

EVIDENCE OF ANTHROPOGENIC CLIMATE EFFECTS IN
SNOW AND FIRN OF EAST ANTARCTICA?
CHARACTERIZATION OF LOW ACCUMULATION AREAS
USING MULTIPARAMETER-ANALYSIS FROM
SNOW AND FIRN CORES

ALEXANDER WEINHART

THESIS BY PUBLICATION FOR THE DEGREE
DOCTOR OF NATURAL SCIENCES (DR. RER. NAT.)

sponsored by



Deutsche
Bundesstiftung Umwelt

www.dbu.de

REVIEWERS

SUPERVISOR:

PROF. DR. OLAF EISEN^{1,2}

FIRST ASSESSOR:

PROF. DR. HUBERTUS FISCHER^{2,3}

SECOND ASSESSOR:

PROF. DR. FRANK WILHELMS^{1,4}

SCIENTIFIC ADVISORS:

DR. JOHANNES FREITAG¹

DR. MARIA HÖRHOLD¹

SUBMISSION: 23 JUNE 2021

COLLOQUIUM: 21 SEPTEMBER 2021

¹ Alfred-Wegener-Institut Helmholtz-Zentrum für Polar- und Meeresforschung, Bremerhaven, Germany

² Fachbereich Geowissenschaften, Universität Bremen, Bremen, Germany

³ Klima und Umweltphysik, University of Bern, Switzerland

⁴ Abteilung Kristallographie, Geowissenschaftliches Zentrum, Universität Göttingen, Göttingen, Germany

AFFIRMATION

Versicherung an Eides Statt

gem. § 5 Abs. 5 der Promotionsordnung vom 18.06.2018

Affirmation in lieu of an oath

according to § 5 (5) of the Doctoral Degree Rules and Regulations of 18 June, 2018

Ich (Vorname, Name | Anschrift | Matr.-Nr.)

Alexander Weinhart

I (First Name, Name | Address | Student ID no.)

versichere an Eides Statt durch meine Unterschrift, dass ich die vorliegende Dissertation selbständig und ohne fremde Hilfe angefertigt und alle Stellen, die ich wörtlich dem Sinne nach aus Veröffentlichungen entnommen habe, als solche kenntlich gemacht habe, mich auch keiner anderen als der angegebenen Literatur oder sonstiger Hilfsmittel bedient habe und die zu Prüfungszwecken beigelegte elektronische Version (PDF) der Dissertation mit der abgegebenen gedruckten Version identisch ist.

Ich versichere an Eides Statt, dass ich die vorgenannten Angaben nach bestem Wissen und Gewissen gemacht habe und dass die Angaben der Wahrheit entsprechen und ich nichts verschwiegen habe.

Die Strafbarkeit einer falschen eidesstattlichen Versicherung ist mir bekannt, namentlich die Strafandrohung gemäß § 156 StGB bis zu drei Jahren Freiheitsstrafe oder Geldstrafe bei vorsätzlicher Begehung der Tat bzw. gemäß § 161 Abs. 1 StGB bis zu einem Jahr Freiheitsstrafe oder Geldstrafe bei fahrlässiger Begehung.

With my signature I affirm in lieu of an oath that I prepared the submitted dissertation independently and without illicit assistance from third parties, that I appropriately referenced any text or content from other sources, that I used only literature and resources listed in the dissertation, and that the electronic (PDF) and printed versions of the dissertation are identical.

I affirm in lieu of an oath that the information provided herein to the best of my knowledge is true and complete. I am aware that a false affidavit is a criminal offence which is punishable by law in accordance with § 156 of the German Criminal Code (StGB) with up to three years imprisonment or a fine in case of intention, or in accordance with § 161 (1) of the German Criminal Code with up to one year imprisonment or a fine in case of negligence.

Brauerhaven, 18.06.2021

A. Weinhart

Ort, Datum

Unterschrift

Place, Date

Signature

„Difficulties are just things to overcome after all.“

Sir Ernest Henry Shackleton

ABSTRACT (ENGLISH)

Antarctica is a fundamental element of the global climate system. On the one hand, the ice masses of Antarctica are a unique climate archive that has steadily piled up over millennia. Analyses of stable water isotopes ($\delta^{18}\text{O}$ and $\delta^2\text{H}$) and aerosols (including ions from sea salt and biogenic emissions), which serve as indirect indicators of climate in ice cores ("climate proxies"), make reconstructions of climate history possible. Gas inclusions in the ice even allow a direct study of the paleoatmosphere. On the other hand, Antarctica is strongly affected by global climate change. Rising temperatures cause a widespread mass loss in West Antarctica and a regional mass loss in East Antarctica. The whole Antarctic ice sheet may contribute to a global sea level rise of about 60 m if it melts entirely.

This work provides important insights into both research aspects of glaciology – the look into the past and into the future. Particularly in areas that are logistically difficult to access, such as the East Antarctic Plateau, field data are scarce. However, these are essential both for studying the signal formation of climate proxies and for validating results from (satellite-based) remote sensing.

The East Antarctic Plateau extends from 20°W to 45°E above an elevation of 2000 m asl. During the Antarctic summer of 2016/17, snow cores were sampled in that area on a traverse between Kohlen Station (0° 4'E, 75° 0'S) and the abandoned Plateau Station (40° 33'E, 79° 15'S). X-ray computed tomography was used to determine the density and stratigraphic properties of the snow. The cores were then cut into individual samples at 1 cm or 2 cm resolution under clean room conditions at -18°C, for which a special instrument was developed as part of this study. The distinct samples were analyzed for stable water isotopes as well as major ions. This approach of a multiparameter analysis allows a combined look at different individual parameters and thus better understand the snowpack history.

Multiple snow cores per sampling location allow a more representative determination of the investigated parameters. The small-scale variability caused by stratigraphic noise or postdepositional processes can thus be filtered.

The surface snow density is needed as a parameter to convert the elevation change of the ice sheet measured by satellites into a mass balance. Due to lack of large-scale data, this density is often modeled. The sampling approach allows us to obtain a representative surface snow density with a relative error of less than 1.5% at each sampling location. Along the traverse route, the mean surface snow density is 355 kg m⁻³ and shows a lower dependence on temperature and accumulation rate than assumed. The modeled values show a significant discrepancy of about -10% from the measured density. A simplified calculation shows that the modeled snow density underestimates the mass budget of the firn column on the East Antarctic Plateau by 3%. Parameterizations of surface snow density can be tuned with the presented data to reduce the uncertainty of the mass balance of East Antarctica.

Crusts in polar snowpacks are a stratigraphic detail that has been used, for example, to characterize environmental conditions in remote regions of the ice sheets. In this work, the first dataset on the spatial distribution of crusts in polar snow is presented – not only with data from the East Antarctic Plateau, but also from Greenland. Contrary to the assumption of finding more crusts in locations with lower accumulation rates, the total number of crusts per meter decreases with decreasing accumulation rates. The results suggest a linear relationship between the number of crusts and the logarithmic accumulation rate. Also the use of crusts for seasonal dating is possible. They can be used as a stratigraphic element supporting the dating with chemical proxies. An effect of crusts on backscatter properties in remote sensing and on firn column ventilation could be future research topics.

An exemplary combined study of stratigraphic and chemical properties of the snowpack allows a reconstruction of the continuous buildup of a dune by drifting snow. Whether the chemical signature is characteristic for this type of deposition, however, remains to be proven with further data.

Measurements of $\delta^{18}\text{O}$ and $\delta^2\text{H}$ can be used to reconstruct paleoclimate from seasonal to millennial time scales because of their direct relationship to precipitation temperature. But on short time scales, mechanical (including redistribution by winds) and physical processes (including sublimation and diffusion) at the surface, especially in areas with low accumulation rates, complicate the temporal assignment of the measured signals. An increase in deuterium excess over the uppermost cm in the majority of the investigated snow cores suggest a strong sublimation effect. Samples over larger depth intervals show stronger correlation with temperature and elevation, as the uppermost snow layers can have a seasonal bias. Cycles in $\delta^{18}\text{O}$ around Kohnen Station can still be interpreted as seasonal signals, but below an accumulation rate of $50 \text{ kg m}^{-2}\text{a}^{-1}$, however, they are overprinted by postdepositional diffusion and consequently no longer suitable for dating the snowpack on short time scales. A comparison with the atmospheric general circulation model ECHAM6-wiso validates the model trend along the traverse, but shows a constant offset in $\delta^{18}\text{O}$. Modeled snow profiles with precipitation values from ECHAM6-wiso and a diffusion model represent the measured profiles well at 1-2 m depth. However, from the surface to 1 m depth, redeposition and sublimation appear to contribute significantly to (postdepositionally) shaping of the $\delta^{18}\text{O}$ signal. These processes need to be further quantified in the future to improve the interpretation of stable water isotopes as a proxy for temperature.

On the one hand, the change in surface snow density between samples from 2005/06 and samples from this study can be attributed to different volume errors in sampling rather than to a change in climatic conditions. On the other hand, mean $\delta^{18}\text{O}$ values over the recent decades show a trend of increasing $\delta^{18}\text{O}$ (and thus increasing temperature) on the East Antarctic Plateau. While these values are within the range of natural variability, they may be early indications that climate proxies in the snow of the East Antarctic Plateau have already recorded the increase of the global temperature.

ABSTRACT (GERMAN)

Die Antarktis ist ein elementarer Bestandteil des globalen Klimasystems. Einerseits sind die Eismassen der Antarktis ein einzigartiges Klimaarchiv, das sich über Jahrtausende stetig aufgebaut hat. Analysen von stabilen Wasserisotopen ($\delta^{18}\text{O}$ und $\delta^2\text{H}$) und Aerosolen (u.a. Ionen aus Meersalz und biogenen Emissionen), die als indirekte Anzeiger des Klimas in Eiskernen („Klimaproxies“) dienen, machen Rekonstruktionen der Klimahistorie möglich. Durch Gaseinschlüsse im Eis kann sogar die Paläoatmosphäre direkt untersucht werden. Andererseits ist die Antarktis stark vom globalen Klimawandel betroffen. Steigende Temperaturen sorgen für flächendeckenden Massenverlust der Westantarktis und regionale Massenverluste der Ostantarktis. Der antarktische Eisschild kann bei vollständigem Abschmelzen zu einer Erhöhung des globalen Meeresspiegels um ca. 60 m beitragen.

Zu beiden Forschungsaspekten der Glaziologie – dem Blick in die Vergangenheit und in die Zukunft – liefert diese Arbeit wichtige Erkenntnisse. Insbesondere aus logistisch schwer zugänglichen Gebieten wie dem ostantarktischen Plateau, gibt es bisher nur wenige Felddaten. Diese sind aber sowohl für die Untersuchung der Signalbildung von Klimaproxies als auch zur Validierung von Ergebnissen aus (satellitengestützter) Fernerkundung unerlässlich.

Das ostantarktische Plateau erstreckt sich von 20°W bis 45°O auf einer Höhe über 2000 m NN. Im antarktischen Sommer 2016/17 wurden dort auf einer Traverse zwischen der Kohlen Station ($0^\circ 4'\text{O}$, $75^\circ 0'\text{S}$) und der verlassenen Plateau Station ($40^\circ 33'\text{O}$, $79^\circ 15'\text{S}$) Schneekerne beprobt. Mittels Röntgen-Computertomographie wurden die Dichte und stratigraphische Eigenschaften des Schnees bestimmt. Danach wurden die Kerne unter Reinraumbedingungen bei -18°C in 1 cm oder 2 cm Auflösung in einzelne Proben geschnitten, wofür im Rahmen dieser Studie ein spezielles Gerät entwickelt wurde. Die Einzelproben wurden auf stabile Wasserisotope sowie auf anorganische Ionen analysiert. Dieser Ansatz der Multiparameteranalyse erlaubt es, verschiedene Einzelparameter kombiniert zu betrachten und somit die Historie der Schneedecke besser nachzuvollziehen.

Mehrere Schneekerne pro Probenahmeort lassen eine repräsentativere Ermittlung der untersuchten Parameter zu. Die kleinräumige Variabilität, die durch stratigraphisches Rauschen oder postdepositionale Prozesse verursacht wird, kann dadurch herausgefiltert werden.

Die Dichte von Oberflächenschnee wird als Parameter benötigt, um die durch Satelliten gemessene Höhenänderung der Eisschilde in eine Massenbilanz umzurechnen. Aufgrund fehlender großflächiger Daten wird diese Dichte häufig modelliert. Durch das Beprobungskonzept kann eine repräsentative Oberflächenschneedichte mit einem relativen Fehler von weniger als 1,5% an jedem Probenahmeort ermittelt werden. Entlang der Traversenroute beträgt die mittlere Oberflächenschneedichte 355 kg m^{-3} und zeigt eine geringere Abhängigkeit von der Temperatur und Akkumulationsrate als angenommen. Die modellierten Werte weisen eine deutliche Diskrepanz von ca. -10% zu der gemessenen Dichte auf. Eine vereinfachte Kalkulation zeigt, dass durch die modellierte Schneedichte das Massenbudget der Firnsäule auf dem ostantarktischen Plateau um 3% unterschätzt wird. Parametrisierungen der Oberflächenschneedichte können mit den präsentierten Daten angepasst werden und somit die Genauigkeit der Massenbilanz der Ostantarktis verbessern.

Krusten in polarem Schnee sind ein stratigraphisches Detail, das beispielsweise zur Charakterisierung der Umweltbedingungen in entlegenen Regionen der Eisschilde genutzt wird. Im Rahmen dieser Arbeit wird der erste Datensatz zur räumlichen Verteilung von Krusten in polarem Schnee vorgestellt – nicht nur mit Daten vom ostantarktischen Plateau, sondern auch aus Grönland. Entgegen der Annahme, mehr Krusten an Orten mit geringerer Akkumulationsrate zu finden, nimmt die Gesamtzahl der Krusten pro Meter mit sinkender

Akkumulationsrate ab. Die Ergebnisse deuten einen linearen Zusammenhang zwischen der Anzahl an Krusten und der logarithmischen Akkumulationsrate an. Eine Nutzung von Krusten zur saisonalen Datierung ist ebenfalls möglich. Sie können als stratigraphisches Element unterstützend zur Datierung mit chemischen Proxies herangezogen werden. Die Auswirkungen von Krusten auf Rückstreueigenschaften in der Fernerkundung und auf die Ventilation der Firnsäule könnten Themen künftiger Forschung sein.

Eine exemplarische, kombinierte Untersuchung aus stratigraphischen und chemischen Eigenschaften der Schneedecke lässt eine Rekonstruktion des kontinuierlichen Aufbaus einer Düne durch Driftschnee zu. Ob die chemische Signatur für diese Depositionsart charakteristisch ist, muss aber mit weiteren Daten noch belegt werden.

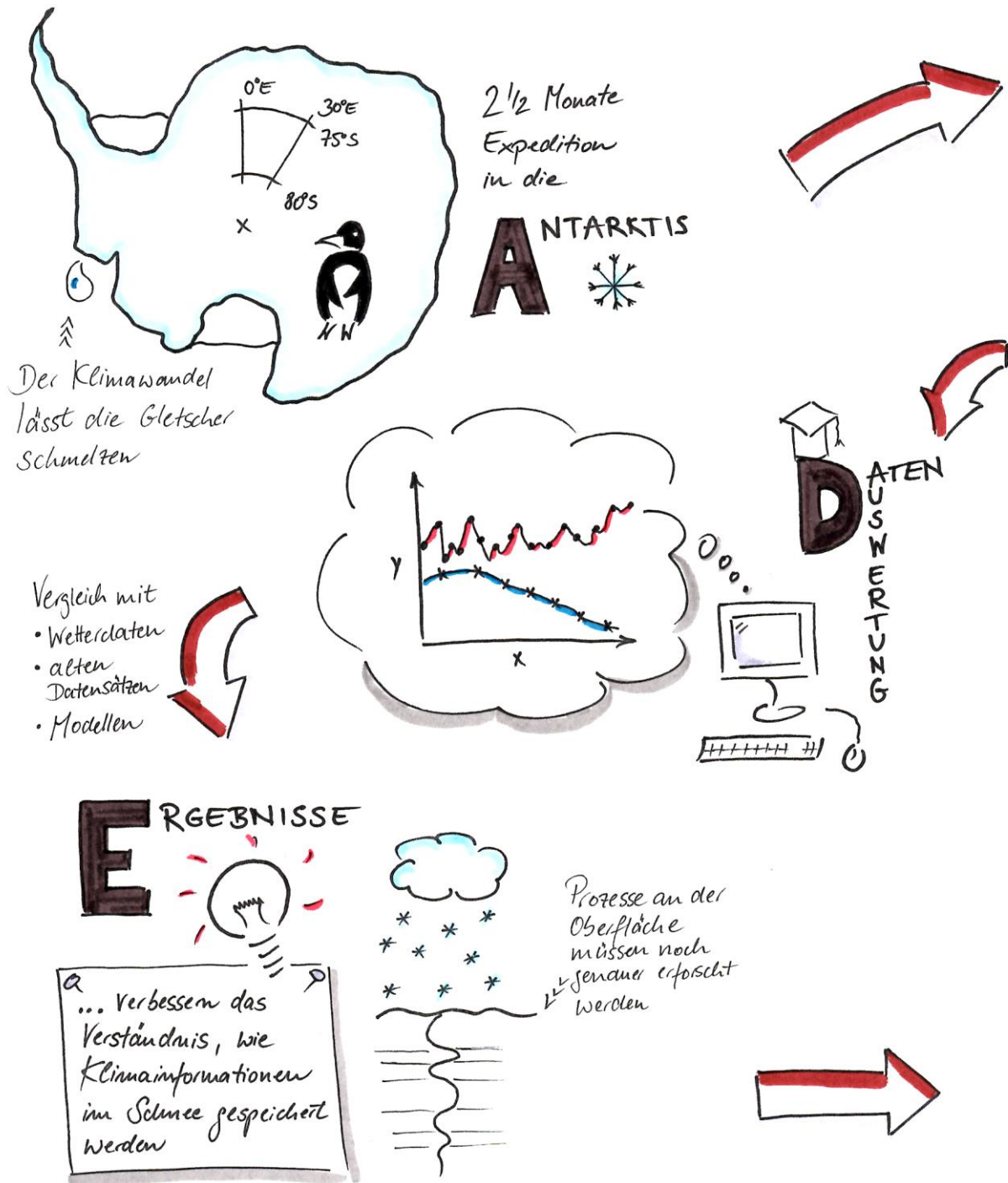
Messungen von $\delta^{18}\text{O}$ und $\delta^2\text{H}$ können durch ihre direkte Beziehung zur Temperatur des Niederschlags zur Rekonstruktion des Paläoklimas von saisonalen bis tausendjährigen Zeitskalen genutzt werden. Doch auf kurzen Zeitskalen erschweren mechanische (u.a. Umlagerung durch Winde) und physikalische Prozesse (u.a. Sublimation und Diffusion) an der Oberfläche, insbesondere in Gebieten mit geringer Akkumulationsrate, die zeitliche Zuordnung der gemessenen Signale. Ein Anstieg des Deuterium-Exzesses über die obersten cm in der Mehrzahl der untersuchten Schneekerne lässt auf einen starken Sublimationseffekt schließen. Deshalb zeigen Proben über größere Tiefenintervalle stärkere Korrelation mit der Temperatur und der geographischen Höhe. Zyklen in $\delta^{18}\text{O}$ lassen sich rund um die Kohnen Station noch als saisonale Signale interpretieren, unter einer Akkumulationsrate von

$50 \text{ kg m}^{-2}\text{a}^{-1}$ jedoch sind sie von postdepositioneller Diffusion überprägt und demzufolge nicht mehr zur Datierung der Schneedecke auf kurzen Zeitskalen geeignet.

Ein Vergleich mit dem atmosphärischen Zirkulationsmodell ECHAM6-wiso validiert den Trend von $\delta^{18}\text{O}$ des Modells entlang der Traverse, zeigt aber einen konstanten Offset. Modellerte Schneeprofile mit den Niederschlagswerten aus ECHAM6-wiso und einem Diffusionsmodell stellen die gemessenen Profile in der Tiefe 1-2 m gut dar. Von der Oberfläche bis 1 m Tiefe aber scheinen Umlagerung und Sublimation das $\delta^{18}\text{O}$ Signal (postdepositionell) wesentlich zu beeinflussen. Diese Prozesse müssen in der Zukunft noch weiter quantifiziert werden, um die Interpretation von stabilen Wasserisotopen als Proxy für die Temperatur zu verbessern.

Auf der einen Seite kann die Veränderung der Oberflächenschneedichte zwischen Proben aus dem Jahr 2005/06 und Proben dieser Studie auf unterschiedliche Volumenfehler bei der Probenahme zurückgeführt werden und nicht auf eine Veränderung der klimatischen Bedingungen. Auf der anderen Seite zeigen Mittelwerte von $\delta^{18}\text{O}$ über die letzten Dekaden eine Tendenz zu steigenden $\delta^{18}\text{O}$ (und damit eine steigende Temperatur) auf dem ostantarktischen Plateau. Diese Werte liegen zwar innerhalb der Schwankungsbreite der natürlichen Variabilität, können aber erste Anzeichen dafür sein, dass Klimaproxies im Schnee des ostantarktischen Plateaus den globalen Temperaturanstieg bereits aufgezeichnet haben.

ABSTRACT (VISUAL)



BEPROBUNG



Proben aus den Polargebieten sind wichtig und kostbar !

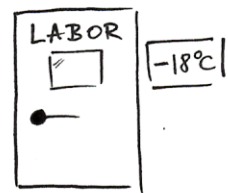
Zahlreiche Schneeprofile aus Schneeschräichten



Die Messdaten können als indirekte Anzeiger des Klimas ("Proxy") genutzt werden, z.B. für die Temperatur oder Ablagerungsbedingungen



CHEMISCHE + PHYSIKALISCHE ANALYSE



- Dichte & Struktur
- Isotope
- Spurenstoffe



FOLGEN

Vergangenheit & Zukunft verstehen



Klimaprognosen werden genauer

Klima-rekonstruktionen werden verbessert



CONTENTS

Reviewers	III
Affirmation.....	V
Abstract (English)	VIII
Abstract (German).....	X
Abstract (Visual)	XII
Contents.....	XIV
Abbreviations & acronyms.....	XVI
Author contributions	XVII
1 Introduction	1
1.1 Continent Antarctica: A brief look at its geography & research history	2
1.2 The past: Ice as climate archive	4
1.3 The present: Increasing temperature in East Antarctica	7
1.4 The future: Contribution of melting ice to a global sea level rise	8
1.5 Area of investigation.....	9
1.5.1 The East Antarctic Plateau.....	9
1.5.2 The CoFi traverse	11
1.6 Motivation and scope of this study.....	13
1.6.1 Spatial & temporal variability of climate signals in snow.....	13
1.6.2 Formation of climate signals in snow and firn on the East Antarctic ice sheet.....	14
1.6.3 Climate change recorded in snow on the East Antarctic Plateau?	15
2 Material & methods	17
2.1 Sample overview	17
2.2 Snow profile sampling	18
2.2.1 Multiple snow profiles.....	18
2.3 Computer tomography	19
2.4 Discrete sampling	20
2.5 Ion chromatography.....	20
2.6 Cavity ring-down spectroscopy.....	21
2.6.1 Delta notation for stable water isotopes	21
2.7 Additional material	22
2.7.1 Single snow profiles along the CoFi traverse	22
2.7.2 The OIR trench.....	22
2.7.3 Snow profiles from different projects	22
2.7.4 Firn cores	23
3 Publication I Representative surface snow density on the East Antarctic Plateau.....	24
4 Publication II Spatial distribution of crusts in Antarctic and Greenland snowpacks and implications for snow and firn studies.....	48
5 Publication III Climate signal or postdepositional modification? Insights on stable water isotopes in Antarctic surface snow.....	65
6 Further results & discussion.....	88
6.1 Deciphering the local snowpack history on the East Antarctic Plateau – using a combination of stratigraphic features and major ions	88

6.2 Is a temperature rise visible in snow of the East Antarctic Plateau? – A comparison of decadal $\delta^{18}\text{O}$ at selected sites.....	94
7 Summary, conclusion & outlook	97
7.1 Summary & conclusions of the scientific results	97
7.2 Suggestions for further studies	99
7.3 Closing remarks.....	100
8 References	101
9 Acknowledgments	110
10 Appendix	113
10.1 Sampling protocols	113
10.2 Datasets.....	117
10.2.1 Snow density.....	117
10.2.1.1 Surface snow density along the CoFi traverse.....	117
10.2.2 Spatial distribution of crusts in Greenland and Antarctica.....	117
10.2.2.1 Crusts in snow from Greenland and Antarctica.....	117
10.2.2.2 Crusts in two Antarctic firn cores	117
10.2.3 Stable water isotopes & major ions.....	118
10.3 Conference poster contributions	119
10.3.1 EGU 2019	119
10.3.2 EGU 2020 #1 (co-authorship).....	120
10.3.3 EGU 2020 #2 (co-authorship).....	120
10.4 Miscellaneous	121
10.4.1 Curiosities from the ice lab.....	121
10.4.2 A visit to abandoned Plateau Station (active 1966-1969)	122

ABBREVIATIONS & ACRONYMS

ASL	Above sea level
AWI	Alfred-Wegener-Institute, Helmholtz Center for Polar and Marine Research
AWS	Automatic weather station
BE-OI	Beyond EPICA – Oldest Ice
CoFi	Coldest Firn
CLP	Crosshair liner project (Kohnen Station)
CRDS	Cavity Ring Down Spectroscopy
DML	Dronning Maud Land
Dome A	Dome Argus
Dome C	Dome Charlie
Dome F	Dome Fuji
EAP	East Antarctic Plateau
EDC	EPICA Dome C
EDML	EPICA Dronning Maud Land
EGRIP	East Greenland ice core project
EPICA	European Project for Ice Coring in Antarctica
GMSL	Global mean sea level
IC	Ion chromatography
IPCC	The Intergovernmental Panel on Climate Change
μ CT	Microfocus computer tomography
OIR	Oldest ice reconnaissance
RCP	Representative concentration pathway
RECAP	Renland ice cap
SLE	Sea level equivalent
SMB	Surface mass balance
SSP	Shared socio-economic pathway
T4M	Trench study in 2018/19 (Kohnen Station)

AUTHOR CONTRIBUTIONS

The CoFi project at AWI was initialized by Dr. Sepp Kipfstuhl and Dr. Johannes Freitag. The sampling for this thesis was carried out within the framework of the joint scientific expedition of the CoFi project and the Beyond EPICA - Oldest Ice pre-site survey in Antarctica in 2016/17.

The research questions, scientific objectives, and concept of this study were designed by myself with scientific support of Dr. Johannes Freitag, Dr. Maria Hörhold and Prof. Dr. Olaf Eisen. The project was funded for three years by the German Environmental Foundation.

I took part in the field campaign and performed the sampling with assistance from Dr. Alexandra Touzeau (chapter 2.2). Chapters 2.3 to 2.6 cover the working process of the main samples (snow profiles) chronologically. I conducted the μ CT measurements, performed the laboratory work (in teams of two – a list of all assistants can be found in the acknowledgments), and managed subsequent IC and CRDS measurements. Other samples (not sampled by myself) used supportively in this thesis are described in chapter 2.7. I performed the data analysis using the software “R” (R Core Team, 2021), evaluated the additional results in chapter 6, and wrote the frame text of this thesis.

I will write in first-person singular when referring to performed working steps by myself or results and conclusions in the context of the thesis. Regarding results and conclusions from the three publications, I will use first-person plural to include the effort of my co-authors. My (Alexander Weinhart) contributions to the three publications are as follows:

Publication I:

Alexander Weinhart and Dr. Sepp Kipfstuhl conducted the fieldwork. Alexander Weinhart performed the majority of the μ CT measurements, subsequent analysis and wrote the manuscript. All authors discussed the results and contributed to revising the manuscript.

Publication II:

Alexander Weinhart created the dataset, prepared the manuscript, and discussed the first results with Dr. Johannes Freitag and Dr. Sepp Kipfstuhl. Dr. Maria Hörhold supervised the chemical measurements, Prof. Dr. Olaf Eisen improved the statistical analysis. All authors contributed to revising the manuscript.

Publication III:

Alexander Weinhart took all presented snow profiles along the CoFi traverse and conducted the sample preparation in the ice laboratories with support from Melissa Mengert, Georgia Micha, and Pia Götz. Alexander Weinhart wrote the manuscript and discussed the results intensively with Dr. Sepp Kipfstuhl, Dr. Johannes Freitag, and Dr. Maria Hörhold. Dr. Martin Werner provided recent ECHAM6-wiso isotope outputs and Dr. Thomas Münch supported the generation of the simulated snow profile. Prof. Dr. Olaf Eisen improved the manuscript with substantial feedback.

1 INTRODUCTION

The Earth's climate system is based on complex interactions between the atmosphere, hydrosphere, lithosphere (also referred to as geosphere), and biosphere. The existing natural greenhouse effect, which traps the heat radiating from the Earth towards space, makes the Earth an inhabitable planet (Lacis et al., 2010). However, since the industrial revolution in the 19th century, humankind has added an anthropogenic component to it. Scientists have observed significant shifts and changes in the climate system (Alexander et al., 2006) and the biosphere (Parmesan & Yohe, 2003) since the preindustrial times, which is a relatively short period of time compared to the 4.55 billion year history of planet Earth (Dalrymple, 2001, Manhes et al., 1980). A rising global mean temperature (Lenssen et al., 2019), warming and acidification of the oceans (Doney et al., 2009, von Schuckmann et al., 2020), changes in precipitation patterns (Held & Soden, 2006) or higher potential for heatwaves (Meehl & Tebaldi, 2004) are just a few of many others. The anthropogenic impact on climate change has become so meaningful that scientists are proclaiming the introduction of the new geological stage called "Anthropocene" (Crutzen, 2002, Steffen et al., 2007).

The scientific consensus of an anthropogenic impact on the climate system is expressed in the output of the Intergovernmental Panel on Climate Change (IPCC), a committee of experts established in 1988 by the United Nations. Its goal is to gather "scientific, technical and socio-economic information relevant to understanding the scientific basis of risk of human-induced climate change, its potential impacts and options for adaptation and mitigation" (IPCC, 1998). Almost three decades have passed before political actions finally lead to the Paris Agreement in 2015, the first binding agreement on climate, with the goal to limit the global warming to less than 2°C compared with preindustrial levels (UNFCCC, 2015). More recently, the Special Report on the Ocean and Cryosphere in a Changing Climate has been published, highlighting the scientific status quo as well as prognoses and risks for and by the hydrosphere (including the cryosphere) in particular (IPCC, 2019).

The long-term consequences of climate change in a biological and physicochemical, geological, climatic and socio-economic context are difficult and sometimes even impossible to forecast. However, irreversible changes (or losses) of certain elements of the Earth system are expected if so-called 'tipping points' are reached or transgressed (Lenton et al., 2008). Among these elements at risk are, e.g., the dieback of the Amazon rainforest and boreal forests, shifts in monsoon systems, permanent changes in the thermohaline circulation (including the Atlantic deep water formation), but also the instability of the Greenland and Antarctic ice sheets and the loss of Arctic sea ice. For some elements, the tipping points are dangerously close, especially within the cryosphere (Lenton et al., 2019, Schellnhuber et al., 2016). A global warming beyond 2°C would cause a deglaciation of almost the entire Northern hemisphere in the long-term, as the tipping point for Greenland is postulated between 0.8°C and 3.2°C and even lower for Arctic summer sea ice (Schellnhuber et al., 2016). As the global mean air temperature rises three times faster in the Arctic than the global mean (AMAP, 2021), a phenomenon called "Arctic amplification" (Cai et al., 2021, Screen & Simmonds, 2010, Serreze & Barry, 2011), the Arctic sea ice extent in September constantly shrinks (Stroeve et al., 2011), a reason why some studies count the Arctic summer sea ice already for lost (Lindsay & Zhang, 2005). Also the melting of the Antarctic ice sheet is an imminent risk and bears the potential for enormous consequences and non-linear, self-enforcing feedback mechanisms, even if the goals of the Paris agreement are reached (Pattyn et al., 2018).

1.1 CONTINENT ANTARCTICA: A BRIEF LOOK AT ITS GEOGRAPHY & RESEARCH HISTORY

In Earth history, the glaciation of the polar regions is not the common situation. Since the beginning of the Proterozoic 2.5 billion years ago, the poles were only covered with ice a few times (Young, 2013). The recent period of glaciation around the South Pole was initiated roughly 34 million years ago when the development of the Antarctic circumpolar current started to isolate Antarctica from the rest of the world (Kennett, 1977). As in consequence the temperature dropped, snow and ice started to accumulate on the Antarctic continent. However, the ice masses did not constantly remain until today. Around 4.7 million years ago, Antarctica was almost ice-free. Only three minor glaciers covered the regions around the South Pole, Dronning Maud Land (DML), and Dome Argus (Dome A) (DeConto & Pollard, 2003). Since then, the ice sheet started to grow again up to its current state. Nowadays, continental Antarctica is covered by an ice volume of 25.4 million km³ (LIMA, 2008). With Antarctica being oriented northward along the Greenwich meridian (0°), the Transantarctic Mountain range divides the continent into a Western and an Eastern part (Fig. 1), appositely named West Antarctica and East Antarctica. The Antarctic ice sheet had its last maximum extent between 26,500 and 19,000 years ago, at the climax of the last glacial maximum. During that period, the global mean sea level (GMSL) was about 126 m below the current sea level (Clark et al., 2009). Today, Antarctica has an area of almost 14 million km² including ice shelves and islands. 99.8% of the area is covered by ice (Burton-Johnson et al., 2016). The two largest shelf ice areas, the Ross Ice Shelf and Filchner-Ronne Ice Shelf, make up more than 6% of the total area. Often considered a flat and white area of snow and ice, it is forgotten that Antarctica is also the continent with the highest mean elevation. On average, the ice masses pile up to a height of 2194 m asl (above sea level), while Asia, the second-highest continent, only reaches an average level of 960 m asl (LIMA, 2008, Spektrum, 2005). The highest elevation of the ice sheet itself is Dome A with 4093 m asl, but the highest point of Antarctica is Mount Vinson with a total height of 4892 m asl, located in the Ellsworth Mountains west of the Filchner-Ronne Ice Shelf (Fig. 1). Below the ice sheet, many subglacial lakes, which formed due to a combination of the overburden pressure of the ice (and consequently a lower melting point) and the geothermal heat flux from the Earth's interior, exist. The largest of over 400 subglacial lakes is Lake Vostok with a size of roughly 14,000 km² (Siegert et al., 2011).

Antarctica fascinates young and old because of its geographic and climatic extremes. It was not until January 1820 that the continent was first sighted, when the Fimbul Ice Shelf in Northern DML was discovered on a Russian expedition led by Fabian Gottlieb von Bellingshausen (World Ocean Review 6, 2019). It is still under debate to whom honor of the first step on the Antarctic continent is due. Rumors say John Davis and his crew set foot on Antarctica as early as 1821 during a seal hunt in Hughes Bay, but without valid evidence. The first confirmed landing on the continent happened 74 years later by the crew members of the expedition Antarctic, namely Carsten Egeberg Borchgrevink, which reached Cape Adare in 1895 (Branagan, 2014).

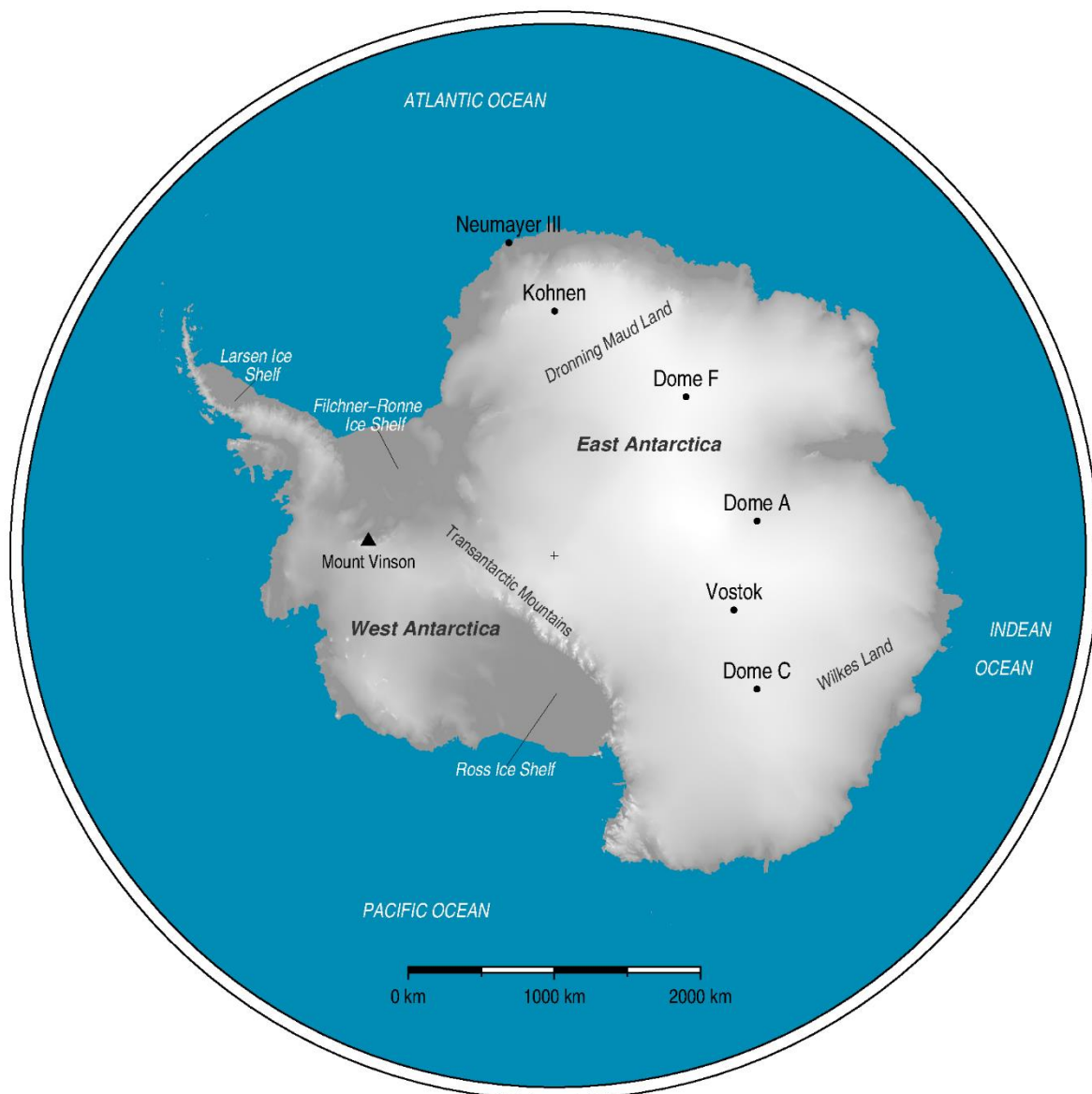


Fig. 1: Overview map of Antarctica with the Greenwich meridian at top. Selected research stations and ice core drill sites mentioned in the text are annotated and marked with a black dot. The geographic South Pole is marked with a small cross. Further annotations show large areas of Antarctica (oblique font, black), mountains (black triangle), ice shelves (oblique font, white) or surrounding oceans (capitals, white).

After this early stage of exploration, the Heroic Age of Antarctic Exploration started with a resolution passed on the sixth International Geographical Congress in 1895, suggesting that “the exploration of the Antarctic regions is the greatest piece of geographical exploration still to be undertaken” (International Geographical Congress, 1896). By that time, pioneering achievements in physics had been made, like the discovery of radioactivity by Ernest Rutherford (1896) and Marie and Pierre Curie (1898). In the meantime, remote Antarctica was still about to be discovered. Great pioneers tried unsuccessfully but returning alive (Ernest Henry Shackleton, Nimrod Expedition 1906-1909), successfully and returning alive (Roald Amundsen, South Pole Expedition 1910-1912), and successfully but never returning (Robert Falcon Scott, Terra Nova Expedition 1910-1913), to reach the geographic South Pole as the first person in history. Other glorious expeditions tried to explore East Antarctica (Gauss Expedition, 1901-1903) or cross the Antarctic continent (Imperial Trans-Antarctic Expedition, 1914-1917). Both ships, ‘Gauss’ and ‘Endurance’, were trapped in ice (World Ocean Review 6, 2019).

Today, thanks to technological progress, expeditions to Antarctica are still challenging but not nearly as dangerous as they were at the beginning of the 20th century. Probably the biggest challenge on Antarctic expeditions is the extremely low temperature, as Antarctica is the coldest and driest continent on Earth. The coldest temperature ever recorded is -89.2°C at the Russian station Vostok (Fig. 1) in July 1983 (Turner et al., 2009). The mean annual air temperature there is given with -55°C (Petit et al., 1999). Using satellite measurements, scientists have recently detected even lower temperatures in depressions on the East Antarctic Plateau (EAP) (Scambos et al., 2018).

1.2 THE PAST: ICE AS CLIMATE ARCHIVE

Over the last 4 million years, the Antarctic ice sheet has accumulated year by year, layer by layer. Information about recent weather (i.e., up to three decades; or on longer time scales: climate) conditions can be preserved in each individual layer. With time passing and accumulation on top of the ice sheet, this information is advected downwards and is embedded in the ice.

Starting at the surface with fresh snow, which has a porosity of 60-70% in polar regions, the overburden pressure of the accumulating snow on top increases the density and lowers the porosity with increasing depth. Firn is defined as a snow layer that has lasted one season without melting (a definition originating from alpine glaciology, Böhm et al., 2007), but sometimes also a specific density or depth value as a threshold to distinguish between snow and firn is taken into account (Pidwirny, 2006). Either way, the porous matrix in firn allows the air to diffuse and exchange with the atmosphere above by wind convection (Colbeck, 1989, Schwander, 1996). The air inside the firn column, therefore, is always younger than the surrounding firn matrix. In glacial periods, this age difference can be up to several thousand years (Schwander & Stauffer, 1984). Until reaching a density of 830 kg m⁻³, the porous matrix vanishes slowly and only single closed gas bubbles remain (Fig. 2). This is defined as the transition from firn to glacial ice. The enclosure of gas with the composition of the atmosphere at the time of the close-off is trapped in these bubbles (Sowers et al., 1992). This phenomenon makes ice a unique environmental archive, as no other archive on Earth directly preserves the paleoatmosphere. The gas composition can be measured directly and tell us a lot about the history of planet Earth, particularly the development of the atmosphere in the past (e.g., Fischer et al., 1999).

Other parameters or species can also be measured and translated into climate information that cannot be measured directly. These parameters are called climate proxies. Examples are stable water isotopes and impurities, which can function as a relative marker for seasons, temperature changes, transport pathways or climatic conditions in general. Isotopes are variants of one chemical element with a constant number of protons and a varying number of neutrons in their nucleus. Depending on the energy equilibrium in the nucleus, isotopes can be stable or decay under radioactive emission. Most elements have a natural variety of isotopes, which occur in a specific ratio. In this thesis, the focus is on the stable isotopes of water (H₂O). The two stable isotope of hydrogen are ¹H (99.984% abundance) and deuterium (²H) (0.016%) (Friedman, 1953). Oxygen has three naturally occurring stable isotopes, which are ¹⁶O (99.76%), ¹⁷O (0.04%) and ¹⁸O (0.20%). These abundances of hydrogen and oxygen isotopes also resemble the natural ratio in water. At phase transitions with condensation and evaporation, sublimation and resublimation, this ratio changes due to the different thermodynamic behaviors of each isotope. Heavier isotopes tend to remain in the condensed phase, while lighter isotopes are enriched in the evaporating phase. This relationship in the hydrological cycle is described with the Rayleigh fractionation, which generally describes the evolution of a system with several phases in which one phase is continuously removed through fractional

distillation. An example of this fractionation in precipitation over Antarctica is shown in Fig. 2. Dansgaard (1964) first described the quantitative relationship in global precipitation, and with that study he initiated the use of stable water isotopes as a measure for paleotemperatures. As the fractionation effect is sensitive to temperature, a measured relationship between heavier and lighter isotopes can be translated into the condensation temperature of precipitation.

While hydrogen and oxygen isotopes as part of the water molecule build the snow, firn and ice matrix itself, other components can be attached to or incorporated in the matrix. Among these are impurities (ions) or insoluble dust particles. The former usually appear in the form of aerosols, tiny solid or liquid particles in a gaseous phase (Shaw, 1988). Sodium and chlorine are two of the most abundant species as they are the major sea salt components. They get dispersed in the air over the open ocean and transported with the wind over high distances onto the polar ice sheets, exhibiting a seasonality due to more frequent advection in winter. Mineral aerosols from continents, like aluminum, silicon, and calcium, are brought into the air via physical erosion. Sulfurous (e.g., sulfate) and nitrogenous (e.g., nitrate) species may have different biogenic and geogenic as well as anthropogenic origins. These can be volcanic eruptions, sea salt, degradation in the atmosphere, denitrification processes, continental erosion or algae bloom (Legrand & Mayewski, 1997). On the other hand, larger insoluble dust particles can represent weathering conditions in the source region (Fig. 2).

To retrieve this information from snow, firn, and ice, scientists started drilling cores and analyzing the different chemical and physical properties. The first ice core from Antarctica was drilled in the framework of the Norwegian-British-Swedish Antarctic Expedition to DML from 1949 to 1952 (Schytt, 1958). Of course, the quality of the almost 100 m long ice core cannot keep up with the quality of ice cores nowadays, but nevertheless this moment found its way into history books (Faria et al., 2014, Jouzel, 2013). The first drilling that reached the bedrock underneath the ice sheet was finished in 1966 in a total depth of 1388 m after six years at Camp Century in the northwest of Greenland (Hansen & Langway, 1966). However, not science was the main motor of this project. In “project iceworm” the United States deposited up to 600 mobile nuclear missiles in Greenland, hidden under the surface in a tube-like system in the ice. In 1967, Camp Century was abandoned, leaving the remnants of a nuclear power plant in the ice. The radioactive fluids will be transported with the ice stream further towards the coast and melt out into the sea in the future (Colgan et al., 2016).

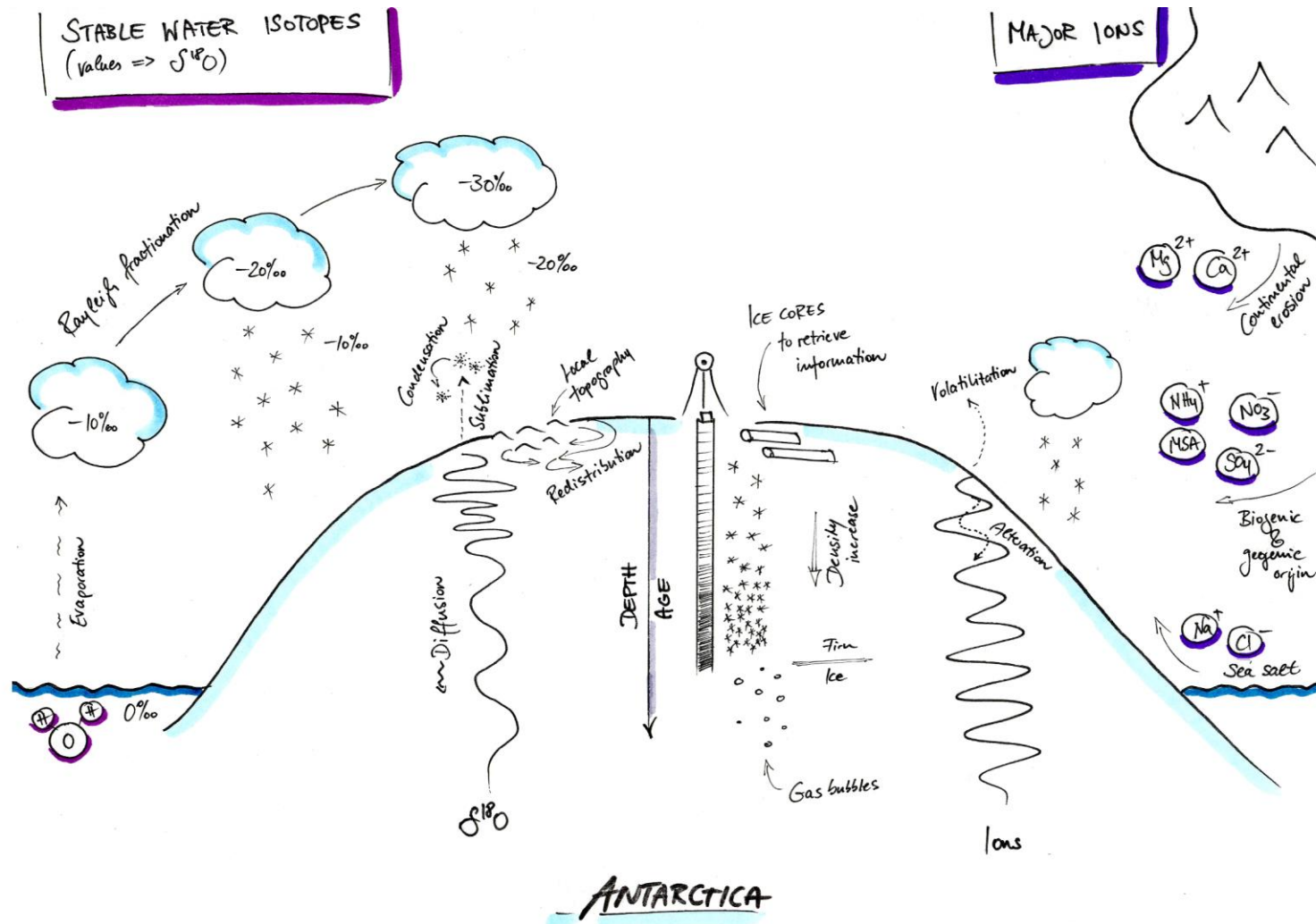


Fig. 2: A drawn scheme summarizing some of the formation processes of the climate archive ice regarding a) density (middle), b) stable water isotopes (left), and c) major ions (right). Apart from the transport pathways to Antarctica (major ions) and the fractionation process at phase transitions (stable water isotopes), I want to highlight the processes that hamper the interpretation of these climate proxies on short (seasonal to annual) time scales in low accumulation areas with this figure. The values in ‰ on the left side of the sketch refer to $\delta^{18}\text{O}$ (s. chapter 2.6).

One of the biggest and most significant ice core projects in history was the European Project for Ice Core Drilling in Antarctica (EPICA). In the framework of this project funded by the European Union, two ice cores were drilled in Antarctica, one of them at Kohnen Station (abbreviated EDML) and the other at Dome C (EDC). Both cores were milestones in the research of younger climate dynamics, especially for the strong interhemispheric coupling via the Atlantic Meridional Overturning Circulation (EPICA Community Members, 2006). The EDC core reveals eight glacial-interglacial cycles over the last 800,000 years from gas bubbles, stable water isotopes as well as impurities (EPICA Community Members, 2004). Furthermore, EDC is the oldest ice core drilled so far, but this age record may be broken in a few years.

The preparations for the project 'Beyond EPICA - Oldest Ice' (BE-OI) started in 2016 with the goal to drill an ice core dating back, in the best case, 1.5 Million years. To get a continuous stratigraphy for paleoclimatic reconstructions far back in time, the setting of accumulation rate and temperature, bedrock topography, ice flow as well as geothermal heat flux has to fit perfectly at the desired drill site (Fischer et al., 2013). After modeling efforts (Parrenin et al., 2017, Young et al., 2017) and intensive pre-site surveys (Cavitte et al., 2018, Karlsson et al., 2018, Sutter et al., 2019, Winter et al., 2019), the final drilling spot has been announced and confirmed in 2019 on subglacial highlands 40 km south-west of Dome Charlie (Dome C), informally called 'Little Dome C' (Barbante & Eisen, 2019, Van Liefferinge et al., 2018). Between 1.2 and 0.8 million years ago, there was a significant change to longer glacial and interglacial periods in Earth history. The climate system switched from a periodicity of 41,000-year cycles (until ~1 million years ago) to 100,000-year cycles (800,000 years ago until today). This interval of change is also called mid-Pleistocene climate transition. The temperature information about this period is gathered, among other records, from benthic foraminifera isotopes (Lisiecki & Raymo, 2005). The cause of the mid-Pleistocene climate transition is still under debate and several theories for that exist (e.g., Elderfield et al., 2012, Hönisch et al., 2009). The lacking information to answer this question is the record of atmospheric carbon dioxide (CO₂) in this time period. One objective of the BE-OI core is to obtain a climatic record of atmospheric CO₂ throughout the mid-Pleistocene climate transition in high resolution and answer the open question of the cause.

1.3 THE PRESENT: INCREASING TEMPERATURE IN EAST ANTARCTICA

Temperatures around the globe can be measured directly where weather stations are available. In each of the last three decades the Earth's surface has been warmer than in the previous one, and since the 1980s a constant warming trend on both hemispheres is visible, with the past 19 years being among the hottest 20 years since weather recordings (GISTEMP Team, 2020, Lenssen et al., 2019, NASA, 2021).

In contrast to inhabited regions, the spatial and temporal coverage of weather stations in Antarctica is sparse and for quite a while, there were no significant evidences for an increased warming of East Antarctica (Monaghan et al., 2008, Monaghan et al., 2006, Turner et al., 2005). However, at research stations often automatic weather stations (AWS) were installed, which recorded, amongst other parameters, the local air temperature. An evaluation of the AWS at Kohnen Station (Reijmer & van den Broeke, 2003) indicated a temperature increase over the past 20 years of 1.13°C (Fig. 3, left). This has been published and discussed as a visible trend by Medley et al. (2018), which could even lead to a sea level mitigation in climate model projections. Also a warming of 0.61 ±0.34 °C per decade at the South Pole has been reported recently (Clem et al., 2020).

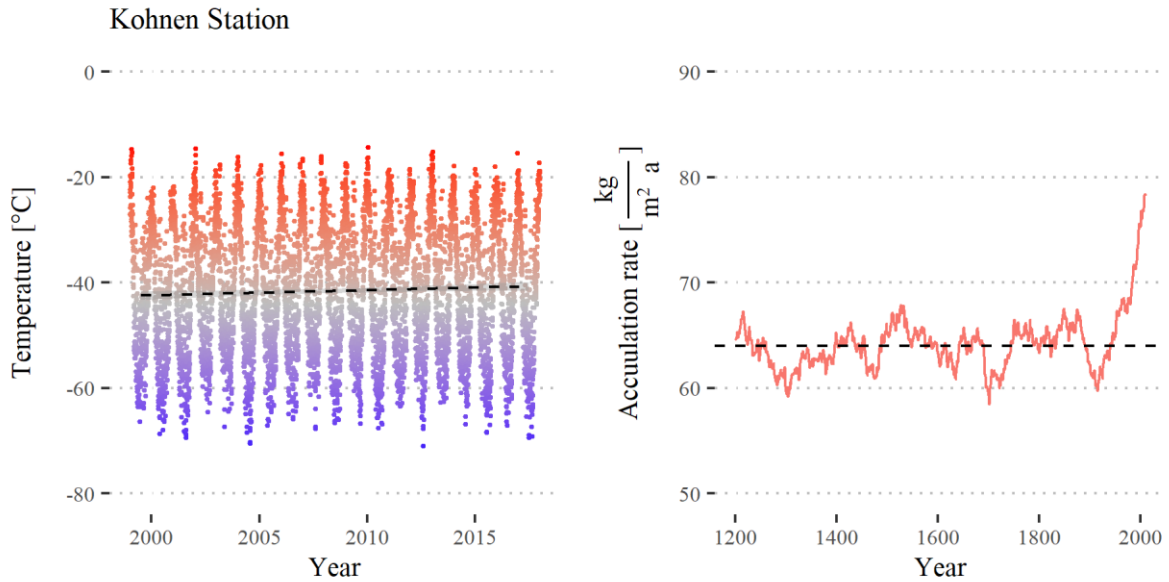


Fig. 3: Left: Air temperature 10 m above the surface at Kohnen Station. The weather station is jointly operated by the Institute for Marine and Atmospheric Research and the Alfred-Wegener-Institute (Reijmer & van den Broeke, 2003). In the plot we show daily mean values starting from 1st of January 1999 until the 1st of December 2017. The black dashed line shows the linear trend in annual mean temperature in the same interval. Right: Accumulation rate determined from density and age scale from continuous flow analysis data of firn core B40 (Medley et al., 2018).

Where no AWS are available, climate information is gathered from snow, firn, and ice. One important property in this context is the accumulation rate which gives valuable information about the local precipitation and is essential for the interpretation of climate proxies in ice cores. Several ground-based (Eisen et al., 2008) and remote measurement techniques (e.g., Arthern et al., 2006) exist to derive accumulation rates on different scales and with varying accuracy. The temperature increase at Kohnen Station is also accompanied by a 25% increase in accumulation rate (relative to preindustrial time), measured in ice core B40 (Fig. 3, right) (Medley et al., 2018). An increase in accumulation rate for all of Antarctica with a significantly higher increase at the coastal areas has been proposed by Frieler et al. (2015) using a combination of ice core data and general circulation models. Increased snowfall leading to a positive surface mass balance (SMB) has also been observed in other parts of DML (Philippe et al., 2016). It is expected that the main reason for these observations is related to an atmospheric pressure decrease over the Weddell Sea and an increase over the EAP. After an anomalously positive SMB in DML in the year 2009, a warmer atmosphere and changed circulation and precipitation patterns may lead to steadily positive SMB in the future (Lenaerts et al., 2013). Increasing temperatures (Muto et al., 2011) accompanied by increasing accumulation rates lead to lower sea level projections from this part of Antarctica (Medley & Thomas, 2019).

1.4 THE FUTURE: CONTRIBUTION OF MELTING ICE TO A GLOBAL SEA LEVEL RISE

In the past decades, glaciers worldwide contributed to a larger amount to the global sea level rise than the large ice sheets (Hugonnet et al., 2021, Marzeion et al., 2012, Meier et al., 2007). However, Greenland and Antarctica combined still store a sea level equivalent (SLE) of 65 m (Alley et al., 2005, Fretwell et al., 2013) and will replace mountain glaciers as the main contributor rather sooner than later. The Antarctic mass balance has remotely been monitored over the last decades showing large regional differences in mass loss (IMBIE Team, 2018, Rignot et

al., 2019). West Antarctica loses mass over almost its entire area caused by rising temperatures (Bromwich & Nicolas, 2014) and the warm surrounding ocean (Payne et al., 2004, Shepherd et al., 2004). Enhanced melting at the bottom of the ice sheet is then caused by the bedrock topography below sea level with a retrograde slope and warm circumpolar deep water entering ice shelf cavities (Scambos et al., 2017). In particular, the situation at the Amundsen Sea Embayment with the large negative mass balance of the Pine Island Glacier and Thwaites Glacier (Rignot et al., 2019) can lead to a destabilization of the whole West Antarctic ice sheet (DeConto & Pollard, 2016, Feldmann & Levermann, 2015, Joughin et al., 2014). In contrast, East Antarctica still seems to be in balance (Gardner et al., 2018, IMBIE Team, 2018, Rignot et al., 2019), although locally glaciers are reported to lose mass, such as in Wilkes Land (Li et al., 2015, Miles et al., 2016, Shen et al., 2018). Due to increasing snowfall, some observations even show a regional mass gain for East Antarctica (Medley et al., 2018, Medley & Thomas, 2019, Zwally et al., 2015) and models predict this also for the future (Seroussi et al., 2020).

Since 1901, GMSL has risen about 19 cm (IPCC, 2014). The development of future GMSL was commonly calculated dependent on different representative concentration pathways (RCP). These pathways stand for parameterized scenarios regarding adaption to and further development of the Earth's climate forced by carbon emissions and solar radiation (Moss et al., 2010). The RCPs will be replaced by shared socio-economic pathways (SSP) for the next IPCC report in 2021 (Meinshausen et al., 2020). DeConto and Pollard (2016) presented a range between 2 cm and 105 cm contribution of Antarctica to GMSL until 2100, depending on different RCP as well as the Pliocene sea level reference. The recent Ice Sheet Model Intercomparison Project forecasts between -7.6 and 30.0 cm of SLE for the same time period under different RCP (Seroussi et al., 2020). The IPCC projections classify a GMSL rise between 0.43 m and 0.84 m relative to the sea level between 1986 and 2005 to be likely (Oppenheimer et al., 2019). The regional impacts of a GMSL rise can be severe within the next century, especially for populated coastlines (Clark et al., 2016).

1.5 AREA OF INVESTIGATION

1.5.1 THE EAST ANTARCTIC PLATEAU

The EAP does not have clear boundaries so that one might find different definitions for this area. A common classification is the region higher than 2000 m asl, east of the Transantarctic Mountains (Fig. 1) (Stenni et al., 2017, Thomas et al., 2017). In the framework of this thesis, the focus is on the region DML between 20°W and 45°E. While several research stations are located along the DML coastline, there are two active research stations on the EAP, which are currently operated only in some austral summer. The first one is Kohonen Station (75°S, 0.6°E, 2892 m asl), which was introduced already in section 1.2 as one location of the EPICA project (Oerter et al., 2009). The other one is the Japanese Dome Fuji Station (77° 19'S, 39° 42'E, 3710 m asl) on the second-highest ice dome in Antarctica (Shiraishi, 2013).

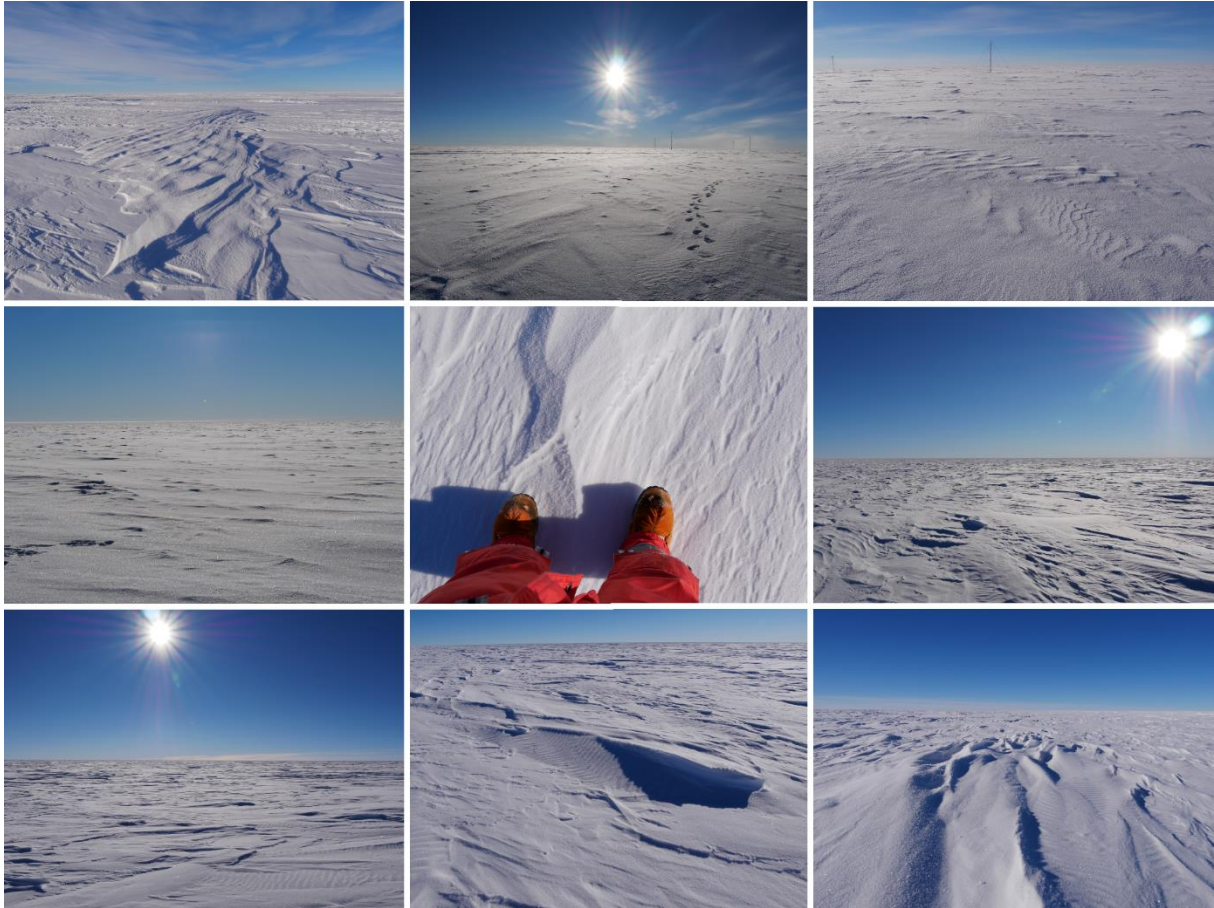


Fig. 4: Snow surface structures photographed along the CoFi field campaign (section 1.5.2). Although the EAP seems infinitely flat on the large scale (see the horizon in some of the pictures), the small-scale surface is highly variable and shows undulations, snow patches, dunes and sastrugi. In relation to the annual accumulation rate (or “annual layer thickness”), this surface roughness becomes relatively large.

As daily and seasonal cycles in temperature only affect the upper meters of snow and firn, the temperature in 10 m depth represents the mean annual temperature at a given place. At Kohlen Station the 10 m firn temperature was measured in 1999 with -44.5°C (Oerter et al., 1999). Temperature records from an automatic weather station at Kohlen Station give a mean annual air temperature of -41.5°C . At Dome F the 10 m firn temperature is given with -58°C (Ageta et al., 1998), the annual mean air temperature in 1.5 m height of -54.3°C was measured between 1996 and 1997 (Watanabe et al., 2003).

The EAP is the major heat sink in the southern hemisphere. Strong radiative cooling during periods of clear sky as well as weak winds and a very dry atmosphere force cold temperatures there. The large temperature difference between the equator and South Pole creates synoptic activity over the southern ocean (King & Turner, 1997). The coastal parts of Antarctica and also of DML have a constant influence of marine air. The EAP, in contrast, is just occasionally influenced by synoptic activities. The most frequent weather patterns are eastward-moving low-pressure systems reaching the plateau, and lows that formed east of 0° longitude moving to the west associated with clouds influencing the plateau. These weather situations can cause single precipitation events, which can make up a large fraction of the annual accumulation in some areas (Birnbaum et al., 2006, Schlosser et al., 2010, Servettaz et al., 2020). A significant fraction of the precipitation on the remote plateau occurs during clear sky conditions due to radiative cooling, also called ‘diamond dust’ (Bromwich, 1988, Bromwich et al., 2004, Stenni et al., 2016). On the high and remote part of the EAP, stratospheric air masses sink in consequence of the Polar

high and get accelerated along the surface slope in the form of katabatic winds. Therefore, also the mean wind speed is lower in the interior part of Antarctica than at the coast. The annual mean wind speed derived from a three year average (1995-1997) at Dome F was reported to be 5.8 ms^{-1} (Watanabe et al., 2003), wind speed maps (Lenaerts & van den Broeke, 2012, Sanz Rodrigo et al., 2012, van Lipzig et al., 2004) show a similar value, but AWS data from years 2015 and 2016 indicate a lower mean wind speed.

The topography of the EAP is generally flat. The surface slope within 30 km around Dome F is $1/5000$ (0.01°) (Ageta et al., 1998). Characteristic for the EAP is the low annual accumulation rate, in a global context one of the driest areas on this planet. At Kohnen Station, the accumulation rate used to be $64 \text{ kg m}^{-2} \text{ a}^{-1}$ (Oerter et al., 1999), with increasing tendency to about $80 \text{ kg m}^{-2} \text{ a}^{-1}$ over the last decades. While Dome F reaches an annual accumulation rate of $32 \text{ kg m}^{-2} \text{ a}^{-1}$ (Ageta et al., 1998), the accumulation rate in the central part of the plateau is estimated to be in the same order of magnitude or even lower. Arthern et al. (2006) derived an accumulation rate map from satellite observations, which gives a range of values from 30 to $40 \text{ kg m}^{-2} \text{ a}^{-1}$. Nevertheless, this range is considered as too high, as, e.g., Anschütz et al. (2011) suggest an overestimation of the accumulation rate on the higher interior part of the EAP.

The temperature inversion and gravity-driven katabatic winds interacting with ice surface topography on the EAP result in a significant spatial variability in snow accumulation (Frezzotti et al., 2005, King et al., 2004, Parish & Bromwich, 1987, Scambos et al., 2012), but is also relevant in several other contexts – e.g., physical and chemical proxies or surface topography and structures (Fig. 4).

1.5.2 THE COFI TRAVERSE

In Antarctica, glacial periods are characterized by much colder temperatures, reduced precipitation and therefore more arid conditions as well as stronger large-scale atmospheric circulation (e.g., Petit et al., 1999) than at present. As these different environmental conditions can cause changes in some physical processes affecting the ice sheet, ice core data covering glacials have to be interpreted adequately. Firnification during glacial periods is modeled, for example, to calculate the age difference between gas and ice (s. section 1.2) and to infer the phase relationship between temperature derived from the isotopes and the CO_2 concentration measured in ice cores. However, these firnification models simulate a deeper firn-ice transition than nitrogen isotope data predict (Sowers et al., 1992). The CoFi project – acronym for Coldest Firn – at the Alfred Wegener Institute (AWI) has the scientific goal of understanding the metamorphosis of snow to ice (s. section 1.2) in the coldest region of Antarctica. As there is no access to glacial firn, the EAP with cold and dry environmental conditions is the best analogue for glacial firn that we currently have in Antarctica (and on Earth).

Five firn cores were drilled in different positions on the EAP that all cover the firn-ice transition. The first part of the CoFi project took part in field season 2012/13, in which the two cores B51 and B53 have been drilled. The second part was organized as a traverse in a joint venture with the BE-OI reconnaissance (OIR) campaign in 2016/17. For the fuel supply of the radar measurements with the AWI Basler BT-67 aircraft, the traverse carried 80,000 liters of fuel (Fig. 5, bottom right) and set up the temporary OIR camp that functioned as an airbase (Karlsson et al., 2018). The three firn cores B54, B55 and B56 have been drilled during this traverse from Neumayer-Station III via Kohnen Station to OIR camp. In the following, we just refer to the part between Kohnen Station and OIR camp, as the samples relevant for this study were taken there. I took part in the traverse (starting

and ending at Kohnen Station), took snow samples along the traverse, which are the main data basis of this thesis, and assisted in the firn-core drilling.



Fig. 5: Top: The traverse car park. Five PistenBully® track vehicles and a Ski-doo® motor sledge parked closely next to each other in a lunch break. Every 50 km the vehicles had to be refueled. Bottom left: Living container for maximum six persons. Inside there is a small entrance area, in the back is a table with three bunk beds. Bottom right: bladder tanks on sledges with 80,000 liters of fuel.

After preparation at Kohnen Station and waiting for the Neumayer III – Kohnen traverse to arrive, the traverse (Fig. 5, top) departed on 14th December 2016 towards B51 drill site (location 5 in Fig. 6 and Tab. 1). After some technical problems in the beginning, the traverse covered on average 100 km per day (average speed of 11-12 km h⁻¹). Just after the B51 drill site, the traverse split into two groups. Group A arrived at OIR camp on 25th December 2016. Group B headed to the B53 drill site and then to OIR camp, arriving there on 27th December. During the radar campaign, core B54 at OIR camp was drilled (29th December 2016 – 4th January 2017). After completion, a smaller group of five (including myself) headed to former Plateau Station to drill core B55 (7th – 14th January 2017) and then 116 km west to drill core B56 (15th – 21th January 2017). Returning to OIR camp, the

whole group went back to Kohnen Station and arrived on 29th January 2017. A detailed overview of the traverse, including all sample and drill sites, names and coordinates can be found in chapter 2.1 (Fig. 6) and in the appendix (Tab. 2).

1.6 MOTIVATION AND SCOPE OF THIS STUDY

This section summarizes the motivation and scientific questions (highlighted in italics and grey shading) of this thesis. These are divided into three thematic blocks, which have been addressed in three publications (chapters 3, 4 & 5) as well as an additional results chapter (chapter 6).

In general, gaining data from the remote ice sheets of Greenland and Antarctica is a key aspect in glaciology. The vast majority of both ice sheets has never been seen or touched by humankind and no sample of snow or ice is reproducible. This makes each sample very precious, considering a lot of logistic efforts hidden behind each single piece of snow, ice or a data point from various measurements. Collecting samples along the CoFi traverse was therefore an important task as especially in the region between Kohnen Station and Dome F barely any samples are available.

Considering the value of the samples, the concept of the study included a multiparameter approach. This means, for each single sample, information about the snow stratigraphy and density as well as the physico-chemical components (i.e., stable water isotopes and major ions) were derived. This allowed contributing to two important aspects of current research in glaciology. On the one hand, the look into the recent past: improving the interpretation of paleoclimatic proxies in snow and ice by investigating the processes related to the signal formation at the snow surface. On the other hand, the assessment of the status quo of the ice sheet: improving the SMB of East Antarctica for climate projections.

1.6.1 SPATIAL & TEMPORAL VARIABILITY OF CLIMATE SIGNALS IN SNOW

As much information as a single sample of snow or ice provides, each sample is just a point information. A high spatial variability of different parameters has been mentioned even on small scales for several sites in Antarctica (Caiazza et al., 2016, Ekaykin et al., 2002, Karlöf et al., 2005, Karlöf et al., 2006, Urbini et al., 2008). In a trench study at Kohnen Station, Laepple et al. (2016) have shown that the correlation of vertical profiles of climate proxies in snow has reached a minimum after 10 m spacing. Snow profiles at this distance are further referred to as spatially independent samples. For a representative (climate) signal on inter-annual timescales, several spatially independent samples are necessary.

There is a crucial need for representative ground-truth values for large-scale assessments of parameters and to investigate the relation of these parameters to environmental properties – this holds especially for the EAP, where sample availability is sparse. While an accurate surface snow density leads to lower uncertainty in SMB of the ice sheets, constraining the spatial distribution of snowpack features, stable water isotopes, and major ions improves the understanding of snowpack formation and their interpretation as a paleoclimatic proxy (see section 1.6.2 and 1.6.3).

How large is the spatial and temporal variability of climate proxies in snow along the CoFi traverse and how representative are these proxies on different spatial scales?

To accomplish this, a sampling setup with four snow profiles per location was applied – covering the local scale at each location (tens of m) and the regional scale along the traverse (hundreds of km).

For an improved sampling routine in the cold laboratories, a new snow cutting device was introduced in the framework of this thesis (publication II).

A recurring problem when collecting field data is the decoupling of spatial (horizontal) and temporal (vertical) variability. Unfortunately, also in this study this problem arose several times. Still, the quantification of the variability for several parameters – in both, spatial and temporal respect – is key for the interpretation of climate records from ice cores.

In publication I, the research question has been addressed for surface snow density and in publication III for stable water isotopes. A dataset with stable water isotopes and major ions was published in the open access repository PANGAEA (appendix: chapter 10.2.3). In the context of publication II, I created the first dataset about the spatial distribution of crusts in snow covering regions in Greenland and Antarctica.

1.6.2 FORMATION OF CLIMATE SIGNALS IN SNOW AND FIRN ON THE EAST ANTARCTIC ICE SHEET

Many meaningful ice cores have been drilled in East Antarctica to reconstruct the climate of the past (e.g., the five ice cores with a temporal record of over 100,000 years: Dome F. Deep Coring Group, 1998, EPICA Community Members, 2004, EPICA Community Members, 2006, Indermühle et al., 1999, Petit et al., 1999). However, especially on short time scales in low accumulation (and low temperature) regions, particularly the EAP, the processes of signal formation of climate proxies are not fully constrained (Fig. 2).

This also applies to stratigraphic elements of the snowpack, which have been used to characterize different environmental regions in East Antarctica (Furukawa et al., 1996, Furukawa et al., 1992). The snowpack layering generally affects the firn metamorphism (Adolph & Albert, 2014, Gregory et al., 2014, Mitchell et al., 2015, Schaller et al., 2017) and can have an impact on the backscatter properties of remote sensing techniques (Dierking et al., 2012, Flach et al., 2005, Winebrenner et al., 2001). Furthermore, high-density crusts in the snowpack have locally been used as a seasonal marker (Hoshina et al., 2016), despite their unclear formation history. Still, stratigraphic snowpack features – which have mostly been observed and well understood (e.g., Colbeck, 1991) – bear the potential to reconstruct the local snowpack history. Using the multiparameter approach for a combined evaluation of stratigraphic snowpack features and chemical parameters, I want to investigate the local snowpack history along the CoFi traverse.

*How are stratigraphic elements correlated to (climate) proxies in snow of low accumulation rate areas?
Can stratigraphic elements function as a support to reconstruct the local snowpack history?*

This question was addressed in publication II and chapter 6.1. The potential of crusts as a proxy for the accumulation rate or former snow surfaces is also discussed in publication II.

Measuring stable water isotopes in ice cores to infer the paleotemperature has become a standard routine in glaciology (Masson-Delmotte et al., 2008). For this intent, a quantitative conversion of $\delta^{18}\text{O}$ and $\delta^2\text{H}$ into temperature is necessary. However, several effects hamper the interpretation of stable water isotopes as a climate proxy, especially on short time scales. The first stage affects the precipitation and its timing: Precipitation intermittency (Casado et al., 2020, Laepple et al., 2011) and clear-sky precipitation can bias the isotope signal, which records the natural climate variability. The second stage affects the time while the snow is exposed to the atmosphere at the very surface: Sublimation influences the relation between oxygen and hydrogen isotopes, which

creates a warm bias in their climatic interpretation (Pang et al., 2019). Additionally, erosion, mixing, and redistribution complicate determining the temporal sequence of the snowpack (Lenaerts & van den Broeke, 2012). At stage three (after deposition), the diffusion of isotopes within snow, firn, and ice smooths the amplitudes of the record (Johnsen et al., 2000). The processes of all three stages are described in more detail in publication III. Due to lack of year-round observations, a close network of AWS and continuous sampling, it is still not completely understood what controls the isotopic composition of snow over time. For a precise interpretation of stable water isotopes in snow on seasonal to decadal time scales, a quantitative description of the processes at the snow-atmosphere interface is necessary.

How many climate signals (of precipitation) are preserved in the snowpack and which surface processes hamper the formation of a seasonal signal on the East Antarctic Plateau?

For this intent in publication III, we compare a simulated snow profile derived from the atmospheric general circulation model ECHAM6 (Cauquoin & Werner, in review, 2021) with the samples collected along the CoFi traverse. Furthermore we elaborate, where the formation of seasonal signals of stable water isotopes in snow reaches its environmental limits. The presented data and analyses will contribute to an improved understanding and interpretation of stable water isotopes in snow, firn, and ice core records in the future.

1.6.3 CLIMATE CHANGE RECORDED IN SNOW ON THE EAST ANTARCTIC PLATEAU?

Altimetry measurements (McMillan et al., 2014, Schröder et al., 2019, Sorensen et al., 2018) are one of the state-of-the-art techniques to derive the mass balance of ice sheets. As mentioned in section 1.4, the SMB for Antarctica is relatively stable. Cryosat2 observations of East Antarctica, for instance, reported a total mass change of -3 Gt yr^{-1} – but with an uncertainty of $\pm 36 \text{ Gt yr}^{-1}$ (McMillan et al., 2014). One of the sources of uncertainty is the low data availability of ground-truth snow and firn density data. More field observations are urgently needed (IPCC, 2019). A monitoring of accumulation in the coast-to-plateau region is crucial to better evaluate and improve the models used to predict Antarctic SMB changes and related contribution to sea level (Genthon et al., 2017). This also includes snow and firn density, which is parameterized on the large scale due to lack of data. However, this parameterized density is assumed too low considered to field measurements on the EAP.

How large is the offset between parameterized and observed surface snow density and what effect can this offset have on the mass budget of the East Antarctic ice sheet?

In publication I we show the importance of ground-truth field data for the accuracy of model predictions, what impacts offsets can have and promote our dataset as basis for snow density parameterizations.

As mentioned in section 1.3, the rise of the annual mean temperature and the accumulation rate at e.g., Kohnen Station (Medley et al., 2018) is one indicator for an arrival of climate change on the EAP. Whether the increasing temperature has also been recorded by different climate proxies in snow between Kohnen Station and former Plateau Station has not been tested yet.

Are the consequences of a warming climate recorded by climate proxies already visible in snow on the East Antarctic Plateau?

In publication I, we answered this question for the snow surface density along the East Antarctic Plateau. In chapter 6 of this thesis, I show an approach to answer this question with stable water isotopes at selected sites along the CoFi traverse.

2 MATERIAL & METHODS

In this chapter, I summarized the samples and analyzing methods that were used in this study. The working steps are shown chronologically from sampling in the field (section 2.2) via non-destructive analysis (section 2.3) and to discrete sampling (section 2.4) and chemical analysis (sections 2.5 and 2.6). Additional samples are presented in section 2.7.

2.1 SAMPLE OVERVIEW

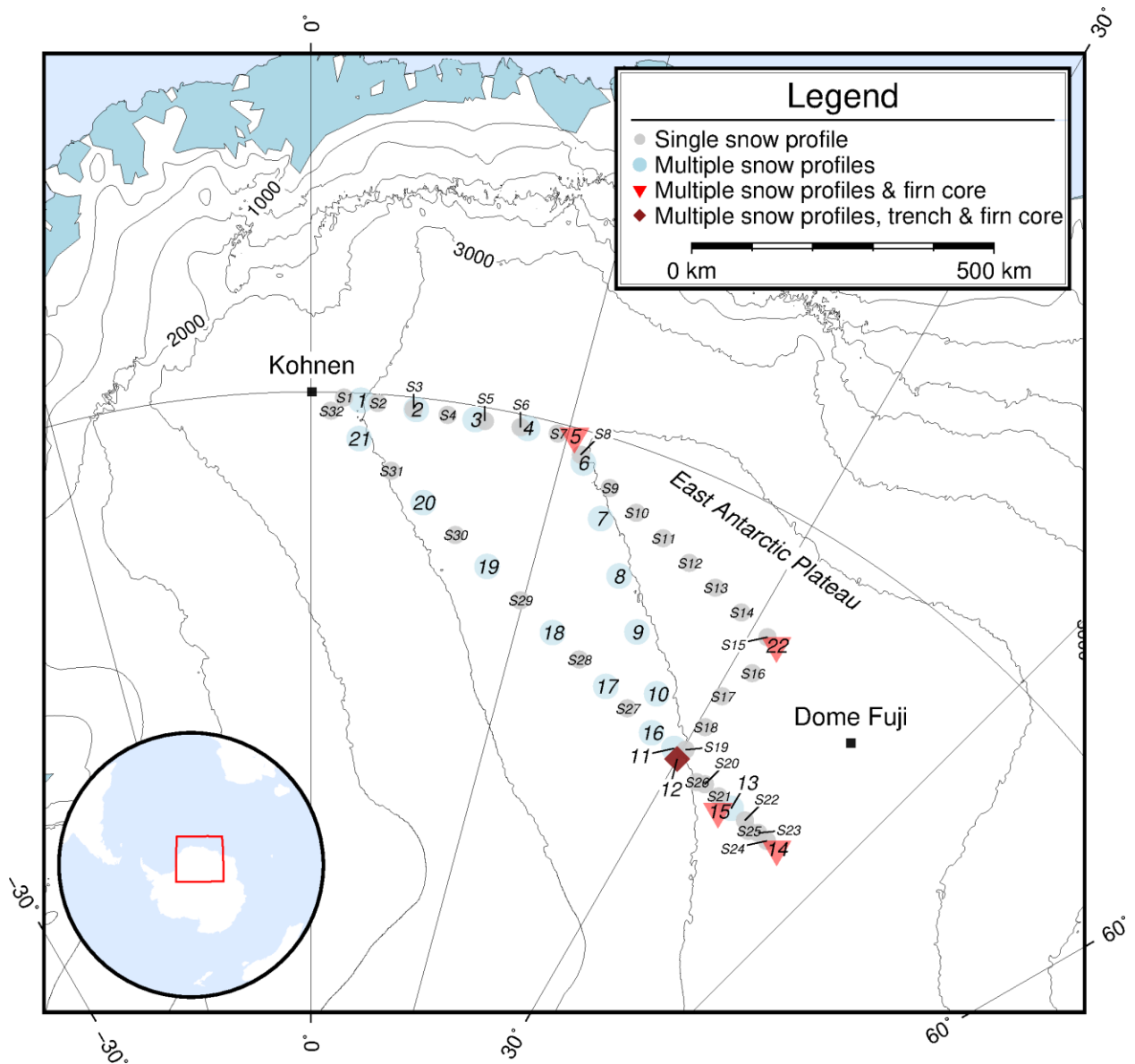


Fig. 6: All sampling locations along the CoFi traverse. Find the main snow profiles for the thesis in light blue (1-22) and further single snow profiles in gray (S1-32). Firn core locations are shown in pale red, OIR camp in dark red.

Tab. 1: Overview of firn cores according to the nomenclature in Fig. 6.

Sampling site	Firn core	Season
5	B51	2012/13
22	B53	2012/13
12	B54	2016/17
14	B55	2016/17
15	B56	2016/17

2.2 SNOW PROFILE SAMPLING

Snow liners are a relatively new and straightforward tool to sample the snow surface for a variety of analyzing methods. Two notable advantages of this method are a preserved original snow stratigraphy as well as time efficiency. It has been used at AWI for several years and was first described by Schaller et al. (2016). Snow liners are tubes made of carbon fiber with 1 m in length, 10 cm in diameter, and 1 mm wall thickness. They are light and easy to transport, robust and transmissive for X-rays, an important characteristic for the upcoming radiographic analysis (section 2.3). In the following, the term liner will refer to the carbon fiber tube itself or the sampling method, the term snow profile is used for the snow retrieved with the liner or the derived data.

The sampling procedure is described in detail in publication I. An impression of the fieldwork can be seen in Fig. 7. A map overview of all samples can be found in section 2.1.



Fig. 7: Digging a snow pit at location 16. In front of the snow pit the liner is already inside the snow, its top is covered with a wooden plate. To dig a snow pit efficiently, it is advisable to saw blocks with a hand saw and lift the blocks with a shovel out of the pit (credit: Sepp Kipfstuhl).

2.2.1 MULTIPLE SNOW PROFILES

Along the traverse route, a sampling scheme was applied retrieving four spatially independent snow profiles according to findings by Laepple et al. (2016). Spatial independence describes in this context a distance, at which a comparison of two samples (e.g., snow profiles) shows significantly different information due to stratigraphic noise (Fisher et al., 1985), which is caused by, e.g., snow patches or dunes.

The relative sampling positions are shown in Fig. 8. The center profile had a length of 2 m. The other three profiles were taken in a 10 m radius, forming an equilateral triangle. The sampling was done at overnight stops of the traverse. Within publications of this thesis, the snow profiles are named according to their location along the traverse (1-22) and their relative orientation (A, B, C, X). Due to lack of time or technical constraints, at location 11 (A, X), 13 (A, B), and 19 (A, B, X) only two or three profiles, respectively, were sampled. At locations 14 and 15, the central profile was extended to 4 m. This way, firn cores B55 and B56 were supported in the top meters

with the liner method as the snow is very soft and unconsolidated, and therefore the core quality is often not sufficient. The sampling of one location took around 2 h and 15 minutes.

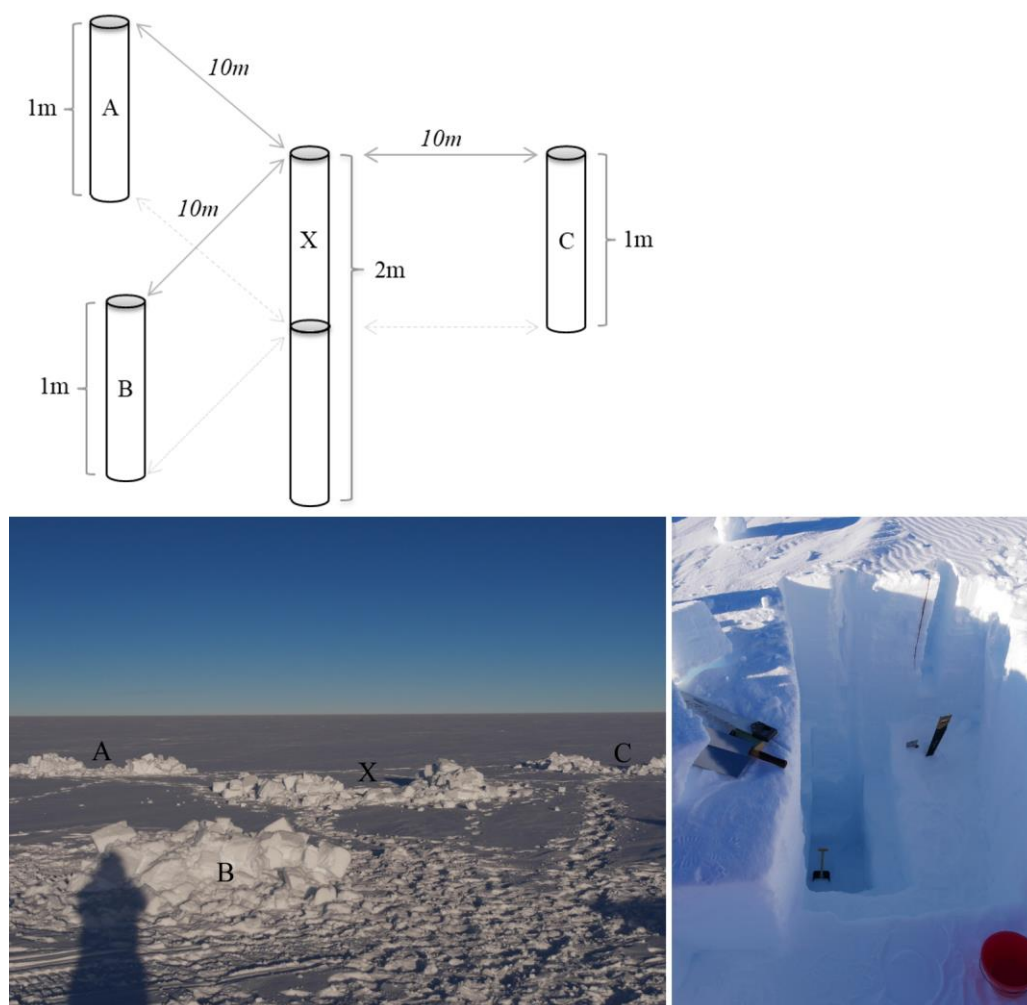


Fig. 8: Top: Scheme of the sampling strategy. The distance to the central profile (X) was always 10 m. Bottom left: location 3 after the sample retrieval. For the snow pits, blocks were sawn as good as possible and lifted out of the pit. The sawn snow blocks can partly still be recognized. Bottom right: snow pit to retrieve a 4 m deep snow profile. The logistical challenge is to find the balance between sufficient space (to work and get out of the pit) and time efficiency.

2.3 COMPUTER TOMOGRAPHY

The non-destructive, core-scale microfocus X-ray computer tomograph (μ CT) in a cold cell (-15°C) is a worldwide unique device specifically constructed for snow, firn and ice cores (Fig. 9). Technically introduced by Freitag et al. (2013) the μ CT offers the opportunity to X-ray meter segments with usually 7.7 cm (3 inches) and 10.2 cm (4 inches) in diameter. The procedure is described in more detail in publication I.

In a 2D scan the measured attenuation by the sample is displayed as a gray value image, which directly visualizes the stratigraphy (the approach to count high-density crusts from the gray value images is presented in publication II). The central part of the measured segment and bubble-free ice of known density and geometry are used to translate this information into a density profile. In a 3D mode, the sample rotates around its central axis during the scan. The records from all angles are composed to a 3D dataset, in which space structure in firn and ice (in

particular surfaces or the porous matrix and gas bubbles) can be imaged. The 3D- μ CT analysis is not subject in this thesis, but will be mentioned in the outlook.

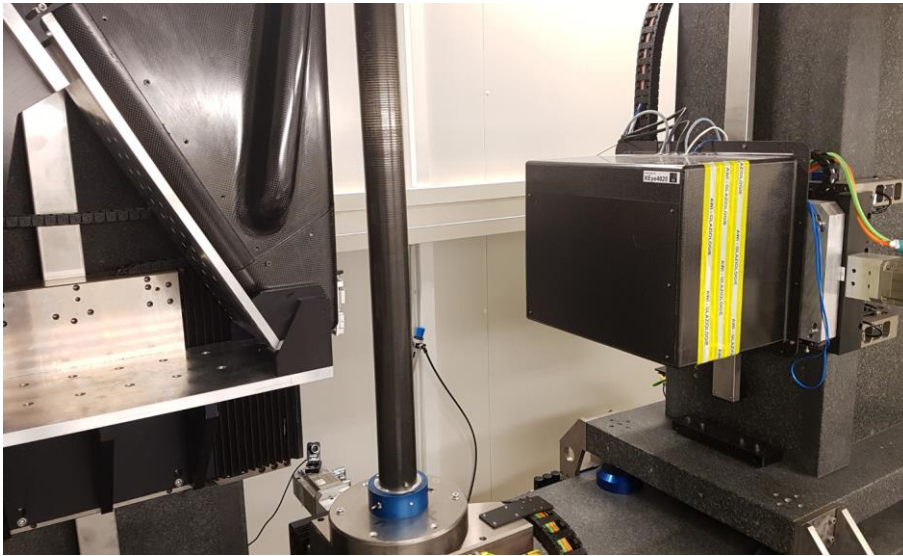


Fig. 9: μ CT at AWI. The left box is the radiation source. In the middle stands an ice core inside a carbon fiber tube. The blue pedestal holds the ice core in position. The calibration unit is at the bottom of the carbon fiber tube directly above the pedestal. The rectangular box on the right is the detector.

2.4 DISCRETE SAMPLING

After the μ CT imaging, the snow profiles were prepared in the AWI ice laboratory at -18°C for further analysis. They were cut into discrete samples using a device specially made for this purpose by the AWI workshop. It consists of a trough with a cutting mounting at the end. A detailed protocol for the cutting procedure including a picture of the device is presented in publication II.

The original plan was to cut every profile in 1 cm resolution. After the first completed profiles, considering the considerable amount of work and time, material and capacity for ion chromatography (IC), and cavity ring-down spectroscopy (CRDS), the plan was adjusted. Profiles A, B, and C were cut in 2 cm resolution, profiles X in 1 cm resolution. Including preparation (i.e., labeling sample bags), cutting one snow profile in higher (1 cm) resolution takes 5 h, in lower (2 cm) resolution about 2.5 h. At this point (31.12.2019), 84 of the aspired 108 profiles were cut.

2.5 ION CHROMATOGRAPHY

The principle of chromatography uses the affinity of molecules to specific phases. The carrier medium (eluent) is pumped into the sample loop, where a defined volume of the snow sample (analyte) is injected. In the separator column, the impurities are separated by their different mobility in the stationary phase. The respective species are identified by their specific retention time. The suppressor decreases the background conductivity of the eluent and enhances detection of single species, which is important for molecules or elements with low concentrations. The integral of the measured conductivity signal in the chromatogram gets transferred into a concentration by referencing it with a known standard.

IC is an established system for the measurement of ions from discrete snow and ice samples (Fischer et al., 2007, Göktaş et al., 2002, Ruth et al., 2008, Wolff et al., 2006), also recently in combination with physical properties

(Eichler et al., 2019). A different approach in glaciology are continuous measurements where firn or ice cores do not have to be cut into discrete samples (e.g., Bigler et al., 2011, Kaufmann et al., 2008). But in combination with the liner method or snow samples in general (Hoshina et al., 2014, Laepple et al., 2016), IC has been the preferred method so far. On the one hand, the resolution can be lower in continuous measurements (dependent on the system) as the signals can smear during the continuous melting process (resulting in smoothed data). On the other hand, due to the low cohesiveness and high porosity of surface snow the discrete sampling in a trough is also easier to carry out. Nevertheless, plans to use continuous measurement techniques for this method exist (similar to Dallmayr et al., 2021).

Anorganic impurities were measured with a Dionex ICS-2100 system. The anion analytics were conducted with potassium hydroxide as eluent, using a Dionex AS 18 (2 mm) separation column and an AERS 500 suppressor. Analyzed anions were chloride (Cl^-), nitrate (NO_3^-), sulfate (SO_4^{2-}) and methanesulfonate (MSA). For the cation analytics MSA was used as eluent and a Dionex CS12a (2 mm) as separation column for analyzing sodium (Na^+), ammonium (NH_4^+), magnesium (Mg^{2+}) and calcium (Ca^{2+}). The suppressor in the cation IC unit was a Dionex ERS 500. Fluoride (F^-), bromide (Br^-) and potassium (K^+) were measured as well, but will not be considered in this thesis. The normative precision for anions is <10%, for cations <20%.

2.6 CAVITY RING-DOWN SPECTROSCOPY

CRDS (Berden et al., 2010, Zalicki & Zare, 1995) uses the unique infrared spectrum of molecules at a characteristic wavelength based upon different energy levels in the atomic orbitals. The CRDS analyzer consists of a laser diode, a cavity piston and a detector unit. Inside the isolated cavity, there are three mirrors installed facing each other (although not used for oxygen and hydrogen isotopes like in this study: find a sketch of the setup in figure 1 in Kratochwil et al. (2018) or figure 1 in Balslev-Clausen et al. (2013)). As the laser enters the cavity, the mirrors create a continuous travelling light wave. After a threshold intensity level is reached, the laser beam is turned off. The light in the cavity still circulates being reflected by the mirrors with exponential intensity decay. This intensity decrease is called 'ring-down'. The same procedure is repeated with the samples in gaseous phase. The measured decrease in intensity and time (ring-down) of the laser beam is characteristic for the gas in the cavity and its specific energy absorption (i.e., the isotopic composition).

Despite mass spectrometry (Maselli et al., 2013), CRDS has established as a state-of-the-art technique for stable water isotope analysis in glaciology (Gupta et al., 2009) and has been used in numerous studies (e.g., Bagheri Dastgerdi et al., in review, 2020, Casado et al., 2016, Jones et al., 2017, Münch et al., 2016, Servettaz et al., 2020, Steen-Larsen et al., 2014, Touzeau et al., 2016).

Samples in this study have been measured with a Picarro L2130-i isotope analyzer using the protocol by van Geldern and Barth (2012) and are presented in publication III and also discussed in chapter 6.

2.6.1 DELTA NOTATION FOR STABLE WATER ISOTOPES

The delta value is a common notation for stable isotopes expressing a relative enrichment or depletion (Craig, 1961). It is always given in reference to a defined standard in order to make measured samples intercomparable. On a global scale, the reference value is the standard mean ocean water. For regional studies with extreme isotopic values (like this one), specific standards are used. Further details are presented in publication III.

$$\delta = \frac{\alpha_{sample} - \alpha_{std}}{\alpha_{std}} \times 1000 \text{ [‰]}$$

δ :	Delta value [‰]
α_{sample} :	Isotopic value of the sample ($^Y A_{sample} / ^X A_{sample}$)
α_{std} :	Isotopic value of the standard ($^Y A_{std} / ^X A_{std}$)
A:	Chemical element (here: H or O)
X & Y :	Sum of protons and neutrons of the respective isotope (of element A)

Relevant δ values in this thesis are $\delta^{18}\text{O}$ and $\delta^2\text{H}$ (further δD).

The second order parameter deuterium excess (d) is defined as

$$d = \delta\text{D} - 8 \times \delta^{18}\text{O}$$

2.7 ADDITIONAL MATERIAL

Unfortunately, during the expedition I could not retrieve shallow firn cores as originally planned in this project. With this procedure, I would have been able to determine the exact accumulation rate and to perform precise temporal comparisons at each sampling site reaching the last volcanic eruption with a firn core. However, the required hand auger was not available at the start of the traverse.

Despite the snow profiles mentioned in section 2.2.1, I used several other samples within this thesis.

2.7.1 SINGLE SNOW PROFILES ALONG THE COFI TRAVERSE

Additionally to the snow profiles mentioned in section 2.2.1, single snow profiles have been sampled along the traverse route roughly every 30 km. On the way back from OIR camp to Kohnen Station the sampling distance increased due to limited liner availability. These 1 m profiles are marked in the overview map (Fig. 6) with S# (# standing for 1 to 32 in chronological order). These profiles were used for μCT analysis in publication I & II and a combined analysis of stratigraphy and major ions in chapter 6.1.

2.7.2 THE OIR TRENCH

For an additional high resolution study on a local scale, at the OIR camp a trench (50 m long, 2.3 m deep) was excavated with a PistenBully®. 30 snow profiles with 3 m length were sampled directly at the trench wall. The profile positions were chosen feature-dependent and not with an equidistant spacing. A description and a picture of the OIR trench are in publication I, a sampling protocol of the OIR trench is in the appendix (Tab. 3).

2.7.3 SNOW PROFILES FROM DIFFERENT PROJECTS

In local projects in Antarctica and Greenland, further snow profiles were sampled using the liner method as described above (sect. 2.2) and used in this thesis:

- Samples taken at Kohnen Station in season 2015/16 (CLP). See Schaller (2017) (page 60) for the sampling scheme.
- Samples from a trench at Kohnen Station in season 2018/19 (T4M).

- Samples at the Renland ice cap drilling site (RECAP) in Greenland taken in May 2015.
- Samples in a trench at the East Greenland ice core project drill site (EGRIP) taken in May 2016.

Samples from Kohlen Station (CLP), EGRIP and RECAP were used in publication II, CLP samples also in publications I & III. T4M samples were used in chapter 6.2.

2.7.4 FIRN CORES

The main focus of this thesis is the snowpack of the recent past. However, to compare the results from the snow profiles to a longer temporal record or simply to another available sample, we used two firn cores within this study. From μ CT gray value of firn cores B40 close to Kohlen Station (Medley et al., 2018) and B54 (Tab. 1), we derived a crust record presented in publication II. Furthermore, stable water isotopes measured in firn core B54 were used for a comparison to the snow profiles in chapter 6.2.

3 PUBLICATION I

REPRESENTATIVE SURFACE SNOW DENSITY ON THE EAST ANTARCTIC PLATEAU

Weinhardt, A. H., Freitag, J., Hörhold, M., Kipfstuhl, S., and Eisen, O.

The Cryosphere, published on 05 November 2020

Doi: 10.5194/tc-14-3663-2020



Representative surface snow density on the East Antarctic Plateau

Alexander H. Weinhart¹, Johannes Freitag¹, Maria Hörhold¹, Sepp Kipfstuhl^{1,2}, and Olaf Eisen^{1,3}

¹Alfred-Wegener-Institut Helmholtz-Zentrum für Polar- und Meeresforschung, Bremerhaven, Germany

²Physics of Ice, Climate and Earth, Niels Bohr Institute, University of Copenhagen, Copenhagen, Denmark

³Fachbereich Geowissenschaften, Universität Bremen, Bremen, Germany

Correspondence: Alexander H. Weinhart (alexander.weinhart@awi.de)

Received: 10 January 2020 – Discussion started: 2 March 2020

Revised: 4 September 2020 – Accepted: 21 September 2020 – Published: 5 November 2020

Abstract. Surface mass balances of polar ice sheets are essential to estimate the contribution of ice sheets to sea level rise. Uncertain snow and firn densities lead to significant uncertainties in surface mass balances, especially in the interior regions of the ice sheets, such as the East Antarctic Plateau (EAP). Robust field measurements of surface snow density are sparse and challenging due to local noise. Here, we present a snow density dataset from an overland traverse in austral summer 2016/17 on the Dronning Maud Land plateau. The sampling strategy using 1 m carbon fiber tubes covered various spatial scales, as well as a high-resolution study in a trench at 79° S, 30° E. The 1 m snow density has been derived volumetrically, and vertical snow profiles have been measured using a core-scale microfocus X-ray computer tomograph. With an error of less than 2 %, our method provides higher precision than other sampling devices of smaller volume. With four spatially independent snow profiles per location, we reduce the local noise and derive a representative 1 m snow density with an error of the mean of less than 1.5 %. Assessing sampling methods used in previous studies, we find the highest horizontal variability in density in the upper 0.3 m and therefore recommend the 1 m snow density as a robust measure of surface snow density in future studies. The average 1 m snow density across the EAP is 355 kg m⁻³, which we identify as representative surface snow density between Kohnen Station and Dome Fuji. We cannot detect a temporal trend caused by the temperature increase over the last 2 decades. A difference of more than 10 % to the density of 320 kg m⁻³ suggested by a semiempirical firn model for the same region indicates the necessity for further calibration of surface snow density parameterizations. Our data provide a solid baseline for tuning the surface

snow density parameterizations for regions with low accumulation and low temperatures like the EAP.

1 Introduction

Various future scenarios of a warming climate as well as current observations in ice sheet mass balance indicate a change in surface mass balance (SMB) of the Greenland and Antarctic ice sheets (IPCC, 2019). Accurate quantification of the SMB is therefore one of the most important tasks to estimate the contribution of the polar ice sheets to the global sea level rise (Lenaerts et al., 2019). Satellite altimetry is a state-of-the-art technique to measure height changes of the major ice sheets on large spatial scales (McMillan et al., 2014; Schröder et al., 2019; Sorensen et al., 2018). These changes are converted to a respective mass gain or loss, which is directly linked to a eustatic change in sea level (Rignot et al., 2019; Shepherd et al., 2018). But this volume change converted to a mass change is subject to large uncertainties (Shepherd et al., 2012). In altimetry, at the margins of the ice sheets the local surface topography is a limiting factor in accuracy, while in the comparably flat and high-elevation interior part of the ice sheet's snow properties like density have a much larger influence on the accuracy (Thomas et al., 2008). Therefore, an accurate snow and firn density on top of the ice sheets, which constantly undergoes the natural process of densification, is crucial. Given the large extent of the ice sheets, the spatial coverage of ground truth snow and firn density data is still sparse. To overcome this shortcoming, surface snow density (usually 1 m) is often parameterized as a function of climatic conditions, such as temperature, wind speed and accumulation rate (Agosta et al., 2019;

Kaspers et al., 2004). Then, this parameterized approach is implemented in firn models, leading to a fresh snow density (e.g., Ligtenberg et al., 2011). But both the parameterized and modeled approach seem to underestimate the snow density when compared to independent ground truth data from Antarctica (Sugiyama et al., 2012; Tian et al., 2018). Inaccurate snow density, especially in the uppermost meter, leads to significant surface mass balance uncertainties (Alexander et al., 2019). Accordingly, ground truth density data are urgently needed to optimize densification models, which are crucial to convert height changes to mass changes in altimetry and therefore reduce the uncertainties in ice sheet mass balance estimates.

One source of uncertainty in the assessment of ground truth density data is the representativeness of the derived density values mainly due to the sampling strategy and sampling tools, as the snow surface on the ice sheet is spatially inhomogeneous at all scales. Apart from climate-induced (e.g., seasonal or event-based) density fluctuations, surface snow density is also influenced by topographic changes of the ice sheet surface and underlying bedrock on small (tens of meters) and large spatial scales (up to hundreds of kilometers) (Frezzotti et al., 2002; Furukawa et al., 1996; Rotschky et al., 2004). On the local scale, surface roughness and the surface slope in combination with dominant wind regimes and varying accumulation rates (Fujita et al., 2011) cause the main variations in density.

Arthern et al. (2006) derived snow accumulation in Antarctica from available field measurements of accumulation and density. To obtain this density, sampling is usually conducted in snow pits with discrete sampling over depth. Between Kohonen Station and Dome Fuji, snow density has been sampled in discrete depth intervals by Sugiyama et al. (2012), who report a high spatial variability on a kilometer scale. A small part of the variability can be attributed to the sampling method. Conger and McClung (2009) compared different snow cutting devices with various volumes between 99 and 490 cm³. The combination of undersampling (usually negligible), variation in the device itself (0.8%–6.2%) and the weight error of the scale can add up to a significant error (dependent on the type up to 6%). Box- or tube-type cutters with larger sampling volumes are suggested for more precise measurements, with the disadvantage of coarser sampling intervals. Other commonly used devices to derive snow density in discrete intervals use dielectric properties of snow (Sihvola and Tiuri, 1986) or penetration force into the snow (Proksch et al., 2015).

In this paper, we present surface snow density data from a traverse covering over 2000 km on the East Antarctic Plateau (EAP). We show snow density data using the recently introduced liner sampling method (Schaller et al., 2016). The focus of this study is on the uppermost meter, echoing the study of Alexander et al. (2019), who emphasized the importance of an accurate 1 m density of polar snowpack. To reduce the stratigraphic noise, we show a strategy with multiple sam-

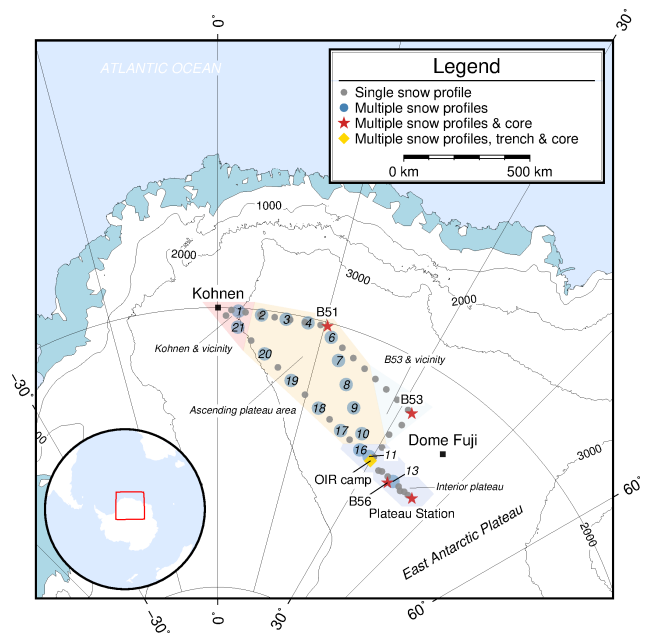


Figure 1. Overview map of the traverse route and sampling locations; inset shows location in Antarctica. Contour lines are given in 1000 m a.s.l. intervals. The first sampling position with multiple liners after Kohonen Station is named location 1. Following the traverse route, B51 is also called location 5, OIR camp location 12, Plateau Station location 14, B56 location 15 and B53 location 22 (see Table 2). The 200 m firn cores were drilled at locations indicated with a red star. Subregions defined in Sect. 2.5 are colored differently (Kohonen and vicinity: purple; ascending plateau area: orange; B53 and vicinity: light blue; interior plateau: lavender).

ples per location. This allows a more representative local 1 m snow density. The spatial representativeness of density profiles in East Antarctica has been recently addressed at the local scale (Laepfle et al., 2016), but correlation studies for larger scales are currently not available. We discuss the representativeness of density on small and large spatial scales as well as on the temporal variability of density. Beyond improving density retrieval, our results can be of particular interest for calibration of surface snow density parameterizations in firn models for this part of the East Antarctic ice sheet.

2 Material and methods

2.1 Study area

We performed an overland traverse in austral summer 2016/17 – a joint venture between the Coldest Firn (CoFi) project and the Beyond EPICA – Oldest Ice Reconnaissance (OIR) pre-site survey (Karlsson et al., 2018; Van Liefferinge et al., 2018) (Fig. 1). The CoFi project aims at an improved understanding of firn densification with samples from the EAP. In its framework, five firn cores have been drilled, re-

Table 1. Definition of terms used in the following sections are listed below.

Term	Symbol	Description
Liner	–	1 m of snow sampled with a carbon fiber tube. This term is used in a methodological context or for the tube itself.
Snow profile	–	(Continuous) snow sample at a given position. It may consist of several consecutively (vertically on top of each other) sampled liners; the length can be 1–3 m.
Location	–	A given place with one or several snow profiles taken within a range of 50 m.
Liner density	ρ_L	Volumetrically derived 1 m density of one single liner. Note: for snow profiles over 1 m length, liner densities for every meter segment are calculated individually.
μ_{CT}^x mean density	$\rho_{\mu_{CT}}^x$	μ_{CT} -derived mean density for the sampling interval x .
Location mean density	ρ_{loc}	Average of liner densities at one location for the same depth interval (usually 0–1 m).
Horizontal standard deviation	σ_H^x	Standard deviation of either liner density or μ_{CT} density for depth interval x over horizontal distance in a given area. Note, for 1 m we use the liner density, for smaller intervals μ_{CT}^x means.
Vertical standard deviation	σ_V^x	Vertical standard deviation of either μ_{CT} density over depth interval x or liner density (only for snow profiles > 1 m) at a given position.
Standard error	σ_n	Definition in Sect. 2.4.

ferred to as B51 and B53 (both drilled in 2012/13) and B54, B55 and B56 (drilled on the traverse in 2016/17).

From Kohonen Station the traverse went to the former B51 drill site. Right after B51 the traverse split up and followed two different legs, to reunite at the OIR field camp at 79° S, 30° E. After accomplishing the OIR survey and drilling the firn core B54, the traverse continued to the former Plateau Station (abandoned in 1969) and then returned back to Kohonen Station.

We follow Stenni et al. (2017) using the term EAP for the region higher than 2000 m above sea level (a.s.l.).

The traverse covers a region with a 10 m firn temperature range of about -44.5°C at Kohonen Station (Oerter et al., 2000) to -58.4°C at Plateau Station (Kane, 1970; Picciotto et al., 1971), which belongs to the lowest firn temperatures ever recorded (cf. Dome A: -58.3°C ; Cunde et al., 2008).

At Kohonen Station the accumulation rate used to be $64\text{ kg m}^{-2}\text{ a}^{-1}$ in the period between 1200 and 2000 (Oerter et al., 2004, 1999) with an increasing tendency to over $80\text{ kg m}^{-2}\text{ a}^{-1}$ over the last decades (Medley et al., 2018). At Dome Fuji $27.3\text{ kg m}^{-2}\text{ a}^{-1}$ was measured (Hoshina et al., 2016). For the locations along the traverse, an accurate value is difficult to obtain. Large-scale accumulation estimated based on remote sensing techniques (Arthern et al., 2006) is assumed to be too high for the EAP (Anschütz et al., 2011). Karlof et al. (2005) determined an accumulation rate of $\sim 45\text{ kg m}^{-2}\text{ a}^{-1}$ close to location 5 (Fig. 1); Anschütz et al. (2009) published $\sim 20\text{ kg m}^{-2}\text{ a}^{-1}$ for sites between location 8 and B53 as well as OIR camp and Dome Fuji. A high interannual variability of accumulation rate is observed

in several places on the EAP (Hoshina et al., 2016, 2014; Oerter et al., 2000). A 1 m deep snow profile can therefore cover a time period of about 4 years at Kohonen Station and up to 20 years on the interior plateau.

While the northern part of the traverse (Kohonen Station – B51) is more strongly influenced by synoptic activities with periodic snowfall (Birnbaum et al., 2006), the interior plateau (OIR camp to Plateau Station) is characterized by diamond dust deposition from a clear-sky atmosphere (Schwerdtfeger, 1969), which was described by Furukawa et al. (1996) as the calm accumulation zone. Wind maps (Lenaerts and van den Broeke, 2012; Parish, 1988; Sanz Rodrigo et al., 2012; van Lipzig et al., 2004) show generally low mean wind speed (around 6 m s^{-1}) from Kohonen Station along the ice divide up the EAP, but lower values for the region around Plateau Station. Due to the prevailing Antarctic high-pressure system over the EAP and the gentle slopes, the katabatic winds reach only moderate wind speeds there. While occasionally snow storms with wind speeds exceeding 15 m s^{-1} can happen at Kohonen Station, this is not the case on the interior plateau.

2.2 Liner sampling

For clarity, we define the terms used in the following paragraphs in Table 1.

Along the traverse route, vertical snow profiles were extracted using the snow liner sampling technique, also described by Schaller et al. (2016). Each vertical profile was taken using a carbon fiber tube of 1 m length and 10 cm in diameter. The liner was pushed into the snow until the liner top

was level with the snow surface. Afterwards, a snow pit next to the liner was dug and the snow was cut at the liner bottom with a metal plate to take the filled liner out of the pit wall. Both ends were covered with a Whirl-Pack® plastic bag to reduce possible contamination by touching the liner ends and air ventilation. During the sampling process, the liner was handled carefully to avoid concussions that destroy the original snow stratigraphy (e.g., not to bounce against the liner with the shovel and placing it softly into the sample box). A 1 m snow profile can be retrieved within 15 min. The liners were stored in isolated polypropylene boxes and shipped to the Alfred Wegener Institute (AWI) in Bremerhaven in a continuous cold chain. In total 144 snow profiles in different setups and total lengths were taken (Sect. 2.2.1–2.2.3). All strategies described in the following sections have been applied independently of each other.

2.2.1 Single snow profiles

Single profiles were taken every 30 km. On the last segment of the traverse (OIR camp to Kohnen Station) the distance increased due to limited liner availability. In total, 31 single snow profiles are available (Fig. 1).

2.2.2 Multiple snow profiles

A total of 22 locations with multiple profiles were sampled during overnight stops of the traverse; therefore the distance between the locations varied (roughly around 100 km). Regularly four snow profiles were sampled, at one location three, at two locations only two profiles because of time constraints (see Table 2). The four profiles were arranged in an even-sided triangular setup with one profile in the center (labeled with “X”) and three profiles around it (labeled with “A”, “B” and “C”). The corner profiles A, B and C are on a radius of 10 m to the central profile X (Fig. 2). A total of 83 profiles were retrieved in this setup. The locations are named in ascending order (Fig. 1 and Table 2).

2.2.3 OIR trench

At the OIR camp (Fig. 1), a 50 m long and ca. 2.3 m deep trench was excavated by a PistenBully snow vehicle (Fig. 3). The trench orientation was perpendicular to the main wind direction (127° true north). Thirty 3 m snow profiles were sampled directly at the trench wall using the liner technique described above. At every sampling position in the trench three liners were taken below each other. The first liners were pushed into the snow around 0.2 m behind the trench wall, to ensure an original stratigraphy not disturbed by excavation of the trench. After removal of the snow, the liners were directly taken out of the wall and the next consecutive liner in depth was placed at the same position (see Fig. 3, where the first liner is already in place). The lateral spacing between neighboring liners varied between 0.4 and 2.4 m, depending on the

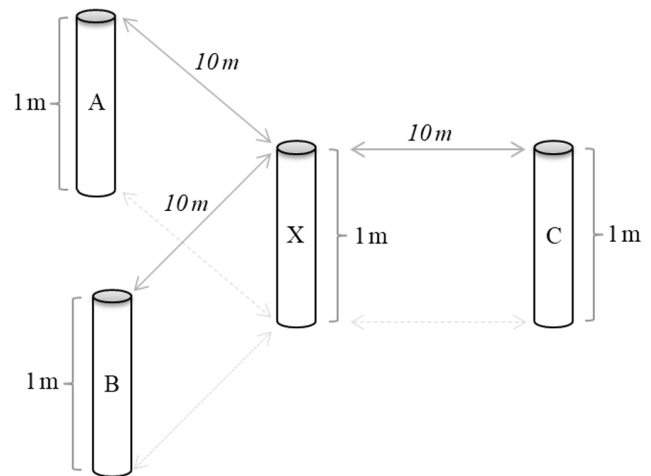


Figure 2. The sampling setup for locations with multiple snow profiles. The profiles A, B and C have a sampling distance of roughly 10 m to the central profile. Due to time constraints, locations 19 (three profiles), 11 and 13 (two profiles) have been sampled differently.



Figure 3. Sampling procedure in the OIR trench. The first carbon fiber tube (liner) is pushed into the snow after excavation of the trench. The positions were marked with a small bamboo pole. After retrieval of the first profile, the vertically consecutive second and third liners were taken. Two empty liners lean at the trench wall. The last liner had to be dug out partly as the trench was only 2 to 2.5 m deep.

surface structure. The profiles were taken within 2 d after excavation of the trench (31 December 2016–2 January 2017).

2.3 Density measurements

The snow liners have been non-destructively analyzed at AWI with the core-scale microfocuss X-ray computer tomograph in a cold cell (μ CT), specifically constructed for snow, firn and ice cores. For technical details see Freitag et

al. (2013) and Schaller et al. (2016). Before the measurement all liners were weighed. The weight of the carbon fiber tube was subtracted. The exact height of filled snow inside the liner was determined using the μ CT. Then, ρ_L was calculated volumetrically. All liners have been measured in a 2D mode using a setup of 140 kV and 470 μ A at -14°C . Breaks and lost snow in the snow profiles have been spotted during the scan and corrected (set to NaN) in the μ CT density profiles, which have a vertical resolution of ca. 0.13 mm (see Appendix).

For the calculation of the μ CT density only the central segment of the liner is used as scattering effects at the outer parts of the liner occur. The used segment corresponds to less than half of the snow volume in the liner. Missing snow at the edges of the profile does not influence the μ CT scan. Accuracy of the $\rho_{\mu\text{CT}}$ can be affected by the calibration, which is done with three cuboids of bubble-free ice with different lengths in every scan individually, or at the horizontal variability on the very small scale, as the central part of the profile can have a different density than the edges.

It is generally possible that the snow profiles are subject to compression during sampling or transport. Therefore the exact snow volume determined with the μ CT is rescaled to the original 1 m length (length of every single snow profile is determined individually) to avoid this potential error source. But lost snow in the liner (or at top or bottom), e.g., in non-cohesive layers (such as depth hoar layers), can lead to lower densities. Thus, ρ_L is also affected by errors. Conger and McClung (2009) reported that snow sampling devices with larger volumes usually result in higher precision in snow density. The volume of the snow liners (radius: 5 cm, length: 1 m) is 7855 cm³, 16 times the volume with the highest precision in their study. As the volume error among single liners is not known, we assume a 0.3 mm variation in both dimensions (length and radius), resulting in a volume error around 1.2 %. As still small parts inside the liner might not be completely filled with snow (e.g., lost snow during the transport), we estimate the undersampling error of the liner method to be less than 1.5 %. Additional error sources are the precision of the used scale (1 g or 0.03 % compared to the mean value along the traverse) as well as weight variations among the carbon tubes (< 0.1 %). The maximum relative error is estimated to be below 1.9 %.

Both $\rho_{\mu\text{CT}}^{1\text{m}}$ and ρ_L are in good agreement with each other (Fig. 4). The differences between the volumetrically calculated ρ_L and $\rho_{\mu\text{CT}}^{1\text{m}}$ are on average only 0.6 %. As the μ CT density is sensitive to calibration, we consider ρ_L to be more accurate for a 1 m interval. Some systematically higher values in the μ CT measurements can be caused by low-quality calibration in single measurements. Therefore, for the 1 m surface snow density we use ρ_L . For the comparison of intervals smaller than 1 m, we use the μ CT-derived density $\rho_{\mu\text{CT}}$ (Table 1).

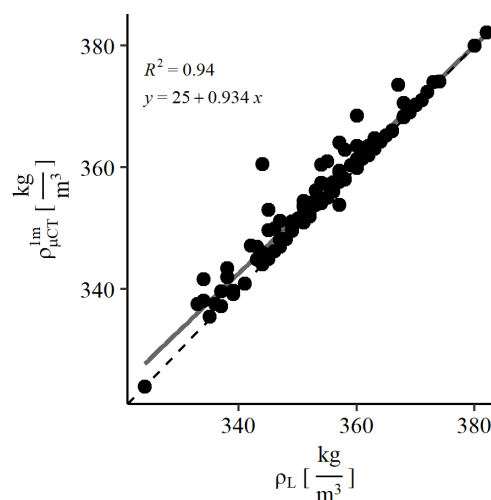


Figure 4. Comparison of liner density (ρ_L) with μ CT density ($\rho_{\mu\text{CT}}^{1\text{m}}$) calculated from the 114 liners along the traverse. Values of both measurements are in good agreement with an R^2 of 0.94. The linear fit is given with a grey solid line; the dashed black line represents $x = y$.

2.4 Finding a representative density

Fisher et al. (1985) defined stratigraphic noise as a “random element caused by the surface irregularities”, which is present in any taken snow profile or ice core. This stratigraphic noise is mainly caused by spatially inhomogeneous deposition in combination with wind, leading to snow patches or dune structures that usually have a spatial extent of several meters. This stratigraphic noise hampers the representative (i.e., for a certain location or area) estimate of surface snow density, when not considered in the sampling strategy. To still be able to get a representative value or profile (of density or other parameters) at a given spot, several samples have to be taken at a distance, at which they are not subject to the same stratigraphic noise. For example, samples should not be taken from the same dune or snow patch, as these values cannot be considered to be spatially independent. By stacking or averaging independent samples, the stratigraphic noise is reduced. For example, this has also been performed for isotopes (Karlöf et al., 2006; Münch et al., 2016), and a common (annual or seasonal) climatic signal can be retrieved despite a high level of stratigraphic noise.

The (minimum) sampling distance between two samples was quantitatively described for snow density by Laepple et al. (2016). In a 2D high-resolution trench study at Kohnen Station they have shown that the correlation coefficient between single profiles decreases rapidly with increasing distance and settles at a constant value after 5–10 m. In the following we refer to samples taken at this distance as “spatially independent”. Consequently, we consider the multiple snow profiles at one location to provide spatially independent ρ_L .

In the OIR trench, we assume a sampling distance of 5 m between two profiles to be sufficient.

For a representative 1 m ρ_{loc} , we aim for a relative error of less than 2%. To test how many snow samples per location are needed for this representativeness, we calculated σ_H^{1m} of ρ_{loc} . We used the maximum number of spatially independent ρ_L for ρ_{loc} (further called n). We did this for both the multiple liners at the traverse locations and the OIR trench. At the locations along the traverse we use all four available ρ_L values ($n = 4$) to calculate σ_H^{1m} of ρ_{loc} . In the trench, we created two sets of ρ_L , which have a minimum sampling distance of 5 m. We get two sets of seven ($n = 7$; using different snow profiles in both sets) and calculated the mean value of both sets. We then derive the standard error (σ_n), which depends on the number n of ρ_L at a given location, by

$$\sigma_n = \sigma_H^{1m} / \sqrt{[2; n = 1]}, \quad (1)$$

with the denominator being a varying number of snow profiles from 2 to $n - 1$. This means, for example, when using seven profiles (like one set in the OIR trench), we are able to calculate the standard error for two to six profiles. In this way we use the maximum sample size without an artificially caused bias in the data. This can happen, for instance, by creating sets with a small sample size and picking ρ_L randomly. Accordingly by (a) using large volumetric samples we improve the accuracy, and by (b) using several profiles at each location we improve the representativeness of the density values derived for each location. We are therefore able to deliver a more accurate and representative density of each site, compared to previous studies.

2.5 Definition of subregions on the EAP

We pooled several snow profiles for further investigation to characterize the surface density of a larger ($\geq 10\,000\text{ km}^2$) region. We chose a minimum number of 10 profiles (0–1 m) per area. We followed the classification of Furukawa et al. (1996) as well as possible and used the 3500 m a.s.l. contour line as the approximate boundary between different wind and accumulation regimes on the katabatic wind zone and the interior plateau (calm accumulation zone). This way we classified one major area “ascending plateau area” (AP) with 64 profiles, covering roughly $140\,000\text{ km}^2$ between Kohnen Station and OIR camp and the smaller “interior plateau” (IP) with 29 profiles between OIR camp and Plateau Station ($28\,500\text{ km}^2$). We did not include the OIR trench, as this specific location would have been overrepresented. The area around B53 ($28\,500\text{ km}^2$) was treated as a separate area as it is on the interior plateau close to the ice divide (“B53 and vicinity” – 10 profiles). Additionally, we handled the area around Kohnen Station (Ko) with roughly $10\,000\text{ km}^2$ as another separate unit (“Kohnen and vicinity” – 45 profiles). The sample availability at Kohnen Station from other studies is sufficient, several liners from other sampling programs in seasons 2015/16 (16 profiles) and 2016/17 (18 profiles)

have been added to the evaluation. The areas are color-coded in the overview map (Fig. 1).

As we present density data on different scales, in this context we use the term “local” scale for distances between profiles at one location and the area around a sampling location (i.e., tens of meters, Table 1). In contrast, the term “regional” scale is used for distances between several locations (100 to 1000 km) and areas in the dimensions of the subregions defined above. For all subsets, we present a spatial distribution of ρ_L and ρ_{loc} .

2.6 Optical leveling

The relative surface elevation of the OIR trench was measured using optical leveling at each profile position and in between two consecutive profiles. Additionally, at the OIR camp and Plateau Station surface roughness transects were measured. The optical level was placed at the transect starting point. The first height measurement was done at a 10 m distance to the starting point and repeated every 2 m up to a 58 m distance relative to the start, resulting in 25 measuring points per transect. In total six transects have been done at one location with 1 m lateral spacing between them.

3 Results

3.1 Snow and firn density in the OIR trench

ρ_L ranges in the OIR trench from 347 to 380 kg m^{-3} . We calculated ρ_{loc} for the OIR trench (\pm standard deviation) with $365 \pm 10\text{ kg m}^{-3}$, which is 3.1% higher than for the whole traverse (Sect. 3.2). σ_H is between 10 and 27 kg m^{-3} for 0.1 m sampling intervals and between 5 and 10 kg m^{-3} for 1 m sampling intervals (Fig. 5 and Table 4). The highest $\sigma_H^{0.1m}$ can be found in the top 0.3 m. σ_V^3m of the 3 m profiles is 34 kg m^{-3} (Table 4).

3.2 Snow and firn density along the traverse

Here we present data from Sect. 2.2.1 and 2.2.2. Along the traverse we find ρ_L ranging from 324 kg m^{-3} (pos. 22C) to 382 kg m^{-3} (pos. 16A). The average ρ_L calculated from 114 liners along the traverse is $354 \pm 11\text{ kg m}^{-3}$ (Fig. 6).

ρ_{loc} (Table 1) is calculated from multiple snow profiles (Sect. 2.2.2) at each location. At locations 21 and 1 close to Kohnen Station we find the lowest ρ_{loc} with 344 and 345 kg m^{-3} , respectively. The highest ρ_{loc} is found at position 5 with 372 kg m^{-3} (Table 2). The average ρ_{loc} along the traverse is $355 \pm 8\text{ kg m}^{-3}$. To characterize the surface variability, we calculated σ_H^{1m} for each location separately. The minimum σ_H^{1m} is 2 kg m^{-3} at position 20 (and position 13 with only two profiles taken); the maximum σ_H^{1m} is 15 kg m^{-3} at position 22.

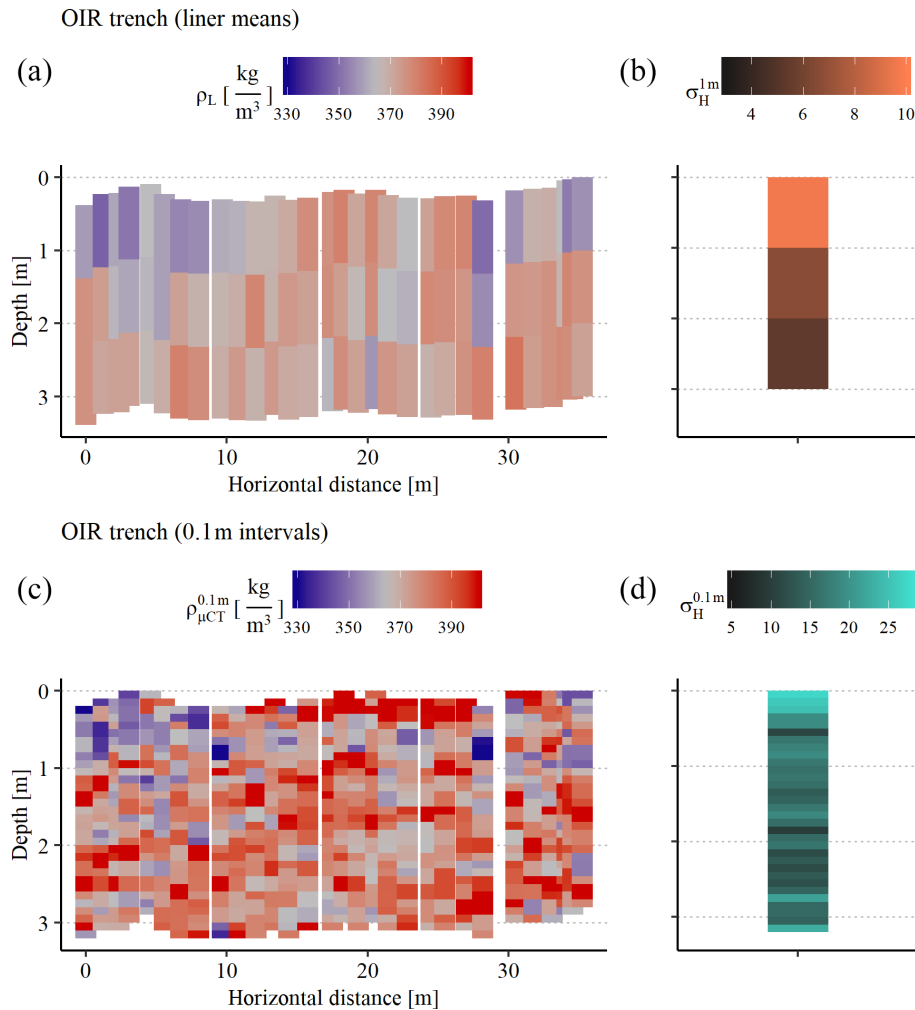


Figure 5. Density of the OIR trench from 30 profiles in vertical 1 m (liner density, **a**, **b**) and 0.1 m sampling intervals (μ CT density, **c**, **d**) in a color-coded plot. For the profiles in 0.1 m intervals, we used a common depth scale for the whole trench starting at the top of the profile with the highest surface elevation (profile 30); all other liners start at the measured relative height. We then calculated the density of each 0.1 m interval according to the common depth scale. ρ_L and $\rho_{\mu CT}^{0.1m}$, respectively, are given in a blue (low density) to red (high density) color code. On the right of each panel, σ_H of the respective depth interval is shown.

A detailed overview of all ρ_{loc} and σ_H^{1m} along the traverse can be found in Table 2, and a visualization is in the appendix (Fig. 13).

3.3 Representativeness of surface snow density on local scales

In Fig. 7 we compare the calculated σ_n according to Sect. 2.4. For four spatially independent snow profiles in the OIR trench, we get a value for σ_n of less than 1.5 % (4.9 kg m^{-3}) relative to ρ_{loc} ($355 \pm 2 \text{ kg m}^{-3}$). We note that on average σ_n in the OIR trench is higher than the average of the four areal subsets (7.0 kg m^{-3} in contrast to 6.1 kg m^{-3} for two profiles and 5.7 kg m^{-3} in contrast to 5.0 kg m^{-3} for three profiles).

Consequently, we consider four snow profiles to be sufficient for a ρ_{loc} with σ_n of less than 2%. Unfortunately, we

cannot test a number of profiles higher than six. But assuming a constant σ_H^{1m} , seven spatially independent profiles are needed to assure a relative σ_n of less than 1%.

3.4 Representativeness of surface snow density on regional scales

In the spatial density distribution of ρ_L and ρ_{loc} , we find similar values for Kohnen and vicinity ($352 \pm 1 \text{ kg m}^{-3}$), ascending plateau area ($356 \pm 1 \text{ kg m}^{-3}$) and the interior plateau ($355 \pm 2 \text{ kg m}^{-3}$) (Fig. 8). These have less than 1% difference from the average value of the whole traverse. Only B53 and vicinity show lower density values ($349 \pm 3 \text{ kg m}^{-3}$, -1.7% compared to the traverse location mean density 355 kg m^{-3}).

Looking at the density distribution of the high-resolution μ CT density profiles (for details, see Appendix), we find

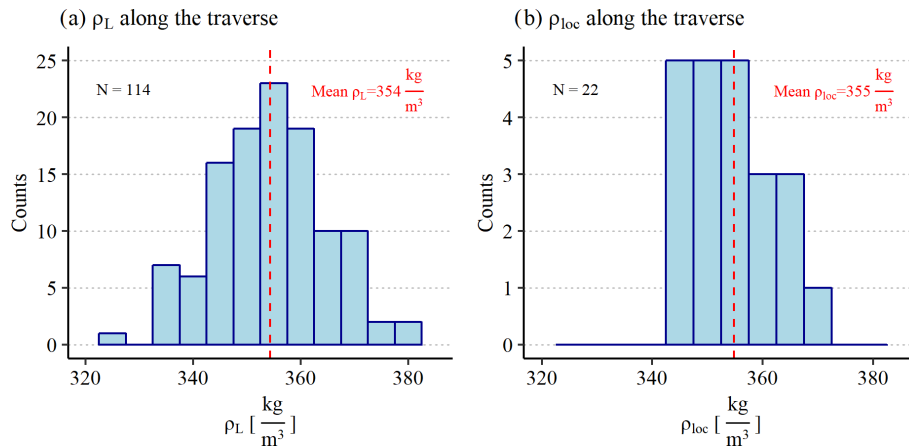


Figure 6. Histogram of (a) liner density (ρ_L) and (b) location mean density (ρ_{loc}) along the whole traverse route (profiles of the OIR trench not included). For both plots we used a bin width of 5 kg m^{-3} . The average liner density and location mean density, respectively, are shown by the red dashed line in (a) and (b).

Table 2. ρ_{loc} at each location with multiple liners and the respective standard deviation. The number of liners at each location is given in brackets. For locations and abbreviations see Fig. 1.

Location (no. of ρ_L values)	Longitude ($^{\circ}$)	Latitude ($^{\circ}$)	Elevation (m a.s.l.)	Sampling date	ρ_{loc} (kg m^{-3})	$\sigma_H^{1 \text{ m}}$ (kg m^{-3})
1 (4)	2.89	-75.11	2990	14 December 2016	345	8
2 (4)	6.12	-75.18	3146	15 December 2016	355	10
3 (4)	9.58	-75.21	3301	16 December 2016	360	13
4 (4)	12.66	-75.18	3400	17 December 2016	350	9
5 (4) – B51	15.40	-75.13	3470	18 December 2016	372	7
6 (4)	16.32	-75.47	3484	19 December 2016	353	14
7 (4)	18.33	-76.19	3463	20 December 2016	346	8
8 (4)	20.66	-76.90	3456	21 December 2016	355	9
9 (4)	23.19	-77.57	3452	22 December 2016	351	12
10 (4)	26.30	-78.29	3455	23 December 2016	346	5
11 (2)	29.38	-78.89	3461	24 December 2016	350	6
12 (4) – OIR/B54	30.00	-79.00	3473	26 December 2016	358	6
13 (2)	35.69	-79.18	3576	6 January 2017	362	2
14 (4) – B55	40.56	-79.24	3665	9–11 January 2017	352	10
15 (4) – B56	34.97	-79.33	3544	16–18 January 2017	351	8
16 (4)	27.28	-78.84	3416	23 January 2017	366	11
17 (4)	22.64	-78.50	3325	24 January 2017	358	7
18 (4)	17.62	-78.02	3259	25 January 2017	356	5
19 (3)	12.03	-77.32	3153	26 January 2017	365	6
20 (4)	7.20	-76.54	3067	27 January 2017	368	2
21 (4)	2.90	-75.67	2959	28 January 2017	344	7
22 (4) – B53	31.91	-76.79	3737	26 December 2016	345	15
Whole traverse (22 ρ_{loc})	–	–	–	–	355	8

a normal distribution of the snow density in the first meter (Fig. 9). We see a shift towards higher densities in the OIR trench and a higher probability for lower densities in B53 and vicinity, but in general a similar distribution of density in all subregions is found.

We calculated the confidence interval (95 %) of ρ_L for each respective subregion (Table 3). We want to stress that

the number of samples of “B53 and vicinity” is lower than recommended for this method. The mean value for the traverse is represented in all four intervals of the subregions. We note that the interval for Kohonen and vicinity just includes this value.

The snow density directly measured at the surface in general shows high spatial variability (Figs. 5 and 10). To char-

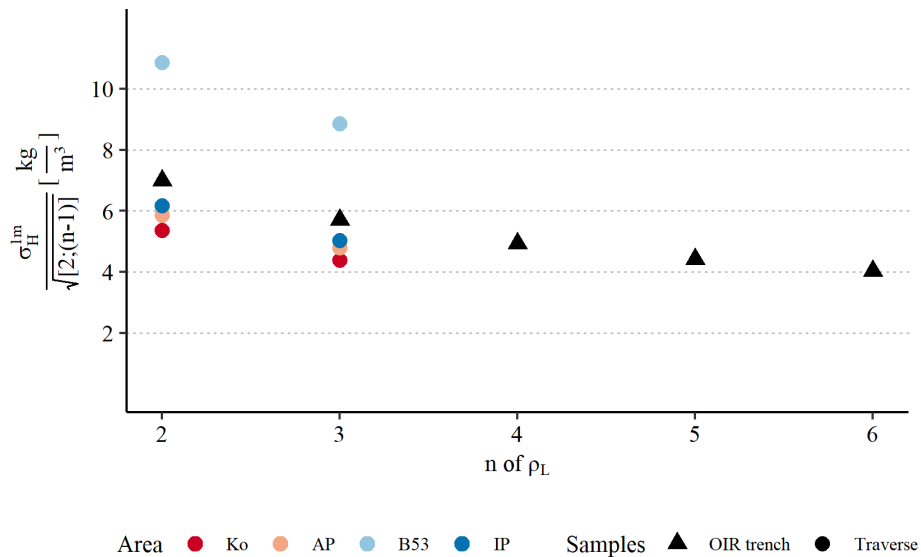


Figure 7. Standard error (σ_n) of the location mean density (ρ_{loc}) as a function of the number of profiles (n). Triangles represent samples from the OIR trench while colored circles show samples along the traverse in the respective subsets (Sect. 2.5).

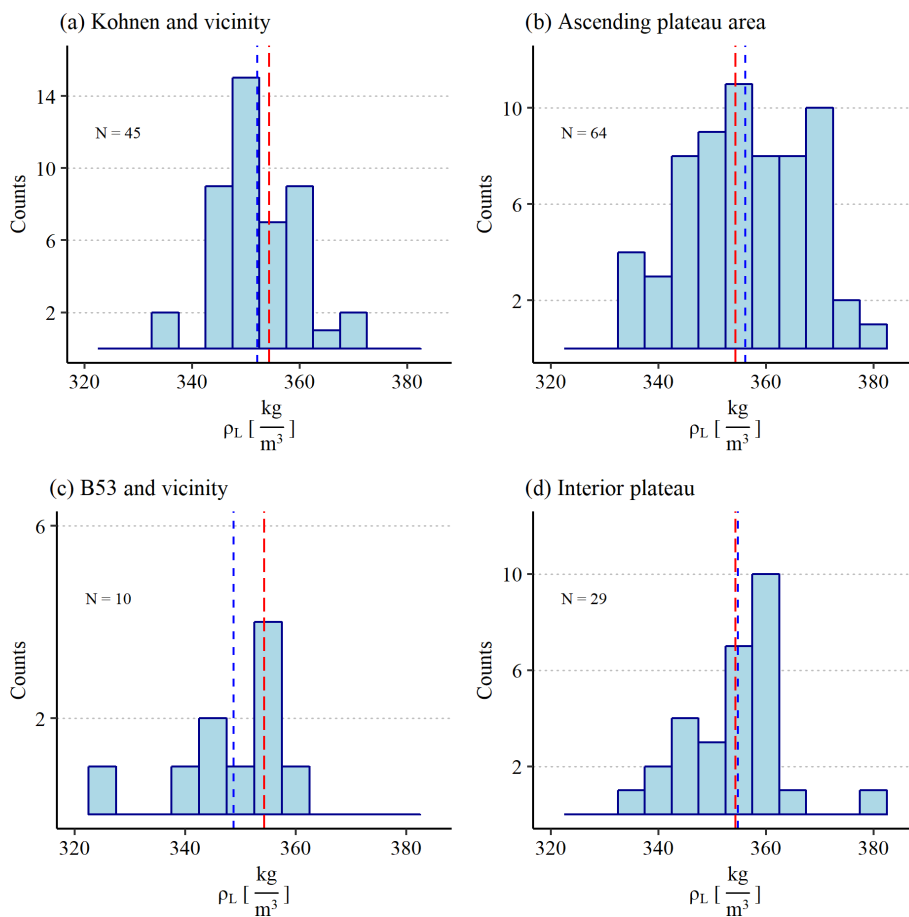


Figure 8. Histograms of the liner density (ρ_L) for the four subregions (Fig. 1). The bin width for each histogram is 5 kg m^{-3} . The average ρ_L (Fig. 6a) is given as a red dashed line while the liner density of the respective subregion is marked with a blue dashed line.

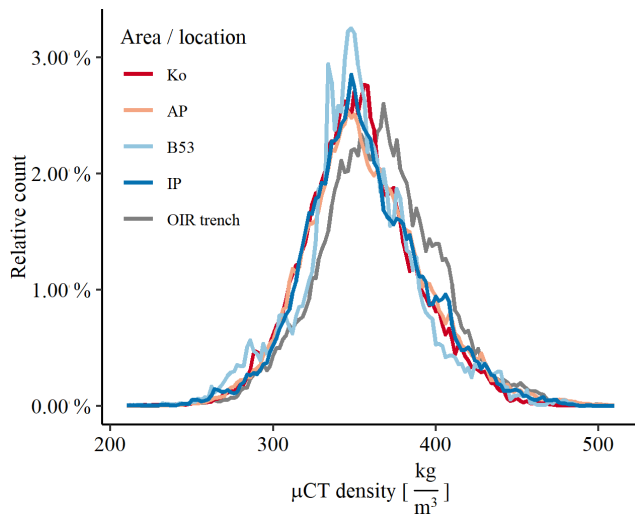


Figure 9. Density distribution from surface to 1 m depth of the μCT density. It is based on all available liners – 114 liners from the traverse (according to their subregion), 30 liners for the OIR trench (grey) and 16 liners from Kohlen Station (not this study) with a bin width of 2 kg m^{-3} . We used the same color code for the subregions (Sect. 2.5) as in Fig. 1.

Table 3. Confidence intervals of 95 % for each pooled area.

Area (number of samples)	Lower boundary (kg m^{-3})	Upper boundary (kg m^{-3})
Whole traverse (114)	352	356
Kohlen and vicinity (45)	350	354
Ascending plateau area (64)	353	358
B53 and vicinity (10)	341	357
Interior plateau (29)	351	358
OIR trench (30)	361	368

acterize the spatial variability of density in a given area (tens of meters for traverse locations and trenches, hundreds of meters for Kohlen Station), we use the parameter σ_{H} . For a comparison we used snow liners along the traverse (liners sampled at OIR trench presented in a separate column), from Kohlen Station (Schaller, 2018) and from East Greenland Ice-core Project (EGRIP) camp site ($75^{\circ}37' \text{ N}$, $35^{\circ}59' \text{ W}$; 2702 m a.s.l.). Shown is also σ_{V} for the respective areas, which can be interpreted as temporal (seasonal or annual) variations in density. We computed both (σ_{H} and σ_{V}) for 0.1, 0.5 and 1 m intervals each (Table 4).

3.5 Small-scale topography at OIR camp and Plateau Station

The maximum height difference between the lowest (first) and highest (last) profiles in the OIR trench is 38.5 cm. The height values of each position are given in the appendix (Ta-

ble 6). We find significant differences in the surface topography at both places. At OIR camp the height differences between the lowest and highest points of the measured transects are 60 % larger than the height differences at Plateau Station (Table 5). The variation in height differences between the six transects at each location is low with a standard deviation of 2.4 cm (OIR camp) and 2.0 cm (Plateau Station).

4 Discussion

4.1 Liner method vs. discrete sampling

To discuss the 1 m snow density using the liner technique, we compare our dataset with data by Oerter (2008). In that study, snow pits with 20 km spacing have been dug and sampled along a small transect from Kohlen Station upstream towards B51 (comp. Fig. 1). A detailed map of the sampled region by Oerter (2008) is available in Huybrechts et al. (2007). Snow density has been measured volumetrically in each snow pit using discrete samples in 0.1 m depth intervals. We compare our results with density data from locations 1 to 4 (including single snow profiles in between) at two different depth resolutions (0.1 and 1 m). For our study, we use $\rho_{\mu\text{CT}}^{0.1\text{m}}$ and ρ_{L} . For the 1 m interval from Oerter (2008) we use the average density value of all discrete samples between 0 and 1 m.

$\rho^{1\text{m}}$ values from both studies are in good agreement with each other. $\rho^{1\text{m}}$ derived with the liner method tends to be 1 %–5 % higher than the one from Oerter (2008) (Fig. 10). A higher discrepancy can be seen in the mean density of the upper 0.1 m. While we find on average $\rho_{\mu\text{CT}}^{0.1\text{m}} = 349 \text{ kg m}^{-3}$ from liner measurements, $\rho^{0.1\text{m}}$ for Oerter (2008) is 293 kg m^{-3} . The calculated $\sigma_{\text{H}}^{0.1\text{m}}$ over the whole distance is 31 kg m^{-3} for our study and 25 kg m^{-3} for Oerter (2008). Interestingly, $\rho^{0.1\text{m}}$ in Oerter (2008) is always lower than $\rho^{1\text{m}}$, which is not the case in samples from our study. Due to the soft and unconsolidated snow at the surface, we assume that the undersampling error is higher at the surface for small sampling devices, which forces a systematic error towards smaller values (Fig. 10). Snow in greater depth has undergone sintering processes and is more coherent; therefore the undersampling error should also be smaller. Additionally, a systematic error with increasing depth in the data by Oerter (2008) cannot be excluded, as the sampling device (core cutter) might densify the snow with each interval due to the thick wall in relation to the sampling volume. In contrast to other devices, the liner method preserves the original stratigraphy of the snow column. In combination with the μCT measurement on different chosen depth intervals, this results in a density value with less uncertainty, especially for small sampling intervals at the snow surface. Despite the sampling strategy, the difference between both datasets can be caused by different weather conditions during the sampling. This affects in particular the upper centimeter of the snow column.

Table 4. Comparison of σ (horizontal and vertical) for each depth interval (from surface to respective depth) of samples from the traverse and OIR trench (this study), Kohnen Station and a trench from EGRIP (Schaller, 2018).

σ^{0-X} (kg m^{-3})	σ_V Traverse (22 locations, 4 profiles)	σ_H Traverse (22 locations, 4 profiles)	σ_V OIR trench (30 profiles)	σ_H OIR trench (30 profiles)	σ_V Kohnen Station (16 profiles)	σ_H Kohnen Station (16 profiles)	σ_V EGRIP trench (22 profiles)	σ_H EGRIP trench (22 profiles)
0.1 m	24	23	19	25	31	23	24	17
0.5 m	33	11	33	14	31	9	33	9
1.0 m	34	8	34	10	33	6	43	7

Table 5. Maximum height differences (m) along transects one to six at Plateau Station and B56.

	1	2	3	4	5	6	Mean
OIR camp	0.268	0.280	0.310	0.330	0.319	0.310	0.303
Plateau Station	0.180	0.211	0.180	0.174	0.150	0.212	0.184

4.2 Comparison of different sampling intervals

In the following we discuss the advantages of a 1 m snow density in contrast to smaller depth intervals. In this context we refer to the data presented in Table 4. At sites with accumulation rates higher than $100 \text{ kg m}^{-2} \text{ a}^{-1}$ (e.g., EGRIP), small sampling intervals ($< 0.5 \text{ m}$) do not contain the seasonal or annual variability over several years (see also data by Oerter, 2008, in Fig. 10), at sites with lower accumulation (in this context $< 60 \text{ kg m}^{-2} \text{ a}^{-1}$) the density might be masked by the high stratigraphic noise. Both effects can be seen in the low $\sigma_V^{0.1\text{m}}$ in contrast to $\sigma_V^{1\text{m}}$ looking at data from different sites in Table 4. Higher $\sigma_V^{1\text{m}}$ in snow profiles from EGRIP are caused by a clearer seasonal density cycle, which is barely or not detectable on the EAP. This can be explained with higher temperatures as well as higher accumulation rates at EGRIP. In the case of surface melting like in the year 2012 (Nghiem et al., 2012), $\sigma_V^{1\text{m}}$ can be even higher. We find lower σ_H at the surface in samples from EGRIP in contrast to EAP. This can be explained by the non-uniform deposition causing high undulations in the surface topography. We measured the topography in the form of dune heights (Table 5), which are often 30 to 40 cm high and exceed the yearly accumulation by far. Snow layers do not form as spatially consistently as at sites where the (predicted) yearly layer thickness is larger than the amplitude of dunes. This also affects the snow density as the signal cannot form homogenously over a larger distance and causes larger σ_H . For all presented sites, the $\sigma_H^{0.1\text{m}}$ is 2.4 to 4 times higher than the $\sigma_H^{1\text{m}}$, which is explainable by the more comprehensive density spectrum over larger depth intervals. This high horizontal variability is mainly caused by the existing small-scale topography, in particular dunes. The variability decreases below the maximum measured dune heights of 30–35 cm below the surface. These dunes have a higher snow density (Birnbaum et al., 2010) than snow that gets deposited in local depressions due to enhanced wind packing (see Sect. 4.3). This is also visualized for the OIR trench in

Fig. 5. A snow patch of low density can be seen at the surface between 0 and 5 m (horizontal distance) and rather high density between 18 and 25 m (horizontal distance) (Fig. 5c). This illustrated the need to choose a far enough distance to reduce the effect of stratigraphic noise (Sect. 2.5).

The temperature-dependent densification effect does not affect the 1 m snow density substantially. By comparing all μCT density profiles over depth, we cannot see a significant increase in density over the first meter. Also according to the model by Herron and Langway (1980), at a temperature of $-43 \text{ }^\circ\text{C}$ (annual mean air temperature at Kohnen Station after Medley et al., 2018), the increase in snow density by densification from the surface to 1 m depth is 10 kg m^{-3} . At a $-53 \text{ }^\circ\text{C}$ annual mean air temperature ($-10 \text{ }^\circ\text{C}$ compared to Kohnen Station) the densification is roughly 8.3 kg m^{-3} . A temperature change of $-1 \text{ }^\circ\text{C}$ would lower the densification-induced density by about 0.17 kg m^{-3} .

In summary, due to the high snow density variability in the upper decimeters of the snowpack, we suggest the 1 m density as a feasible approach to derive the surface snow density independently of local recent weather conditions. For a representative value, at least four samples should be taken per location with the respective sampling distance. The densification of snow over the first meter is negligibly small. Furthermore, we want to advert to the time efficiency of the liner method here. A 1 m snowpack density with four samples can be obtained within 1 h. Even if a high-resolution study in a snow pit is done, a snow profile using a liner can always be added to the discrete sampling in a snow pit for comparison.

4.3 Temporal and vertical variation in density along the traverse

Long-term changes in temperature, accumulation rate or wind systems can also affect fluctuations in density. At Kohnen Station a $1 \text{ }^\circ\text{C}$ temperature rise per decade has been recorded by an automatic weather station, jointly operated by

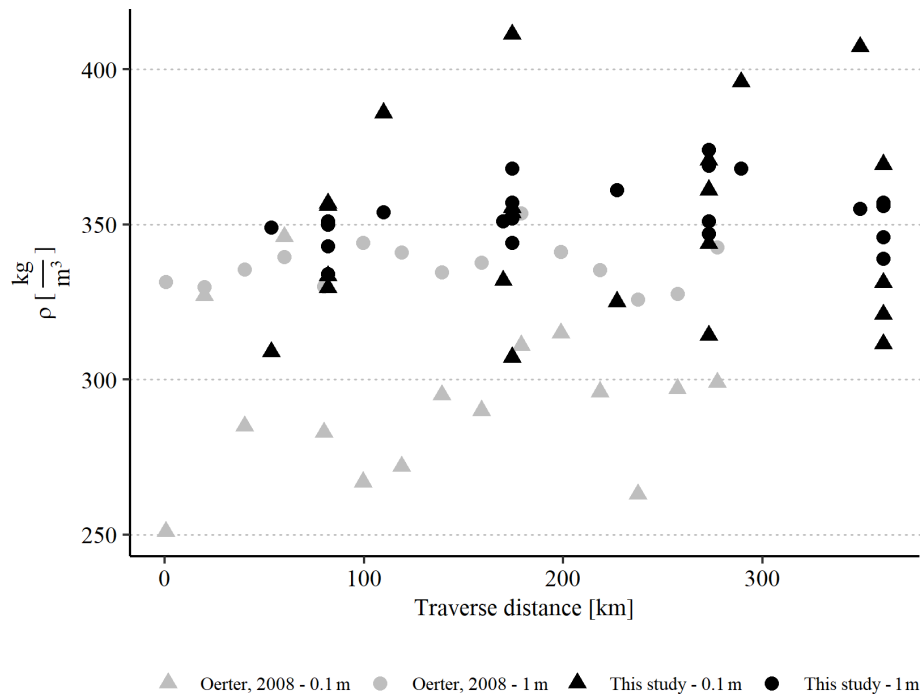


Figure 10. Density values of this study (black) in comparison with those from snow pit sampling by Oerter (2008) (grey). The samples are taken along a comparable transect line. Density is given as mean value from the snow surface to the respective depth. The spatial variability in both 1 and 0.1 m intervals can be seen by the spread of points in data of this study at one sampling location (comp. Table 3).

the Institute for Marine and Atmospheric Research (IMAU) and AWI (Reijmer and van den Broeke, 2003) over the past 20 years and discussed by Medley et al. (2018). Recent studies postulate in some areas of Antarctica, partly also on the EAP, an increase in the accumulation rate (Frierler et al., 2015; Medley and Thomas, 2019) caused by a temperature rise. However, accurate accumulation rates for the interior EAP are hard to determine and are generally overestimated (Anschütz et al., 2011).

We test the impact on surface snow density of a 1 °C temperature rise as well as a 15 % increase in accumulation rate at Kohonen Station. We use the surface snow density parameterization after Kaspers et al. (2004):

$$\rho = 7.36 \times 10^{-2} + 1.06 \times 10^{-3}T + 6.69 \times 10^{-2}\dot{A} + 4.77 \times 10^{-3}W, \quad (2)$$

where T is the 10 m firm temperature (K), \dot{A} the accumulation rate ($\text{kg m}^2 \text{a}^{-1}$) and W the mean wind speed (m s^{-1}).

For comparison we also use the surface snow density parameterization after Sugiyama et al. (2012), as this one has been calibrated in particular with samples along a traverse over the EAP:

$$\rho = 305 + 0.629T + 0.150\dot{A} + 13.5W, \quad (3)$$

with T (°C), \dot{A} ($\text{kg m}^2 \text{a}^{-1}$) and W (m s^{-1}) at the given location.

A temperature rise of 1 °C and an increase in accumulation rate of 15 % at Kohonen Station would increase the surface snow density by 1.7 kg m^{-3} according to Kaspers et al. (2004) and by 2.0 kg m^{-3} according to Sugiyama et al. (2012). According to both parameterizations, the difference in density between this study and Oerter (2008) cannot be solely attributed to these climatic changes as both potential increases are inside the error range of ρ_{loc} . Despite uncertainties in the precision of the sampling method or natural (climatic) variability, the discrepancy in surface density between both datasets can also be caused by stratigraphic noise over time. To give an example here, we compare ρ_{loc} of snow profiles from Kohonen Station taken in two different seasons at the same position. We use 17 profiles along a transect line with 0.5 m spacing from the season in 16/17, which were re-sampled in the season in 18/19 (both unpublished). The climatic conditions during this time span did not change significantly. $\rho_{\text{loc}}(16/17)$ and $\rho_{\text{loc}}(18/19)$ both have the same value and the same standard deviation $350 \pm 6 \text{ kg m}^{-3}$. Although this example can give an estimate for the robustness of our density measurements using the liner method, we are not able to completely decouple the spatial variability and the temporal variability as we cannot resample the exact same position (and thus the exact same snow).

In a second test, we use an annual mean temperature of -50 °C (223.15 K), accumulation rate of $40 \text{ kg m}^2 \text{a}^{-1}$ and wind speed of 6 m s^{-1} , which are roughly the mean values of

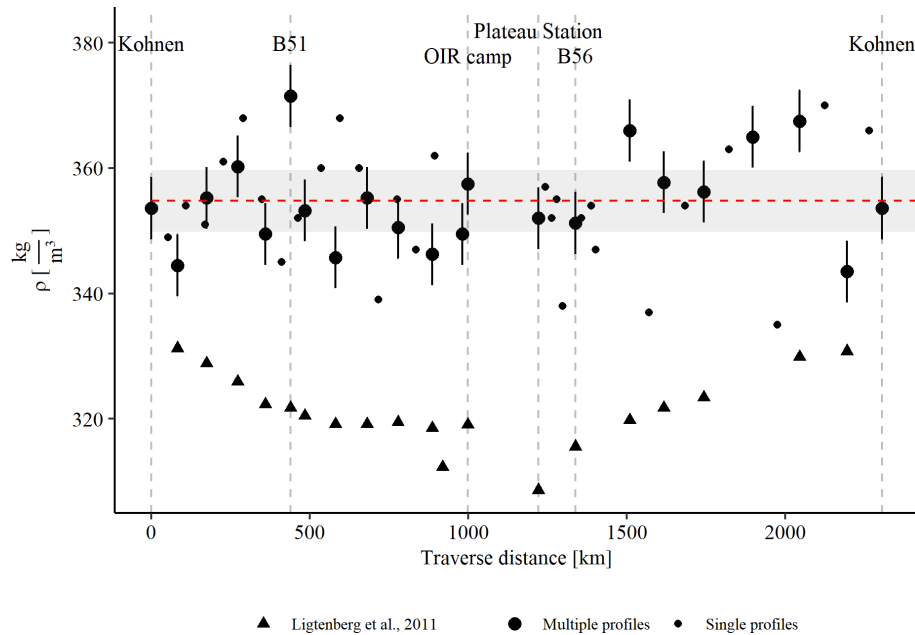


Figure 11. Location mean density (ρ_{loc}) as well as liner density (ρ_L) along one leg of the traverse route, from Kohnen Station to B51, further along the ice divide to B53 and from Plateau Station straight back to Kohnen Station. σ_n calculated from the OIR trench (Sect. 3.3) is given by vertical error bars at each location. A mean density value for Kohnen Station was calculated from samples not collected in this study (Sect. 2.5). The red dashed horizontal line indicates the mean density along the whole traverse, and the standard error (σ_n) is indicated with grey shading. The triangles show the parameterized density values according to Ligtenberg et al. (2011).

the area covered with the traverse. While the parameterization by Sugiyama et al. (2012) is fairly accurate compared to our 1 m snow density ($+5 \text{ kg m}^{-3}$), keeping the temperature and accumulation rate constant we have to increase the wind speed to 9 m s^{-1} to reach the surface snow density along the traverse using the parameterization by Kaspers et al. (2004).

In general we conclude that several parameterizations for the surface snow density (Kaspers et al., 2004; Sugiyama et al., 2012) need further tuning for regions with low accumulation and low temperatures like the EAP. Rather, local parameterizations should be used for regions with similar environmental conditions instead of continent-wide parameterizations.

4.4 A representative surface snow density on the EAP

In order to overcome the sparsity of ground truth surface snow density, regional climate models and derivatives with adequate snow deposition modules are often used to obtain estimates of accumulation and surface snow density on a full regional scale. Ligtenberg et al. (2011) presented firm density averaged from surface to 1 m depth over a period from 1979 to 2011. It is forced by RACMO2.3p1 mass fluxes and skin temperature and gridded at 27 km resolution.

Compared to the firm densification model presented by Ligtenberg et al. (2011), we find systematically higher values for density on the interior EAP than the model predicts for the same locations. While ρ_{loc} spans the range from 346

to 372 kg m^{-3} , the firm model provides a range from 308 to 332 kg m^{-3} (Fig. 11). Having sound statistics at these locations, we exclude the systematic bias to be caused by our observations, but rather we assume a shortcoming of the model to yield densities which are about 10% too low. This could be caused by a multitude of reasons, e.g., model physics, spatial and temporal resolution, or forcing. As the parameterization by Kaspers et al. (2004) provides density values closer to our ground truth data than the model output by Ligtenberg et al. (2011), we suggest revising the used slope correction (Helsen et al., 2008) for the EAP.

Our observation is consistent with recent field observations on the EAP (Sugiyama et al., 2012) or snow density collections from over 2 decades (Tian et al., 2018). Sugiyama et al. (2012) found a density around 350 kg m^{-3} for the same depth interval (0–1 m) along a traverse between Dome F and Kohnen Station, with a similar spatial variability. Nevertheless, we cannot detect a clear trend in density along the whole traverse route. A potential reason might be the increase in elevation, distance to the coast and major Dronning Maud Land (DML) ice divide on the one hand and the decrease in temperature as well as accumulation rate (Fig. 11) on the other hand. As the sampling took 6 weeks in total (Table 2), we exclude an effect of seasonal density variability as well as a significant effect of accumulation during the traverse (as the only observed accumulation on the traverse was a few diamond dust events above 3500 m a.s.l. during the nights and

some drift snow). We explain the increase in surface density along the ice divide from Kohnen Station towards B51 (Figs. 8b and 11) by smaller grain sizes due to decreasing temperature. The combination of the lower accumulation rate and longer exposition and mixing at the snow surface seems to create a higher surface snow density here. The observation of this systematic change in density is also visible in results of Sugiyama et al. (2012) and not captured by firn models. In fact, the model by Ligtenberg et al. (2011) shows the opposite trend along this traverse section (km 0–500 in Fig. 11). High density at B51 goes along with stronger dune formation than at Kohnen Station, which was observed to increase along this traverse part, and higher potential for wind packing due to lower accumulation rates. This is consistent with observations of dune formation at wind speeds exceeding 10 m s^{-1} (Birnbaum et al., 2010) or observation of wind-packing events (Sommer et al., 2018) causing increased snow density.

Modeled density is parameterized by wind speed, but the process of denser packing by wind scouring and redistribution over the time until the snow is finally buried might be underestimated. We assume that the modeled low density values for locations 14 and 15 (Plateau Station and B56, Fig. 11) in the calm accumulation zone are caused by the relatively low wind speed (Lenaerts and van den Broeke, 2012; Sanz Rodrigo et al., 2012), in combination with low temperatures and humidity (Picciotto et al., 1971). But the wind on the interior plateau is not strong enough to cause wind packing and sintering of snow crystals. It rather redistributes them smoothly at the surface, which also happens at low wind speeds. This process is significantly different from wind packing at high wind speeds. Thus as the sintering process is prolonged it increases the density on the long term, which also causes an increase in density variability at the surface. But as the low densities cannot be seen for the whole interior plateau region (Fig. 8d), we consider it to be a process that needs very specific settings on the high plateau than average characteristics. The abundance of wind speeds higher than 10 m s^{-1} might be a limiting factor in this context.

Different environmental conditions at B53 and vicinity might cause lower density here as well (Fig. 8c). High σ_n for subset B53 and vicinity should not be over-interpreted, as only one sampling location with four profiles is present there. Still, σ_{loc} is highest here amongst all locations with multiple liners along the traverse (compare also $\sigma_{\text{H}}^{1\text{m}}$ in Table 2). An explanation can be a different wind and accumulation regime at the distant side of the ice divide causing high heterogeneity on a very small scale.

Small fluctuations in density within the error range at nearby locations can be explained by stratigraphic noise (Laepple et al., 2016; Münch et al., 2016). Stronger variations in density, e.g., beyond 1 standard variation, can be caused by a complex interaction between wind speed and surface roughness on the small scale but also have been shown to originate from dynamic interaction of ice flow over bedrock

undulations, thus altering surface slope and in turn elevation and accumulation rate on the large scale in this region (Anschütz et al., 2011; Eisen et al., 2005; Rotschky et al., 2004). For a detailed conclusion regarding the influence of bedrock topography on the density fluctuations in our data, we consider the local scale (10 m) to be too small and the regional scale (100 km) to be too large. We suggest a different sampling scale (i.e., 10 km spacing of representative density) for this purpose.

As already stated above, we cannot conclusively attribute a cause to the model behavior as we also neglected the atmospheric forcing of the firn densification models, which could explain parts of the density discrepancy between field data and modeled values. Unfortunately, it is also difficult to pin down the mechanism for the observed systematic spatial distribution of density. As the surface snow density parameterizations are mainly dependent on temperature and wind speed, the influence of both might be too high while processes acting on the snow surface like snow redistribution and packing play a major role in snow density. Obviously, a dedicated sensitivity study with a snow deposition and firn model is needed to discriminate the various processes affecting post-depositional snow metamorphism and densification. We suggest setting up a specific model test designed for the EAP and using datasets like ours and those from comparable studies as the standard against which to evaluate model outcomes.

4.5 Application to satellite altimetry of ice sheets

Firn densification models are used in altimetry to convert height changes of the ice sheets to mass changes. The more accurate the modeled firn density provided by these models is, the lower the uncertainties in the calculated mass changes will be. Therefore, our presented density data can be of particular interest to improve the accuracy of ice sheet mass balances.

One way in altimetry is to use a simple density mask as an input parameter (e.g., McMillan et al., 2014; Schröder et al., 2019). In regions with a strong influence of ice dynamics, only the density of ice is used. In the remaining areas, also in large parts of East Antarctica where the ice flow velocities are low (Rignot et al., 2011), the density of firn is used. In this conversion, uncertainties in snow density have a direct impact on the result in mass. In our case, the 10 % density underestimation in previous studies can lead to a 10 % mass error (e.g., Alexander et al., 2019). Shepherd et al. (2019), in contrast, use firn or ice density by defining areas of dynamic imbalance, which depend on surface uplift or lowering in relation to firn column changes. This method is even more sensitive to uncertainties in the firn densification models, as it subtracts variations in firn density over time.

Despite the impact of density on the height-to-mass conversion, the snowpack properties can also influence the microwave penetration into the snow and therefore considerably

affect the radar altimetric measurements. Generally, snow properties like density, grain size and liquid water content can influence the permittivity (Mätzler, 1996), but spatiotemporal variations in these parameters also influence the measurements (Davis and Zwally, 1993). Furthermore layering of the snowpack seems to affect the penetration depth, like shown in Slater et al. (2019) for Greenland. Interestingly, the density distribution of density (Fig. 9) does not show as much difference between the subregions as previously expected due to different accumulation rates. While we can see differences on the local scale (OIR trench), on the regional scale the vertical density distribution of the subregions is very congruent. Therefore further high-resolution studies on the vertical variability of the snowpack are needed on the EAP, especially with regard to high surface variability.

4.6 Impact of surface snow density on the firm depth on the EAP

In the following we provide an idea of how the mass of the firm column depends on the choice of the surface density. Based on our findings we employ a simple quantitative calculation of the mass in the firm column with the density data presented in this study (average ρ_{loc}) using the semiempirical firm densification model by Herron and Langway (1980). We use an annual mean temperature of -50°C and an accumulation rate of $40\text{ kg m}^2\text{ a}^{-1}$ as input parameters. We use the two different surface snow densities $\rho_0(1) = 320\text{ kg m}^{-3}$ (Ligtenberg et al., 2011) and $\rho_0(2) = 355\text{ kg m}^{-3}$ (this study) and sum up the water equivalent (w.e.; based on 1000 kg m^{-3}) in the firm column.

We calculated 59.0 m w.e. for $\rho_0(1)$ and 61.0 m w.e. for $\rho_0(2)$ in the firm column down to the firm–ice transition in 92.9 m, where scenario $\rho_0(2)$ reaches the critical density of 830 kg m^{-3} . The calculation is in good agreement with firm density (μCT) measured in core B53 (unpublished data). This difference of +2 m w.e. corresponds roughly to an underestimation of 3 % mass for the firm column only using the modeled initial density. Other effects like an overestimation of the accumulation rate on the interior plateau are not taken into account.

5 Conclusion

We presented surface snow density data along a traverse route from Kohnen Station to former Plateau Station on the EAP using the time-efficient liner method. By using the liner technique (this study and, for example, Schaller et al., 2016) we can reduce the sampling error from up to $\pm 4\%$ for other measurement techniques (Conger and McClung, 2009) to less than 2 % relative error for a 1 m snow density. The method covers seasonal and annual variations at sites of high accumulation and reduces the influence of high surface roughness in relation to the annual accumulation in low-

accumulation areas. Especially in the upper 30 cm we see the highest stratigraphic variability in snow density. As long as the accumulation does not exceed 0.5 m of snow per year (independent of the snow density), we suggest a 1 m snow density using the liner method as the best way to quantify surface snow density as the 1 m interval offers high accuracy and is representative when repeated several times. It is not biased by the seasonal density variations or weather conditions, balances high surface roughness with multiple samples, has negligible undersampling errors as well as snow compaction and is very time efficient.

We compared the presented snow profiles to density data from snow pits by Oerter (2008). We found 1 %–5 % lower 1 m snow densities, which cannot be attributed to a temperature change between the sampling dates only. For the density from the surface to 0.1 m depth we find a considerable 16 % difference in density that we explain with a systematic sampling error. This systematic error makes comparisons of old and new datasets with different sampling devices difficult, as an increase in mass in Antarctica or an underestimation of mass in the past is hard to detect.

Especially on the EAP, field data are sparse. We conclude that four spatially independent snow profiles are necessary to determine a snow density value with an error lower than 1.5 % of the mean. To further verify this result in future studies, we suggest testing this with a similar sampling scheme with five and more profiles using the liner technique. A circular setup with one profile in the midpoint and four to six profiles along a circle with a radius of 10 m to keep spatial independency might be a feasible approach.

Our results are in good agreement with earlier density studies partly made in the same region (Sugiyama et al., 2012). We suggest a representative mean density of 355 kg m^{-3} for surface snow on regional scales on the EAP. As we find a high variability on different spatial scales, we suggest averaging point measurements for snow density over regional scales to find a spatially representative density value for surface snow instead of using single measurements. We divided the area covered by the traverse into subregions due to different environmental regimes, but we cannot find significant differences in surface snow density among them. Natural variability in snow density seems to be higher than previously assumed. Especially on the regional scale, we cannot see a clear correlation between temperature and accumulation rate with snow density. For future studies we therefore suggest sampling transects of 50–100 km with representative density samples every 1 km to investigate the influence of topography changes on snow density in more detail.

We also suggest further tuning of parameterizations of the surface snow density in firm models, especially for regions with environmental conditions like the EAP, which currently produce densities which are almost 10 % lower than our observed values. We did not test the climatic forcing in firm models, which also can contribute to this significant offset. Neglecting the forcing, an underestimation of surface snow

density can lead to a 3 % mass underestimation in the firn column of East Antarctica. These errors or biases in 1 m snow density can lead to large uncertainties in SMB. Improving densification models with the presented density data can also increase the accuracy of ice sheet SMB derived by altimetry, as a 10 % offset in snow density, as presented in this study, can lead to a 10 % error in SMB. We suggest further investigation of the density variability in depth (temporal variability) with local snowpack studies in high resolution and whether this can affect altimetry measurements.

Appendix A: Snow density profile

For a better understanding of Fig. 9, we show a density profile over depth measured with the μ CT. In the radioscopic image the stratification of the snowpack is visible. In Fig. 9 we took all high-resolution μ CT density profiles along the traverse, according to their subregion, as well as the OIR trench and plotted the relative abundance of the density values in 2 kg m^{-3} intervals.

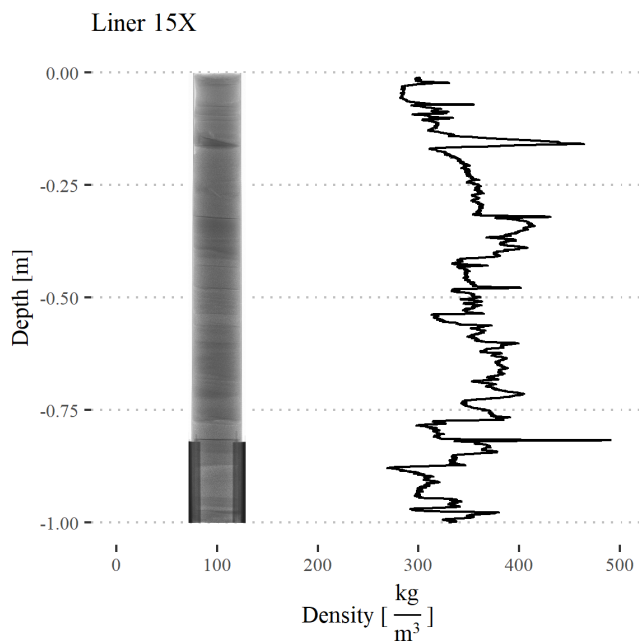


Figure A1. μ CT density of a snow profile at position 15X. On the left the radioscopic image of the snow profile is visible. Dark grey color represents high-density values, and bright grey represents low-density values. On the right, the corresponding density profile over depth is shown.

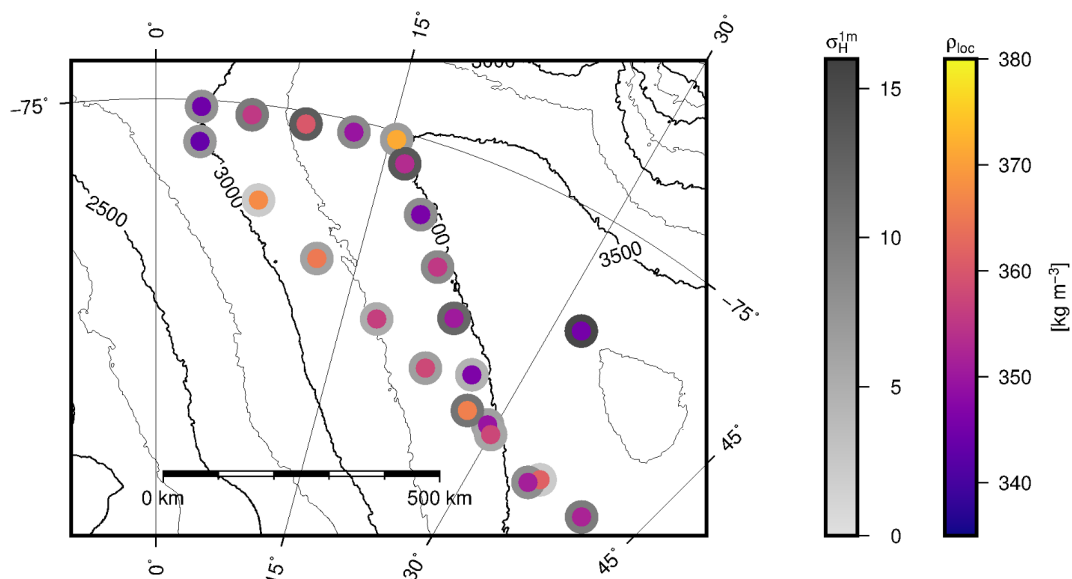
Appendix B: Geographical map of ρ_{loc} and σ_H^{1m} 

Figure B1. Location mean density (ρ_{loc}) and the horizontal standard deviation (σ_H^{1m}) along the traverse. The according values can be found in Table 2. Colored points show ρ_{loc} , grey edges σ_H^{1m} .

Appendix C: Height measurements along the OIR trench surface

Table C1. Surface leveling along the OIR trench. Surface height was measured at and in between subsequent sampling positions. In column two we show the distance along the trench and in column three the relative surface height in relation to the last profile.

Sample position	Distance (cm)	Relative surface height (to profile 30) (cm)
1	0	−38.5
	59	−31
2	125	−23.4
	178	−33
3	237	−21.6
	274	−16.1
4	309	−12.7
	391	−17.8
5	462	−9.7
	510	−19.3
6	556	−22.7
	610	−30.1
7	672	−30.2
	740	−34.7
8	800	−32.1
	895	−35.7
9	970	−30.5
	1030	−32.6
10	1088	−32.3
	1150	−35
11	1209	−33.4
	1278	−33.5
12	1343	−24.9
	1395	−30.4
13	1440	−31.3
	1510	−29.6
14	1575	−28.4
	1675	−30.4
15	1750	−20.2
	1790	−19.6

Table C1. Continued.

Sample position	Distance (cm)	Relative surface height (to profile 30) (cm)
16	1832	−17.6
	1880	−20.4
17	1934	−22.6
	1998	−25.2
18	2056	−17.1
	2100	−25
19	2145	−24.6
	2230	−27.9
20	2282	−28.2
	2380	−30
21	2449	−28.9
	2500	−26.8
22	2545	−25.6
	2619	−27.8
23	2700	−25.2
	2760	−29.9
24	2815	−31.8
	2940	−30.9
25	3051	−18.3
	3120	−21.9
26	3177	−16
	3245	−12.7
27	3310	−14.6
	3368	−8.7
28	3412	−4.6
	3432	−4.2
29	3453	−3.2
	3488	−1.1
30	3522	0

Data availability. Datasets will be uploaded to the open-access repository Pangaea. They are available upon request to the authors in the meantime.

Author contributions. JF and SK were in charge of planning the scientific expedition. AW and SK conducted the fieldwork. AW performed the majority of the μ CT measurements and subsequent analysis and wrote the manuscript. All authors discussed the results and contributed to revising the manuscript.

Competing interests. Olaf Eisen is Co-Editor-in-Chief of *The Cryosphere*.

Acknowledgements. We want to thank the whole logistic team of the traverse for technical support during the expedition and Alexandra Touzeau for assisting in taking snow liners in the field. Thanks to Melissa Mengert for conducting parts of the μ CT measurements, Christoph Schaller for interesting discussions, Thomas Laepple for sharing his experience regarding representativeness of climate proxies and Ludwig Schroeder for his help regarding the impact of our data on altimetry.

Financial support. Alexander Weinhart is funded by the German environmental foundation (Deutsche Bundesstiftung Umwelt).

The article processing charges for this open-access publication were covered by a Research Centre of the Helmholtz Association.

Review statement. This paper was edited by Jürg Schweizer and reviewed by two anonymous referees.

References

- Agosta, C., Amory, C., Kittel, C., Orsi, A., Favier, V., Gallée, H., van den Broeke, M. R., Lenaerts, J. T. M., van Wessem, J. M., van de Berg, W. J., and Fettweis, X.: Estimation of the Antarctic surface mass balance using the regional climate model MAR (1979–2015) and identification of dominant processes, *The Cryosphere*, 13, 281–296, <https://doi.org/10.5194/tc-13-281-2019>, 2019.
- Alexander, P. M., Tedesco, M., Koenig, L., and Fettweis, X.: Evaluating a Regional Climate Model Simulation of Greenland Ice Sheet Snow and Firm Density for Improved Surface Mass Balance Estimates, *Geophys. Res. Lett.*, 46, 12073–12082, <https://doi.org/10.1029/2019gl084101>, 2019.
- Anschütz, H., Muller, K., Isaksson, E., McConnell, J. R., Fischer, H., Miller, H., Albert, M., and Winther, J. G.: Revisiting sites of the South Pole Queen Maud Land Traverses in East Antarctica: Accumulation data from shallow firn cores, *J. Geophys. Res.-Atmos.*, 114, D24106, <https://doi.org/10.1029/2009jd012204>, 2009.
- Anschütz, H., Sinisalo, A., Isaksson, E., McConnell, J. R., Hamran, S. E., Bisiaux, M. M., Pasteris, D., Neumann, T. A., and Winther, J. G.: Variation of accumulation rates over the last eight centuries on the East Antarctic Plateau derived from volcanic signals in ice cores, *J. Geophys. Res.-Atmos.*, 116, D20103, <https://doi.org/10.1029/2011jd015753>, 2011.
- Arthern, R. J., Winebrenner, D. P., and Vaughan, D. G.: Antarctic snow accumulation mapped using polarization of 4.3-cm wavelength microwave emission, *J. Geophys. Res.-Atmos.*, 111, D06107, <https://doi.org/10.1029/2004jd005667>, 2006.
- Birnbaum, G., Brauner, R., and Ries, H.: Synoptic situations causing high precipitation rates on the Antarctic plateau: observations from Kohnen Station, Dronning Maud Land, *Antarctic Science*, 18, 279–288, <https://doi.org/10.1017/s0954102006000320>, 2006.
- Birnbaum, G., Freitag, J., Brauner, R., König-Langlo, G., Schulz, E., Kipfstuhl, S., Oerter, H., Reijmer, C. H., Schlosser, E., Faria, S. H., Ries, H., Loose, B., Herber, A., Duda, M. G., Powers, J. G., Manning, K. W., and van den Broeke, M. R.: Strong-wind events and their influence on the formation of snow dunes: observations from Kohnen station, Dronning Maud Land, Antarctica, *J. Glaciology*, 56, 891–902, <https://doi.org/10.3189/002214310794457272>, 2010.
- Conger, S. M. and McClung, D. M.: Comparison of density cutters for snow profile observations, *J. Glaciol.*, 55, 163–169, <https://doi.org/10.3189/002214309788609038>, 2009.
- Cunde, X., Yuansheng, L., Allison, I., Shugui, H., Dreyfus, G., Barnola, J.-M., Jiawen, R., Lingen, B., Shenkai, Z., and Kameda, T.: Surface characteristics at Dome A, Antarctica: first measurements and a guide to future ice-coring sites, *Ann. Glaciol.*, 48, 82–87, <https://doi.org/10.3189/172756408784700653>, 2008.
- Davis, C. H. and Zwally, H. J.: Geographic and seasonal variations in the surface properties of the ice sheets by satellite-radar altimetry, *J. Glaciol.*, 39, 687–697, <https://doi.org/10.3189/s0022143000016580>, 1993.
- Eisen, O., Rack, W., Nixdorf, U., and Wilhelms, F.: Characteristics of accumulation around the EPICA deep-drilling site in Dronning Maud Land, Antarctica, *Ann. Glaciol.*, 41, 41–46, <https://doi.org/10.3189/172756405781813276>, 2005.
- Fisher, D. A., Reeh, N., and Clausen, H. B.: Stratigraphic noise in time series derived from ice cores, *Ann. Glaciol.*, 7, 76–83, <https://doi.org/10.3189/S0260305500005942>, 1985.
- Freitag, J., Kipfstuhl, S., and Laepple, T.: Core-scale radioscopic imaging: a new method reveals density–calcium link in Antarctic firn, *J. Glaciol.*, 59, 1009–1014, <https://doi.org/10.3189/2013JoG13J028>, 2013.
- Frezzotti, M., Gandolfi, S., La Marca, F., and Urbini, S.: Snow dunes and glazed surfaces in Antarctica: new field and remote-sensing data, *Annals of Glaciology*, 34, 81–88, <https://doi.org/10.3189/172756402781817851>, 2002.
- Frieler, K., Clark, P. U., He, F., Buizert, C., Reese, R., Ligtenberg, S. R. M., van den Broeke, M. R., Winkelmann, R., and Levermann, A.: Consistent evidence of increasing Antarctic accumulation with warming, *Nat. Clim. Change*, 5, 348–352, <https://doi.org/10.1038/nclimate2574>, 2015.
- Fujita, S., Holmlund, P., Andersson, I., Brown, I., Enomoto, H., Fujii, Y., Fujita, K., Fukui, K., Furukawa, T., Hansson, M., Hara, K., Hoshina, Y., Igarashi, M., Iizuka, Y., Imura, S., Ingvander, S., Karlin, T., Motoyama, H., Nakazawa, F., Oerter,

- H., Sjöberg, L. E., Sugiyama, S., Surdyk, S., Ström, J., Uemura, R., and Wilhelms, F.: Spatial and temporal variability of snow accumulation rate on the East Antarctic ice divide between Dome Fuji and EPICA DML, *The Cryosphere*, 5, 1057–1081, <https://doi.org/10.5194/tc-5-1057-2011>, 2011.
- Furukawa, T., Kamiyama, K., and Maeno, H.: Snow surface features along the traverse route from the coast to Dome Fuji Station, Queen Maud Land, Antarctica, *Proceedings of the NIPR Symposium on Polar Meteorology and Glaciology*, 10, 13–24, 1996.
- Helsen, M. M., van den Broeke, M. R., van de Wal, R. S. W., van de Berg, W. J., van Meijgaard, E., Davis, C. H., Li, Y. H., and Goodwin, I.: Elevation changes in Antarctica mainly determined by accumulation variability, *Science*, 320, 1626–1629, <https://doi.org/10.1126/science.1153894>, 2008.
- Herron, M. M. and Langway, C. C.: Firn Densification – an Empirical-Model, *J. Glaciol.*, 25, 373–385, <https://doi.org/10.3189/S0022143000015239>, 1980.
- Hoshina, Y., Fujita, K., Iizuka, Y., and Motoyama, H.: Inconsistent relationships between major ions and water stable isotopes in Antarctic snow under different accumulation environments, *Polar Science*, 10, 1–10, <https://doi.org/10.1016/j.polar.2015.12.003>, 2016.
- Hoshina, Y., Fujita, K., Nakazawa, F., Iizuka, Y., Miyake, T., Hirabayashi, M., Kuramoto, T., Fujita, S., and Motoyama, H.: Effect of accumulation rate on water stable isotopes of near-surface snow in inland Antarctica, *J. Geophys. Res.-Atmos.*, 119, 274–283, <https://doi.org/10.1002/2013jd020771>, 2014.
- Huybrechts, P., Rybak, O., Pattyn, F., Ruth, U., and Steinhage, D.: Ice thinning, upstream advection, and non-climatic biases for the upper 89 % of the EDML ice core from a nested model of the Antarctic ice sheet, *Clim. Past*, 3, 577–589, <https://doi.org/10.5194/cp-3-577-2007>, 2007.
- IPCC: IPCC Special Report on the Ocean and Cryosphere in a Changing Climate, edited by: Poertner, H.-O., Roberts, D. C., Masson-Delmotte, V., Zhai, P., Tignor, M., Poloczanska, E., Mintenbeck, K., Alegria, A., Nicolai, M., Okem, A., Petzold, J., Rama, B., and Weyer, N. M., IPCC, in press, 2019.
- Kane, H. S.: A study of 10 m firn temperatures in central East Antarctica, *IAHS*, 86, 165–174, 1970.
- Karlov, L., Isaksson, E., Winther, J. G., Gundestrup, N., Meijer, H. A. J., Mulvaney, R., Pourchet, M., Hofstede, C., Lappégard, G., Pettersson, R., Van den Broeke, M., and Van De Wal, R. S. W.: Accumulation variability over a small area in east Dronning Maud Land, Antarctica, as determined from shallow firn cores and snow pits: some implications for ice-core records, *J. Glaciol.*, 51, 343–352, <https://doi.org/10.3189/172756505781829232>, 2005.
- Karlöf, L., Winebrenner, D. P., and Percival, D. B.: How representative is a time series derived from a firn core? A study at a low-accumulation site on the Antarctic plateau, *J. Geophys. Res.*, 111, F04001, <https://doi.org/10.1029/2006jf000552>, 2006.
- Karlsson, N. B., Binder, T., Eagles, G., Helm, V., Pattyn, F., Van Liefferinge, B., and Eisen, O.: Glaciological characteristics in the Dome Fuji region and new assessment for “Oldest Ice”, *The Cryosphere*, 12, 2413–2424, <https://doi.org/10.5194/tc-12-2413-2018>, 2018.
- Kaspers, K. A., van de Wal, R. S. W., van den Broeke, M. R., Schwander, J., van Lipzig, N. P. M., and Brenninkmeijer, C. A. M.: Model calculations of the age of firn air across the Antarctic continent, *Atmos. Chem. Phys.*, 4, 1365–1380, <https://doi.org/10.5194/acp-4-1365-2004>, 2004.
- Laepple, T., Hörhold, M., Münch, T., Freitag, J., Wegner, A., and Kipfstuhl, S.: Layering of surface snow and firn at Kohnen Station, Antarctica: Noise or seasonal signal?, *J. Geophys. Res.-Ea. Surf.*, 121, 1849–1860, <https://doi.org/10.1002/2016jg003919>, 2016.
- Lenaerts, J. T. M. and van den Broeke, M. R.: Modeling drifting snow in Antarctica with a regional climate model: 2. Results, *J. Geophys. Res.-Atmos.*, 117, D05109, <https://doi.org/10.1029/2010jd015419>, 2012.
- Lenaerts, J. T. M., Medley, B., van den Broeke, M. R., and Wouters, B.: Observing and Modeling Ice Sheet Surface Mass Balance, *Rev. Geophys.*, 57, 376–420, <https://doi.org/10.1029/2018rg000622>, 2019.
- Ligtenberg, S. R. M., Helsen, M. M., and van den Broeke, M. R.: An improved semi-empirical model for the densification of Antarctic firn, *The Cryosphere*, 5, 809–819, <https://doi.org/10.5194/tc-5-809-2011>, 2011.
- Mätzler, C.: Microwave permittivity of dry snow, *IEEE Trans. Geosci. Remote*, 34, 573–581, <https://doi.org/10.1109/36.485133>, 1996.
- McMillan, M., Shepherd, A., Sundal, A., Briggs, K., Muir, A., Ridout, A., Hogg, A., and Wingham, D.: Increased ice losses from Antarctica detected by CryoSat-2, *Geophys. Res. Lett.*, 41, 3899–3905, <https://doi.org/10.1002/2014gl060111>, 2014.
- Medley, B., McConnell, J. R., Neumann, T. A., Reijmer, C. H., Chellman, N., Sigl, M., and Kipfstuhl, S.: Temperature and Snowfall in Western Queen Maud Land Increasing Faster Than Climate Model Projections, *Geophys. Res. Lett.*, 45, 1472–1480, <https://doi.org/10.1002/2017gl075992>, 2018.
- Medley, B. and Thomas, E. R.: Increased snowfall over the Antarctic Ice Sheet mitigated twentieth-century sea-level rise, *Nat. Clim. Change*, 9, 34–39, <https://doi.org/10.1038/s41558-018-0356-x>, 2019.
- Münch, T., Kipfstuhl, S., Freitag, J., Meyer, H., and Laepple, T.: Regional climate signal vs. local noise: a two-dimensional view of water isotopes in Antarctic firn at Kohnen Station, Dronning Maud Land, *Clim. Past*, 12, 1565–1581, <https://doi.org/10.5194/cp-12-1565-2016>, 2016.
- Nghiem, S. V., Hall, D. K., Mote, T. L., Tedesco, M., Albert, M. R., Keegan, K., Shuman, C. A., DiGirolamo, N. E., and Neumann, G.: The extreme melt across the Greenland ice sheet in 2012, *Geophys. Res. Lett.*, 39, L20502, <https://doi.org/10.1029/2012gl053611>, 2012.
- Oerter, H.: High resolution density and d18O of snow pits DML76S05_11 to DML90S05_25, *Pangaea*, <https://doi.org/10.1594/PANGAEA.708082>, 2008.
- Oerter, H., Graf, W., Meyer, H., and Wilhelms, F.: The EPICA ice core from Dronning Maud Land: first results from stable-isotope measurements, *Ann. Glaciol.*, 39, 307–312, <https://doi.org/10.3189/172756404781814032>, 2004.
- Oerter, H., Graf, W., Wilhelms, F., Minikin, A., and Miller, H.: Accumulation studies on Amundsenisen, Dronning Maud Land, Antarctica, by means of tritium, dielectric profiling and stable-isotope measurements: first results from the 1995–96 and 1996–97 field seasons, *Ann. Glaciol.*, 29, 1–9, <https://doi.org/10.3189/172756499781820914>, 1999.

- Oerter, H., Wilhelms, F., Jung-Rothenhausler, F., Goktas, F., Miller, H., Graf, W., and Sommer, S.: Accumulation rates in Dronning Maud Land, Antarctica, as revealed by dielectric-profiling measurements of shallow firn cores, *Ann. Glaciol.*, 30, 27–34, <https://doi.org/10.3189/172756400781820705>, 2000.
- Parish, T. R.: Surface winds over the Antarctic continent – a review, *Rev. Geophys.*, 26, 169–180, <https://doi.org/10.1029/RG026i001p00169>, 1988.
- Picciotto, E., Crozaz, G., and De Breuck, W.: Accumulation on the South Pole-Queen Maud Land Traverse, 1964–1968, in: *Antarctic Snow and Ice Studies II*, edited by: Crary, A. P., Antarctic Research Series, Washington, DC, 1971.
- Proksch, M., Lowe, H., and Schneebeli, M.: Density, specific surface area, and correlation length of snow measured by high-resolution penetrometry, *J. Geophys. Res.-Ea. Surf.*, 120, 346–362, <https://doi.org/10.1002/2014jfg003266>, 2015.
- Reijmer, C. H. and van den Broeke, M. R.: Temporal and spatial variability of the surface mass balance in Dronning Maud Land, Antarctica, as derived from automatic weather stations, *J. Glaciol.*, 49, 512–520, <https://doi.org/10.3189/172756503781830494>, 2003.
- Rignot, E., Mouginot, J., and Scheuchl, B.: Ice flow of the Antarctic ice sheet, *Science*, 333, 1427–1430, 2011.
- Rignot, E., Mouginot, J., Scheuchl, B., van den Broeke, M., van Wessem, M. J., and Morlighem, M.: Four decades of Antarctic Ice Sheet mass balance from 1979–2017, *P. Natl. Acad. Sci. USA*, 116, 1095–1103, <https://doi.org/10.1073/pnas.1812883116>, 2019.
- Rotschky, G., Eisen, O., Wilhelms, F., Nixdorf, U., and Oerter, H.: Spatial distribution of surface mass balance on Amundsenisen plateau, Antarctica, derived from ice-penetrating radar studies, *Ann. Glaciol.*, 39, 265–270, <https://doi.org/10.3189/172756404781814618>, 2004.
- Sanz Rodrigo, J., Buchlin, J.-M., van Beeck, J., Lenaerts, J. T. M., and van den Broeke, M. R.: Evaluation of the antarctic surface wind climate from ERA reanalyses and RACMO2/ANT simulations based on automatic weather stations, *Clim. Dynam.*, 40, 353–376, <https://doi.org/10.1007/s00382-012-1396-y>, 2012.
- Schaller, C. F.: Towards understanding the signal formation in polar snow, firn and ice using X-ray computed tomography, PhD Thesis, Department of Geosciences, University Bremen, Bremen, 2018.
- Schaller, C. F., Freitag, J., Kipfstuhl, S., Laepple, T., Steen-Larsen, H. C., and Eisen, O.: A representative density profile of the North Greenland snowpack, *The Cryosphere*, 10, 1991–2002, <https://doi.org/10.5194/tc-10-1991-2016>, 2016.
- Schröder, L., Horwath, M., Dietrich, R., Helm, V., van den Broeke, M. R., and Ligtenberg, S. R. M.: Four decades of Antarctic surface elevation changes from multi-mission satellite altimetry, *The Cryosphere*, 13, 427–449, <https://doi.org/10.5194/tc-13-427-2019>, 2019.
- Schwerdtfeger, W.: Ice Crystal Precipitation on the Antarctic Plateau, *Antarctic Journal of the United States*, 4, 221–222, 1969.
- Shepherd, A., Gilbert, L., Muir, A. S., Konrad, H., McMillan, M., Slater, T., Briggs, K. H., Sundal, A. V., Hogg, A. E., and Engdahl, M. E.: Trends in Antarctic Ice Sheet Elevation and Mass, *Geophys. Res. Lett.*, 46, 8174–8183, <https://doi.org/10.1029/2019gl082182>, 2019.
- Shepherd, A., Ivins, E., Rignot, E., Smith, B., van den Broeke, M., Velicogna, I., Whitehouse, P., Briggs, K., Joughin, I., Krinner, G., Nowicki, S., Payne, T., Scambos, T., Schlegel, N., Geruo, A., Agosta, C., Ahlstrom, A., Babonis, G., Barletta, V., Blazquez, A., Bonin, J., Csatho, B., Cullather, R., Felikson, D., Fettweis, X., Forsberg, R., Gallee, H., Gardner, A., Gilbert, L., Groh, A., Gunter, B., Hanna, E., Harig, C., Helm, V., Horvath, A., Horwath, M., Khan, S., Kjeldsen, K. K., Konrad, H., Langen, P., Lecavalier, B., Loomis, B., Luthcke, S., McMillan, M., Melini, D., Mernild, S., Mohajerani, Y., Moore, P., Mouginot, J., Moyano, G., Muir, A., Nagler, T., Nield, G., Nilsson, J., Noel, B., Otosaka, I., Pattle, M. E., Peltier, W. R., Pie, N., Rietbroek, R., Rott, H., Sandberg-Sorensen, L., Sasgen, I., Save, H., Scheuchl, B., Schrama, E., Schroder, L., Seo, K. W., Simonsen, S., Slater, T., Spada, G., Sutterley, T., Talpe, M., Tarasov, L., van de Berg, W. J., van der Wal, W., van Wessem, M., Vishwakarma, B. D., Wiese, D., Wouters, B., and Team, I.: Mass balance of the Antarctic Ice Sheet from 1992 to 2017, *Nature*, 558, 219–222, <https://doi.org/10.1038/s41586-018-0179-y>, 2018.
- Shepherd, A., Ivins, E. R., A. G., Barletta, V. R., Bentley, M. J., Bettadpur, S., Briggs, K. H., Bromwich, D. H., Forsberg, R., Galin, N., Horwath, M., Jacobs, S., Joughin, I., King, M. A., Lenaerts, J. T., Li, J., Ligtenberg, S. R., Luckman, A., Luthcke, S. B., McMillan, M., Meister, R., Milne, G., Mouginot, J., Muir, A., Nicolas, J. P., Paden, J., Payne, A. J., Pritchard, H., Rignot, E., Rott, H., Sorensen, L. S., Scambos, T. A., Scheuchl, B., Schrama, E. J., Smith, B., Sundal, A. V., van Angelen, J. H., van de Berg, W. J., van den Broeke, M. R., Vaughan, D. G., Velicogna, I., Wahr, J., Whitehouse, P. L., Wingham, D. J., Yi, D., Young, D., and Zwally, H. J.: A reconciled estimate of ice-sheet mass balance, *Science*, 338, 1183–1189, <https://doi.org/10.1126/science.1228102>, 2012.
- Sihvola, A. and Tiuri, M.: Snow fork for field determination of the density and wetness profiles of a snow pack, *IEEE Trans. Geosci. Remote*, 24, 717–721, <https://doi.org/10.1109/tgrs.1986.289619>, 1986.
- Slater, T., Shepherd, A., McMillan, M., Armitage, T. W. K., Otosaka, I., and Arthern, R. J.: Compensating Changes in the Penetration Depth of Pulse-Limited Radar Altimetry Over the Greenland Ice Sheet, *IEEE Trans. Geosci. Remote*, 57, 9633–9642, <https://doi.org/10.1109/tgrs.2019.2928232>, 2019.
- Sommer, C. G., Wever, N., Fierz, C., and Lehning, M.: Investigation of a wind-packing event in Queen Maud Land, Antarctica, *The Cryosphere*, 12, 2923–2939, <https://doi.org/10.5194/tc-12-2923-2018>, 2018.
- Sorensen, L. S., Simonsen, S. B., Langley, K., Gray, L., Helm, V., Nilsson, J., Stenseng, L., Skourup, H., Forsberg, R., and Davidson, M. W. J.: Validation of CryoSat-2 SARIn Data over Austfonna Ice Cap Using Airborne Laser Scanner Measurements, *Remote Sens.*, 10, 1354, <https://doi.org/10.3390/rs10091354>, 2018.
- Stenni, B., Curran, M. A. J., Abram, N. J., Orsi, A., Goursaud, S., Masson-Delmotte, V., Neukom, R., Goosse, H., Divine, D., van Ommen, T., Steig, E. J., Dixon, D. A., Thomas, E. R., Bertler, N. A. N., Isaksson, E., Ekaykin, A., Werner, M., and Frezzotti, M.: Antarctic climate variability on regional and continental scales over the last 2000 years, *Clim. Past*, 13, 1609–1634, <https://doi.org/10.5194/cp-13-1609-2017>, 2017.
- Sugiyama, S., Enomoto, H., Fujita, S., Fukui, K., Nakazawa, F., Holmlund, P., and Surdyk, S.: Snow density along the route tra-

- versed by the Japanese-Swedish Antarctic Expedition 2007/08, *J. Glaciol.*, 58, 529–539, <https://doi.org/10.3189/2012JoG11J201>, 2012.
- Thomas, R., Davis, C., Frederick, E., Krabill, W., Li, Y., Manizade, S., and Martin, C.: A comparison of Greenland ice-sheet volume changes derived from altimetry measurements, *J. Glaciol.*, 54, 203–212, <https://doi.org/10.3189/002214308784886225>, 2008.
- Tian, Y., Zhang, S., Du, W., Chen, J., Xie, H., Tong, X., and Li, R.: Surface snow density of east antarctica derived from in-situ observations, *Int. Arch. Photogramm. Remote Sens. Spatial Inf. Sci.*, XLII-3, 1657–1660, <https://doi.org/10.5194/isprs-archives-XLII-3-1657-2018>, 2018.
- Van Liefferinge, B., Pattyn, F., Cavitte, M. G. P., Karlsson, N. B., Young, D. A., Sutter, J., and Eisen, O.: Promising Oldest Ice sites in East Antarctica based on thermodynamical modelling, *The Cryosphere*, 12, 2773–2787, <https://doi.org/10.5194/tc-12-2773-2018>, 2018.
- van Lipzig, N. P. M., Turner, J., Colwell, S. R., and van Den Broeke, M. R.: The near-surface wind field over the Antarctic continent, *Int. J. Climatol.*, 24, 1973–1982, <https://doi.org/10.1002/joc.1090>, 2004.

4 PUBLICATION II

SPATIAL DISTRIBUTION OF CRUSTS IN ANTARCTIC AND GREENLAND SNOWPACKS AND IMPLICATIONS FOR SNOW AND FIRN STUDIES

Weinhart, A. H., Kipfstuhl, S., Hörhold, M., Eisen, O., and Freitag, J.

Frontiers in Earth Science, published on 25 March 2021

Doi: 10.3389/feart.2021.630070



Spatial Distribution of Crusts in Antarctic and Greenland Snowpacks and Implications for Snow and Firn Studies

Alexander H. Weinhart^{1*}, Sepp Kipfstuhl¹, Maria Hörhold¹, Olaf Eisen^{1,2} and Johannes Freitag^{1*}

¹Alfred-Wegener-Institut Helmholtz-Zentrum für Polar- und Meeresforschung, Bremerhaven, Germany, ²Universität Bremen, Fachbereich Geowissenschaften, Bremen, Germany

OPEN ACCESS

Edited by:

Markus Michael Frey,
British Antarctic Survey (BAS),
United Kingdom

Reviewed by:

Martin Schneebeli,
WSL Institute for Snow and Avalanche
Research SLF, Switzerland
Amaelle Adeline Landais,
Centre National de la Recherche
Scientifique (CNRS), France

*Correspondence:

Alexander H. Weinhart
alexander.weinhart@awi.de
Johannes Freitag
johannes.freitag@awi.de

Specialty section:

This article was submitted to
Cryospheric Sciences,
a section of the journal
Frontiers in Earth Science

Received: 16 November 2020

Accepted: 09 February 2021

Published: 25 March 2021

Citation:

Weinhart AH, Kipfstuhl S, Hörhold M,
Eisen O and Freitag J (2021) Spatial
Distribution of Crusts in Antarctic and
Greenland Snowpacks and
Implications for Snow and Firn Studies.
Front. Earth Sci. 9:630070.
doi: 10.3389/feart.2021.630070

The occurrence of snowpack features has been used in the past to classify environmental regimes on the polar ice sheets. Among these features are thin crusts with high density, which contribute to firn stratigraphy and can have significant impact on firn ventilation as well as on remotely inferred properties like accumulation rate or surface mass balance. The importance of crusts in polar snowpack has been acknowledged, but nonetheless little is known about their large-scale distribution. From snow profiles measured by means of microfocuss X-ray computer tomography we created a unique dataset showing the spatial distribution of crusts in snow on the East Antarctic Plateau as well as in northern Greenland including a measure for their local variability. With this method, we are able to find also weak and oblique crusts, to count their frequency of occurrence and to measure the high-resolution density. Crusts are local features with a small spatial extent in the range of tens of meters. From several profiles per sampling site we are able to show a decreasing number of crusts in surface snow along a traverse on the East Antarctic Plateau. Combining samples from Antarctica and Greenland with a wide range of annual accumulation rate, we find a positive correlation ($R^2 = 0.89$) between the logarithmic accumulation rate and crusts per annual layer in surface snow. By counting crusts in two Antarctic firn cores, we can show the preservation of crusts with depth and discuss their temporal variability as well as the sensitivity to accumulation rate. In local applications we test the robustness of crusts as a seasonal proxy in comparison to chemical records like impurities or stable water isotopes. While in regions with high accumulation rates the occurrence of crusts shows signs of seasonality, in low accumulation areas dating of the snowpack should be done using a combination of volumetric and stratigraphic elements. Our data can bring new insights for the study of firn permeability, improving of remote sensing signals or the development of new proxies in snow and firn core research.

Keywords: Antarctica, Greenland, polar snow, snow stratigraphy, crusts, snow properties, accumulation rate

INTRODUCTION

Densification of snow to ice is one of the key processes at the surface of ice sheets and glaciers (Herron and Langway, 1980). The (local) characteristics at the interface of the atmosphere and the ice pre-condition the rates of further densification (Hörhold et al., 2011), which are of primary importance for the paleo-atmospheric archive of air bubbles as well as observations of mass balance (Zwally and Jun, 2017). Due to the rapid and significant technological progress, there are plenty of methods to derive snow properties of the polar ice sheets remotely. In contrast, field observations are still preciously scarce, albeit of their necessity to validate remote measurements of e.g. accumulation rate (Arthern et al., 2006), surface snow density (Champollion et al., 2019), grain size (Picard et al., 2012) or surface roughness (Tran et al., 2008), or for properties which cannot be obtained remotely (yet) like stratigraphic elements in the snow column.

By observing and describing the snow surface and snowpack stratigraphy, regions of different environmental regimes have been characterized, for instance, along overland traverses from the coast to the interior plateau of East Antarctica (Furukawa et al., 1992; Furukawa et al., 1996). These classifications, based on field observations, are commonly used to explain regional accumulation behavior or the influence of wind action on the snow surface. Examples for observed snow characteristics are megadunes in parts of Antarctica (Frezzotti et al., 2002) and smaller wind-induced dunes in Dronning Maud Land (DML) where a wind speed threshold of 10 ms^{-1} for dune formation at Kohnen Station was reported (Birnbaum et al., 2010).

Directly at the snow surface formation conditions for glazed surfaces on the West Antarctic Ice Sheet Divide ($79^{\circ}27.78'S$, $112^{\circ}7.51'W$) have been monitored by Fegyveresi et al. (2018). Glazed surfaces have low porosity, can be one to several millimeters thick and form throughout the year, but according to the case study by Fegyveresi et al. (2018) primarily in summer. Glazed surfaces are reported to form after an event with high wind speed and eventually accumulation, followed by clear-sky conditions, low wind speed and higher atmospheric pressure enhancing the possibility of water vapor transport vertically upwards and the formation of subsurface hoar (Albert et al., 2004; Fegyveresi et al., 2018). They can have an extent of up to 200 km^2 and are often found in leeward slopes of large-scale dunes formed by katabatic winds (Scambos et al., 2012). A very similar structural feature are smaller crusts, sometimes also referred to as windcrusts (Sommer et al., 2018a), which can be defined as very thin ($<2 \text{ mm}$) high-density layers that form at the snow surface. In many field studies their appearance at the very surface as well as recurring features in firn and ice is reported as a side note in stratigraphy description. Monitoring of a wind-packing event in DML (Sommer et al., 2018b) and wind tunnel experiments (Sommer et al., 2018a) have indicated that snow deposition and wind (drift) in combination with exposition at the surface are necessary to form a crust. But the exact formation of both features (glazed surfaces and crusts) is still not completely clear, as the temporal development was rarely observed and methodical approaches for this intention are hardly available (Fegyveresi et al., 2018). This also applies to studies on

the spatial distribution of crusts or quantitative studies of crust appearance in general. Based on this sparse knowledge, also their relevance for ice core studies is not well understood. As at the snow-atmosphere interface many physical and chemical processes take place in a complex way, especially the exchange of energy and mass, a variety of processes must interact to form a crust at the snow surface. Nevertheless, crusts have been counted and used in combination with impurities as relative dating approach in low accumulation areas and are interpreted in a very local application as a summer marker (Ren et al., 2004; Hoshina et al., 2014).

In general, dating reference horizons from volcanic eruptions in ice cores and calculating the water equivalent in a given period of time is a state of the art method to derive accumulation rates at certain positions on the ice sheets (Eisen et al., 2008). If an absolute time marker is missing, proxies like impurities or stable water isotopes can be used as relative temporal markers on a decadal, annual or even seasonal scale (Münch et al., 2016). In central Greenland, sea salt aerosols chloride and sodium (Cl^- and Na^+) are interpreted to reflect the winter to spring transition, while maxima in the ratio of chloride to sodium (further Cl^-/Na^+) are attributed to summer (Whitlow et al., 1992). Also ammonium (NH_4^+), nitrate (NO_3^-) and methanesulphonic acid (MSA) can be interpreted as a summer signal (Du et al., 2019). On the plateau of the Antarctic ice sheet, sulphate (SO_4^{2-}) as well as Cl^-/Na^+ can be interpreted as seasonal summer to late summer signals (Weller and Wagenbach, 2007) and also NH_4^+ , calcium (Ca^{2+}) and Na^+ have been used successfully as seasonal markers in DML ice cores for the past 2 ka (Sommer et al., 2000). At Kohnen Station (Figure 1), a link of crusts to seasonal anisotropy has been proposed (Moser et al., 2020). But so far, there has been no study backing crusts as a solid summer proxy in low accumulation areas. Especially on short (annual to seasonal) time scales the determination of an annual layer thickness from stratigraphy is problematic, as the accumulation is not evenly distributed over the year (precipitation intermittency) and the original deposited climate signal is not preserved in the snow column (Laepple et al., 2011). The exposition of snow at the surface can lead to erosion and redistribution by wind, resulting in a hiatus or overestimating a precipitation event in a time series. These postdepositional alterations also hamper the interpretation of impurities (Weller et al., 2004; Jonsell et al., 2007) or stable water isotopes (Hoshina et al., 2014) in snow, firn and ice. These processes generally occur on the surface of ice sheets, but are much more dominant in areas with low accumulation rates. The extent of these alterations of chemical impurities depends on the individual physico-chemical properties, like volatility, solubility or reactivity, with mineral dust and sea salt being less affected (e.g. Curran et al., 2002; Weller et al., 2004).

The layering of polar firn, and therefore the stratigraphic elements therein, can also serve as a paleoclimatic record. At the same time crusts can block, or at least reduce, the exchange of gases between the atmosphere and the pore space in the firn column (Mitchell et al., 2015). In this context, the open pore structure is a main parameter controlling the permeability and gas transport in firn (Adolph and Albert, 2014). To what extent

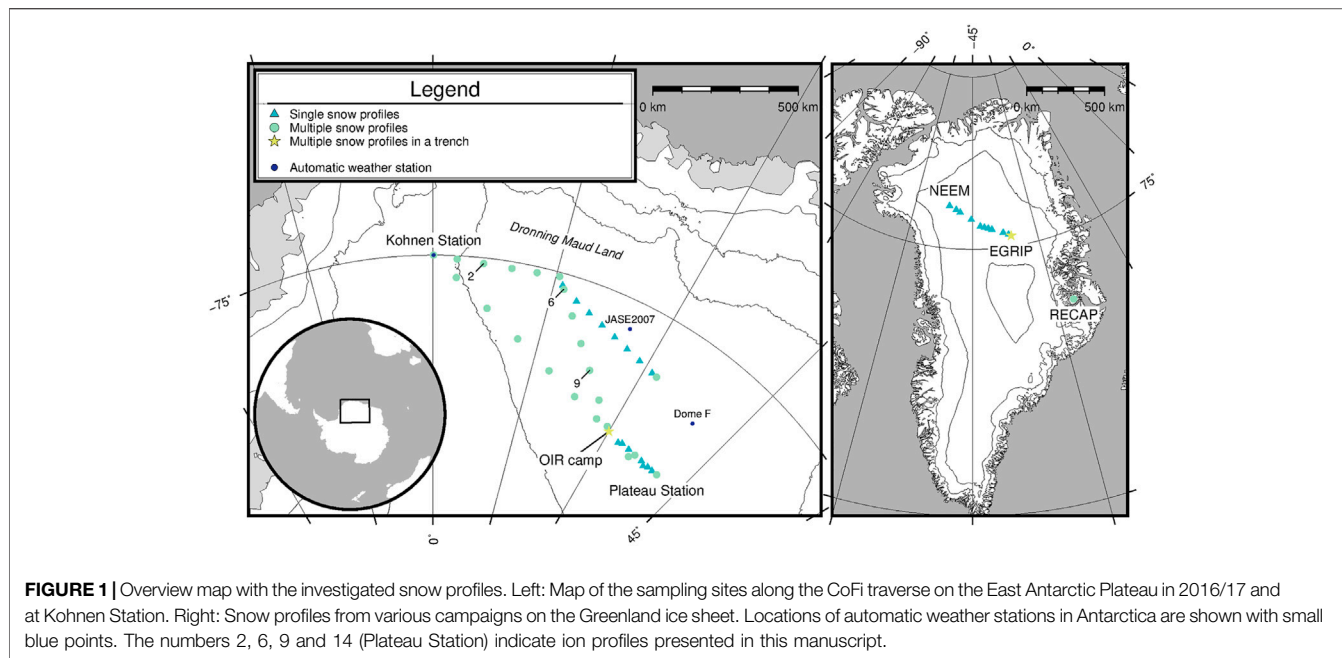


FIGURE 1 | Overview map with the investigated snow profiles. Left: Map of the sampling sites along the CoFi traverse on the East Antarctic Plateau in 2016/17 and at Kohnen Station. Right: Snow profiles from various campaigns on the Greenland ice sheet. Locations of automatic weather stations in Antarctica are shown with small blue points. The numbers 2, 6, 9 and 14 (Plateau Station) indicate ion profiles presented in this manuscript.

layers of low porosity, can impact the pore close-off at the firn-ice transition (Gregory et al., 2014) is still subject to research. Nevertheless, the variability of porosity has been proposed to be a significant factor for the pore close-off depth (Schaller et al., 2017).

Furthermore, crusts are also considered to affect remote sensing backscatter properties (Arthern and Wingham, 1998). The strong density gradient over very short depth intervals can influence (passive) microwave emission and (active) reflection (Wilheit, 1978). Firn volume characteristics have been proposed to be important when remotely deriving accumulation rates in DML (Arthern et al., 2006; Dierking et al., 2012), and there are observations of microwave brightness temperature linked to snowpack properties (Rotschky et al., 2006)—but still there is no conclusive physical explanation. Several approaches try to link these observations to the stratigraphy, i.e. the density layering of the snow and firn (Liang et al., 2008). Here, thin crusts could play an important role, but as they are not always reported in field observations, a systematic analysis of their impact remains open.

In this study, we present a crust dataset from snow cores (snow profiles) along a traverse route on the East Antarctic Plateau as well as from different sites on the Greenland ice sheet. In the results, we show for the first time a spatial distribution of crusts in the snowpack by means of statistical analysis on the local (tens of m) and regional (hundreds of km) scale. With this dataset, we cover an accumulation rate range from $30 \text{ kg m}^{-2} \text{ a}^{-1}$ – $200 \text{ kg m}^{-2} \text{ a}^{-1}$ (and even single samples at $500 \text{ kg m}^{-2} \text{ a}^{-1}$). Additionally, we show a crust record in two firn cores from DML, which gives insights on the temporal variability of crusts, and suggest an explanation for preservation of crusts over depth. With our dataset we contribute some evidence to ideas how crust formation on the polar ice sheets take place (Fegyveresi et al., 2018), in particular in low accumulation areas ($<60 \text{ kg m}^{-2} \text{ a}^{-1}$) like on the East

Antarctic Plateau. We test whether a correlation between the accumulation rate and crust concentration exists and compare our data with environmental parameters like wind speed. In a second step, we follow pilot studies (Ren et al., 2004; Hoshina et al., 2014; Moser et al., 2020) to investigate the link between crusts and chemical proxies in snow. In this context we introduce a cutting device specifically made for snow profiles. For selected samples we show the impurities NH_4^+ , SO_4^{2-} and Cl^-/Na^+ and combine them with our stratigraphic analysis. We discuss the deposition history of the snowpack in Greenland and Antarctica as well as the constraints of dating in low accumulation areas.

MATERIAL AND METHODS

Commonly (wind)crusts and glazed surfaces describe a high density layer at the snow surface, but can form through different processes. Nevertheless, in a snow profile, firn or ice core, these features simply occur as high density layers and are difficult to distinguish. Therefore we will simply use the term ‘crust’, implying that this feature could have been created by either process.

Sampling Area, Snow and Firn Profiles

In this study, we investigated 138 snow profiles from both polar ice sheets covering various environmental conditions. The majority of the profiles (108) was sampled in Antarctica in the framework of the Coldest Firn (CoFi) project at the Alfred Wegener Institute (AWI) in December 2016 and January 2017. One to four snow profiles per sampling site were taken along a traverse on the East Antarctic Plateau between Kohnen Station and former Plateau Station (further called CoFi traverse). Several profiles along a transect line (trench) were sampled at the Oldest Ice Reconnaissance camp (OIR camp; e.g. Karlsson et al.,

TABLE 1 | Overview of investigated firn cores and snow profiles. See **Figure 1** for the locations on both ice sheets.

Type	Name	Site	Ice sheet	Date (mm/yyyy)	Latitude	Longitude	Approx. annual layer thickness (cm)
Snow profile	W10	EGRIP	Greenland	05/2016	75°37'N	35°59'W	50
Firn core	B40	Kohnen Station	Antarctica	01/2013	75°0'S	0°04'E	25
Firn core	B54	OIR camp	Antarctica	01/2017	79°0'S	30°0'E	14
Snow profile	2		Antarctica	12/2016	75°06'S	02°53'E	16
Snow profile	6		Antarctica	12/2016	75°29'S	16°19'E	13
Snow profile	9		Antarctica	12/2016	77°34'S	23°11'E	11
Snow profile	14	Plateau Station	Antarctica	01/2017	79°15'S	40°33'E	9

2018). Eight samples were from Kohnen Station, taken in December 2015 (**Figure 1**, left).

The remaining 22 snow profiles originated from different campaigns in Greenland. Several profiles were sampled at Renland Ice Cap drilling site (RECAP; e.g. Holmes et al., 2019; Simonsen et al., 2019) in May 2015 and in a trench at the East Greenland Ice-Core Project site (EGRIP; e.g. Vallelonga et al., 2014; Du et al., 2019) in May 2016. Single samples (one profile per site) were taken on a traverse between the North Greenland Eemian Ice Drilling site (NEEM; e.g. Steen-Larsen et al., 2011; NEEM Community Members, 2013) and EGRIP in May 2015 (**Figure 1**, right).

The sampling sites (distinguishing between single profiles, multiple profiles and profiles in a trench) are shown in **Figure 1**. For the retrieval of the snow profiles the liner method was used, which was first described by Schaller et al. (2016). The used carbon fiber tubes conserve the original snow stratigraphy with negligible small compaction within the tube. The snow profiles had various lengths, covering the interval from the surface to 1 m or 2 m depth, respectively. More details on the sampling protocols in Antarctica are provided in Weinhart et al. (2020).

Additionally, we analyzed nine 2 m snow profiles along the CoFi traverse and ten 2 m snow profiles in the OIR trench to see the development of crusts with depth. For the investigation of the deeper firn, two firn cores were used in this study, both drilled on the East Antarctic Plateau (**Table 1**). The core B40 was drilled in season 2012/13, B54 in season 2016/17. Both have a total length of 200 m. As we focus on the firn structure, both cores were only considered from surface to 30 m depth.

We use data of the University of Wisconsin-Madison Automatic Weather Station (AWS) Program (JASE2007 and Dome F) as well as data from an AWS9 at Kohnen Station, which was jointly operated by the Institute for Marine and Atmospheric Research and AWI (Reijmer and van den Broeke, 2003), from the years 2016 and 2017.

Non-Destructive Analysis Using μ CT

The snow profiles were analyzed by means of core-scale microfocus X-ray computer tomography (μ CT) at AWI (Freitag et al., 2013). The X-ray source produces a (fan-shaped) cone beam, which is recorded by the detector after being transmitted through the sample. X-ray source and detector move simultaneously along the profile (snow, firn or ice) and record gray value images.

For a density profile of the sample, only the parts of the images parallel to the central radiographic line are processed and the gray values (representing the transmissivity of the radiation) translated into density using a calibration function and ice pieces of known geometry and density (**Figure 2A**). A possible application of the μ CT density can be found in Schaller et al. (2016). The gray value images of the profiles contain visual information about the snow stratigraphy.

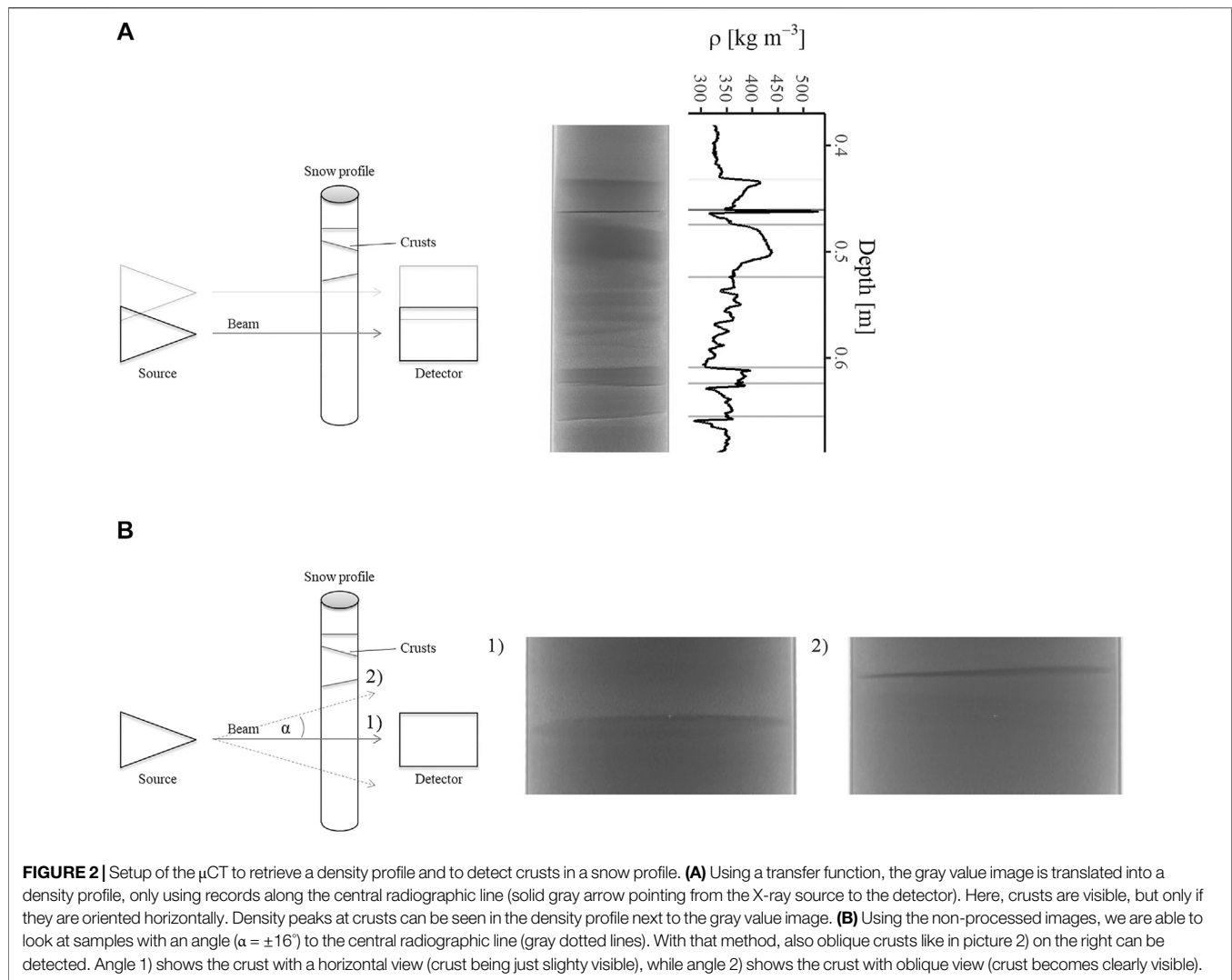
We defined crusts as thin layers with a strong gradient in the gray value in contrast to the surrounding snow (but we did not use a density threshold). In order to identify crusts, we used the non-processed μ CT image sequences, which also store structural information with an angle to the horizontal central radiographic line of $\pm 16^\circ$. With this procedure also oblique crusts could be spotted (**Figure 2B**), which are barely or not visible at all in the processed images. By moving along the snow profile and changing the angle of view, we detected crusts and looked for the angle of view with the highest contrast to the surrounding snow to find their orientation. From this information we calculated the position of the crusts center within the snow profile. Strong crusts can exhibit densities between 400 and 550 kg m⁻³ as determined in the central radiographic line (s. examples in **Figure 2A**). To ensure consistency in detecting the crusts, one person did the manual detection of crusts in all profiles.

Reproducibility of the Method

Counting and categorizing the visible crusts of a 1 m snow or firn section based on the gray value image took roughly 10 min. To validate the method, we also counted crusts in three profiles using 3D-volume imaging from the μ CT like performed in Moser et al. (2020) (s. **Figure 3** therein). In 3D mode, the profiles were investigated in 50 μ m resolution. Exact surfaces of the crusts could be found and detected. The absolute difference in crust counting per profile between both methods was on average ± 1.5 counts (from a total of 20–30 crusts). As we did not see a large difference and the 3D visualization is much more time consuming, the 2D method is the preferred option to count crusts when the 3D microstructure is not part of the investigation.

Calculation of Crust Abundance

To compare the regional presence of crusts in snow, we used the number of crusts in a depth interval of 1 m as a proxy for crust abundance, further called crust concentration (c_m). We also calculated the distribution of crusts over depth locally at



EGRIP, Kohnen Station and the OIR camp by stacking all available profiles and show the result as a histogram.

The densification process begins below a depth of 2–3 m (Weinhart et al., 2020) and evolves differently dependent on mainly temperature and accumulation rate at the different sites (Hörhold et al., 2011). For the investigated firn cores, we calculated the crusts per kg ice (c_{ice}) by dividing c_m by the density of firn (snow in the upper meter, respectively) for each meter interval to account for the differing bulk density and for a better comparability of our results from different locations.

We calculated an ‘annual layer thickness’ at each sampling site of the snow profiles using the snow density and accumulation rate (find values for the profiles that were analyzed for impurities in **Table 1**). For Antarctica we used a surface snow density of 355 kg m^{-3} (Weinhart et al., 2020) and accumulation data from Arthern et al. (2006). In Greenland we used a surface snow density of 335 kg m^{-3} as well as accumulation data derived from reference horizons at the sampling sites (Schaller et al., 2016). Then, we multiplied c_m by the annual layer thickness [m a^{-1}] resulting in the number of crusts per annual layer (c_{al}) in the rate unit a^{-1} .

Discrete Sampling and Chemical Analysis

After the μCT -measurements, selected snow profiles from the CoFi traverse in East Antarctica were cut in discrete samples of 1 cm thickness in the AWI cold laboratory at -18°C . We used a cutting device for snow profiles developed with the AWI workshop (**Figure 3**, left). For the sampling, the snow profile was carefully pushed out of the carbon fiber tube into the holding trough. The snow is cohesive enough to remain as whole piece in the trough (**Figure 3**, right). Length, position of possible breaks and noteworthy features (e.g. visible changes in grain structure, surface undulations, slivered carbon fibers) were noted. An attachment was placed at the end of the cutting device, which controls the thickness of the cut sample width. After pushing the profile forward and cutting one sample, a piston was used to cut out the inner part of the snow profile. As this part is assumed to be contamination-free, it was used for the analysis of impurities by means of ion chromatography (IC). Removing the attachment, the remaining outer part of the cut slice is stored in a separate bag for e.g. isotopic analysis (only presented for EGRIP). Then the area was cleaned with a brush for the next sample. The effective

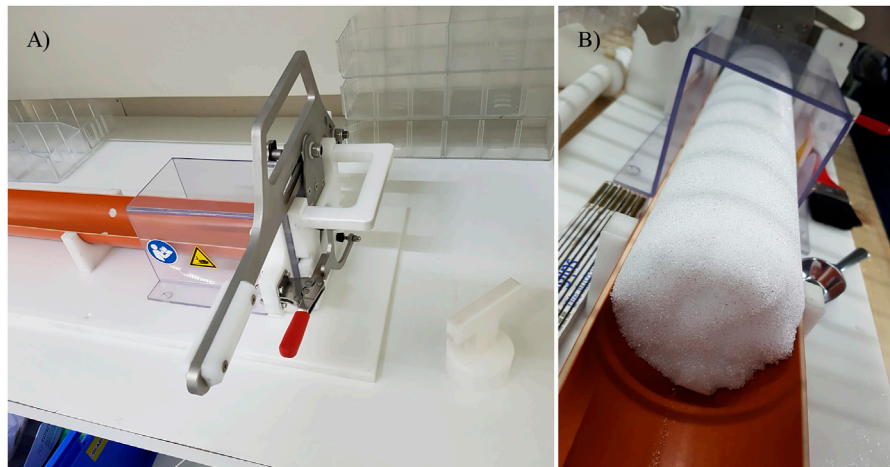


FIGURE 3 | Sampling device for the snow profiles **(A)** Front part of the snow profile cutting device with trough (orange), blade with handle (metal), attachment (white synthetic material, hold in place by clamp with red handle), piston to cut the interior part of the snow profile **(B)** Due to the sampling method and the cohesiveness of the snow the profile remains as one piece, unless breaks or layers with high porosity occur.

sample thickness was slightly below 1 cm as the blade cuts away a small fraction of the snow profile. This is acknowledged in the depth assignment, where the position of each sample with respect to depth is kept constant during the cutting procedure (without a consequence of a possible offset for the depth scale). The sampling was done in teams of two, in which one person was in charge for cutting and collecting the outer part of the snow profile, the other one sampled the contamination-free inner part wearing protective gloves.

Each sample was measured for major ions (Na^+ , NH_4^+ , Ca^{2+} , MSA, Cl^- , SO_4^{2-} , NO_3^-) using a Dionex[®] IC 2100 ion chromatograph. We compare the recognized crusts with the measured ions at selected sampling sites along the CoFi traverse in Antarctica (with decreasing temperature and accumulation rate) and in one profile at EGRIP, Greenland. The profiles in Antarctica are named profile 2, 6, 9 and 14, the profile at EGRIP is called W10 (**Table 1**). As we focus on the seasonality aspect in this study, we only present the ionic species NH_4^+ , SO_4^{2-} as well as Cl^-/Na^+ in the following. For the profile W10 we also show stable water isotopes, which were measured by Ring Down Spectroscopy following the protocol by van Geldern and Barth (2012) with a precision of $<0.1\%$ for $\delta^{18}\text{O}$.

RESULTS

Most crusts are in the thickness range of 0.5–1 mm. The thickest crusts can be up to 2 mm thick, which is rather an exception. We do not find a trend or striking differences in crust thickness at the different sampling sites, i.e. the crust thickness is not higher at warmer sites with higher accumulation rate. We can report a high potential for depth hoar layers just below the crusts (s. *Stratification of the Snow Column Through Crusts* Section).

Spatial Distribution of Crusts On the DML Plateau, East Antarctica

Within the samples from Antarctica, we find the maximum c_m (23.5 m^{-1}) from the surface to 1 m depth close to Kohnen Station. Along the CoFi traverse c_m decreases and has its minimum on the plateau between OIR camp and Plateau Station, where we count an average c_m of 9 m^{-1} (**Figure 4**). The mean standard deviation at sampling sites with four profiles along the traverse is 3.8 m^{-1} . We record the maximum standard deviation at OIR camp with 7.5 m^{-1} .

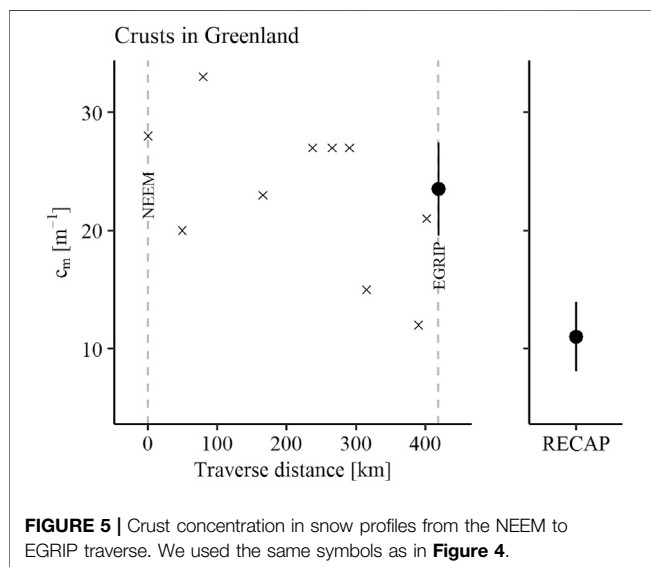
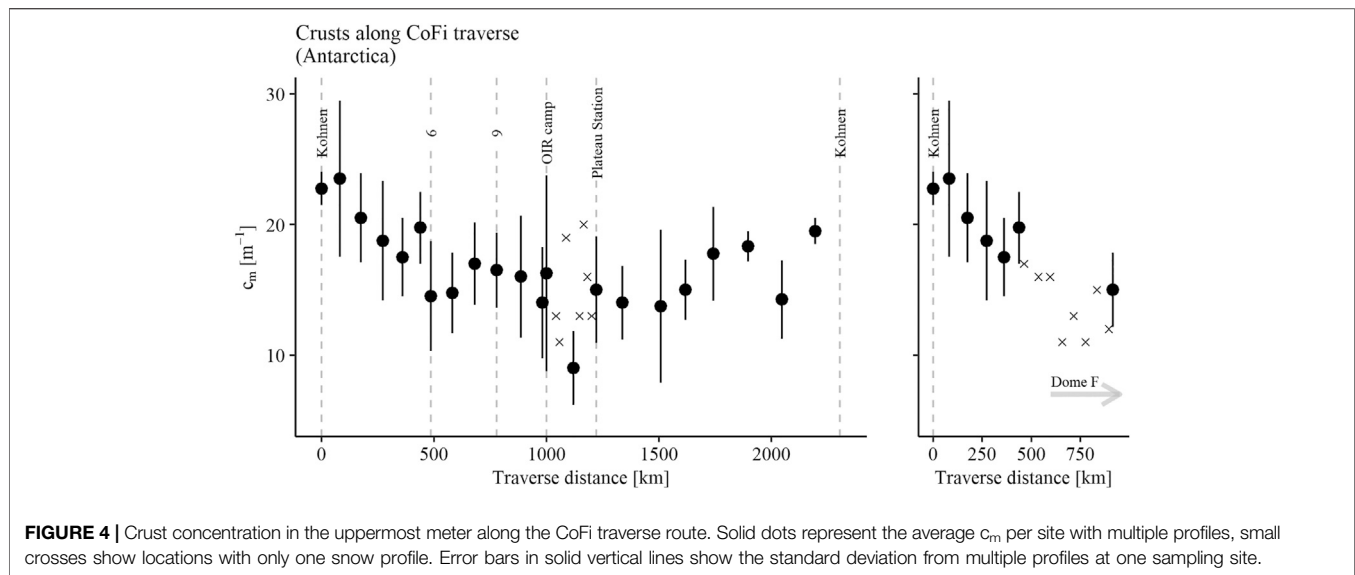
On the Greenland Plateau

In Greenland, the highest c_m is found at NEEM (28 m^{-1}) and close to NEEM (33 m^{-1}) (**Figure 5**). As we only have one snow profile per site along the traverse, the statistics are not as solid as for the CoFi traverse in Antarctica. The average c_m in the depth range 0–1 m along the whole traverse amounts to 23.3 m^{-1} . This fits well with c_m of 23.5 m^{-1} at EGRIP from eight samples. At EGRIP, we calculated a standard deviation of 3.9 m^{-1} , at RECAP of 2.9 m^{-1} (four samples).

Crusts vs. Accumulation Rate

We show c_m (**Figure 6A**) and c_{al} (**Figure 6B**) plotted against the logarithmic accumulation rate. We see a steady increase in c_{al} with increasing accumulation rate. A linear fit between the logarithmic accumulation rate and c_{al} results in a coefficient of determination (R^2) of 0.89 (plotted in **Figure 6B**). Note that this spatial correlation applies to the total dataset, i.e. from Greenland and Antarctica.

For an estimation of the temporal sensitivity of crusts to accumulation rate, we calculated c_{al} in B40 up to 15 m depth using a five-year running mean for both, crusts and accumulation rate, as the latter is subject to large interannual variability (in some cases roughly a factor of two in consecutive years—note that this is an artifact of a



single point measurement and not necessarily representative for a larger area). The regression analysis on the temporal scale also results in a positive correlation, but with a much lower R^2 (0.36) than on the spatial scale (**Figure 6C**). A potential bias of the slope is discussed in *Crust concentration in relation to accumulation rate* Section. We consider the temporal resolution of the accumulation rate in B54 and thus c_{ai} as not precise enough to perform a regression analysis here as well.

Vertical Record of Crusts in East Antarctic Firm

We see a decrease in c_m from 0 to 2 m depth. The relative decrease seems to be higher at sites with a higher c_m in the first meter. At Kohnen Station, from the first to the second meter in depth there

is a reduction in c_m of 27% (average of eight samples), at OIR camp of 25% (ten samples). But single samples along the traverse also show a reduction of over 50%.

The maximum lateral extent of crusts can be followed in the OIR trench, where it ranges between 10 and 15 m, typical dimensions of the snow patches perpendicular to the mean wind direction. In addition, the depth position of crusts is rarely consistent among nearby sampling sites on the East Antarctic Plateau. This can be explained by the high surface roughness relative to the annual accumulation rate as dune heights can exceed two or three times the annual layer thickness (Weinhart et al., 2020).

c_m in the firn cores at Kohnen Station and the OIR camp agrees well with c_m in snow profiles in the vicinity of the firn cores. In core B40 we count 21 crusts in the first meter and 18 in the second meter, whereas in core B54 we only find eight and seven crusts in the first and second meter, respectively. In both cores, c_{ice} decreases steadily but does not fall below 10 kg^{-1} (**Figures 7A,B**).

Local Vertical Crust Distribution

We also find profiles where multiple crusts form on top of each other, also oblique to each other with only few millimeters between them. The question arises, whether a preference for the crusts to form in a distinct period of time is visible in several profiles from the same location. This could then indicate the annual layering on a local scale. At EGRIP in a stack of several profiles the crust distribution over depth agrees with the annual layer thickness (**Table 1; Figure 8A**). At Kohnen Station five local maxima in the crust count can be seen, which is consistent with the local accumulation rate (**Figure 8B**). At the OIR camp, the histogram is not as clear. The higher the surface roughness and the lower the accumulation rate, the more difficult is the recognition of a lateral consistency of crusts. For the smaller bin width (2.5 cm), we count eight local maxima, which could be

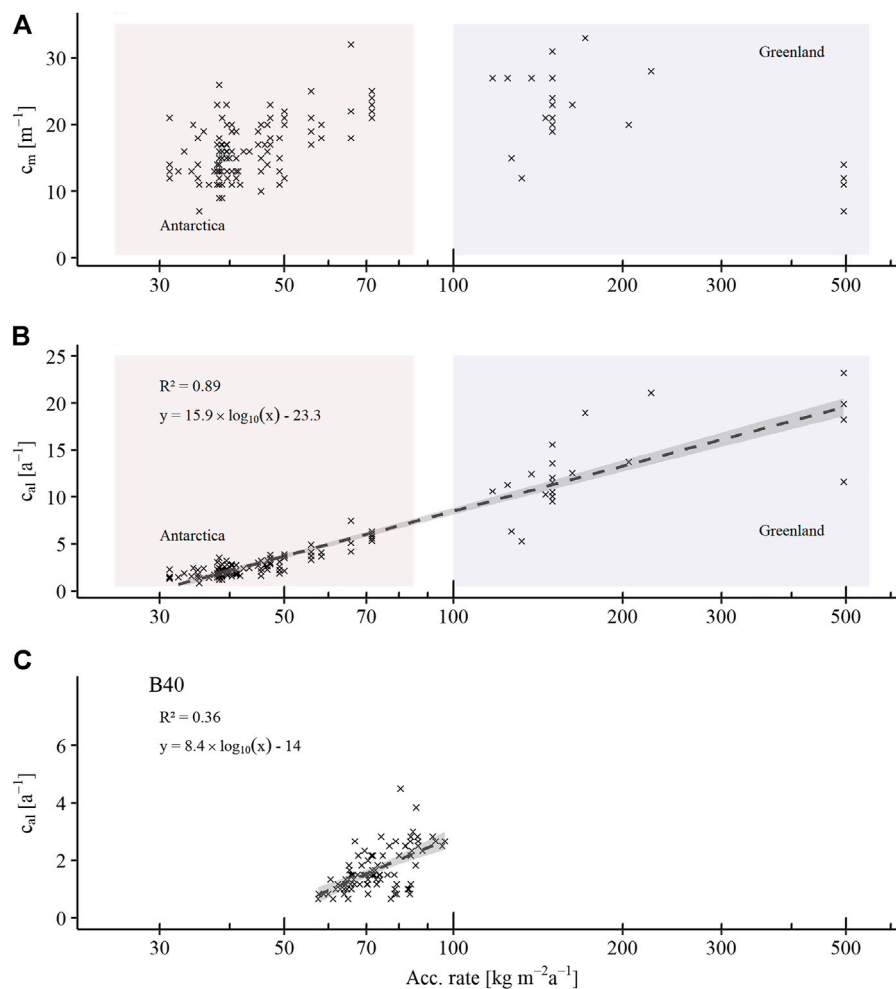


FIGURE 6 | (A) and (B): Spatial crust statistics for Antarctica and Greenland. We used the crust information in snow of the top meter at all sampling sites. In **(A)** the crust concentration, in **(B)** the crust concentration per annual layer is plotted against the accumulation rate (logarithmic scale) at each sampling position. With increasing accumulation rate, also the number of crusts per year increases **(C)**: Five-year running mean of crust concentration per annual layer, also plotted against the accumulation rate (logarithmic scale), in firm core B40 (up to 15 m depth) over the last 100 years at Kohlen Station. It shows the temporal evolution of crusts with changing accumulation rate, possibly affected/biased by the destruction of crusts through metamorphism with depth (and time).

congruent with the local accumulation rate or the number of deposition events (**Figure 8C**).

Impurities in Snow Profiles From Antarctica and Greenland

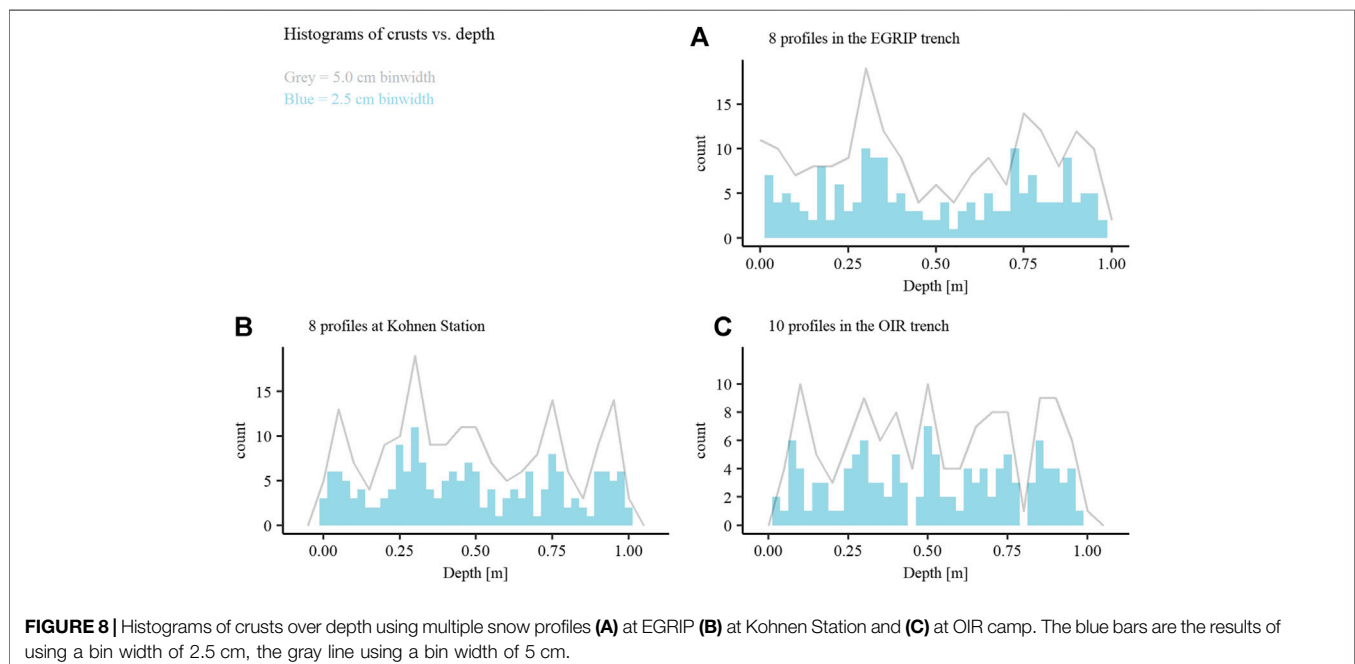
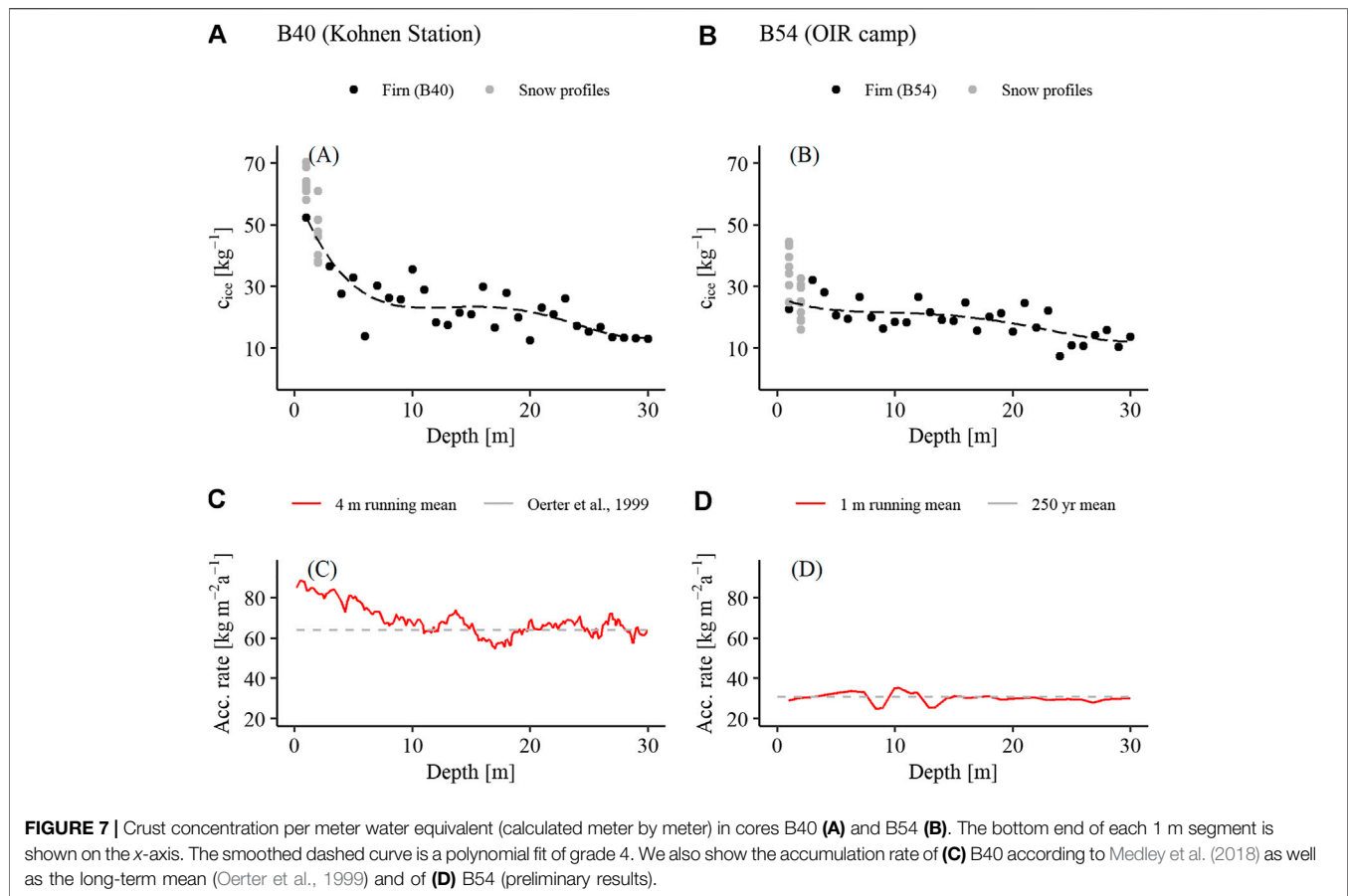
The corresponding impurity profiles to the results presented in this section are shown in **Figure 9** and **Figure 10** in *Case study at EGRIP (Greenland)* and *Case study in DML (Antarctica)* Sections.

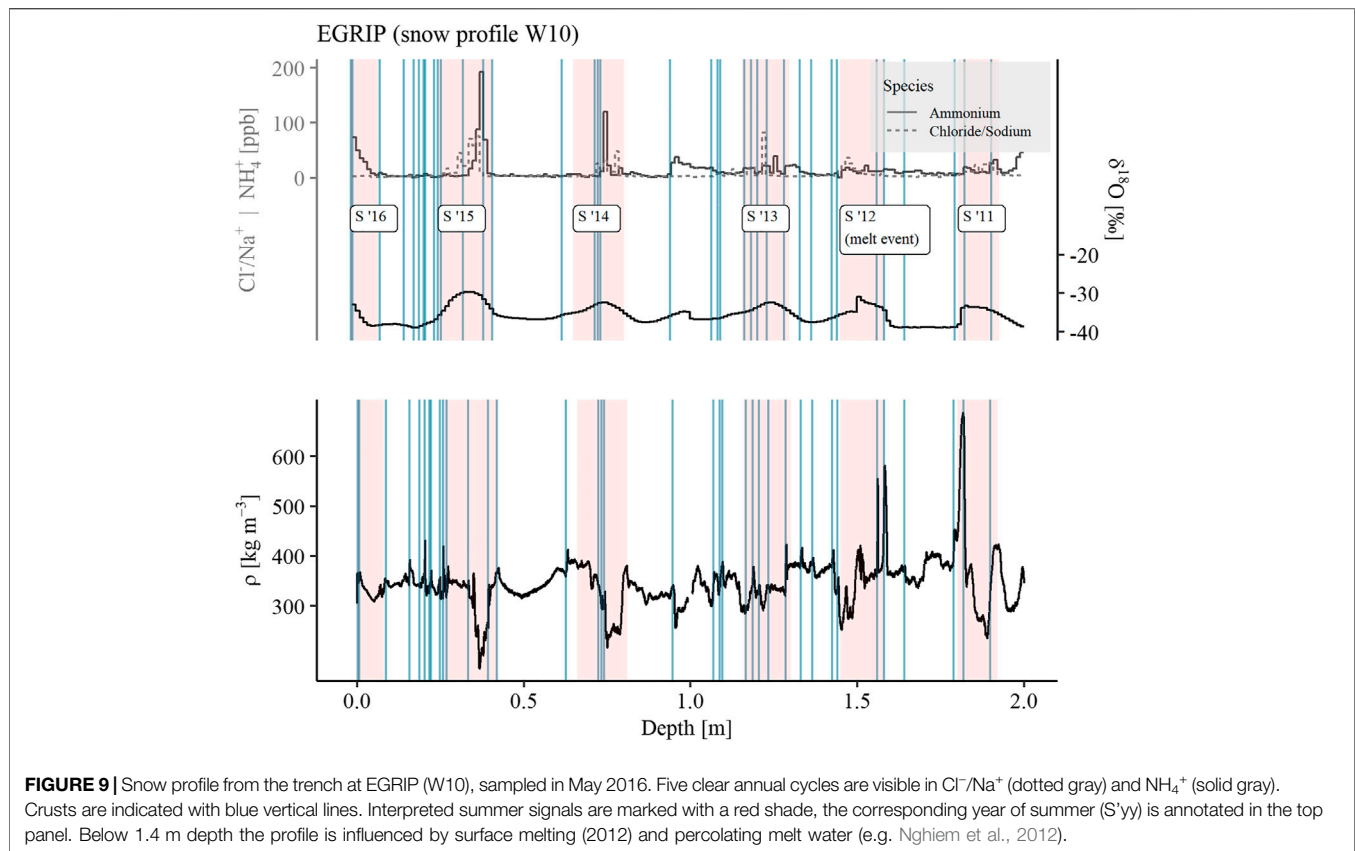
In Antarctica, Cl^-/Na^+ increases from profile 2 close to Kohlen Station (mean: 3.6, max. peak: 15.3) toward the interior Plateau. In profile 14 at Plateau Station, the mean is 4.0 and the maximum peak at 21.4. The peak of Cl^-/Na^+ in Greenland can reach values up to 82.3, the mean of the profile is 7.7. The mean SO_4^{2-} concentration is a bit lower in Greenland (W10: 90.8 ppb) than for the interior part of the East Antarctic

Plateau (profile 2: 72.3 ppb; profile 6: 79.7 ppb; profile 9: 104.1 ppb; profile 14: 101.6 ppb).

We do not find seasonal cycles in impurities measured in the Antarctic profiles. While a seasonal signal in density (not shown) is not pronounced at low-accumulation sites (Landais et al., 2006; Laepple et al., 2016), we see rather some profiles (or parts of profiles), in which we recognize a strong coincidence of crusts, SO_4^{2-} and Cl^-/Na^+ peaks, in some profiles the ions and crusts seem to have just an arbitrary connection (**Figure 10**). In profile 9 most of the crusts are located directly at the Cl^-/Na^+ peaks and (temporally) after the SO_4^{2-} peaks.

In contrast to the Antarctic profiles, in the profile at EGRIP seasonal cycles in several ionic species are much easier and clearer to detect. As NH_4^+ seems to exhibit a clearer seasonality than sulphurous species like SO_4^{2-} (Du et al., 2019), for the dating of the profile we rather use NH_4^+ and Cl^-/Na^+ . The seasonal cycle in Cl^-/Na^+ corresponds well with the accumulation rate. NH_4^+





peaks set in a bit earlier but do not show a high amplitude like Cl^-/Na^+ . For this profile, we also show $\delta^{18}\text{O}$ as well as the high resolution μCT density (ρ) (Schaller et al., 2016). Both, local maxima in $\delta^{18}\text{O}$ and minima in density, indicate summer seasons in Greenland as well. The crusts partly seem to cluster at the (temporal) end of the Cl^-/Na^+ peaks (Figure 9).

DISCUSSION

Spatial and Temporal Variability of Crusts and Validity of the Method

On the interior plateau c_m agrees well with data from snow pits in the vicinity of Dome Fuji (Sugiyama et al., 2012; Hoshina et al., 2014). But the number of crusts can vary a lot in space, especially on small scales (in the order of tens of meters), which is visible in the standard deviation at single sampling sites in Figure 4. This shows, that crusts are a rather local feature and several samples are needed to obtain a representative value. The high small-scale variability seems to be related to the dimension of snow patches and dune structures at the snow surface (Birnbaum et al., 2010). Sugiyama et al. (2012) reported a lower c_m at Kohnen Station than we find in this study. We consider this offset to originate from the different methods and the higher potential of crust clusters (two or more crusts within 1 cm) at Kohnen Station than along the traverse. But also the temporal variability in c_m can be a possible explanation.

In general, our method shows numbers of crusts in the same order of magnitude as other sparse published field observations so far. A big advantage we see in our method to derive crusts in comparison to observations in the field, is the detection of crust clusters and weak crusts, which can be easily overlooked in the field. In addition, the distinct density of the crusts itself and the surrounding snow (s. *Stratification of the snow column through crusts* Section) can be an important point for the classification of polar snowpacks.

On Crust Formation and Potential Implications for Snow and Firn Studies

Crusts in cold dry snow, which are not the result of melting processes, occur in the wide temperature range between 0°C and -60°C . Our crust count from various sampling sites in Greenland and Antarctica suggests that, surprisingly, at warm sites the crusts do not seem to grow thicker than at cold sites. This is different to our experience from granular materials with a high vapor pressure. Since crusts in polar snow form over a wide diversity of environmental conditions (temperature, wind, sunshine duration, relative and absolute humidity, etc.) it is difficult to give more than general assumptions for crust formation.

In areas of low accumulation (here: $<60 \text{ kg m}^{-2} \text{ a}^{-1}$) the snow surface must be considered dynamic and exposed to the atmosphere for up to or even more than one year. Snow

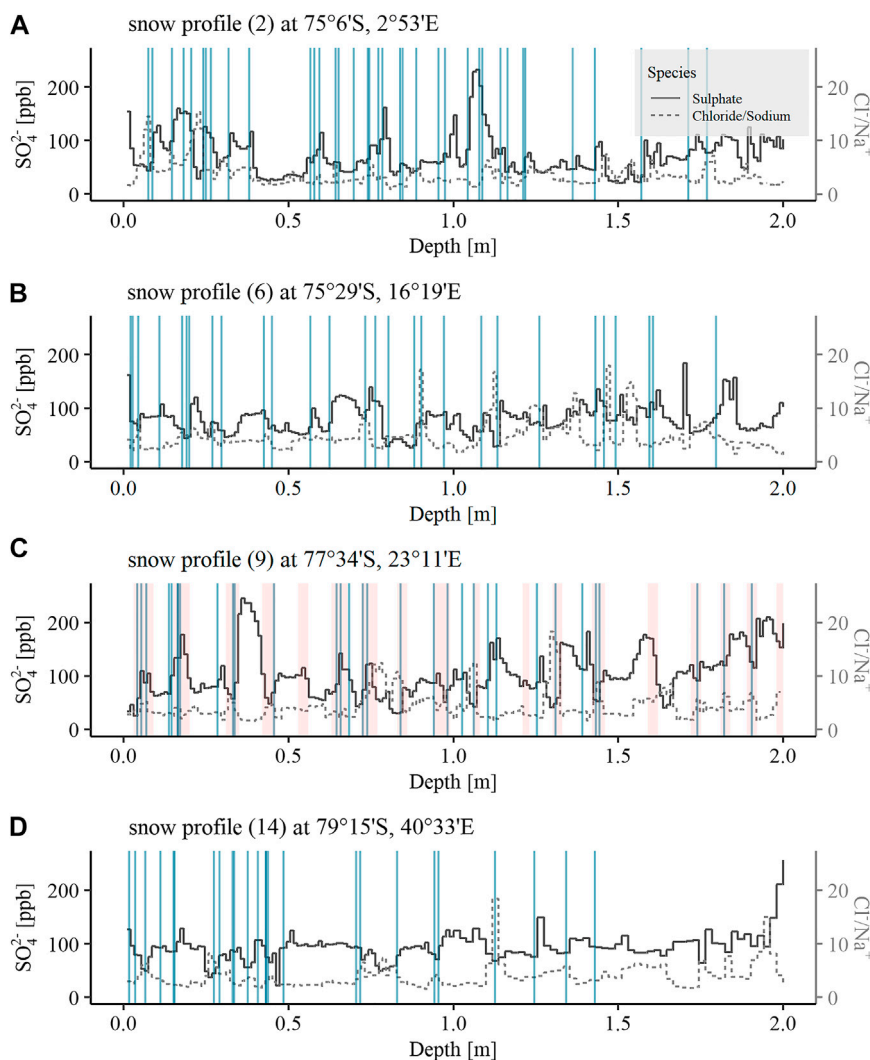


FIGURE 10 | Four exemplary profiles of SO_4^{2-} (black line), Cl^-/Na^+ (gray dotted line) and crusts (blue vertical lines). All ion profiles have a 1 cm resolution. A possible dating version of profile 9 shows summer intervals in shaded red vertical bars. Corresponding locations can be found in **Figure 1**.

dunes with heights of 20–30 cm may well be exposed for more than one year.

Crust Concentration in Relation to Accumulation Rate

With decreasing accumulation rate and therefore more years covered in 1 m snow, one would intuitively expect c_m to increase toward the East Antarctic Plateau. Surprisingly, we observe the opposite trend. The number of crusts decreases with decreasing accumulation rate (Anschütz et al., 2011) and temperature along the CoFi traverse (**Figure 4**). Comparing our results to the temperature and accumulation rate at each site, we find a similar trend for both parameters to c_m . In contrast, the surface snow density (surface to 1 m depth, Weinhart et al., 2020) is not influenced by c_m , as there is no correlation between both parameters. The crusts are too thin to make a significant impact on the surface snow density.

From a dating perspective, a rather important measure is the number of crusts that form per year. A relationship between

surface features and accumulation rate has been proposed by Craven and Allison (1998), as higher accumulation rates lower the time of exposition of upper layers to surface conditions. On average, at least one crust per year forms on the interior plateau of East Antarctica due to the limited formation conditions (**Figure 6**). On the one hand, the annual accumulation rate can be a factor for the preservation of crusts over time. On the other hand, we conclude that the formation of crusts is also directly related to the number of deposition events per year. We also observe a non-linear behavior toward lower accumulation rates. In areas with higher accumulation rate (especially in the investigated areas in Greenland), there are more periods and conditions present, which favor crust formation.

A reduction of c_m (and c_a) on the plateau can generally also come from a higher destruction rate of crusts after formation. This objection has also been raised by Fegyveresi et al. (2018) and might in particular be relevant for areas with low accumulation

rate and very mobile snow grains at the surface. Interestingly, as it could not confirm a correlation of crust hardness and duration of exposition at the snow surface, which causes phase transformations and sublimation-condensation cycles in the uppermost snow layer. We also did not find crusts with higher density on the interior East Antarctic Plateau. A possible explanation might be the higher mobility or the higher potential for destruction of crusts, but the formation conditions of crusts can be rather diverse.

We assume that only strong crusts survive the further firn metamorphism as both cores B40 and B54 show a similar decrease in c_{ice} from a depth of 5 m on (Figure 7). Unfortunately, we are not able to separate the temporal variability from thinning of crusts with time due to firn metamorphism. This finding would have been in particular interesting at Kohnen Station, whether the increase in accumulation rate over the last decades (Medley et al., 2018) caused an increase in c_{ice} , or the drop of c_{ice} in the first meters is only due to destruction because of firn metamorphism (Figures 7A,C).

Both regression analyses of c_{al} with the logarithmic accumulation rate on the spatial and temporal scale result in a positive correlation (compare Figures 6B,C). We explain the offset between the temporal and spatial regression with the destruction of crusts with depth. The cause for the lower slope in B40 in contrast to the spatial overview is not completely clear. We observe an increase in accumulation rate in the upper 10 m which is also the depth interval in which we would expect the strongest crust destruction by firn metamorphism. This would theoretically lead to a higher slope, which is not the case for B40. Nevertheless, the correlation on the spatial and temporal scale proves a high sensitivity of crusts to accumulation rate. For future studies we suggest to investigate further firn and ice cores with an additional focus on the depth interval below 10 m (due to high crust destruction) in order to better separate the effect of accumulation rate from firn metamorphism.

At the moment, we assume that there are no regional differences how crusts vanish with depth and that the variability in crust strength is not stronger than the temporal variability, but c_{al} can still be determined precisely in firn and ice cores. In the EPICA ice core at Kohnen Station (EPICA Community Members, 2006), single crusts are even visible down to the ice clathrate transition zone. If this relationship between c_{al} and the accumulation rate can be proven in the future, taking the densification rate into account crusts can be used as proxy for accumulation rate variability in firn and ice cores.

Discussion of Wind Speed and Snow Mobility as Important Parameters for Crust Formation

While drifting snow seems to be an important factor for wind packing and crust formation as they are also grain size and their mobility might play a role in that context. Picard et al. (2012) reported an increased grain index in summer around Kohnen Station, which decreases toward the sampling sites on the interior plateau. Larger grains with lower mobility might be in favor for crust formation. Smaller grains, which form in particular at low temperatures (Endo and Fujiwara, 1973) like on the interior East

Antarctic Plateau, are prone to wind erosion and redistribution. But more important could be the coordination number and the potential of particles to sinter together. Sintered grains remain at the snow surface while weakly bonded particles get blown away. The mobility and grain size distribution might not be optimal for crust formation on the interior plateau as the uppermost layer of the snowpack has the tendency to be eroded or redistributed completely and has no chance to build a crust.

While we discuss temperature (gradients) later in the text (Stratification of the Snow Column Through Crusts Section), we also compare the wind speed distribution over the last two years of the three mentioned AWS (Figure 1) with our crust record. Large scale weather events are visible at all three locations, but especially the wind speed maxima are significantly different. We find, that the abundance of events with wind speed exceeding 10 m s^{-1} is considerably higher at Kohnen Station than at JASE2007. At Dome Fuji, there are barely more than four events per year above that threshold. As we cannot date the formation of the crusts to link them to the wind events and the high wind speeds are recorded all over the year, we cannot conclude a direct dependence between crusts and events with high wind speed. Nevertheless, the abundance of events with high wind speeds fits with the general trend of c_{al} along the CoFi traverse. To classify them unequivocally as marker for event-based accumulation or seasonality, additional observations of the snow surface coupled with weather data (in particular precipitation and wind speed) are necessary. To avoid crust destruction, the wind speeds should not exceed a level, at which erosion of the whole surface layer takes place. In this context, the wind speed thresholds might vary for different areas dependent on the environmental conditions and grain mobility. Wind scour areas, which are spread over the Antarctic continent and are characterized by high wind erosion (Das et al., 2013), might additionally hamper or prevent the formation of crusts.

Stratification of the Snow Column Through Crusts

From the local histograms in Figure 8 we conclude that at least a slight preference for crust formation in a specific time frame (fitting environmental conditions) seems to be likely. As a consequence of that distribution, crusts can indicate some sort of seasonal layering for a local application, but a sufficient amount of samples (we suggest at least six) is necessary. In low accumulation areas, the stacked signal does not show an unequivocal result due to the high amount of stratigraphic noise (Fisher et al., 1985).

Despite the direct effect of stratification, crusts can also have an indirect effect, altering the (surrounding) snowpack after crust formation. Vertical temperature gradients can enhance mass transport upwards during clear sky weather conditions with lower air temperatures than snow temperatures (Fegyveresi et al., 2018). This mass transport from the snow layer (or layers, dependent on the thickness and permeability) can create layers of low density and high porosity below crusts with increased grain size. This was also observed in radar profiles in West Antarctica (Arcone et al., 2004). The crust on top in turn absorbs the transported mass and increases in density

and decreases in porosity. Similar effects are observed at the formation of firnspiegel (Schlatter, 1984).

But also the opposing effect of hard depth hoar is possible, dependent on the original snow type and density. An additional exposure to a temperature gradient of $20^{\circ}\text{C m}^{-1}$ or higher was observed to produce a hard and cohesive snow layer (Pfeffer and Mrugala, 2002), while high temperature gradients can lead to a preferred crystal growth in vertical direction (Calonne et al., 2017).

Over half of the layers (56%) between 0.2 cm and 3 cm below crusts in our samples from Antarctica have a lower density than the average 1 m density of the snow profiles. This is a higher percentage as we report for Greenland (43%), where the mean surface snow density is generally lower and a seasonal cycle in density (Figure 9) may be stronger than the postdepositional formation of low porosity layers. The formation of (low density) depth hoar seems to be more likely on the East Antarctic Plateau than on the Greenlandic plateau [but has also been observed there, see Alley et al. (1990)]. Also the relative contribution of crust formation to density variations within the snowpack is potentially larger on the East Antarctic Plateau than on the Greenlandic Plateau. In both ways, crusts can influence the stratigraphy significantly even after their formation. We see our results as a good starting point for snowpack models that can capture these processes.

These findings can have impact on remote sensing techniques as both, passive and active remote sensing methods reveal a sensitivity to accumulation rate (e.g. Winebrenner et al., 2001; Flach et al., 2005; Arthern et al., 2006; Dierking et al., 2012). The reason for this relationship is assumed in the density layering of firn (Liang et al., 2008) as the density stratification affects the polarization of the horizontally polarized microwave radiation (Winebrenner et al., 2001; Macelloni et al., 2007). Even more, a few millimeters thin and high-density crusts can influence the polarization considerably as the density gradients at layer boundaries can be huge (Winebrenner et al., 2001; Arthern et al., 2006). For example, Surdyk (2002) interpreted local differences in measured brightness temperatures with the appearance of windcrusts. However, the effect will be limited by the considered wavelength of the sensor, as at lower frequencies the influence of the surface meter(s) are small (Macelloni et al., 2007). It is beyond the scope of this study to go into the physical explanation and the possible effect of crusts on the microwave signal. Nevertheless, we see potential for further studies on this topic based on our records.

The Potential of Crusts as Dating Proxy

We tested a correlation between ion peaks (SO_4^{2-} , Cl^-/Na^+) and crusts, which has also been done by Moser et al. (2020). Nevertheless, crusts only make a small amount of the 1 cm thick samples and a direct conclusion between the ion concentration of the sample and the crust cannot be made. A potential solution based on sampling and measuring the crust only is technically very difficult. While the detection of crusts with the μCT is fairly precise, spotting the crusts by eye working in the field or in the ice lab is not very straightforward. While cutting the crust still might work technically, the volume is not sufficient for an IC measurement.

For a better understanding of the discussion of crusts as a climatic or temporal proxy, we show the annual layer thicknesses for the profiles presented in Figures 9 and 10 in Table 1. At this point we want to mention, that crusts are interpreted as markers for a specific point (or interval) in time. This structural information is in principle independent from an impurity or stable water isotope signal in deposited snow. Still, both structural and chemical components can of course indicate the same point in time (season or year).

Case Study at EGRIP (Greenland)

Interpreting Cl^-/Na^+ and NH_4^+ as a clear summer signal and assuming that accumulation is to some extent evenly distributed, then in Greenland the majority of the crusts seems to form in late summer or autumn. A formation in spring seems less likely. Weather conditions or lack of exposition time at the snow surface might be reasons why less crusts form in that period. In general we conclude that crusts in Greenland have the potential to indicate seasonal transitions, i.e. could be used as an annual marker, but should remain second priority for dating. In between single deposition events there seems to be enough time for a crust to form. Whether crusts can be used as an annual marker for firn core records from other regions in Greenland and in future studies in general, requires the investigation of additional data.

Case Study in DML (Antarctica)

Snow profiles at Kohnen Station indicate the presence of a seasonal cycles in some impurities there (Göktas et al., 2002; Weller and Wagenbach, 2007; Moser et al., 2020), but going further inland (increasing distance to the coast and decreasing accumulation rate), this seasonal signal vanishes. In profile 9 the clarity of the ion peaks is good and also the correlation between ions and crusts is fine, therefore we tried to assign summer periods there (Figure 10C, red shaded areas). We interpret a combination of at least two proxies (SO_4^{2-} , Cl^-/Na^+ or crust) as summer marker and find 16-18 summer periods from surface to 2 m depth, which is reasonable comparing it to the approximate annual layer thickness (Table 1). In contrast in profile 2 (Figure 10A), which is close to Kohnen Station and the accumulation rate can be derived with lower uncertainty, it is hard to assign four to five clear peaks per meter. In profile 14 (Figure 10D), the SO_4^{2-} signal shows rather a constant value over 2 m depth instead of clear peaks and we cannot assign summer or winter periods to specific layers. This profile in turn is an excellent example for dating problems of chemical signals (stable water isotopes, impurities) in low accumulation areas as well. Structural elements in the snow column (density, anisotropy, crusts) have the potential for an additional annual marker when chemical signals fail to show a clear seasonality. They are not biased by the physico-chemical exchange reactions between snow and atmosphere like diffusion, sublimation or volatilization. But, of course, they are also subject to erosion and probably sensitive to specific weather conditions. We assume that the potential for crust destruction is higher for a lower annual accumulation rate. For a reliable dating application in low accumulation areas we suggest a combination of several parameters derived from a sufficiently large amount of samples.

CONCLUSION

In this study, we presented for the first time a crust record derived from radioscopic scan images using X-rays. With this method, we can detect weak crusts as well as crust clusters and also the density of horizontal crusts and the surrounding layers can be determined. We investigated samples from the East Antarctic Plateau and the Greenland interior. Although the lateral extent of crusts is limited to few meters and the small-scale variability is high, in Antarctica we find a clear trend of decreasing c_m (crusts per meter) going from Kohnen Station (75.00°S, 0.06°E) to the interior Antarctic Plateau (79.24°S, 40.33°E). Looking at samples from both ice sheets and taking the annual layer thickness into account, c_{al} (crusts per annual layer) decreases constantly from high to low accumulation rate areas. A linear relationship between c_{al} and the logarithmic accumulation rate seems likely on the spatial scale, as well as on the temporal scale as shown for firn core B40. We recommend further studies to test this positive correlation, especially to decouple the crust destruction with increasing depth from an accumulation rate (or climate) driven temporal variability of crusts. This crust abundance (and variability) might play a role for firn ventilation and pore close-off at the firn-ice transition, especially in the diffusive zone (Birner et al., 2018).

Assessing the formation theory for glazed surfaces by Fegyveresi et al. (2018) and observations by Sommer et al. (2018b) in combination with our data, we conclude that the most important factor for crust formation is time with absence of persistent snow deposition. Due to the reduced metamorphism under cold temperatures, on the interior Antarctic plateau the surface snow is rather soft and remains mobile even under moderate winds. It prevents longer residence times at the surface and therefore crust formation. In addition, less annual accumulation reduces the seasonal supply of snow leading to a further reduction of formed crusts. It is shown that crusts on the East Antarctic plateau are more frequently associated with porous layers below them than at the investigated sites in Greenland. We conclude that the contribution of crusts to the overall stratigraphy of the snowpack is therefore stronger on the East Antarctic plateau.

Future studies could deal with a microstructure analysis of crusts (e.g. grain size distribution), the thickness of depth hoar layers in consequence of temperature and vapor pressure gradients and the mass loss within these layers and the mass gain at crusts. Our crust record can serve as a physically constrained dataset on which radiation of scattering modeling can build, both, subscribing vertical distribution as well as horizontal variations. The observations in this study indicate that crusts might have a direct (stratification through crusts) as well as an indirect effect (stratification through low porosity layers below crusts), but this topic needs further investigation.

The distribution of crusts over depth from several samples and the combination of crusts with chemical data at EGRIP, where seasonal signals of impurities are clearly visible, have shown that structural elements can be used for dating on a seasonal scale, although several samples are necessary for a reliable result. If the accumulation rate is completely unknown, it is difficult to identify the annual layer thickness in low accumulation areas just based

on a crust record. A multitude of different mechanisms interact for crust formation, the general formation mechanism is not limited to one specific season only and a correlation to ions cannot be seen in all investigated profiles. But stable water isotopes and some impurities face postdepositional, physico-chemical alterations in their concentration at the snow-atmosphere interphase (i.e. diffusion, sublimation, chemical reactions) and redistribution by wind (i.e. change of the stratigraphic order). Crusts, which form at the snow surface and are advected downwards by snow accumulation unless they are eroded, can be seen as a rather immobile proxy and can support dating approaches with other proxies.

DATA AVAILABILITY STATEMENT

The crust dataset of this study and another dataset containing the impurity data are available from the open-access repository PANGAEA at <https://www.pangaea.de/>.

AUTHOR CONTRIBUTIONS

The CoFi project was initialized by SK and JF. AW sampled the snow profiles along the CoFi traverse and the OIR trench, analysed the profiles and created the dataset. AW prepared the manuscript and discussed the first results with JF and SK. MH supervised the chemical measurements, OE improved the statistical analysis. All authors contributed to revising the manuscript.

FUNDING

AW is funded by the German environmental foundation (Deutsche Bundesstiftung Umwelt). SK has received support from the Villum Investigator Project IceFlow (no. 16572).

ACKNOWLEDGMENTS

We are grateful to the AWI logistic team for their support during the field work and to the AWI workshop for the production of the snow cutting device. We thank Birthe Twarloh for the conduct of IC measurements. Accumulation rate of core B54 has been calculated from continuous flow measurements at Desert Research Institute lead by Joe McConnell.

A part of the Greenland samples were obtained in the framework of the EGRIP—directed and organized by the Center for Ice and Climate at the Niels Bohr Institute, University of Copenhagen. It is supported by funding agencies and institutions in Denmark (A. P. Møller Foundation, University of Copenhagen), USA (US National Science Foundation, Office of Polar Programs), Germany (Alfred Wegener Institute, Helmholtz Centre for Polar and Marine Research), Japan (National Institute of Polar Research and Arctic Challenge for Sustainability), Norway (University of Bergen and Bergen Research Foundation), Switzerland (Swiss National Science Foundation), France

(French Polar Institute Paul-Emile Victor, Institute for Geosciences and Environmental research) and China (Chinese Academy of Sciences and Beijing Normal University).

REFERENCES

- Adolph, A. C., and Albert, M. R. (2014). Gas diffusivity and permeability through the firn column at Summit, Greenland: measurements and comparison to microstructural properties. *The Cryosphere* 8, 319–328. doi:10.5194/tc-8-319-2014
- Albert, M., Shuman, C., Courville, Z., Bauer, R., Fahnestock, M., and Scambos, T. (2004). Extreme firn metamorphism: impact of decades of vapor transport on near-surface firn at a low-accumulation glazed site on the East Antarctic plateau. *Ann. Glaciol.* 39, 73–78. doi:10.3189/172756404781814041
- Alley, R. B., Saltzman, E. S., Cuffey, K. M., and Fitzpatrick, J. J. (1990). Summertime formation of depth hoar in central Greenland. *Geophys. Res. Lett.* 17, 2393–2396. doi:10.1029/g1017i013p02393
- Anschütz, H., Sinisalo, A., Isaksson, E., McConnell, J. R., Hamran, S. E., Bisiaux, M. M., et al. (2011). Variation of accumulation rates over the last eight centuries on the East Antarctic Plateau derived from volcanic signals in ice cores. *J. Geophys. Research-Atmospheres* 116, 12. doi:10.1029/2011jd015753
- Arcone, S. A., Spikes, V. B., Hamilton, G. S., and Mayewski, P. A. (2004). “Stratigraphic continuity in 400 MHz short-pulse radar profiles of firn in West Antarctica,” in *Annals of glaciology*. Editor J. Jacka (Cambridge: Int Glaciological Soc), 39, 195–200.
- Arthern, R. J., Winebrenner, D. P., and Vaughan, D. G. (2006). Antarctic snow accumulation mapped using polarization of 4.3-cm wavelength microwave emission. *J. Geophys. Research-Atmospheres* 111, 10. doi:10.1029/2004jd005667
- Arthern, R. J., and Wingham, D. J. (1998). The natural fluctuations of firn densification and their effect on the geodetic determination of ice sheet mass balance. *Climatic Change* 40, 605–624. doi:10.1023/a:1005320713306
- Birnbaum, G., Freitag, J., Brauner, R., König-Langlo, G., Schulz, E., Kipfstuhl, S., et al. (2010). Strong-wind events and their influence on the formation of snow dunes: observations from Kohnen station, Dronning Maud Land, Antarctica. *J. Glaciol.* 56, 891–902. doi:10.3189/002214310794457272
- Birner, B., Buizert, C., Wagner, T. J. W., and Severinghaus, J. P. (2018). The influence of layering and barometric pumping on firn air transport in a 2-D model. *The Cryosphere* 12, 2021–2037. doi:10.5194/tc-12-2021-2018
- Calonne, N., Montagnat, M., Matzl, M., and Schneebeli, M. (2017). The layered evolution of fabric and microstructure of snow at Point Barnola, Central East Antarctica. *Earth Planet. Sci. Lett.* 460, 293–301. doi:10.1016/j.epsl.2016.11.041
- Champollion, N., Picard, G., Arnaud, L., Lefebvre, É., Macelloni, G., Rémy, F., et al. (2019). Marked decrease in the near-surface snow density retrieved by AMSR-E satellite at Dome C, Antarctica, between 2002 and 2011. *The Cryosphere* 13, 1215–1232. doi:10.5194/tc-13-1215-2019
- Craven, M., and Allison, I. (1998). Firnification and the effects of wind-packing on Antarctic snow. *A. Glaciology* 27, 239–245. doi:10.3189/1998aog27-1-239-245
- Curran, M. A. J., Palmer, A. S., Van Ommen, T. D., Morgan, V. I., Phillips, K. L., McMorrow, A. J., et al. (2002). Post-depositional movement of methanesulphonic acid at Law Dome, Antarctica, and the influence of accumulation rate. *Ann. Glaciol.* 35, 333–339. doi:10.3189/172756402781816528
- Das, I., Bell, R. E., Scambos, T. A., Wolovick, M., Creyts, T. T., Studinger, M., et al. (2013). Influence of persistent wind scour on the surface mass balance of Antarctica. *Nat. Geosci* 6, 367–371. doi:10.1038/ngeo1766
- Dierking, W., Linow, S., and Rack, W. (2012). Toward a robust retrieval of snow accumulation over the Antarctic ice sheet using satellite radar. *J. Geophys. Research-Atmospheres* 117, 17. doi:10.1029/2011jd017227
- Du, Z., Xiao, C., Zhang, Q., Li, C., Wang, F., Liu, K., et al. (2019). Climatic and environmental signals recorded in the EGRIP snowpit, Greenland. *Environ. Earth Sci.* 78. doi:10.1007/s12665-019-8177-4
- Eisen, O., Frezzotti, M., Genthon, C., Isaksson, E., Magand, O., Van Den Broeke, M. R., et al. (2008). Ground-based measurements of spatial and temporal variability of snow accumulation in East Antarctica. *Rev. Geophys.* 46, 39. doi:10.1029/2006rg000218
- Endo, Y., and Fujiwara, K. (1973). Characteristics of the snow cover in East Antarctica along the route of the JARE South Pole traverse and factors controlling such characteristics. *JARE Sci. Rep.* 7, 1–27.
- The authors used available datasets of the Automatic Weather Station Program (NSF grants number ARC-0713843, ANT-0944018 and ANT-1141908).
- Epica Community Members (2006). One-to-one coupling of glacial climate variability in Greenland and Antarctica. *Nature* 444, 195–198. doi:10.1038/nature05301
- Fegyveresi, J. M., Alley, R. B., Muto, A., Orsi, A. J., and Spencer, M. K. (2018). Surface formation, preservation, and history of low-porosity crusts at the WAIS Divide site, West Antarctica. *The Cryosphere* 12, 325–341. doi:10.5194/tc-12-325-2018
- Fisher, D. A., Reeh, N., and Clausen, H. B. (1985). Stratigraphic noise in time series derived from ice cores. *A. Glaciology* 7, 76–83. doi:10.3189/s0260305500005942
- Flach, J. D., Partington, K. C., Ruiz, C., Jeansou, E., and Drinkwater, M. R. (2005). Inversion of the surface properties of ice sheets from satellite microwave data. *IEEE Trans. Geosci. Remote Sensing* 43, 743–752. doi:10.1109/tgrs.2005.844287
- Freitag, J., Kipfstuhl, S., and Laepple, T. (2013). Core-scale radiosopic imaging: a new method reveals density-calcium link in Antarctic firn. *J. Glaciol.* 59, 1009–1014. doi:10.3189/2013jog13j028
- Frezzotti, M., Gandolfi, S., and Urbini, S. (2002). Snow megadunes in Antarctica: sedimentary structure and genesis. *J. Geophys. Research-Atmospheres* 107. doi:10.1029/2001jd000673
- Furukawa, T., Kamiyama, K., and Maeno, H. (1996). Snow surface features along the traverse route from the coast to Dome Fuji station, queen Maud Land, Antarctica. *Proc. NIPR Symp. Polar Meteorology Glaciology* 10, 13–24.
- Furukawa, T., Watanabe, O., Seko, K., and Fujii, Y. (1992). Distribution of surface conditions of ice sheet in enderby Land and east queen Maud Land, east Antarctica. *Proc. NIPR Symp. Polar Meteorol. Glaciol* 5, 140–144.
- Göktas, F., Fischer, H., Oerter, H., Weller, R., Sommer, S., and Miller, H. (2002). A glacio-chemical characterization of the new EPICA deep-drilling site on Amundsenisen, Dronning Maud Land, Antarctica. *Ann. Glaciol.* 35, 347–354. doi:10.3189/172756402781816474
- Gregory, S. A., Albert, M. R., and Baker, I. (2014). Impact of physical properties and accumulation rate on pore close-off in layered firn. *The Cryosphere* 8, 91–105. doi:10.5194/tc-8-91-2014
- Herron, M. M., and Langway, C. C. (1980). Firn densification: an empirical model. *J. Glaciol.* 25, 373–385. doi:10.1017/s0022143000015239
- Holme, C., Gkinis, V., Lanzky, M., Morris, V., Olesen, M., Thayer, A., et al. (2019). Varying regional $\delta^{18}\text{O}$ -temperature relationship in high-resolution stable water isotopes from east Greenland. *Clim. Past* 15, 893–912. doi:10.5194/cp-15-893-2019
- Hörhold, M., Kipfstuhl, S., Wilhelms, F., Freitag, J., and Frenzel, A. (2011). The densification of layered polar firn. *J. Geophys. Research-Earth Surf.* 116. doi:10.1029/2009jf001630
- Hoshina, Y., Fujita, K., Nakazawa, F., Iizuka, Y., Miyake, T., Hirabayashi, M., et al. (2014). Effect of accumulation rate on water stable isotopes of near-surface snow in inland Antarctica. *J. Geophys. Res. Atmos.* 119, 274–283. doi:10.1002/2013jd020771
- Jonsell, U., Hansson, M. E., and Mörth, C.-M. (2007). Correlations between concentrations of acids and oxygen isotope ratios in polar surface snow. *Tellus B* 59, 326–335. doi:10.1111/j.1600-0889.2007.00272.x
- Karlsson, N. B., Binder, T., Eagles, G., Helm, V., Pattyn, F., Van Liefferinge, B., et al. (2018). Glaciological characteristics in the Dome Fuji region and new assessment for “oldest ice”. *The Cryosphere* 12, 2413–2424. doi:10.5194/tc-12-2413-2018
- Laepple, T., Werner, M., and Lohmann, G. (2011). Synchronicity of Antarctic temperatures and local solar insolation on orbital timescales. *Nature* 471, 91–94. doi:10.1038/nature09825
- Laepple, T., Hörhold, M., Münch, T., Freitag, J., Wegner, A., and Kipfstuhl, S. (2016). Layering of surface snow and firn at Kohnen Station, Antarctica: noise or seasonal signal? *J. Geophys. Res. Earth Surf.* 121, 1849–1860. doi:10.1002/2016jf003919
- Landais, A., Barnola, J. M., Kawamura, K., Cailion, N., Delmotte, M., Van Ommen, T., et al. (2006). Firn-air $\delta^{15}\text{N}$ in modern polar sites and glacial-interglacial ice: a model-data mismatch during glacial periods in Antarctica? *Quat. Sci. Rev.* 25, 49–62. doi:10.1016/j.quascirev.2005.06.007
- Liang, D., Xu, X., Tsang, L., Andreadis, K. M., and Josberger, E. G. (2008). The effects of layers in dry snow on its passive microwave emissions using dense

- media radiative transfer theory based on the quasicrystalline approximation (QCA/DMRT). *IEEE Trans. Geosci. Remote Sensing* 46, 3663–3671. doi:10.1109/tgrs.2008.922143
- Macelloni, G., Brogioni, M., and Santi, E. (2007). *Retrieval from AMSR-E data of the snow temperature profile at Dome-C Antarctica*, IEEE International Geoscience and Remote Sensing Symposium, Barcelona, Spain 4233–4236. doi:10.1109/IGARSS.2007.4423785
- Medley, B., McConnell, J. R., Neumann, T. A., Reijmer, C. H., Chellman, N., Sigl, M., et al. (2018). Temperature and snowfall in western queen Maud Land increasing faster than climate model projections. *Geophys. Res. Lett.* 45, 1472–1480. doi:10.1002/2017gl075992
- Mitchell, L. E., Buizert, C., Brook, E. J., Breton, D. J., Fegyveresi, J., Baggenstos, D., et al. (2015). Observing and modeling the influence of layering on bubble trapping in polar firn. *J. Geophys. Res. Atmos.* 120, 2558–2574. doi:10.1002/2014jd022766
- Moser, D. E., Horhold, M., Kipfstuhl, S., and Freitag, J. (2020). Microstructure of snow and its link to trace elements and isotopic composition at kohnen station, dronning Maud Land, Antarctica. *Front. Earth Sci.* 8, 13. doi:10.3389/feart.2020.00023
- Münch, T., Kipfstuhl, S., Freitag, J., Meyer, H., and Laepple, T. (2016). Regional climate signal vs. local noise: a two-dimensional view of water isotopes in Antarctic firn at Kohnen Station, Dronning Maud Land. *Clim. Past* 12, 1565–1581. doi:10.5194/cp-12-1565-2016
- Neem Community Members (2013). Eemian interglacial reconstructed from a Greenland folded ice core. *Nature* 493, 489–494. doi:10.1038/nature11789
- Nghiem, S. V., Hall, D. K., Mote, T. L., Tedesco, M., Albert, M. R., Keegan, K., et al. (2012). The extreme melt across the Greenland ice sheet in 2012. *Geophys. Res. Lett.* 39, 6. doi:10.1029/2012gl053611
- Oerter, H., Graf, W., Wilhelms, F., Minikin, A., and Miller, H. (1999). Accumulation studies on Amundsenisen, Dronning Maud Land, Antarctica, by means of tritium, dielectric profiling and stable-isotope measurements: first results from the 1995–96 and 1996–97 field seasons. *Ann. Glaciol.* 29, 1–9. doi:10.3189/172756499781820914
- Pfeffer, W. T., and Mrugala, R. (2002). Temperature gradient and initial snow density as controlling factors in the formation and structure of hard depth hoar. *J. Glaciol.* 48, 485–494. doi:10.3189/172756502781831098
- Picard, G., Domine, F., Krinner, G., Arnaud, L., and Lefebvre, E. (2012). Inhibition of the positive snow-albedo feedback by precipitation in interior Antarctica. *Nat. Clim Change* 2, 795–798. doi:10.1038/nclimate1590
- Reijmer, C. H., and van den Broeke, M. R. (2003). Temporal and spatial variability of the surface mass balance in Dronning Maud Land, Antarctica, as derived from automatic weather stations. *J. Glaciol.* 49, 512–520. doi:10.3189/172756503781830494
- Ren, J. W., Sun, J. Y., and Qin, D. H. (2004). Preliminary results of ionic concentrations in snow pits along the Zhongshan-Dome A traverse route, Antarctica. *Ann. Glaciology* 39 (39), 155–160.
- Rotschky, G., Rack, W., Dierking, W., and Oerter, H. (2006). Retrieving snowpack properties and accumulation estimates from a combination of SAR and scatterometer measurements. *IEEE Trans. Geosci. Remote Sensing* 44, 943–956. doi:10.1109/tgrs.2005.862524
- Scambos, T. A., Frezzotti, M., Haran, T., Bohlander, J., Lenaerts, J. T. M., Van Den Broeke, M. R., et al. (2012). Extent of low-accumulation ‘wind glaze’ areas on the East Antarctic plateau: implications for continental ice mass balance. *J. Glaciol.* 58, 633–647. doi:10.3189/2012jog11j232
- Schaller, C. F., Freitag, J., and Eisen, O. (2017). Critical porosity of gas enclosure in polar firn independent of climate. *Clim. Past* 13, 1685–1693. doi:10.5194/cp-13-1685-2017
- Schaller, C. F., Freitag, J., Kipfstuhl, S., Laepple, T., Steen-Larsen, H. C., and Eisen, O. (2016). A representative density profile of the North Greenland snowpack. *The Cryosphere* 10, 1991–2002. doi:10.5194/tc-10-1991-2016
- Schlatter, T. (1984). Weather queries: firnspiegel: an “ice mirror”. *Weatherwise* 37, 317. doi:10.1080/00431672.1984.9933268
- Simonsen, M. F., Baccolo, G., Blunier, T., Borunda, A., Delmonte, B., Frei, R., et al. (2019). East Greenland ice core dust record reveals timing of Greenland ice sheet advance and retreat. *Nat. Commun.* 10, 4494. doi:10.1038/s41467-019-12546-2
- Sommer, C. G., Lehning, M., and Fierz, C. (2018a). Wind tunnel experiments: influence of erosion and deposition on wind-packing of new snow. *Front. Earth Sci.* 6. doi:10.3389/feart.2018.00004
- Sommer, C. G., Wever, N., Fierz, C., and Lehning, M. (2018b). Investigation of a wind-packing event in queen Maud Land, Antarctica. *The Cryosphere* 12, 2923–2939. doi:10.5194/tc-12-2923-2018
- Sommer, S., Wagenbach, D., Mulvaney, R., and Fischer, H. (2000). Glacio-chemical study spanning the past 2 kyr on three ice cores from Dronning Maud Land, Antarctica: 2. Seasonally resolved chemical records. *J. Geophys. Res.* 105, 29423–29433. doi:10.1029/2000jd900450
- Steen-Larsen, H. C., Masson-Delmotte, V., Sjolte, J., Johnsen, S. J., Vinther, B. M., Breon, F. M., et al. (2011). Understanding the climatic signal in the water stable isotope records from the NEEM shallow firn/ice cores in northwest Greenland. *J. Geophys. Research-Atmospheres* 116. doi:10.1029/2010jd014311
- Sugiyama, S., Enomoto, H., Fujita, S., Fukui, K., Nakazawa, F., Holmlund, P., et al. (2012). Snow density along the route traversed by the Japanese-Swedish Antarctic Expedition 2007/08. *J. Glaciol.* 58, 529–539. doi:10.3189/2012jog11j201
- Surdyk, S. (2002). “Low microwave brightness temperatures in central Antarctica: observed features and implications,” in *Annals of glaciology*. Editors J. G. Winther and R. Solberg (Cambridge: Int Glaciological Soc.), 34, 134–140.
- Tran, N., Remy, F., Feng, H., and Femenias, P. (2008). Snow facies over ice sheets derived from envisat active and passive observations. *IEEE Trans. Geosci. Remote Sensing* 46, 3694–3708. doi:10.1109/tgrs.2008.2000818
- Vallelonga, P., Christianson, K., Alley, R. B., Anandakrishnan, S., Christian, J. E. M., Dahl-Jensen, D., et al. (2014). Initial results from geophysical surveys and shallow coring of the Northeast Greenland Ice Stream (NEGIS). *The Cryosphere* 8, 1275–1287. doi:10.5194/tc-8-1275-2014
- van Geldern, R., and Barth, J. A. C. (2012). Optimization of instrument setup and post-run corrections for oxygen and hydrogen stable isotope measurements of water by isotope ratio infrared spectroscopy (IRIS). *Limnol. Oceanogr. Methods* 10, 1024–1036. doi:10.4319/lom.2012.10.1024
- Weinhart, A. H., Freitag, J., Hörhold, M., Kipfstuhl, S., and Eisen, O. (2020). Representative surface snow density on the East Antarctic plateau. *The Cryosphere* 14, 3663–3685. doi:10.5194/tc-14-3663-2020
- Weller, R., Trauffer, F., Fischer, H., Oerter, H., Piel, C., and Miller, H. (2004). Postdepositional losses of methane sulfonate, nitrate, and chloride at the European Project for Ice Coring in Antarctica deep-drilling site in Dronning Maud Land, Antarctica. *J. Geophys. Research-Atmospheres* 109. doi:10.1029/2003jd004189
- Weller, R., and Wagenbach, D. (2007). Year-round chemical aerosol records in continental Antarctica obtained by automatic samplings. *Tellus B: Chem. Phys. Meteorology* 59, 755–765. doi:10.1111/j.1600-0889.2007.00293.x
- Whitlow, S., Mayewski, P. A., and Dibb, J. E. (1992). A comparison of major chemical species seasonal concentration and accumulation at the South Pole and summit, Greenland. *Atmos. Environ. A. Gen. Top.* 26, 2045–2054. doi:10.1016/0960-1686(92)90089-4
- Wilheit, T. T. (1978). Radiative transfer in a plane stratified dielectric. *IEEE Trans. Geosci. Electron.* 16, 138–143. doi:10.1109/tge.1978.294577
- Winebrenner, D. P., Arthern, R. J., and Shuman, C. A. (2001). Mapping Greenland accumulation rates using observations of thermal emission at 4.5-cm wavelength. *J. Geophys. Res.* 106, 33919–33934. doi:10.1029/2001jd900235
- Zwally, H. J., and Jun, L. (2017). Seasonal and interannual variations of firn densification and ice-sheet surface elevation at the Greenland summit. *J. Glaciology* 48, 199–207. doi:10.3189/172756502781831403

Conflict of Interest: The authors declare that the research was conducted in the absence of any commercial or financial relationships that could be construed as a potential conflict of interest.

Copyright © 2021 Weinhart, Kipfstuhl, Hörhold, Eisen and Freitag. This is an open-access article distributed under the terms of the Creative Commons Attribution License (CC BY). The use, distribution or reproduction in other forums is permitted, provided the original author(s) and the copyright owner(s) are credited and that the original publication in this journal is cited, in accordance with accepted academic practice. No use, distribution or reproduction is permitted which does not comply with these terms.

5 PUBLICATION III

CLIMATE SIGNAL OR POSTDEPOSITIONAL MODIFICATION? INSIGHTS ON STABLE WATER ISOTOPES IN ANTARCTIC SURFACE SNOW

*Weinhart, A. H., Kipfstuhl, S., Freitag, J., Werner, M.,
Mengert, M., Micha, G., Götz, P., Eisen, O., Münch, T., and Hörhold, M.*

To be submitted to Climate of the past

Doi: -

Climate signal or postdepositional modification? Insights on stable water isotopes in Antarctic surface snow

Alexander H. Weinhart¹, Sepp Kipfstuhl^{1,2}, Johannes Freitag¹, Martin Werner¹, Melissa Mengert^{1,*}, Georgia Micha¹, Pia Götz¹, Olaf Eisen^{1,3}, Thomas Münch⁴, Maria Hörhold¹

- 5 ¹ Alfred-Wegener-Institut Helmholtz-Zentrum für Polar- und Meeresforschung, Bremerhaven, Germany
² Physics of Ice, Climate and Earth, Niels Bohr Institute, University of Copenhagen, Copenhagen, Denmark
³ Universität Bremen, Fachbereich Geowissenschaften, Bremen, Germany
⁴ Alfred-Wegener-Institut Helmholtz-Zentrum für Polar- und Meeresforschung, Potsdam, Germany
* Now at: Universität Bremen, Fachbereich Geographie, Bremen, Germany

10

Correspondence to: Alexander H. Weinhart (alexander.weinhart@awi.de), Maria Hörhold (maria.hoerhold@awi.de)

Abstract

Stable water isotopes in snow and ice can function as a proxy for paleotemperatures from seasonal to orbital time scales. However, as several processes – occurring from precipitation to downward advection into the snowpack – influence the measured signals in ice cores, a further understanding of these processes at the snow-atmosphere interface is crucial. In this study, snow cores were taken along a traverse route from Kohnen Station to former Plateau Station on the East Antarctic ice sheet. They were cut into discrete samples of 1 cm or 2 cm resolution and analyzed by means of cavity-ring-down spectroscopy for $\delta^{18}\text{O}$ and δD . We see the textbook relationship between both δD and $\delta^{18}\text{O}$ with temperature on the spatial scale, but we report a larger scatter and lower deuterium excess values in relation to elevation when only considering the upper snow layer instead of a 1 m mean. A temporal variability in form of seasonal cycles is visible in the first part of the traverse until an accumulation rate of $\sim 50 \text{ kg m}^{-2}\text{a}^{-1}$. Further inland, this variability is not consistent anymore with the local accumulation rate. Postdepositional processes shape the isotope profiles with a dominating cycle length of around 20 cm, which is primarily attributed to snow and firn diffusion. A comparison of our observed snow isotopic composition with the isotopic composition of precipitation from the atmospheric general circulation model ECHAM6-wiso shows an offset in $\delta^{18}\text{O}$ and deuterium excess, which we attribute mostly to postdepositional effects. Furthermore, we simulated profiles at three selected sites along the traverse from the isotopic ECHAM6-wiso output with diffusion applied. They resemble the observed snow profile very well below 1 m depth. In turn, from surface to 1 m depth, the simulated profiles show too much temporal (seasonal) variability. As the diffusion in snow and firn is well constrained, we relate this discrepancy to the processes of mechanical mixing at the snow surface and sublimation. Without a quantitative description of the sublimation process and a record of the climatic conditions, the interpretation of cycles in $\delta^{18}\text{O}$ on the seasonal scale in snow and ice core records from sites below an accumulation rate of $50 \text{ kg m}^{-2}\text{a}^{-1}$ is not possible.

1 Introduction

Stable water isotopes as a paleoclimatic proxy

Since the observation that the isotopic composition of precipitation is directly linked to the condensation temperature in the air (Dansgaard, 1964), stable water isotopes retrieved from climate archives have been used for paleoclimatic reconstructions, also called “isotopic thermometer”. The isotopic composition of water molecules (H_2O , HDO , or H_2^{18}O with D standing for deuterium) is commonly expressed as δD or $\delta^{18}\text{O}$ with respect to the Standard Mean Ocean Water (Craig, 1961). Stable water isotope records from ice cores in Greenland (e.g., Rasmussen et al., 2006) and Antarctica (e.g., EPICA Community Members, 2004; EPICA Community Members, 2006) dating back hundreds of thousands of years into the past brought milestones in paleoclimatic research. To translate the isotopic composition measured in ice cores into paleotemperature, a quantitative conversion assuming a specific relationship between the isotopic composition of snow (ice) and the local annual mean temperature is applied. In the past, this was done using the spatial slope between (mean) $\delta^{18}\text{O}$ and the local annual mean (10 m firn) temperature (T) (Lorius and Merlivat, 1975 for Antarctica). Then this slope was used as an equivalent surrogate for a temporal relationship between stable water isotopes and paleotemperatures, assuming that the relationship remains constant over time (e.g., over glacial-interglacial time scales). Nowadays, this approach is only used in a qualitative manner. An overview of available stable water isotope data in surface snow of Antarctica was given by Masson-Delmotte et al. (2008). They also discussed the relationship to environmental properties and suggested a $\delta^{18}\text{O}/T$ slope around $0.8 \text{‰ } ^\circ\text{C}^{-1}$ for the whole Antarctic continent. However, this relationship is known to vary spatially and can be hampered by local to regional processes.

Influence of postdepositional modifications

For the interpretation of a stable water isotope record as a paleoclimatic proxy, several processes have to be considered, which we want to distinguish into three phases: a) syndepositional (the timing, amount, and type of precipitation and processes during deposition), b) mechanical postdepositional (e.g., erosion and redeposition at the snow surface) and c) physico-chemical postdepositional processes (including firn diffusion).

Syndepositional aspects include single precipitation events caused by synoptic activity. In many areas of the East Antarctic Plateau (higher than 2000 m asl), this synoptic precipitation is responsible for a large fraction of the annual accumulation (Birnbaum et al., 2006; Schlosser and Oerter, 2002) and affects interannual variability in surface mass balance as well as temperature and, in consequence, stable water isotopes (Servettaz et al., 2020). Also precipitation intermittency on the interannual scale can complicate interpreting stable water isotopes in firn and ice cores (Casado et al., 2020; Laepple et al., 2011). Additionally, diamond dust deposition as well as hoar frost can constitute a significant amount of the annual deposition on the East Antarctic Plateau (e.g., 65% at Dome C; Stenni et al., 2016). Both (precipitation intermittency and diamond dust) hamper the consecutive recording of “temperature-driven” isotopic composition of precipitation.

Mechanically the interaction of wind with the surface (Lenaerts and van den Broeke, 2012) creates a significant amount of noise in isotopic composition on small time scales (Ekaykin et al., 2002; Fisher et al., 1985; Münch et al., 2016), especially in regions with low annual accumulation rates (i.e., lower than $50 \text{ kg m}^{-2} \text{ a}^{-1}$). Erosion and redistribution contribute to a high spatial variability in the local accumulation rate (Zuhr et al., in review, 2021), affecting isotopic signals on short time scales (Karlöf et al., 2005). Filtering datasets from stratigraphic noise has been applied recently in firn cores from Dronning Maud Land (DML) and the West Antarctic ice sheet (Münch and Laepple, 2018). With a sufficient amount of samples, stacking several records can help filter out the noise and reconstruct the deposited climate signal (Altnau et al., 2015; Münch et al., 2016).

More challenging for the interpretation of climate signals can be snow-air interactions and their effects on the snow isotopic composition in a physico-chemical context. Amongst these processes are sublimation and condensation, which have been shown to have a significant impact on the isotopic composition of snow (Hughes et al., in review; Madsen et al., 2019).

Laboratory experiments (Moser and Stichler, 1974; Sokratov and Golubev, 2009) and field observations (Stichler et al., 2001) show that the specific surface area and exposition time are two controlling factors here. This surface sublimation is also mentioned to be stronger during snow drift (van den Broeke et al., 2006) and influences snow height changes over time (Steffen and Box, 2001). Generally, snow-atmosphere interactions alter the deposited signal in the upper snow layers and can produce
5 a seasonal signal independent of precipitation (Casado et al., 2018). These processes were found to happen on diurnal scales, which have been studied in Greenland (Steen-Larsen et al., 2014) and Antarctica (Ritter et al., 2016).

Once the snow is finally deposited, diffusion smoothes the amplitudes of the isotopic record (Gkinis et al., 2014; Johnsen et al., 2000; Town et al., 2008; Whillans and Grootes, 1985), but seems not to affect the net isotopic composition. Previous studies postulated (depth-dependent) diffusion to cause a cyclicity in stable water isotope records dependent on temperature
10 and accumulation rate with similar diffusion lengths along the East Antarctic Plateau (Casado et al., 2020; Laepple et al., 2018).

The Deuterium excess (d) is defined as $\delta D - 8 \times \delta^{18}O$. In several studies of climate reconstruction d is used as a proxy for the moisture source temperature when combining ice core data and model simulations (Pfahl and Sodemann, 2014; Sodemann and Stohl, 2009; Stenni et al., 2004; Uemura et al., 2012; Vimeux et al., 1999). However, if kinetic fractionation takes place, this
15 second order isotopic property d is strongly affected. While on the East Antarctic Plateau the main control on d in precipitation seems to be the local condensation temperature (Touzeau et al., 2016; Uemura et al., 2012), another driver of d is sublimation of surface snow (Kopec et al., 2019). This sublimated snow can be recycled and deposited again, and make up a large proportion (~40%) of the condensating moisture over Antarctica (Noone and Simmonds, 2002). Recently, a δ -scale effect has been proposed to influence d significantly in high latitudes and altitudes (Dütsch et al., 2017). Studies at Dome Argus (Pang
20 et al., 2019) and Kohlen Station (Kipfstuhl, unpublished) have shown that d in snow precipitation (fresh snow) is much higher than in e.g., snow pits. d measured in deposited snow seems to be superimposed by sublimation effects happening at the snow surface directly after deposition. This explains a much higher d in fresh snow samples and creates a warm bias in $\delta^{18}O$ when the altered signal is archived in firn and ice. In contrast to mechanical mixing, the sublimation causes kinetic fractionation. However, the major factor of uncertainty in signal formation is the not well constrained isotopic composition of fresh snow,
25 although $\delta^{18}O$ and δD in snow precipitation have been analyzed locally (e.g., Fujita and Abe, 2006; Landais et al., 2012; Ma et al., 2020b; Motoyama et al., 2005; Pang et al., 2019).

Isotopic composition of precipitation in atmospheric general circulation models

Atmospheric general circulation models (AGCM) like ECHAM5-wiso (Werner et al., 2011) mathematically describe the atmospheric dynamics. ECHAM5-wiso captures the global pattern of precipitation and water vapor isotopic composition of
30 past and future precipitation on Earth. As these AGCM work on a global scale, they are not specifically tailored to the Polar Regions. Still, previous studies have compared modeled precipitation of ECHAM5-wiso to $\delta^{18}O$, δD , and d in Antarctic snow to test the model performance, but often only the uppermost cm of the snowpack were sampled for this approach (e.g., Ding et al., 2010; Xiao et al., 2012). Goursaud et al. (2018) have reported a general warm bias of ECHAM5-wiso in winters on the remote plateau of East Antarctica.

35 Motivation & scope of this study

All of the above-mentioned processes – from precipitation-related to postdepositional – shape and modify the isotopic records retrieved from firn and ice cores. In order to interpret stable water isotopes as paleoclimatic proxies, it is crucial to understand the processes related to signal formation. Comprehending and quantifying all relevant processes will improve not only the interpretation of isotope records, but also (isotopic) climate models and thus their applications. Whereas spatial variability and
40 diffusion are well constrained, synoptic effects, precipitation intermittency, and especially snow-air exchange reactions are topics of recent research. Our study targets this objective and presents stable water isotope data from snow profiles taken on a

5 traverse on the East Antarctic Plateau – covering a region of low temperatures, accumulation rates, and sparse sample availability. With multiple samples per sampling site, we can quantify the spatial variability of stable water isotopes on a local and regional scale and reduce the impact of stratigraphic noise. Furthermore, we analyze the data in relation to environmental properties like performed by Masson-Delmotte et al. (2008) in order to assess the effect of postdepositional processes on ice core records. From several long-time snow sampling projects at Kohnen Station (Münch et al., 2016), we know that isotopes can be interpreted as proxies of annual and seasonal temperature variations. By counting local maxima and minima in the vertical isotope records along the traverse with its systematically varying accumulation rate, we aim to answer the question up to which critical minimal value of accumulation rate a seasonal signal appears to be still preserved in Antarctic snow.

10 In the second step of this manuscript, we compare our field measurement to simulation results of the recently updated ECHAM6-wiso model (Cauquoin et al., 2019) on the spatial (hundreds of km) and temporal (months to decades) scale. This comparison serves as a validation for the new ECHAM6-wiso to capture the extreme environmental conditions on the East Antarctic Plateau. We discuss whether the sampling depth (here 5 cm vs. 1 m) affects the relation to geographical properties. In case studies at selected sites, we compare simulated snow profiles derived from the ECHAM6-wiso model results with sampled snow profiles to find out whether climatic signals are preserved and which processes dominate in the postdepositional phase. The change of d in snow exposed at the surface over time (starting from fresh snow to deposited snow) can be a measure for sublimation or warm bias of $\delta^{18}\text{O}$. Still, for a quantitative analysis, we are missing the isotopic values of the respective fresh snow in our samples. Instead, we address the question how many depositional events prognosed by ECHAM6-wiso are later visible in the snowpack. A related question is how an isotopic signal is formed, altered, and connected with stratigraphy (and therefore depositional events) on the East Antarctic Plateau. Finally, the surface snow on the interior East Antarctic Plateau can be exposed to the atmosphere for months up to several years. We use our observations and utilize the model to assess the link between snow precipitation to in-fact deposition.

2 Material & methods

Sampling area & snow profiles

25 In the framework of the Coldest Firn project (CoFi; Weinhart et al., 2020), an overland traverse from Kohnen Station to former Plateau Station was conducted in austral summer 2016/17, further called CoFi traverse.

50 snow cores taken along this traverse were analyzed in this study. The sampling sites (Figure 1a) are numbered chronologically (site 14 was sampled before site 15). Data of omitted sampling site numbers 11 and 13 are not presented here (partly not measured yet). The sampling distance between the sites ranges mostly between 80 km and 100 km, dependent on the overnight stops during the traverse (except for the distance between sites 5 and 6: ~46 km). Site 14 was close to former Plateau Station.

30 The mean annual temperature at Kohnen Station used to be -44.5°C (Oerter et al., 2000). Over the last two decades, an increase of 1°C per decade has been measured by the automatic weather station, jointly operated by the Institute for Marine and Atmospheric Research (IMAU) and the Alfred Wegener Institute (AWI) (Medley et al., 2018). The mean annual 10 m firn temperature at former Plateau Station is -58.4°C (Kane, 1970), one of the lowest in Antarctica. According to previous field measurements, the accumulation rate along the traverse ranges from $80\text{ kg m}^{-2}\text{ a}^{-1}$ at Kohnen Station to roughly $25\text{ kg m}^{-2}\text{ a}^{-1}$ at Plateau Station (Radok and Lile, 1977). Coming along with the temperature increase at Kohnen Station, a firn-core analysis also indicates a simultaneous increase in accumulation by almost 20% over two decades (Medley et al., 2018). Close to site 5, an accumulation rate of $49\text{ kg m}^{-2}\text{ a}^{-1}$ was measured (Karlöf et al., 2005).

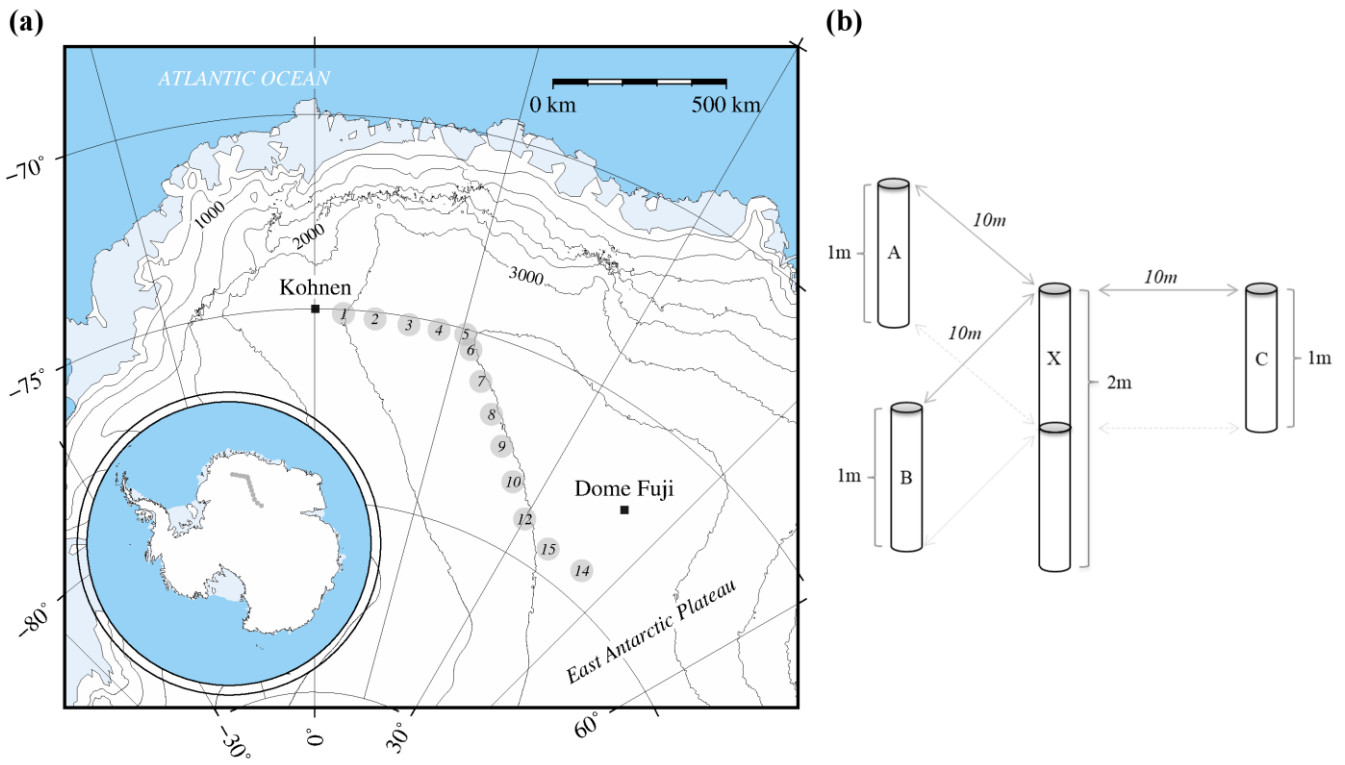


Figure 1: a) Map of the investigated area in Antarctica. Grey dots represent the sampling sites along the CoFi traverse in this study. At each site, snow profiles according to the setup in b) were taken. Contour lines show height above sea level (in 500 m increments).

At each sampling site, snow cores were taken with carbon fiber tubes of 1 m in length and 10 cm in diameter. In the following, we use the term ‘profile’ for a continuous snow record (i.e., one profile can consist of multiple cores sampled consecutively in depth). From a central position (labeled ‘X’) the surrounding sampling positions (labeled ‘A’, ‘B’, ‘C’) had 10 m distance to assure spatial independence according to Laepple et al. (2016) (Figure 1b). Profiles at position X have a total length of 2 m (at sites 14 and 15: 4 m), the surrounding profiles A, B and C have a length of 1 m. For a more detailed description of the sampling procedure, we refer to Schaller et al. (2016) or Weinhart et al. (2020). After sampling, the profiles were transported to AWI in polypropylene boxes in a continuous cold chain below -20°C .

Further in the text, we will distinguish between three different transects along the traverse. The first one is about coast parallel following the ice divide between Kohnen Station and sampling site 5. The second one is contour line parallel at 3500 m asl from site 5 to site 12. The third transect, which contains sites 12, 14, and 15, is called interior plateau.

Discrete sampling and cavity ring-down spectroscopy

For further analysis, the snow profiles are cut into discrete samples in the AWI ice laboratory at -18°C . We used the snow cutting device presented in Weinhart et al. (2021a) to process the snow cores. The cut samples were put into plastic bags, which were welded to prevent exchange reactions with the surrounding air before the analysis. Usually, profiles taken at position X have been cut in 1 cm intervals, profiles from positions A, B, and C have been cut in 2 cm intervals (at sites 5 and 8, all profiles were cut in 1 cm resolution). The depth scale of each individual snow core has been adjusted to the 1 m tube length. At site 5 and site 12 only three measured profiles are available.

Stable water isotopes have been measured using cavity-ring-down-spectroscopy (CRDS) with a Picarro L2130-i isotope analyzer using the protocol by van Geldern and Barth (2012) for memory and drift correction. Results are presented in the common δ -notation in per-mill [‰] according to

$$\delta = \left(\frac{R_{\text{sample}}}{R_{\text{reference}}} - 1 \right) \times 10^3$$

with the isotopic ratio ($^{18}\text{O}/^{16}\text{O}$ or D/H, respectively) of the sample (R_{sample}) and a standard ($R_{\text{reference}}$). Due to the low isotopic values in the area of investigation, we used an in-house snow standard collected at site 14. For $\delta^{18}\text{O}$ we report a precision of $<0.1\%$.

In this manuscript, we present $\delta^{18}\text{O}$ (δD and d) over depth of single profiles. Furthermore, we calculated mean values over
5 depth and use the following terms:

- ${}_z\delta^{18}\text{O}$ as the mean value from surface to depth z (e.g., 5 cm and 1 m) of a single snow profile
- $\sigma_v({}_z\delta^{18}\text{O})$ as vertical standard deviation from surface to depth z of $\delta^{18}\text{O}$ (variability over depth) of a single snow profile
- ${}_z\delta^{18}\text{O}_{\text{Site}}$ as the mean ${}_z\delta^{18}\text{O}$ of all available profiles to depth z at a given sampling site (Figure 1)
- $\sigma_h({}_z\delta^{18}\text{O}_{\text{Site}})$ as horizontal standard deviation of all ${}_z\delta^{18}\text{O}$ (variability in space to the same depth z) at a given site

10 Used climatic parameters on the East Antarctic Plateau

We use the temperature derived from ECHAM6-wiso at each site for a large-scale comparison of our data with temperature. Additionally to the accumulation rates presented earlier, at sites 14 and 15, we used sulfate (SO_4^{2-}) measurements of the 4 m snow profiles (Weinhart et al., 2021b) to calculate a more recent local accumulation rate. Maxima in SO_4^{2-} concentration can reflect volcanic horizons in snow and ice cores and are used to derive the local accumulation rate (e.g., done in the vicinity of
15 Kohnen by Traufetter et al., 2004). As the ionic budget on the Antarctic plateau is not sea-salt dominant like in coastal regions (Legrand and Mayewski, 1997) and our calculation of non-sea-salt SO_4^{2-} (e.g., Ma et al., 2020b; Traufetter et al., 2004) did not significantly differ from SO_4^{2-} , we use SO_4^{2-} here.

We counted local maxima (and minima) of $\delta^{18}\text{O}$ in all available profiles, and for comparison also in SO_4^{2-} . Additionally, we estimated an annual layer thickness at each sampling site by multiplying snow density and annual accumulation rate (see
20 Weinhart et al., 2021a).

Isotopic mean values and vertical profiles derived from ECHAM6-wiso

We use $\delta^{18}\text{O}$ and δD precipitation-weighted model output from an ECHAM6-wiso simulation nudged to ERA5 reanalysis data, covering the period 1979-2020 (Cauquoin and Werner, in review, 2021) in annual resolution for all sampling sites, and in daily resolution for the selected sites 5 and 14 as well as at Kohnen Station. The ECHAM6-wiso simulation was performed at a
25 mean horizontal grid resolution of approximately $1.1^\circ \times 1.1^\circ$ with 31 vertical model levels.

For the comparison of the annual mean values we calculated the mean $\delta^{18}\text{O}$ (δD and d) of the same time period that is covered in the uppermost 1 m of the snow profile at the respective sampling site (according to the local accumulation rate) using the ECHAM6-wiso data in annual resolution.

To compare the ECHAM6-wiso data to the vertical snow profiles, we decided to use just one snow profile at each location
30 instead of a stacked profile to avoid the loss of the amplitude of the temporal variability. At locations 5 and 14, we used profile X (Figure 1b). We use a snow profile from season 2015/16 (Schaller et al., 2017) at Kohnen Station, as in the framework of this study no samples were taken there.

In order to simulate the $\delta^{18}\text{O}$ profiles, we apply a similar concept as explained in Casado et al. (2020). The daily precipitation amount from ECHAM6-wiso was piled up in layers, as if deposited onto the surface day by day, to a simulated snow profile,
35 applying a minimum precipitation threshold of $10^{-7} \text{ kg m}^{-2} \text{ d}^{-1}$, where each layer is converted into snow equivalent thickness assuming a density profile according to Herron and Langway (1980) and associated with the corresponding daily ECHAM6-wiso $\delta^{18}\text{O}$ value. The top of the artificial profile is chosen to correspond to the sampling date of the taken snow profile. To account for the postdepositional firn diffusion (Johnsen et al., 2000), we apply the method used in Münch et al. (2017). For this, we interpolate the artificial snow profile to an equidistant depth resolution of $\sim 0.1 \text{ mm}$ and calculate the depth-dependent
40 diffusion length with site-specific parameters (i.e., annual mean temperature, annual mean accumulation rate, and Herron-

Langway density profile). Finally, we sample the simulated snow profile virtually in 1 cm intervals to mimic the cutting into discrete samples.

3 Results

$\delta^{18}\text{O}$, δD & d in surface snow

5 In the following sections, we present the isotopic data along the traverse and their spatial variability. We describe them in relation to their geographical context, using properties like temperature and elevation. A list of ${}_{1\text{m}}\delta^{18}\text{O}_{\text{Site}}$, ${}_{1\text{m}}\delta\text{D}_{\text{Site}}$, ${}_{1\text{m}}d_{\text{Site}}$ and the respective horizontal standard deviations can be found in the appendix (Table 3).

Spatial distribution along the traverse

We record the highest values for ${}_{1\text{m}}\delta^{18}\text{O}_{\text{Site}}$ (-45.2‰) and ${}_{1\text{m}}\delta\text{D}_{\text{Site}}$ (-355.7‰) close to Kohnen Station at site 1 and the lowest values at site 14 (${}_{1\text{m}}\delta^{18}\text{O}_{\text{Site}}=-55.5‰$, ${}_{1\text{m}}\delta\text{D}_{\text{Site}}=-428.4‰$). Both values decrease steadily from Kohnen Station towards the interior plateau. In contrast, values of ${}_{1\text{m}}d_{\text{Site}}$ are lowest at site 2 (5.8‰) and increase towards site 14 (15.8‰) (s. appendix). The same trends are visible in the samples from surface to 5 cm depth, i.e., ${}_{5\text{cm}}\delta^{18}\text{O}_{\text{Site}}$, ${}_{5\text{cm}}\delta\text{D}_{\text{Site}}$ and ${}_{5\text{cm}}d_{\text{Site}}$ (not shown). We find the minimum of $\sigma_{\text{h}}({}_{1\text{m}}\delta^{18}\text{O}_{\text{Site}})$ and $\sigma_{\text{h}}({}_{1\text{m}}d_{\text{Site}})$ at site 9. Generally, we record a slight increase in $\sigma_{\text{h}}({}_{1\text{m}}\delta^{18}\text{O}_{\text{Site}})$ from Kohnen Station towards site 14 (Table 3).

15 Stable water isotopes vs. environmental properties

Putting our data into the context of the Antarctic-wide dataset from Masson-Delmotte et al. (2008) we find our sites among those with the coldest temperatures and highest elevations. For the isotope ratios we record a slope of ${}_{1\text{m}}\delta\text{D}/{}_{1\text{m}}\delta^{18}\text{O}=7.01$ (Figure 2a) and also see a trend in ${}_{1\text{m}}d$ towards higher values at altitudes higher than 3000 m asl (Figure 2b). From our observations we calculate a slope of ${}_{1\text{m}}\delta^{18}\text{O}/T=1.04 \text{‰ } ^\circ\text{C}^{-1}$ and ${}_{1\text{m}}\delta\text{D}/T=7.21 \text{‰ } ^\circ\text{C}^{-1}$ (Figure 2c and d). Regional differences are also visible in the coast parallel part of the traverse ($1.16 \text{‰ } ^\circ\text{C}^{-1}$), the contour line parallel part ($1.30 \text{‰ } ^\circ\text{C}^{-1}$) and the interior plateau ($0.61 \text{‰ } ^\circ\text{C}^{-1}$). Here we want to mention that the traverse starts at already 2892 m asl.

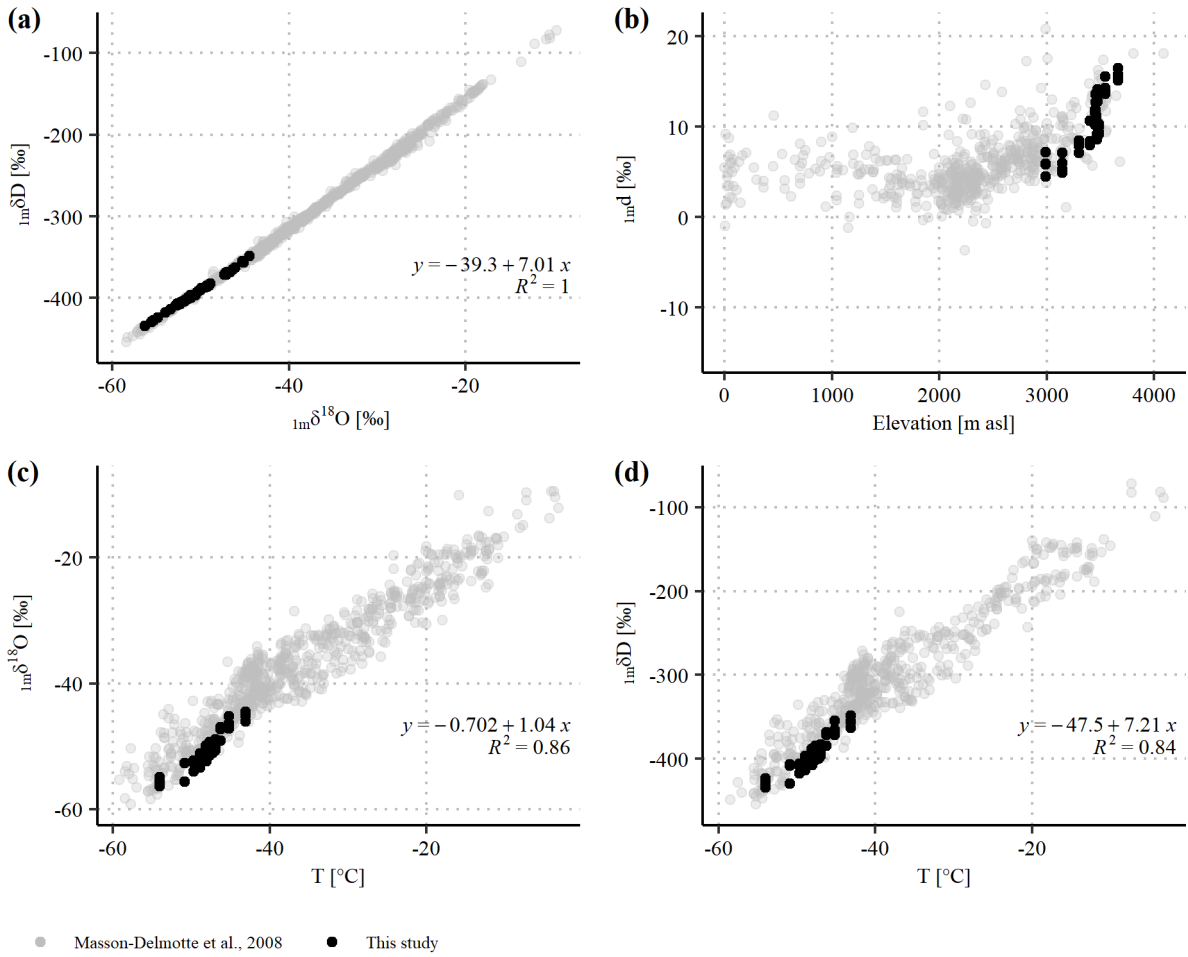


Figure 2: Plots of a) $1m\delta D$ against $1m\delta^{18}O$, b) $1md$ against elevation, c) $1m\delta^{18}O$ against 10 m firn temperature, d) $1md$ against 10 m firn temperature. Results of this study are plotted in black, for comparison we plotted the data from Masson-Delmotte et al. (2008) in grey.

- 5 In contrast, the same calculations with values from the upper 5 cm reflect the general trend not as good as the 1 m mean values (Appendix, Figure 7). The relationship between $5cm\delta D$ and $5cm\delta^{18}O$ is closer to the GMWL with a slope of 7.3. However, the relationship with temperature at the very surface ($5cm\delta^{18}O/T$ and $5cm\delta D/T$) results in an R^2 of only 0.49 and 0.43, respectively. In particular the behavior at low temperatures is not depicted very well ($5cm\delta^{18}O$ and $5cm\delta D$ tend to be too high). Also, $5cmd$ at sites with an elevation higher than 3000 m asl are lower compared to $1md$. We see an increase of R^2 for the correlation of $z\delta^{18}O$ to the local temperature when increasing the depth interval from 5 cm to 1 m (Table 1).

Table 1: Relationships of $z\delta D$ with $z\delta^{18}O$ and $z\delta^{18}O$ with T along the CoFi traverse dependent on the sampling depth.

Depth interval (z)	$z\delta D/z\delta^{18}O$	$z\delta^{18}O/T$	$R^2 (z\delta^{18}O/T)$
5 cm	$5cm\delta D = 7.30 \times 5cm\delta^{18}O - 26.2$	$5cm\delta^{18}O = 0.58 \times T - 1.5$	0.49
10 cm	$10cm\delta D = 7.31 \times 10cm\delta^{18}O - 24.8$	$10cm\delta^{18}O = 0.68 \times T + 7.1$	0.62
20 cm	$20cm\delta D = 7.31 \times 20cm\delta^{18}O - 24.7$	$20cm\delta^{18}O = 1.38 \times T + 15.9$	0.73
40 cm	$40cm\delta D = 7.13 \times 40cm\delta^{18}O - 33.9$	$40cm\delta^{18}O = 1.17 \times T + 5.4$	0.78
1 m	$1m\delta D = 7.01 \times 1m\delta^{18}O - 39.3$	$1m\delta^{18}O = 1.04 \times T - 0.7$	0.86

Accumulation rate derived from snow pits at sampling sites 14 and 15

- As an independent measure to evaluate the annual layer thickness and consequently the presence of seasonal signals, we use the two 4 m profiles to determine the mean decadal accumulation rate. There are two significant local maxima in SO_4^{2-} concentration in both 4 m profiles at sites 14 and 15 (Figure 3). Both peaks appear more apparent in the profile at location 14. We assigned the local maxima around 2 m and 4 m depth to the volcanic eruptions of Pinatubo and Agung, respectively (Traufetter et al., 2004). Cole-Dai et al. (1997) reported high SO_4^{2-} concentrations in snow layers of 1993 and 1994 at South

Pole and assigned them to the Pinatubo eruption. The deposition of volcanic material was delayed due to long-distance transport in high altitudes to the South Pole region. According to this information, we also dated this snow layer to 1993.

We derive a mean accumulation rate of $25.8 \pm 0.5 \text{ kg m}^{-2} \text{ a}^{-1}$ at site 14 and $25.9 \pm 0.5 \text{ kg m}^{-2} \text{ a}^{-1}$ at site 15 since 1964 ($27.7 \pm 1.1 \text{ kg m}^{-2} \text{ a}^{-1}$ and $27.8 \pm 1.1 \text{ kg m}^{-2} \text{ a}^{-1}$ since 1993, respectively), which is consistent with observations at Plateau Station (Radok and Lile, 1977) and around Dome F (Fujita et al., 2011). The uncertainty comes from the unclear deposition time (after the eruption as well as the time interval of deposition itself) of the volcanic material in Antarctica.

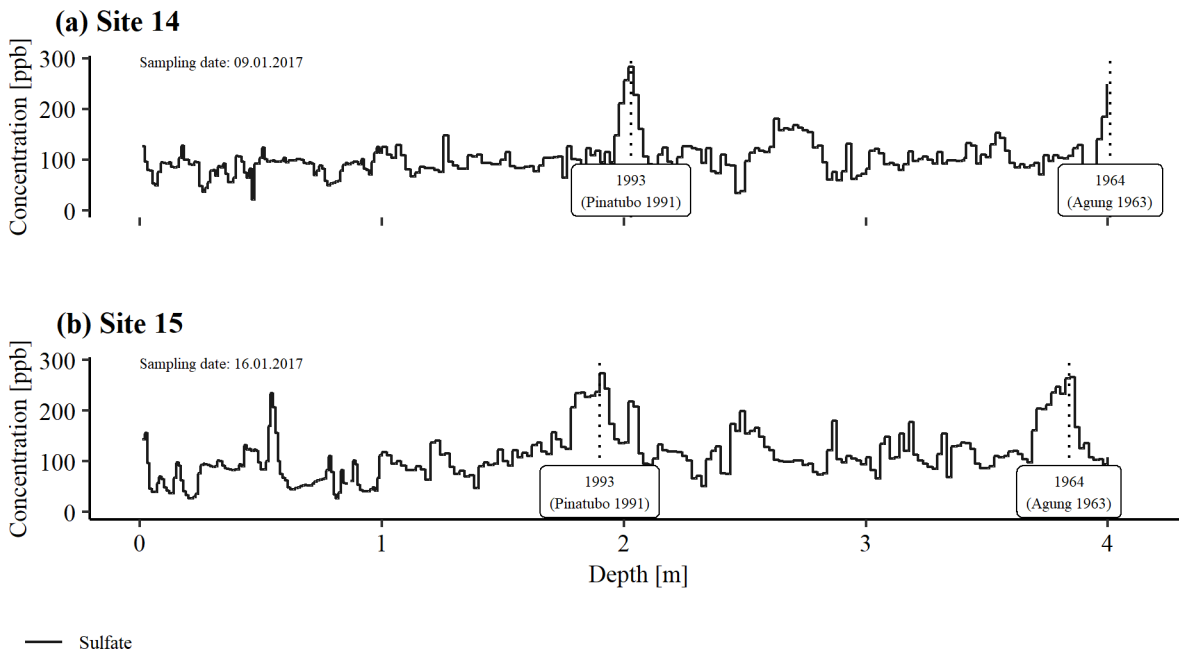


Figure 3: Sulfate concentrations over 4 m depth for sites 14 (a) and 15 (b) measured by means of ion chromatography. We used the dataset by Weinhart et al. (2021b).

10 $\delta^{18}\text{O}$ over depth

Generally, we cannot see one specific relationship between $\delta^{18}\text{O}$ and d in all snow profiles as a function of depth. In most cases we see an anticorrelation, but also correlated patterns or a change between both within a profile is possible. In most snow profiles, d increases from the very surface to about 15 cm depth, mostly independent of the $\delta^{18}\text{O}$ trend. Vertical profiles at some locations can be found in the appendix for comparison.

15 According to the counted $\delta^{18}\text{O}$ cycles in the snow profiles (Table 2), from sites 1-5 the numbers are consistent with the number of years expected from estimates of the accumulation rate. In the contour line parallel part of the traverse this seasonal signal vanishes and is not present at all on the interior plateau (Figure 4). Nevertheless, there is still variability in the order of 4-6 maxima per meter visible in most profiles, which however is not consistent with the annual accumulation rate (compare selected profiles in the Appendix, Figure 8).

Table 2: Average of local maxima counted in $\delta^{18}\text{O}$ over 1 m depth in each profile at each sampling site. The shown accumulation rate is according to the Antarctic-wide dataset by (Arthern et al., 2006)

Sampling site (number of profiles)	Cycles in $\delta^{18}\text{O}$ (\pm standard deviation)	Expected cycles per meter [m^{-1}]	Accumulation rate [$\text{kg m}^{-2}\text{a}^{-1}$]
1 (4)	5 \pm 0.5	4.3	65.7 comp. Medley et al. (2018)
2 (4)	5 \pm 1.0	5.1	55.8
3 (4)	5 \pm 0.9	5.6	50.0
4 (4)	6 \pm 0.5	6.0	46.6
5 (3)	6 \pm 1.2	6.0	47.2 comp. Karlöf et al. (2005)
6 (4)	5 \pm 1.0	6.2	45.5
7 (4)	6 \pm 0.5	6.9	41.1
8 (4)	5 \pm 1.0	7.0	40.3
9 (4)	4 \pm 1.3	7.1	39.5
10 (4)	5 \pm 0.5	7.4	38.0
12 (3)	5 \pm 1.0	7.4	38.3
14 (4)	5 \pm 1.7	9.0	31.3 comp. Figure 3
15 (4)	4 \pm 0.8	8.0	35.1 comp. Figure 3

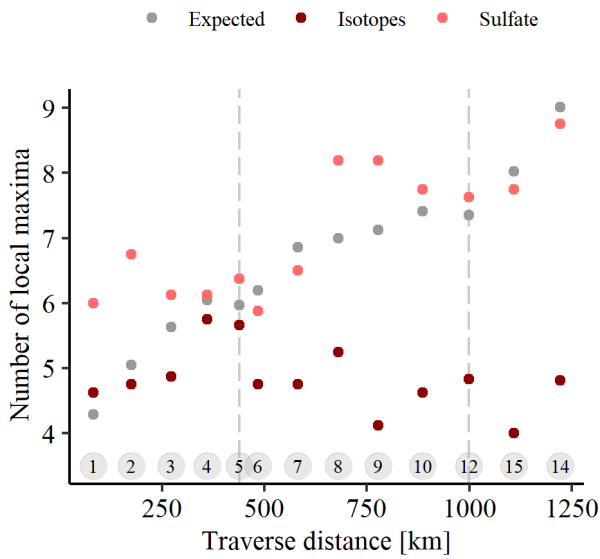


Figure 4: Counted seasonal cycles in $\delta^{18}\text{O}$ (dark red, Table 2) and SO_4^{2-} (red) as well as number of expected cycles according to the accumulation rate (grey). Vertical dashed lines separate the different transects along the traverse (coast parallel, contour line parallel, interior plateau).

Observations vs. ECHAM6-wiso

In the next two sections, we present the results of the comparison between observed isotopic data and ECHAM6-wiso output on a) the spatial scale and b) the temporal scale at the selected sites.

Along the CoFi traverse

Comparing the ECHAM6-wiso model output to the field data, we see that the model depicts very well the trend in $\delta^{18}\text{O}$, but with an offset that slightly increases from Kohnen Station (+4‰) to the interior plateau (+6‰). In contrast, the increase in d of the modeled data along the traverse is too flat (offset on the interior plateau of around +7‰), although d is captured very well close to Kohnen Station.

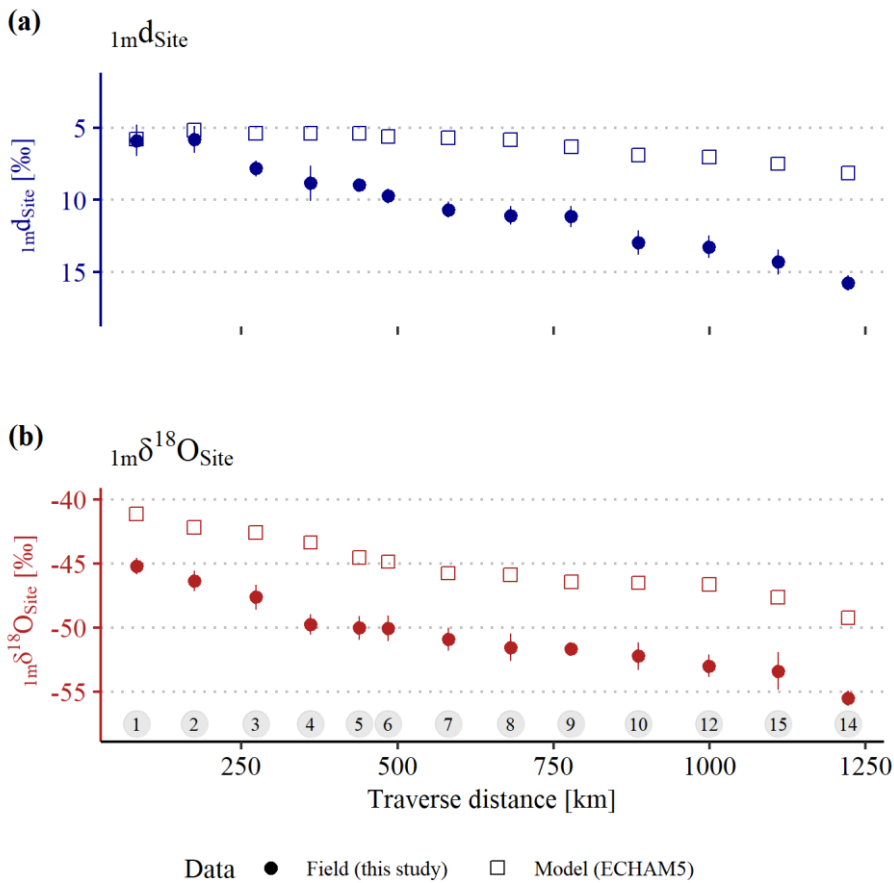


Figure 5: Isotope values a) $1m d_{Site}$ (blue, inverted y-axis) and b) $1m \delta^{18}O_{Site}$ (red) along the CoFi traverse displayed as solid circles with the respective σ_h as vertical error bars. The isotopic composition of the precipitation in ECHAM6-wiso for $\delta^{18}O$ and d for the same time interval is displayed in empty squares. The number of the sampling site is shown in grey circles at the bottom of b).

5 Vertical profiles at selected sites

Comparing the snow profiles with the simulated profiles, we generally see the offset in $\delta^{18}O$, which is also visible on the spatial scale (Figure 6). Some local maxima and minima seem well reflected in the profiles below 1 m at Kohnen Station and site 5. In the upper meter, the simulated profiles show too many temperature-induced variations (seasonal cycles), particularly at site 14, which we consider as representative for the interior plateau.

- 10 At site 5 we note an offset in $\delta^{18}O$ between the first and the second meter possibly originating from daily measurement drift.

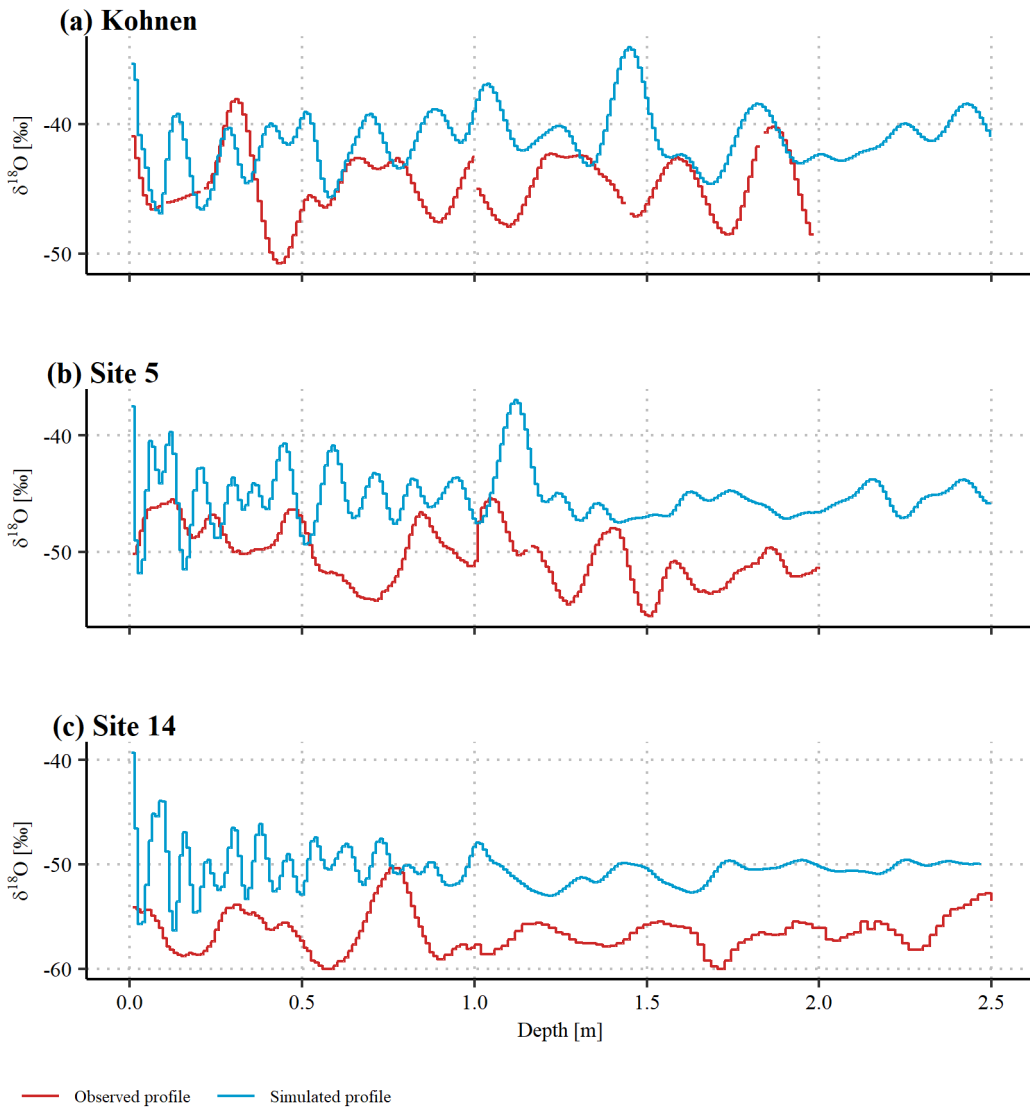


Figure 6: Observed $\delta^{18}\text{O}$ snow profiles (red) and simulated snow profile (blue) from daily ECHAM6-wiso output including precipitation threshold, postdepositional diffusion and virtual sampling for a) Kohnen Station, b) site 5, and c) site 14. The panels have a common depth axis.

5 4 Discussion

In this chapter, we first want to discuss $\delta^{18}\text{O}$, δD , and d in the measured snow profiles in terms of spatial variability and of postdepositional processes in a qualitative manner. Later, we will focus on the comparison between observed and modeled snow profiles and evaluate the processes, which lead to similarities and differences between both.

Spatial variability of $\delta^{18}\text{O}$, δD and d

- 10 Considering the environmental conditions on the remote plateau of East Antarctica – a decreasing accumulation rate and higher relative surface roughness (Weinhart et al., 2020) – we assumed an increase of σ_{H} at each site along the traverse. Non-uniform deposition on the local scale, longer residence time at the surface, and a higher potential for mixing of snow from different deposition events were expected to affect the small-scale spatial variability (i.e., σ_{H}) of the isotopic composition in the samples significantly. In turn, σ_{H} fluctuates around a mean value along the traverse. Four spatially independent snow profiles seem to
- 15 be sufficient to assure a standard error (of the mean at one sampling location: σ_{H} divided by the square root of the number of samples) of below 1‰ for $_{1\text{m}}\delta^{18}\text{O}$ and below 6‰ for $_{1\text{m}}\delta\text{D}$ in the sampling area. The 1 m mean value seems not to be strongly affected by the local surface topography, which can strongly impact the local accumulation behavior (King et al., 2004).

Along several traverses from Zhongshan Station to Dome A in different seasons, the top snow layer (5 cm) was sampled. Ding et al. (2010) reported a $\delta^{18}\text{O}/T$ slope of $0.84 \text{ ‰ } ^\circ\text{C}^{-1}$ using samples from two seasons, Ma et al. (2020a) reported a slope of $0.91 \text{ ‰ } ^\circ\text{C}^{-1}$ with data from four seasons. In general, the $\delta^{18}\text{O}/T$ slopes reflect the overall dependence of the isotopic composition on temperature as well as the specific situation in the condensation layer in different regions and, therefore, may vary regionally. Lower $\delta^{18}\text{O}/T$ slopes on both short (seasonal to annual) and long (glacial-interglacial) time scales have been found (e.g., Stenni et al., 2016; Touzeau et al., 2016) as well as for regions higher than 3000 m asl or generally with increasing elevation and lower temperatures (Li et al., 2021; Satow et al., 1999). This is also consistent with the slopes we find in the different transects in our study, ranging between 0.61 and $1.30 \text{ ‰ } ^\circ\text{C}^{-1}$. Casado et al. (2017) pointed out to be careful with the use of spatial slopes, as they have a much lower span than temporal slopes do (0.2 to $1.5 \text{ ‰ } ^\circ\text{C}^{-1}$), especially when applying to time series covering glacial-interglacial cycles like the whole Holocene.

Ma et al. (2020a) mentioned the interannual variability of $\delta^{18}\text{O}$ to be low and evaporation for stable water isotopes to be limited. This can explain a similar spatial trend of $\delta^{18}\text{O}$ along the traverse for both sampling intervals (5 cm and 1 m). On the other hand, we report a larger scatter in the 5 cm interval when plotting them against local temperature (Table 1 and Figure 7). $_{5\text{cm}}d$ can be considered as too low, especially at sites with high elevations and cold annual mean temperatures. We explain this observation with surface-related processes (probably during summer) that are transient and not fully diffused into the snowpack. Especially the processes redistribution and sublimation are overrepresented in samples from the very surface and can generate a seasonal bias. Therefore we suggest using 1 m to obtain representative isotope samples instead of just the upper cm of the snow column if there are no logistical constraints. 1 m depth-averages cover the interannual variability of stable water isotopes in low accumulation rate areas, and the effect of sublimation (affecting d ; see next section) is not overrepresented.

Postdepositional processes impair conservation of temporal variability in $\delta^{18}\text{O}$, δD and d

Alteration at the snow-atmosphere interface

The isotopic composition of snow after deposition is subject to strong alterations at the very surface. Diurnal cycles in the isotopic composition of surface snow can be larger than day-by-day means in temporal observations (Hughes et al., in review; Ritter et al., 2016). The quantification of these sublimation effects on stable water isotopes archived in ice cores is one of the recent scientific questions (Pang et al., 2019) for higher accuracy in paleotemperature reconstructions. Unfortunately, in our study, we only have one observation in time and can therefore only indirectly reconstruct the temporal signal at each site.

Still, the antiphase we observe between d and $\delta^{18}\text{O}$ present in most profiles is consistent with observations at Dome F by Stenni et al. (2016) and at Dome C by Fujita and Abe (2006). The sublimation effect causes an enrichment in δD at the snow-atmosphere interface and, therefore, lower d values (Moser and Stichler, 1974). We interpret the increase in d from the surface to 15 cm depth (independent of $\delta^{18}\text{O}$) as an ongoing manifestation of the sublimation process (strong at the surface, decreasing with depth). From a comparison with snow profiles from a previous season at Kohnen Station (Schaller et al., 2017), we also see that this is no general behavior, but probably strongly depends on the timing of the last snow deposition, exposition time of the snow surface, and generally the weather conditions. We conclude that d is strongly affected by sublimation in most profiles, independent of the $\delta^{18}\text{O}$ signal. Whether this effect is stronger on the remote plateau than in the other regions still has to be investigated, especially with analyzing the isotopic composition of fresh snow (i.e., before deposition). Laboratory experiments showed that sublimation in the snow is temperature-dependent (Ekaykin et al., 2009), and also the much higher values of d on the interior plateau (Figure 5a) could support this argument.

Postdepositional alterations dominate over seasonal variability in isotope profiles on the East Antarctic Plateau

Assuming that seasonal variations in air temperature modulate the isotopic composition of the snow (either by precipitation or by snow-air interaction), the succession of high/low $\delta^{18}\text{O}$ can be interpreted as a seasonal signal (e.g., Du et al., 2019;

Fernandoy et al., 2010; Furukawa et al., 2017; Nakazawa et al., 2021). However, it has been shown that diffusion only, even if irregular layers with noisy isotopic composition were deposited at the surface, can lead to this kind of observed cycles in the isotopic composition (Laepplé et al., 2018).

Hoshina et al. (2016) have discussed that seasonal cycles in several proxies (major ions and stable water isotopes) are preserved at sites with an accumulation rate $>100 \text{ kg m}^{-2} \text{ a}^{-1}$ and calm wind conditions. Also stable water isotopes at Kohnen Station show sinusoidal patterns, especially after reducing local noise by stacking multiple profiles (Münch et al., 2016), although cycles in single isotope profiles cannot always be seen clearly (e.g., Moser et al., 2020). This is then commonly interpreted as a seasonal signal, but a significant impact of postdepositional alterations cannot be excluded. Considering these observations and interpretations, we also interpret the isotopic cycles in the profiles at sampling sites 1-5 still as seasonal. This is consistent with observations from Karlöf et al. (2005), who discussed seasonal $\delta^{18}\text{O}$ signals close to sampling site 5. Further along the traverse towards the interior plateau, a combination of different processes seems to suppress seasonal isotope signals as the discrepancy between expected annual layers and counted local maxima in $\delta^{18}\text{O}$ increases. At site 14, according to our dating, we should expect 9 cycles m^{-1} snow or firn (Figure 4). At this point, we want to mention that the cyclicity in sulfate fits the expected one adequately, but also major ions reach their limits in the usage as annual markers in low accumulation rate areas (Weinhart et al., 2021a). Vertical $\delta^{18}\text{O}$ profiles with a cycle length of 20 cm have also been observed at Dome A (Ma et al., 2020b). This behavior is generally described at several sites in East Antarctica and explained with a combination of local noise and diffusion (Laepplé et al., 2018). All three stages of isotopic alteration mentioned in the introduction (syndepositional, mechanical postdepositional, and physico-chemical postdepositional) play a decisive role by overprinting the isotopic signals from precipitation. We also want to emphasize the diamond dust deposition and hoar frost, which could add an isotopic value, which is barely known (Stenni et al., 2016). However, as the wave-shape signal with 4-6 local maxima ($\sim 20 \text{ cm}$ cycle length) is present in the vast majority of all profiles, the retrieved diffusion lengths explain the similarity of cycles in snow pits across the East Antarctic Plateau, despite the very different accumulation rates.

The diffusion length at the surface is not very large and increases with depth (and density) (Johnsen et al., 2000; Laepplé et al., 2018; Münch et al., 2017). Therefore we conclude that a seasonal signal is still present along the ice divide but vanishes shortly behind site 5 (accumulation rate of about $50 \text{ kg m}^{-2} \text{ a}^{-1}$), which is a bit lower than pointed out by Hoshina et al. (2016). Further samples in the precipitation shadow of the main DML ice divide are needed to investigate whether certain environmental conditions (e.g., wind speed) have an additional influence here.

Comparison of measured and simulated snow profiles

The absolute offset in $\delta^{18}\text{O}$ (Figure 5 and Figure 6) between observations and model output (or simulated profiles, respectively) can originate either from a lower ice sheet elevation, higher temperatures, or missing fractionation processes (after precipitation). In the following, we will focus on the differences between observations and simulations in the variability over depth.

Before contrasting $\delta^{18}\text{O}$ in simulated and observed snow profiles, we briefly compare the annual precipitation from ECHAM6 with the local accumulation rates (see section 2 and Figure 3). Generally, the modeled annual precipitation is slightly lower than the accumulation rate at Kohnen ($56 \text{ kg m}^{-2} \text{ a}^{-1}$), site 5 ($41 \text{ kg m}^{-2} \text{ a}^{-1}$), and site 14 ($21 \text{ kg m}^{-2} \text{ a}^{-1}$). This is no surprise, as the AGCM does not capture diamond dust and recycled water vapor. Considered the latter two account for over half of the annual accumulation at Dome C (Stenni et al., 2016) and we estimate a similar amount for the interior plateau, we evaluate the precipitation in ECHAM6 at site 14 as rather too high than too low. This overrepresentation of (temperature-driven synoptic) snowfall can explain a higher number of $\delta^{18}\text{O}$ cycles in the simulated profile than expected.

The applied diffusion in the simulated profiles is not significantly different at the sites because the site-specific parameters (accumulation rate, temperature, and density) produce similar diffusion lengths. Assuming that the diffusion in the simulated profiles depicts the environmental conditions on the East Antarctic Plateau, the smooth $\delta^{18}\text{O}$ curves at the surface (especially

0-1 m in Figure 6) in the observed snow profiles are an indicator for strong influences of mechanical mixing and sublimation on the isotopic record in this depth interval. Lower than 1 m, the diffusion seems to control the shape of the isotope profiles, which is captured by our diffusion modeling. This also fits the observation that firn density is the main driver for the depth dependence of the diffusion length (Johnsen et al., 2000).

5 On short time scales, stable water isotope records from the East Antarctic Plateau often are inconsistent with temperature (Ma et al., 2020b; Münch et al., 2017). Some of the previously mentioned postdepositional effects also are suggested to further lead to a correlation between $\delta^{18}\text{O}$ and temperature (again) (Touzeau et al., 2016). In Greenland, a case study implies that only 40-60% of deposited snow is later preserved in the snowpack (Zuhr et al., in review, 2021). Still, we consider the simulated profile to depict the trend at Kohnen Station very well, especially below 1 m depth. Single (climatic) signals in the observed profiles
10 at site 5 and site 14 are visible in the simulated profile as well, although in the upper meter too many (seasonal) cycles appear in the simulated profile.

We observe that the diffusion modeling is well constrained, but at the very surface, other processes dominate the alteration of $\delta^{18}\text{O}$. Of course, the discrepancy between our observed profiles and the simulated profiles can come from a mismatch of the precipitation in ECHAM6 with Antarctic precipitation or errors with the applied diffusion modeling scheme. Nevertheless, as
15 the diffusion is generally well constrained, we qualitatively assign the discrepancy to a) the not well-constrained impact of mechanical mixing, sublimation, and recondensation as well as b) the barely known $\delta^{18}\text{O}$ composition of diamond dust and hoar frost. Therefore, further studies on these processes are highly recommended. This could be accomplished by field experiments comparing fresh snow with deposited snow and a continuous record of $\delta^{18}\text{O}$ in precipitation and temperature.

5 Summary and conclusion

20 In this study, we presented the spatial distribution of stable water isotope data ($\delta^{18}\text{O}$, δD & d) in the top meters along a traverse over the East Antarctic Plateau. On the spatial scale, 1 m averages of $\delta^{18}\text{O}$ and δD show the expected correlation with increasing elevation and decreasing temperature. We report a higher scatter in the correlation of isotopic composition with temperature the smaller the sampling depth is. This indicates a seasonal bias in $\delta^{18}\text{O}$, while a lower deuterium excess in relation to the elevation does indicate an influence of sublimation. For a precise spatial relation of the isotopic composition of snow with
25 environmental properties, we suggest a 1 m sampling depth to avoid a superimposition of surface processes.

An increase of the deuterium excess from the surface to roughly 15 cm depth in most vertical snow profiles, which happens independently of the $\delta^{18}\text{O}$ signal, is interpreted as an ongoing sublimation process. To comprehensively understand the history of a local snowpack, $\delta^{18}\text{O}$ and δD cannot be interpreted independently from each other, d always has to be taken into account. A quantification of the sublimation effect, which we were not able to accomplish within this study, is the subject of current
30 research (Ma et al., 2020b) and is essential for the climatic interpretation of isotopes in ice core records.

Seasonal cycles of $\delta^{18}\text{O}$ (even if postdepositionally altered) are visible in profiles at sites along the ice divide from Kohnen Station eastwards until an accumulation rate of roughly $50 \text{ kg m}^{-2}\text{a}^{-1}$. On the interior plateau, the observed cycles are no longer consistent with the local accumulation rate. The cyclicity with roughly 20 cm length would fit with previously published values for postdepositional diffusion, but in the uppermost meter diffusion alone is probably too weak to cause the observed
35 patterns alone. The processes of sublimation, mechanical mixing, and diffusion together overprint a seasonal signal in areas with an accumulation rate lower than $50 \text{ kg m}^{-2}\text{a}^{-1}$.

A comparison with model results of a recent ECHAM6-wiso simulation covering the same time span shows a similar trend for $\delta^{18}\text{O}$ like in surface snow, but with a constant offset of on average +5‰. The simulated trend in d , in turn, is rather too weak, but the high deuterium excess in snow on the interior plateau is probably strongly influenced by postdepositional sublimation.

40 At selected sites, we compared snow profiles to simulated profiles derived from ECHAM6-wiso data from the surface to 2 m depth. In the first meter, the simulated profiles show distinct variations (i.e., seasonal $\delta^{18}\text{O}$ signals), which are not present in

observed profiles, especially on the interior plateau. In the second meter, the general trends of the profiles are depicted well by the simulation. We come to the conclusion that in the upper meter, the processes of sublimation and mechanical mixing – which are not included in the simulation – are very dominant and can therefore explain the discrepancy between observed and simulated profiles. Below 1 m – with increasing diffusion length – the diffusion gets stronger and results in a better representation of the observed profile. How many of the “depositional events” create a measurable isotopic signal remains a major question, but some precipitation events from ECHAM6-wiso were visible in the measured snow profiles.

Our findings imply that the interpretation of seasonal signals in ice cores from low accumulation areas in East Antarctica (lower than 50 kg m⁻²a⁻¹) is barely possible. However, the temporal signals of prominent years can be visible in snow profiles. Therefore we strongly encourage further studies to quantify the sublimation and mixing at the snow surface.

10 6 Data availability

The isotope dataset is archived in the open-access repository PANGAEA under the DOI: 10.1594/PANGAEA.929966. PANGAEA is hosted by the Alfred Wegener Institute Helmholtz Centre for Polar and Marine Research (AWI), Bremerhaven, and the Center for Marine Environmental Sciences (MARUM), Bremen, Germany.

7 Author contributions and conflict of interest

15 JF and SK planned the CoFi project. AW, JF and MH designed the sampling strategy. AW took all snow profiles along the CoFi traverse and conducted the sample preparation in the ice laboratories with support from MM, GM, and PG. AW wrote the manuscript and discussed the results intensively with SK, JF, and MH. MW provided recent ECHAM6-wiso isotope outputs, TM supported the generation of the simulated snow profile, OE improved the manuscript with substantial feedback. All authors declare that they have no conflict of interest.

20 8 Acknowledgements

We are grateful to the AWI logistic team for technical support and Alexandra Touzeau for assisting in the sampling during the fieldwork. Furthermore, the authors want to thank York Schломann for the conduction of the CRDS measurements.

9 Financial support

AW was funded by the German environmental foundation (Deutsche Bundesstiftung Umwelt).

25 10 References

- Altnau, S., Schlosser, E., Isaksson, E., and Divine, D.: Climatic signals from 76 shallow firn cores in Dronning Maud Land, East Antarctica, *The Cryosphere*, 9, 925-944, <https://doi.org/10.5194/tc-9-925-2015>, 2015.
- Arthern, R. J., Winebrenner, D. P., and Vaughan, D. G.: Antarctic snow accumulation mapped using polarization of 4.3-cm wavelength microwave emission, *Journal of Geophysical Research-Atmospheres*, 111, <https://doi.org/10.1029/2004jd005667>, 2006.
- 30 Birnbaum, G., Brauner, R., and Ries, H.: Synoptic situations causing high precipitation rates on the Antarctic plateau: observations from Kohnen Station, Dronning Maud Land, *Antarctic Science*, 18, 279-288, <https://doi.org/10.1017/s0954102006000320>, 2006.
- Casado, M., Landais, A., Picard, G., Münch, T., Laepple, T., Stenni, B., Dreossi, G., Ekaykin, A., Arnaud, L., Genthon, C., Touzeau, A., Masson-Delmotte, V., and Jouzel, J.: Archival processes of the water stable isotope signal in East Antarctic ice cores, *The Cryosphere*, 12, 1745-1766, <https://doi.org/10.5194/tc-12-1745-2018>, 2018.
- 35 Casado, M., Münch, T., and Laepple, T.: Climatic information archived in ice cores: impact of intermittency and diffusion on the recorded isotopic signal in Antarctica, *Climate of the Past*, 16, 1581-1598, <https://doi.org/10.5194/cp-16-1581-2020>, 2020.
- Casado, M., Orsi, A. J., and Landais, A.: On the limits of climate reconstruction from water stable isotopes in polar ice cores, *Past Global Changes Magazine*, 25, 146-147, <https://doi.org/10.22498/pages.25.3.146>, 2017.

- Cauquoin, A. and Werner, M.: High-resolution isotope modeling with ECHAM6-wiso nudged to ERA5 reanalyses: evaluation and perspectives for a better understanding of the water cycle, *Journal of Advances in Modelling Earth Systems*, in review, 2021. in review, 2021.
- 5 Cauquoin, A., Werner, M., and Lohmann, G.: Water isotopes – climate relationships for the mid-Holocene and preindustrial period simulated with an isotope-enabled version of MPI-ESM, *Climate of the Past*, 15, 1913-1937, <https://doi.org/10.5194/cp-15-1913-2019>, 2019.
- Cole-Dai, J., Mosley-Thompson, E., and Thompson, L. G.: Quantifying the Pinatubo volcanic signal in south polar snow, *Geophysical Research Letters*, 24, 2679-2682, <https://doi.org/10.1029/97gl02734>, 1997.
- Craig, H.: Isotopic Variations in Meteoric Waters, *Science*, 133, 1702-1703, <https://doi.org/10.1126/science.133.3465.1702>, 1961.
- Dansgaard, W.: Stable isotopes in precipitation, *Tellus*, 16, 436-468, <https://doi.org/10.1111/j.2153-3490.1964.tb00181.x>, 1964.
- 10 Ding, M., Xiao, C., Jin, B., Ren, J., Qin, D., and Sun, W.: Distribution of δ 18O in surface snow along a transect from Zhongshan Station to Dome A, East Antarctica, *Chinese Science Bulletin*, 55, 2709-2714, <https://doi.org/10.1007/s11434-010-3179-3>, 2010.
- Du, Z., Xiao, C., Zhang, Q., Li, C., Wang, F., Liu, K., and Ma, X.: Climatic and environmental signals recorded in the EGRIP snowpit, Greenland, *Environ. Earth Sci.*, 78, <https://doi.org/10.1007/s12665-019-8177-4>, 2019.
- Dütsch, M., Pfahl, S., and Sodemann, H.: The Impact of Nonequilibrium and Equilibrium Fractionation on Two Different Deuterium Excess Definitions, *Journal of Geophysical Research: Atmospheres*, 122, <https://doi.org/10.1002/2017jd027085>, 2017.
- 15 Ekaykin, A. A., Hondoh, T., Lipenkov, V. Y., and Miyamoto, A.: Post-depositional changes in snow isotope content: Preliminary results of laboratory experiments, *Clim. Past Discuss.*, 5, <https://doi.org/10.5194/cpd-5-2239-2009>, 2009.
- Ekaykin, A. A., Lipenkov, V. Y., Barkov, N. I., Petit, J. R., and Masson-Delmotte, V.: Spatial and temporal variability in isotope composition of recent snow in the vicinity of Vostok station, Antarctica: implications for ice-core record interpretation, *Annals of Glaciology*, Vol 35, 35, 181-186, <https://doi.org/10.3189/172756402781816726>, 2002.
- 20 EPICA Community Members: Eight glacial cycles from an Antarctic ice core, *Nature*, 429, 623-628, <https://doi.org/10.1038/nature02599>, 2004.
- EPICA Community Members: One-to-one coupling of glacial climate variability in Greenland and Antarctica, *Nature*, 444, 195-198, <https://doi.org/10.1038/nature05301>, 2006.
- 25 Fernandoy, F., Meyer, H., Oerter, H., Wilhelms, F., Graf, W., and Schwander, J.: Temporal and spatial variation of stable-isotope ratios and accumulation rates in the hinterland of Neumayer station, East Antarctica, *Journal of Glaciology*, 56, 673-687, 2010.
- Fisher, D. A., Reeh, N., and Clausen, H. B.: Stratigraphic noise in time series derived from ice cores, *Annals of Glaciology*, 7, 76-83, <https://doi.org/10.3189/S0260305500005942>, 1985.
- Fujita, K. and Abe, O.: Stable isotopes in daily precipitation at Dome Fuji, East Antarctica, *Geophysical Research Letters*, 33, <https://doi.org/10.1029/2006gl026936>, 2006.
- 30 Fujita, S., Holmlund, P., Andersson, I., Brown, I., Enomoto, H., Fujii, Y., Fujita, K., Fukui, K., Furukawa, T., Hansson, M., Hara, K., Hoshina, Y., Igarashi, M., Iizuka, Y., Imura, S., Ingvander, S., Karlin, T., Motoyama, H., Nakazawa, F., Oerter, H., Sjoberg, L. E., Sugiyama, S., Surdyk, S., Strom, J., Uemura, R., and Wilhelms, F.: Spatial and temporal variability of snow accumulation rate on the East Antarctic ice divide between Dome Fuji and EPICA DML, *Cryosphere*, 5, 1057-1081, <https://doi.org/10.5194/tc-5-1057-2011>, 2011.
- 35 Furukawa, R., Uemura, R., Fujita, K., Sjolte, J., Yoshimura, K., Matoba, S., and Iizuka, Y.: Seasonal-Scale Dating of a Shallow Ice Core From Greenland Using Oxygen Isotope Matching Between Data and Simulation, *Journal of Geophysical Research-Atmospheres*, 122, 10873-10887, <https://doi.org/10.1002/2017jd026716>, 2017.
- Gkinis, V., Simonsen, S. B., Buchardt, S. L., White, J. W. C., and Vinther, B. M.: Water isotope diffusion rates from the NorthGRIP ice core for the last 16,000 years – Glaciological and paleoclimatic implications, *Earth and Planetary Science Letters*, 405, 132-141, <https://doi.org/10.1016/j.epsl.2014.08.022>, 2014.
- 40 Goursaud, S., Masson-Delmotte, V., Favier, V., Orsi, A., and Werner, M.: Water stable isotope spatio-temporal variability in Antarctica in 1960-2013: observations and simulations from the ECHAM5-wiso atmospheric general circulation model, *Climate of the Past*, 14, 923-946, <https://doi.org/10.5194/cp-14-923-2018>, 2018.
- Herron, M. M. and Langway, C. C.: Firn Densification - an Empirical-Model, *Journal of Glaciology*, 25, 373-385, <https://doi.org/10.3189/S0022143000015239>, 1980.
- 45 Hoshina, Y., Fujita, K., Iizuka, Y., and Motoyama, H.: Inconsistent relationships between major ions and water stable isotopes in Antarctic snow under different accumulation environments, *Polar Science*, 10, 1-10, <https://doi.org/10.1016/j.polar.2015.12.003>, 2016.
- Hughes, A. G., Wahl, S., Jones, T. R., Zühr, A., Hörhold, M., White, J. W. C., and Steen-Larsen, H. C.: The role of sublimation as a driver of climate signals in the water isotope content of surface snow: Laboratory and field experimental results, *The Cryosphere Discussions*, doi: 10.5194/tc-2021-87, in review. <https://doi.org/10.5194/tc-2021-87>, in review.
- 50 Johnsen, S., Clausen, H. B., Cuffey, K. M., Hoffmann, G., Schwander, J., and Creyts, T.: Diffusion of stable isotopes in polar firn and ice: the isotope effect in firn diffusion. In: *Physics of ice core records*, Hokkaido University, Sapporo, 2000.
- Kane, H. S.: A study of 10m firn temperatures in central East Antarctica, *IAHS*, 86, 165-174, 1970.
- Karlöf, L., Isaksson, E., Winther, J. G., Gundestrup, N., Meijer, H. A. J., Mulvaney, R., Pourchet, M., Hofstede, C., Lappegard, G., 55 Pettersson, R., Van den Broeke, M., and Van De Wal, R. S. W.: Accumulation variability over a small area in east Dronning Maud Land, Antarctica, as determined from shallow firn cores and snow pits: some implications for ice-core records, *Journal of Glaciology*, 51, 343-352, <https://doi.org/10.3189/172756505781829232>, 2005.
- King, J. C., Anderson, P. S., Vaughan, D. G., Mann, G. W., Mobbs, S. D., and Vosper, S. B.: Wind-borne redistribution of snow across an Antarctic ice rise, *Journal of Geophysical Research-Atmospheres*, 109, <https://doi.org/10.1029/2003jd004361>, 2004.
- 60 Kopec, B. G., Feng, X., Posmentier, E. S., and Sonder, L. J.: Seasonal Deuterium Excess Variations of Precipitation at Summit, Greenland, and their Climatological Significance, *Journal of Geophysical Research: Atmospheres*, 124, 72-91, <https://doi.org/10.1029/2018jd028750>, 2019.
- Laepple, T., Hörhold, M., Münch, T., Freitag, J., Wegner, A., and Kipfstuhl, S.: Layering of surface snow and firn at Kohlen Station, Antarctica: Noise or seasonal signal?, *Journal of Geophysical Research-Earth Surface*, 121, 1849-1860, <https://doi.org/10.1002/2016jf003919>, 2016.
- 65 Laepple, T., Münch, T., Casado, M., Hörhold, M., Landais, A., and Kipfstuhl, S.: On the similarity and apparent cycles of isotopic variations in East Antarctic snow pits, *Cryosphere*, 12, 169-187, <https://doi.org/10.5194/tc-12-169-2018>, 2018.
- Laepple, T., Werner, M., and Lohmann, G.: Synchronicity of Antarctic temperatures and local solar insolation on orbital timescales, *Nature*, 471, 91-94, <https://doi.org/10.1038/nature09825>, 2011.
- 70 Landais, A., Ekaykin, A., Barkan, E., Winkler, R., and Luz, B.: Seasonal variations of 17 O-excess and d-excess in snow precipitation at Vostok station, East Antarctica, *Journal of Glaciology*, 58, 725-733, <https://doi.org/10.3189/2012JoG11J237>, 2012.

- Legrand, M. and Mayewski, P.: Glaciochemistry of polar ice cores: A review, *Reviews of Geophysics*, 35, 219-243, <https://doi.org/10.1029/96rg03527>, 1997.
- Lenaerts, J. T. M. and van den Broeke, M. R.: Modeling drifting snow in Antarctica with a regional climate model: 2. Results, *Journal of Geophysical Research: Atmospheres*, 117, <https://doi.org/10.1029/2010jd015419>, 2012.
- 5 Li, C., Ren, J., Shi, G., Pang, H., Wang, Y., Hou, S., Li, Z., Du, Z., Ding, M., Ma, X., Yang, J., Xie, A., Wang, P., Wang, X., Sun, B., and Xiao, C.: Spatial and temporal variations of fractionation of stable isotopes in East-Antarctic snow, *Journal of Glaciology*, doi: 10.1017/jog.2021.5, 2021. 1-10, <https://doi.org/10.1017/jog.2021.5>, 2021.
- Lorius, C. and Merlivat, L.: Distribution of mean surface stable isotopes values in east Antarctica; observed changes with depth in coastal area, in: *Proceedings of the Grenoble Symposium*, August/September 1975, Grenoble 1975.
- 10 Ma, T., Li, L., Li, Y., An, C., Yu, J., Ma, H., Jiang, S., and Shi, G.: Stable isotopic composition in snowpack along the traverse from a coastal location to Dome A (East Antarctica): Results from observations and numerical modeling, *Polar Science*, 24, 100510, <https://doi.org/10.1016/j.polar.2020.100510>, 2020a.
- Ma, T. M., Li, L., Shi, G. T., and Li, Y. S.: Acquisition of Post-Depositional Effects on Stable Isotopes (δ O-18 and δ D) of Snow and Firn at Dome A, East Antarctica, *Water*, 12, 14, <https://doi.org/10.3390/w12061707>, 2020b.
- 15 Madsen, M. V., Steen-Larsen, H. C., Horhold, M., Box, J., Berben, S. M. P., Capron, E., Faber, A. K., Hubbard, A., Jensen, M. F., Jones, T. R., Kipfstuhl, S., Koldtoft, I., Pillar, H. R., Vaughn, B. H., Vladimirova, D., and Dahl-Jensen, D.: Evidence of Isotopic Fractionation During Vapor Exchange Between the Atmosphere and the Snow Surface in Greenland, *Journal of Geophysical Research-Atmospheres*, 124, 2932-2945, <https://doi.org/10.1029/2018jd029619>, 2019.
- 20 Masson-Delmotte, V., Hou, S., Ekaykin, A., Jouzel, J., Aristarain, A., Bernardo, R. T., Bromwich, D., Cattani, O., Delmotte, M., Falourd, S., Frezzotti, M., Gallee, H., Genoni, L., Isaksson, E., Landais, A., Helsen, M. M., Hoffmann, G., Lopez, J., Morgan, V., Motoyama, H., Noone, D., Oerter, H., Petit, J. R., Royer, A., Uemura, R., Schmidt, G. A., Schlosser, E., Simoes, J. C., Steig, E. J., Stenni, B., Stievenard, M., van den Broeke, M. R., de Wal, R. S. W. V., de Berg, W. J. V., Vimeux, F., and White, J. W. C.: A review of Antarctic surface snow isotopic composition: Observations, atmospheric circulation, and isotopic modeling, *Journal of Climate*, 21, 3359-3387, <https://doi.org/10.1175/2007jcli2139.1>, 2008.
- 25 Medley, B., McConnell, J. R., Neumann, T. A., Reijmer, C. H., Chellman, N., Sigl, M., and Kipfstuhl, S.: Temperature and Snowfall in Western Queen Maud Land Increasing Faster Than Climate Model Projections, *Geophysical Research Letters*, 45, 1472-1480, <https://doi.org/10.1002/2017gl075992>, 2018.
- Moser, D. E., Horhold, M., Kipfstuhl, S., and Freitag, J.: Microstructure of Snow and Its Link to Trace Elements and Isotopic Composition at Kohnen Station, Dronning Maud Land, Antarctica, *Front. Earth Sci.*, 8, <https://doi.org/10.3389/feart.2020.00023>, 2020.
- 30 Moser, H. and Stichler, W.: Deuterium and oxygen-18 contents as an index of the properties of snow covers, *International Association of Hydrological Sciences Publication*, 114, 122-135, 1974.
- Motoyama, H., Hirasawa, N., Satow, K., and Watanabe, O.: Seasonal variations in oxygen isotope ratios of daily collected precipitation and wind drift samples and in the final snow cover at Dome Fuji Station, Antarctica, *Journal of Geophysical Research*, 110, <https://doi.org/10.1029/2004jd004953>, 2005.
- 35 Münch, T., Kipfstuhl, S., Freitag, J., Meyer, H., and Laepple, T.: Constraints on post-depositional isotope modifications in East Antarctic firn from analysing temporal changes of isotope profiles, *The Cryosphere*, 11, 2175-2188, <https://doi.org/10.5194/tc-11-2175-2017>, 2017.
- Münch, T., Kipfstuhl, S., Freitag, J., Meyer, H., and Laepple, T.: Regional climate signal vs. local noise: a two-dimensional view of water isotopes in Antarctic firn at Kohnen Station, Dronning Maud Land, *Climate of the Past*, 12, 1565-1581, <https://doi.org/10.5194/cp-12-1565-2016>, 2016.
- 40 Münch, T. and Laepple, T.: What climate signal is contained in decadal- to centennial-scale isotope variations from Antarctic ice cores?, *Climate of the Past*, 14, 2053-2070, <https://doi.org/10.5194/cp-14-2053-2018>, 2018.
- Nakazawa, F., Nagatsuka, N., Hirabayashi, M., Goto-Azuma, K., Steffensen, J. P., and Dahl-Jensen, D.: Variation in recent annual snow deposition and seasonality of snow chemistry at the east Greenland ice core project (EGRIP) camp, Greenland, *Polar Science*, 27, 11, <https://doi.org/10.1016/j.polar.2020.100597>, 2021.
- 45 Noone, D. and Simmonds, I.: Annular variations in moisture transport mechanisms and the abundance of δ 18O in Antarctic snow, *Journal of Geophysical Research*, 107, <https://doi.org/10.1029/2002jd002262>, 2002.
- Oerter, H., Wilhelms, F., Jung-Rothenhausler, F., Goktas, F., Miller, H., Graf, W., and Sommer, S.: Accumulation rates in Dronning Maud Land, Antarctica, as revealed by dielectric-profiling measurements of shallow firn cores, *Annals of Glaciology*, Vol 30, 2000, 30, 27-34, <https://doi.org/10.3189/172756400781820705>, 2000.
- 50 Pang, H., Hou, S., Landais, A., Masson-Delmotte, V., Jouzel, J., Steen-Larsen, H. C., Risi, C., Zhang, W., Wu, S., Li, Y., An, C., Wang, Y., Prie, F., Minster, B., Falourd, S., Stenni, B., Scarchilli, C., Fujita, K., and Grigioni, P.: Influence of Summer Sublimation on δ D, δ 18O, and δ 17O in Precipitation, East Antarctica, and Implications for Climate Reconstruction From Ice Cores, *Journal of Geophysical Research: Atmospheres*, doi: 10.1029/2018jd030218, 2019. <https://doi.org/10.1029/2018jd030218>, 2019.
- Pfahl, S. and Sodemann, H.: What controls deuterium excess in global precipitation?, *Climate of the Past*, 10, 771-781, <https://doi.org/10.5194/cp-10-771-2014>, 2014.
- 55 Radok, U. and Lile, R. C.: A year of snow accumulation at Plateau Station, Antarctic Research Series, 1977. 1977.
- Rasmussen, S. O., Andersen, K. K., Svensson, A. M., Steffensen, J. P., Vinther, B. M., Clausen, H. B., Siggaard-Andersen, M. L., Johnsen, S. J., Larsen, L. B., Dahl-Jensen, D., Bigler, M., Röthlisberger, R., Fischer, H., Goto-Azuma, K., Hansson, M. E., and Ruth, U.: A new Greenland ice core chronology for the last glacial termination, *Journal of Geophysical Research*, 111, <https://doi.org/10.1029/2005jd006079>, 2006.
- 60 Ritter, F., Steen-Larsen, H. C., Werner, M., Masson-Delmotte, V., Orsi, A., Behrens, M., Birnbaum, G., Freitag, J., Risi, C., and Kipfstuhl, S.: Isotopic exchange on the diurnal scale between near-surface snow and lower atmospheric water vapor at Kohnen station, East Antarctica, *Cryosphere*, 10, 1647-1663, <https://doi.org/10.5194/tc-10-1647-2016>, 2016.
- Satow, K., Watanabe, O., Shoji, H., and Motoyama, H.: The relationship among accumulation rate, stable isotope ratio and surface temperature on the plateau of east Dronning Maud Land, Antarctica, *Polar Meteorol. Glaciol.*, 13, 43-52, 1999.
- 65 Schaller, C. F., Freitag, J., Kipfstuhl, S., Laepple, T., Steen-Larsen, H. C., and Eisen, O.: A representative density profile of the North Greenland snowpack, *Cryosphere*, 10, 1991-2002, <https://doi.org/10.5194/tc-10-1991-2016>, 2016.
- Schaller, C. F., Kipfstuhl, S., Steen-Larsen, H. C., Freitag, J., and Eisen, O.: Spatial variability of density stratigraphy and melt features for two polar snowpacks in Greenland and East Antarctica. *PANGAEA*, 10.1594/PANGAEA.884003, 2017.
- 70 Schlosser, E. and Oerter, H.: Seasonal variations of accumulation and the isotope record in ice cores: a study with surface snow samples and firn cores from Neumayer station, Antarctica, *Annals of Glaciology*, Vol 35, 35, 97-101, <https://doi.org/10.3189/172756402781817374>, 2002.

- Servettaz, A. P. M., Orsi, A. J., Curran, M. A. J., Moy, A. D., Landais, A., Agosta, C., Winton, V. H. L., Touzeau, A., McConnell, J. R., Werner, M., and Baroni, M.: Snowfall and Water Stable Isotope Variability in East Antarctica Controlled by Warm Synoptic Events, *Journal of Geophysical Research-Atmospheres*, 125, 14, <https://doi.org/10.1029/2020jd032863>, 2020.
- 5 Sodemann, H. and Stohl, A.: Asymmetries in the moisture origin of Antarctic precipitation, *Geophysical Research Letters*, 36, <https://doi.org/10.1029/2009gl040242>, 2009.
- Sokratov, S. A. and Golubev, V. N.: Snow isotopic content change by sublimation, *Journal of Glaciology*, 55, 823-828, <https://doi.org/10.3189/002214309790152456>, 2009.
- 10 Steen-Larsen, H. C., Masson-Delmotte, V., Hirabayashi, M., Winkler, R., Satow, K., Prié, F., Bayou, N., Brun, E., Cuffey, K. M., Dahl-Jensen, D., Dumont, M., Guillevic, M., Kipfstuhl, S., Landais, A., Popp, T., Risi, C., Steffen, K., Stenni, B., and Sveinbjörnsdóttir, A. E.: What controls the isotopic composition of Greenland surface snow?, *Climate of the Past*, 10, 377-392, <https://doi.org/10.5194/cp-10-377-2014>, 2014.
- Steffen, K. and Box, J.: Surface climatology of the Greenland Ice Sheet: Greenland Climate Network 1995-1999, *Journal of Geophysical Research: Atmospheres*, 106, 33951-33964, <https://doi.org/10.1029/2001jd900161>, 2001.
- 15 Stenni, B., Jouzel, J., Masson-Delmotte, V., Rothlisberger, R., Castellano, E., Cattani, O., Falourd, S., Johnsen, S. J., Longinelli, A., Sachs, J. P., Selmo, E., Souchez, R., Steffensen, J. P., and Udisti, R.: A late-glacial high-resolution site and source temperature record derived from the EPICA Dome C isotope records (East Antarctica), *Earth and Planetary Science Letters*, 217, 183-195, [https://doi.org/10.1016/S0012-821x\(03\)00574-0](https://doi.org/10.1016/S0012-821x(03)00574-0), 2004.
- 20 Stenni, B., Scarchilli, C., Masson-Delmotte, V., Schlosser, E., Ciardini, V., Dreossi, G., Grigioni, P., Bonazza, M., Cagnati, A., Karlicek, D., Risi, C., Udisti, R., and Valt, M.: Three-year monitoring of stable isotopes of precipitation at Concordia Station, East Antarctica, *The Cryosphere*, 10, 2415-2428, <https://doi.org/10.5194/tc-10-2415-2016>, 2016.
- Stichler, W., Schotterer, U., Fröhlich, K., Ginot, P., Kull, C., Gäggeler, H., and Pouyaud, B.: Influence of sublimation on stable isotope records recovered from high-altitude glaciers in the tropical Andes, *Journal of Geophysical Research: Atmospheres*, 106, 22613-22620, <https://doi.org/10.1029/2001jd900179>, 2001.
- 25 Touzeau, A., Landais, A., Stenni, B., Uemura, R., Fukui, K., Fujita, S., Guilbaud, S., Ekaykin, A., Casado, M., Barkan, E., Luz, B., Magand, O., Teste, G., Le Meur, E., Baroni, M., Savarino, J., Bourgeois, I., and Risi, C.: Acquisition of isotopic composition for surface snow in East Antarctica and the links to climatic parameters, *Cryosphere*, 10, 837-852, <https://doi.org/10.5194/tc-10-837-2016>, 2016.
- Town, M. S., Warren, S. G., Walden, V. P., and Waddington, E. D.: Effect of atmospheric water vapor on modification of stable isotopes in near-surface snow on ice sheets, *Journal of Geophysical Research-Atmospheres*, 113, <https://doi.org/10.1029/2008jd009852>, 2008.
- 30 Traufetter, F., Oerter, H., Fischer, H., Weller, R., and Miller, H.: Spatio-temporal variability in volcanic sulphate deposition over the past 2 kyr in snow pits and firn cores from Amundsenisen, Antarctica, *Journal of Glaciology*, 50, 137-146, <https://doi.org/10.3189/172756504781830222>, 2004.
- Uemura, R., Masson-Delmotte, V., Jouzel, J., Landais, A., Motoyama, H., and Stenni, B.: Ranges of moisture-source temperature estimated from Antarctic ice cores stable isotope records over glacial-interglacial cycles, *Climate of the Past*, 8, 1109-1125, <https://doi.org/10.5194/cp-8-1109-2012>, 2012.
- 35 van den Broeke, M., van de Berg, W. J., van Meijgaard, E., and Reijmer, C.: Identification of Antarctic ablation areas using a regional atmospheric climate model, *Journal of Geophysical Research*, 111, <https://doi.org/10.1029/2006jd007127>, 2006.
- van Geldern, R. and Barth, J. A. C.: Optimization of instrument setup and post-run corrections for oxygen and hydrogen stable isotope measurements of water by isotope ratio infrared spectroscopy (IRIS), *Limnology and Oceanography: Methods*, 10, 1024-1036, <https://doi.org/10.4319/lom.2012.10.1024>, 2012.
- 40 Vimeux, F., Masson, V., Jouzel, J., Stievenard, M., and Petit, J. R.: Glacial-interglacial changes in ocean surface conditions in the southern hemisphere, *Nature*, 398, 410-413, <https://doi.org/10.1038/18860>, 1999.
- Weinhart, A. H., Freitag, J., Hörhold, M., Kipfstuhl, S., and Eisen, O.: Representative surface snow density on the East Antarctic Plateau, *The Cryosphere*, 14, 3663-3685, <https://doi.org/10.5194/tc-14-3663-2020>, 2020.
- 45 Weinhart, A. H., Kipfstuhl, S., Hörhold, M., Eisen, O., and Freitag, J.: Spatial Distribution of Crusts in Antarctic and Greenland Snowpacks and Implications for Snow and Firn Studies, *Front. Earth Sci.*, 9, <https://doi.org/10.3389/feart.2021.630070>, 2021a.
- Weinhart, A. H., Kipfstuhl, S., Mengert, M., Götz, P., Micha, G., Freitag, J., and Hörhold, M.: Stable water isotopes and major ions in snow along a traverse route between Kohnen Station and Plateau Station, East Antarctica. PANGAEA, 10.1594/PANGAEA.930965, 2021b.
- Werner, M., Langebroek, P. M., Carlsen, T., Herold, M., and Lohmann, G.: Stable water isotopes in the ECHAM5 general circulation model: Toward high-resolution isotope modeling on a global scale, *Journal of Geophysical Research*, 116, <https://doi.org/10.1029/2011jd015681>, 2011.
- 50 Whillans, I. M. and Grootes, P. M.: Isotopic diffusion in cold snow and firn, *Journal of Geophysical Research*, 90, 3910, <https://doi.org/10.1029/JD090iD02p03910>, 1985.
- Xiao, C., Ding, M., Masson-Delmotte, V., Zhang, R., Jin, B., Ren, J., Li, C., Werner, M., Wang, Y., Cui, X., and Wang, X.: Stable isotopes in surface snow along a traverse route from Zhongshan station to Dome A, East Antarctica, *Climate Dynamics*, 41, 2427-2438, <https://doi.org/10.1007/s00382-012-1580-0>, 2012.
- 55 Zuhr, A. M., Münch, T., Steen-Larsen, H. C., Hörhold, M., and Laepple, T.: Local scale depositional processes of surface snow on the Greenland ice sheet, *The Cryosphere Discuss.*, [preprint], <https://doi.org/10.5194/tc-2021-36>, in review, 2021.

11 Appendix

Spatial variability of $\delta^{18}\text{O}$, δD and d

Table 3: Overview of $1\text{m}\delta^{18}\text{O}_{\text{Site}}$, $1\text{m}\delta\text{D}_{\text{Site}}$ and $1\text{m}d_{\text{Site}}$

Sampling site (number of profiles)	Latitude [°]	Longitude [°]	Elevation [m asl]	Sampling date	$1\text{m}\delta^{18}\text{O}_{\text{Site}}$ [‰]	$\sigma_{\text{H}}(1\text{m}\delta^{18}\text{O}_{\text{Site}})$ [‰]	$1\text{m}\delta\text{D}_{\text{Site}}$ [‰]	$\sigma_{\text{H}}(1\text{m}\delta\text{D}_{\text{Site}})$ [‰]	$1\text{m}d_{\text{Site}}$ [‰]	$\sigma_{\text{H}}(1\text{m}d_{\text{Site}})$ [‰]
1 (4)	-75.11	2.89	2995	14.12.2016	-45.2	0.7	-355.7	5.7	5.9	1.1
2 (4)	-75.18	6.12	3153	15.12.2016	-46.4	0.8	-365.1	7.1	5.8	1.0
3 (4)	-75.21	9.58	3306	16.12.2016	-47.6	1.0	-373.3	7.7	7.8	0.6
4 (4)	-75.18	12.66	3406	17.12.2016	-49.8	0.8	-389.3	6.1	8.9	1.2
5 (3)	-75.13	15.40	3474	18.12.2016	-50.0	0.9	-391.3	7.1	9.0	0.3
6 (4)	-75.48	16.32	3491	19.12.2016	-50.1	1.0	-390.7	7.6	9.7	0.5
7 (4)	-76.19	18.33	3470	20.12.2016	-50.9	0.9	-396.7	7.3	10.7	0.6
8 (4)	-76.90	20.66	3462	21.12.2016	-51.5	1.1	-401.3	8.0	11.1	0.6
9 (4)	-77.57	23.19	3458	22.12.2016	-51.7	0.2	-402.2	1.5	11.2	0.7
10 (4)	-78.29	26.30	3461	23.12.2016	-52.2	1.1	-404.8	7.9	13.0	0.9
12 (3)	-79.00	30.00	3473	26.12.2016	-53.0	0.9	-410.7	6.3	13.3	0.8
14 (4)	-79.24	40.56	3665	09-11.01.2017	-55.5	0.6	-428.4	4.0	15.8	0.5
15 (4)	-79.33	34.96	3550	16-18.01.2017	-53.4	1.5	-412.9	11.0	14.3	0.9

Stable water isotopes (upper 5 cm) vs. environmental properties

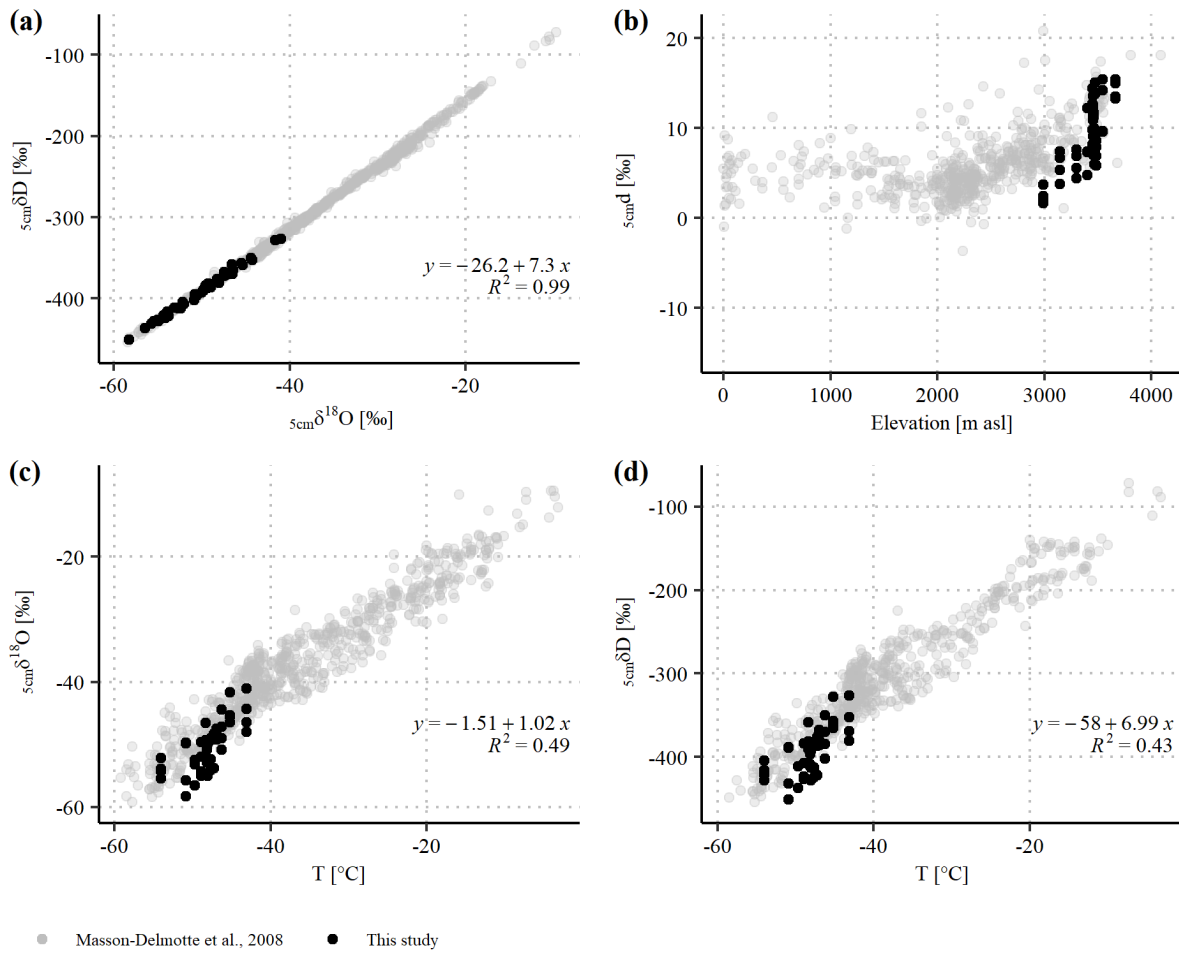


Figure 7: Same data presentation as Figure 2 considering the upper 5 cm of the snow column only.

Isotope profiles at selected sites

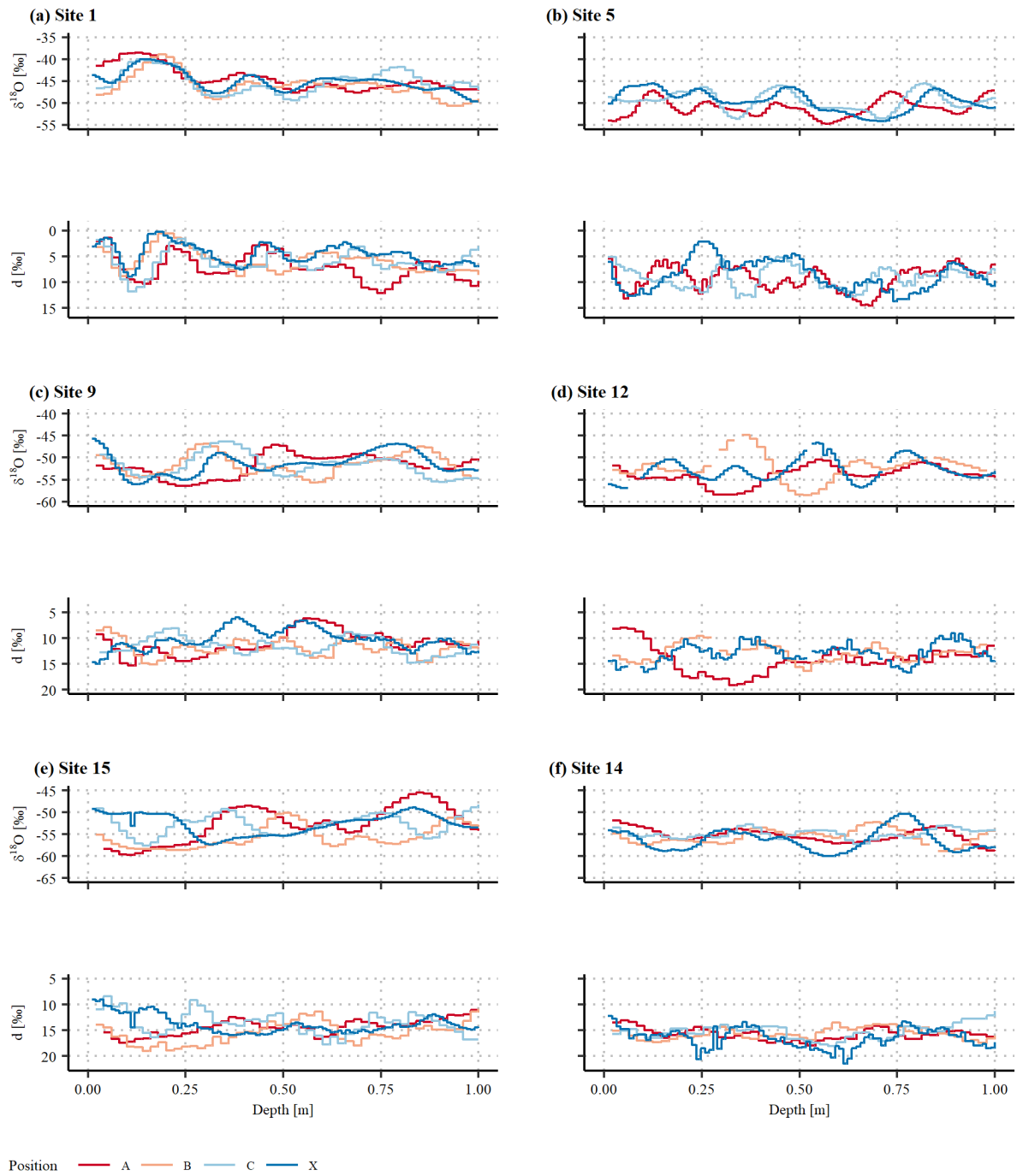


Figure 8: $\delta^{18}\text{O}$ (upper graph of the respective panel) and d (lower graph of the respective panel) from 0 to 1 m depth at the selected sites 1, 5, 9, 12, 15 and 14. Note the inverted scale for d .

6 FURTHER RESULTS & DISCUSSION

In this chapter, I want to summarize results that were not part of the three publications. This chapter includes a combined analysis of density measurements, structural properties and major ions (section 6.1) and an analysis of the decadal variability of stable water isotopes (section 6.2).

6.1 DECIPHERING THE LOCAL SNOWPACK HISTORY ON THE EAST ANTARCTIC PLATEAU – USING A COMBINATION OF STRATIGRAPHIC FEATURES AND MAJOR IONS

INTRODUCTION

Recording snowpack features and snow stratigraphy was an essential task in field glaciology in the past (e.g., Colbeck, 1991, Furukawa et al., 1996, Furukawa et al., 1992, Picciotto et al., 1971, Rundle, 1971) and is still done today. Numerous snowpack features were described in the past. Among them are crusts and depth hoar. Theories for their formation (depth hoar: Colbeck, 1991, crusts: Fegyveresi et al., 2018, Sommer et al., 2018) are already mentioned in publication II. The use of crusts as a paleoclimatic proxy (Hoshina et al., 2016) in combination with major ions has also been discussed there.

Many ionic species can exhibit a cyclicity due to seasonal deposition if the accumulation rate is high enough (Legrand & Mayewski, 1997), but volatile species (especially Cl^- , SO_4^{2-} , NO_3^-) are strongly affected by postdepositional losses (Weller et al., 2004). In a study at the South Pole, Dibb and Whitlow (1996) did not find the expected spring maxima in NO_3^- concentration in their snow profiles, but a peak in near the surface. They concluded that these spring NO_3^- peaks are not related to an atmospheric signal and are influenced by postdepositional effects.

Understanding the link between stratigraphy and climate proxies in snow as well as associated processes is an essential step for reconstructing snowpack history. This can improve the interpretation of climate proxies at the very surface and also in ice cores. Therefore recent studies investigate depositional processes at the snow surface (Zuhr et al., in review, 2021).

The main focus of this section is to investigate the connection of depositional features in combination with snow chemistry. I will show exemplary gray value images of snow profiles along the EAP with recurring stratigraphic features. Then go into detail on one special feature, which shows fine layering over a large part of the profile and is recognized in just few other snow profiles. Further, I want to characterize this fine layered feature in a combination with major ions and isotopes and discuss its deposition history. Lastly, I will tackle the question whether the (density and ion) characteristics of this feature can function as a general identification pattern to reconstruct the snowpack history through single snow profiles and a multiparameter analysis.

In this section, the term ‘layer’ describes a coherent section (especially visually in the radioscopic gray value images – and in consequence also in density) of snow of particular thickness, which may vary as a function of position. One layer might originate from one depositional event (be it precipitation, constant diamond dust deposition or reworked snow and wind drift deposition) but can also be caused by an interaction of many processes. Usually, the term layer is not clearly defined and used rather in a descriptive manner than a quantitative analysis. The classic understanding of a layered snowpack is rather present in high accumulation areas and disturbed by many processes in low accumulation areas (e.g., uneven distribution of precipitation, erosion, and wind redeposition). This subject is also tackled in publications I, II & III.

MATERIAL & METHODS

Snow profiles were measured by means of μ CT (s. publications I & II). The gray value images are the interim step of 2D μ CT measurements before the translation into (snow, firn, or ice) density. However, these gray value images better visualize the layering of the snow than a graph with the plotted density. In Fig. 10, sections from the following profiles are shown:

1A (0.25 m – 0.62 m depth)

8B (0.31 m – 0.68 m depth)

9A (0.30 m – 0.67 m depth)

14C (0 m – 0.37 m depth)

S15 (0 m – 0.37 m depth)

The procedure to count crusts in snow profiles is described in publication II.

From profile S15, selected major ion concentrations (Na^+ , Cl^- , NO_3^- , SO_4^{2-} , MSA) measured using IC (chapter 2.5) and d through CRDS (chapter 2.6) are presented over depth. Then for all available snow profiles at locations 1, 3, 5, 7, 9, 10, 12, 14, and 15, the NO_3^- concentration is shown over depth as well.

RESULTS

SNOWPACK FEATURES

Crusts can be found in every profile, here very present in Fig. 10a to d. Depth hoar can be identified in the gray value images by light gray color and high porosity, which visually appears ‘grainy’ in the images. Depth hoar is often associated with a crust at the top (very clear in the middle of Fig. 10b and at the bottom of d), which is caused by vertical mass transport upwards and therefore depletion in the (depth hoar) layer (Albert et al., 2004, Arcone et al., 2004, Fegyveresi et al., 2018). However, the opposite can be found as well. It is described as hard depth hoar (Pfeffer & Mrugala, 2002), when below a crust a layer with higher density is found. This can be seen very prominently in Fig. 10c.

Profile 14C (Fig. 10d) shows a disturbed structure at the top. It is characterized by erosional, discontinuous and diagonal layer boundaries between two layers of snow. Such chaotic patterns can indicate sastrugi, old dune structures or similar features. Dunes and sastrugi can easily reach 30 cm in height on the EAP. In the following the focus will be on the special feature that was found in snow profile S15 and is present to a lesser extent in few other profiles as well. Profile S15 (Fig. 10e) contains an impressive continuous and fine (almost laminar) layering with an extent of roughly 35 cm. The most interesting observations are first of all the total thickness, but also the gradual small changes in the angle of inclination as well as in density, which makes the fine layering only visible in the μ CT images.

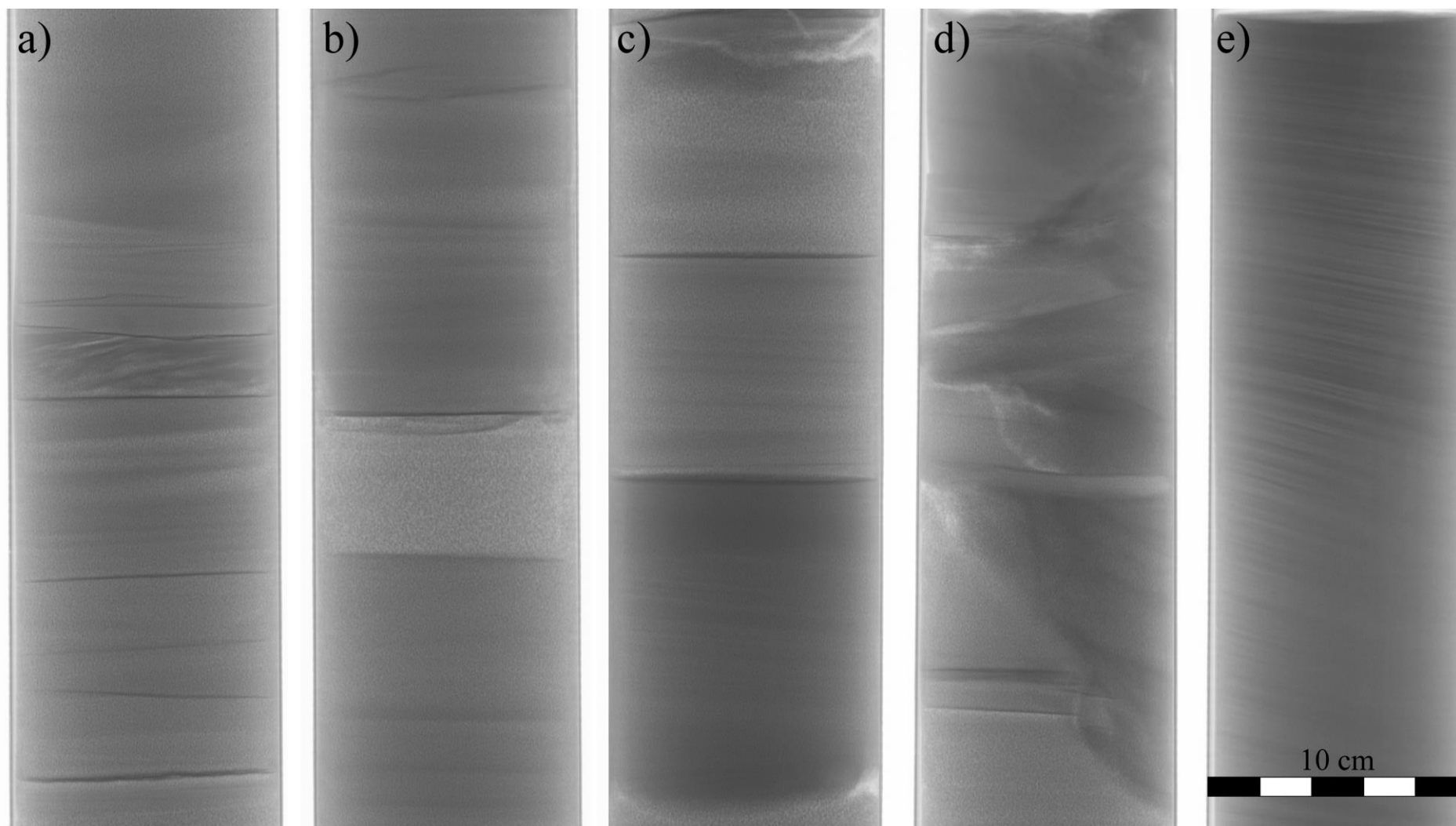


Fig. 10: Here μ CT gray value images are shown highlighting typical snowpack features along the CoFi traverse as well as special structures that are not captured very often. The scans are from positions a) 1A (0.25 m – 0.62 m depth), b) 8B (0.31 m – 0.68 m depth), c) 9A (0.30 m – 0.67 m depth), d) 14C (0 m – 0.37 m depth), e) S15 (0 m – 0.37 m depth) (s. Fig. 6).

PROFILE S15

Taking the IC measurements into account, at the very surface (0-4 cm), an increased concentration of several ion species (Fig. 11, bottom) is visible. It is possible that this increase originates from contamination or is a true climate signal. An interval with very constant Na^+ , Cl^- and SO_4^{2-} concentrations follows, corresponding with the interval of fine-layering in the gray value image (shaded gray in Fig. 11). In the same interval, MSA slightly increases with depth while we find a steady increase in NO_3^- . d increases from the surface to 30 cm depth as we see in the majority of the snow profiles as well (publication III). The increase of d in the upper 25 cm is negatively correlated with the snow density, which decreases from the surface to 35 cm.

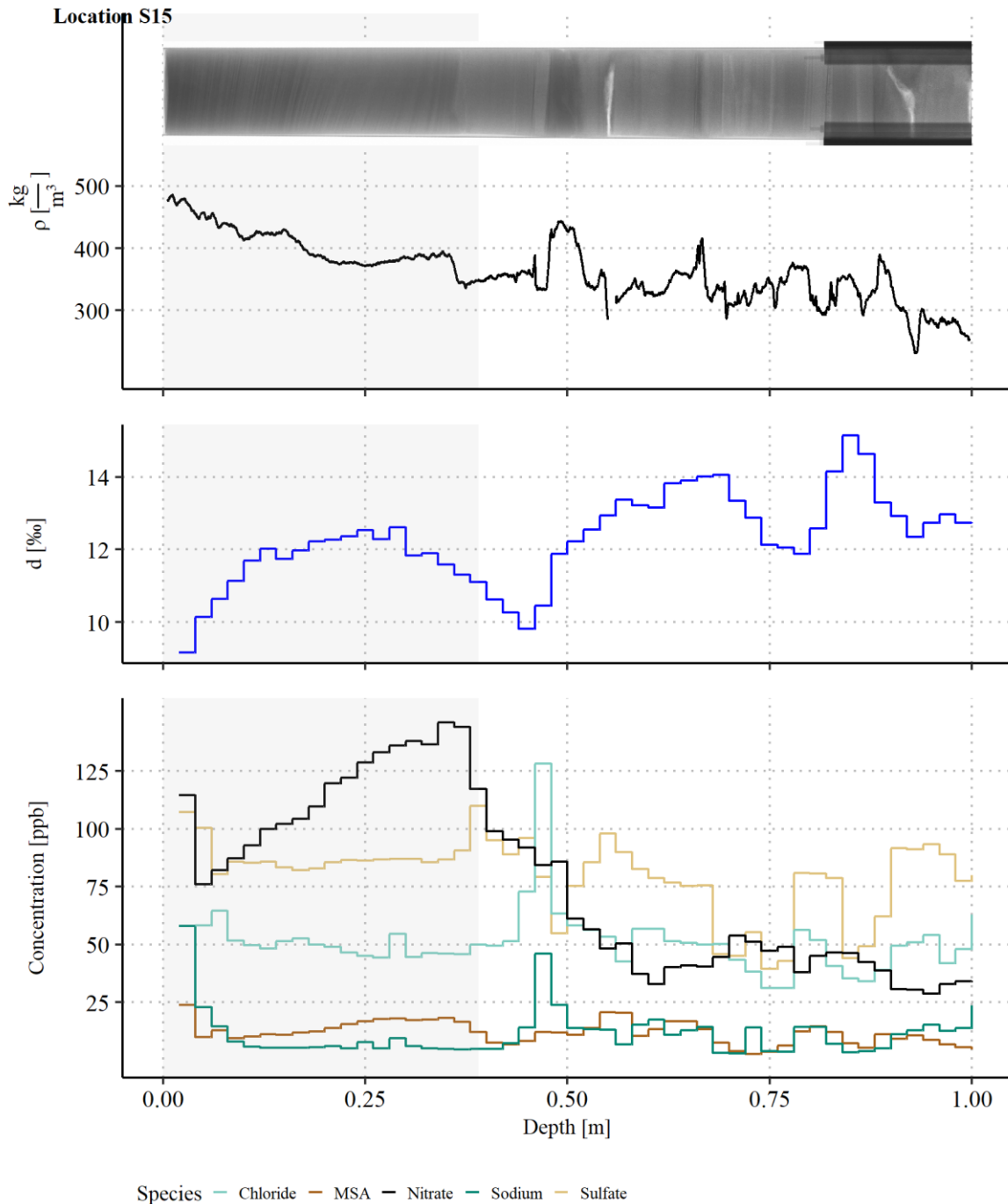


Fig. 11: Density (upper panel), deuterium excess (middle panel), and selected major ions (lower panel) of snow profile S15. The gray value image is plotted on top. The gray-shaded area represents the depth interval shown in Fig. 10e.

NITRATE PROFILES ALONG THE COFI TRAVERSE

The correlation of the fine layering with the increase in NO_3^- in profile S15 raised the question, whether this pattern is also visible in other snow profiles. In Fig. 12 NO_3^- concentrations in snow profiles from several selected locations are shown. Until location 7, there are notable local maxima and minima over depth, starting with concentrations around 100 ppb and decreasing tendency with increasing depth. Especially at location 1, a distinct cyclicity seems to be visible. From locations 8 or 9 further inland (with decreasing temperature and accumulation rate), this local variation diminishes while the concentrations at the surface are higher than close to Kohnen Station.

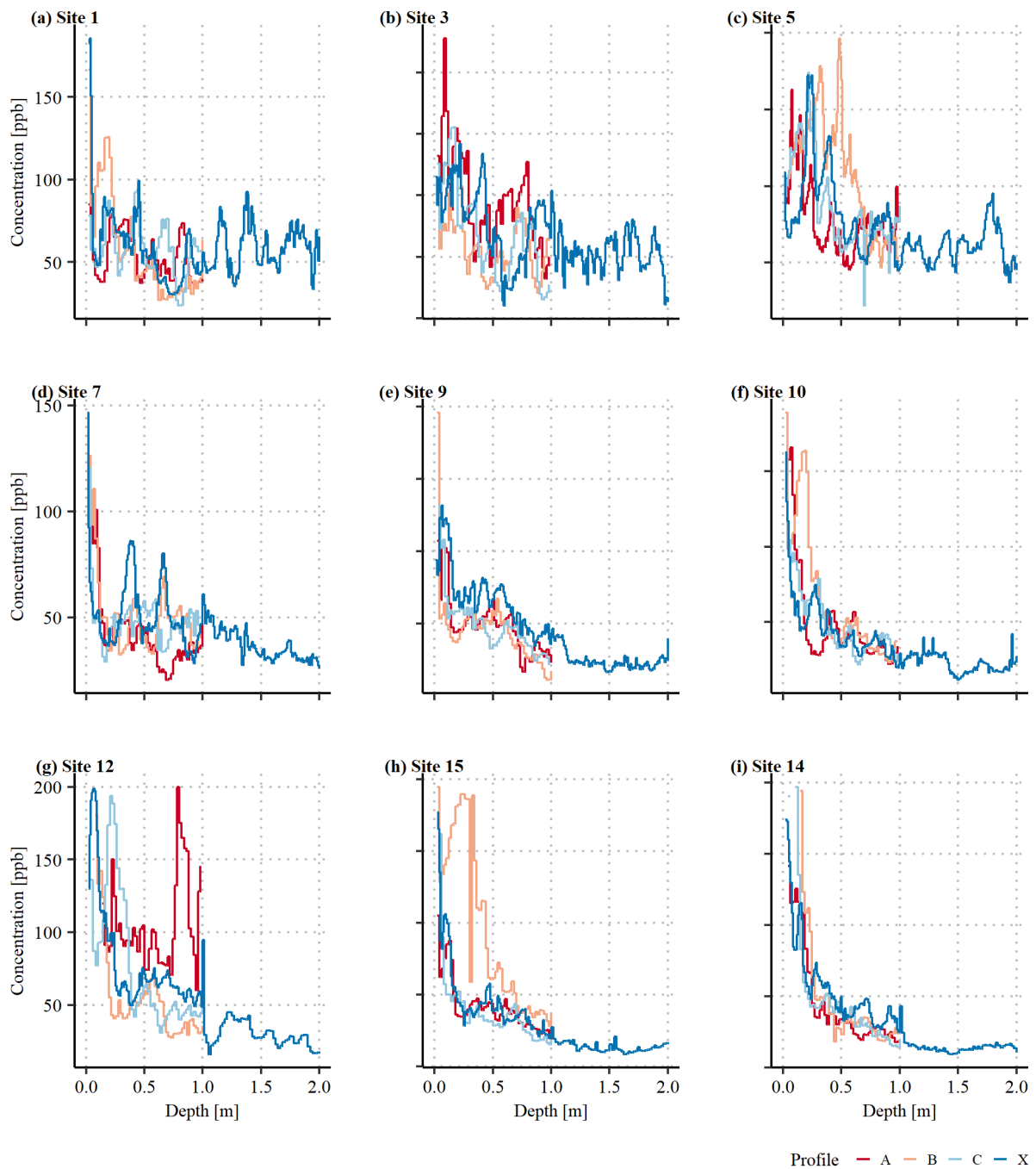


Fig. 12: Nitrate concentrations over depth for all available profiles (A, B, C and X; color coded) at the respective sampling sites. All panels a) to i) have the same depth axis. The annotation of the y axis applies to all panels on the same horizontal line.

Interestingly also in profiles 10B, 12A, 15B, a (rather high) maximum in NO_3^- is visible within the first meter, independent from high concentrations at the very surface. These maxima seem preserved and not level off like in other profiles on the interior plateau. They furthermore correspond with intervals of homogenous gray values (or one snow layer), i.e., rather constant density.

DISCUSSION

I can only speculate about the timespan and the number of accumulation events that have caused the layer in profile S15 (Fig. 10e). This gradual layering seems to form either under constant surface conditions without any erosion (i.e., the snow surface was exposed for a long period of time without erosion and uneven deposition) or during a prolonged drift event with low to medium wind speed. The constant values of several ion species indicate a rather homogenous snow source, which could come from eroded and mixed snow (King et al., 2004). This makes the latter of the scenarios more likely. In this context, the constant decrease (from surface to top) in density is a really interesting observation, but the low small-scale fluctuations compared to other profiles (appendix of publication I) support this hypothesis (Fig. 11, top). The increasing d from the very surface with depth additionally indicates the slow pile-up of a dune structure (Freitag & Kipfstuhl, pers. commun.). While the snow in 20-30 cm depth was buried constantly with snow, the snow close to the surface had a longer exposition to the atmosphere. In this part, sublimation strongly alters the deposited d value towards lower d values (Ekaykin et al., 2009, Pang et al., 2019).

The high ion concentrations at the top of snow profile S15 can be explained by contamination (estimated as rather unlikely) or a true climate (or depositional) signal (e.g., clear sky precipitation). Cl on the other hand, seems not to be that much influenced by volatilization into the atmosphere (comp. Weller et al., 2004).

The layers corresponding with the local maxima in NO_3^- in the other profiles do not show extensive and fine layering as in profile S15, but might have a similar deposition history. The high NO_3^- concentrations there can unlikely be interpreted as a climatic signal, especially not on the EAP (s. Fig. 11 and, e.g., Dibb and Whitlow (1996)). Maybe the origin of the snow in all those layers is a homogenous snow source (caused by mixing). Unfortunately, further investigations were not possible during the time of the project. Nevertheless, I strongly encourage a combined analysis of NO_3^- and density layering in the future. Perhaps a combined analysis of both parameters can indicate a certain type of deposition or the exposition time at the surface with reduced photochemical reactions raising the NO_3^- concentration (Wolff et al., 2002). In areas with higher accumulation rate, this might interfere with seasonal cycles in NO_3^- . Similar approaches could also be followed with other ions, but a regional classification using the optically detected features is barely possible – at least we did not have an applicable idea or parameter to do so (except for the abundance of crusts, s. publication II). This could also include 3D- μCT of other snow profiles. These data allow the calculation of physical properties such as grain size and structure, anisotropy and coordination number and can give even more insights into the snowpack evolution over depth and time. Profiles 14X and 15X have also been analyzed in 3D mode. A first step can be a comparison between Kohlen Station (Moser et al., 2020) and Plateau Station (14X) including chemical analysis.

Continuous observations or tracer experiments are one possibility to learn more about processes at the snow surface, but these are usually time-consuming and require logistical planning and respective instruments. A rather simple improvement for future studies using the liner method or similar sampling tools (with which the snow stratigraphy can be analyzed) is to mark the carbon fiber tubes at the outside and analyze them in the same orientation as taken in the field. This becomes relevant when sampling in the dimension of snow patches on local scales (e.g., sampling increments of 1 m) like small transects or trenches. The original (relative) orientation to the

next sample is recorded and stratigraphic elements can be reconstructed and followed accordingly on the spatial scale.

6.2 IS A TEMPERATURE RISE VISIBLE IN SNOW OF THE EAST ANTARCTIC PLATEAU? – A COMPARISON OF DECADAL $\delta^{18}\text{O}$ AT SELECTED SITES

INTRODUCTION

As presented in chapter 1.3, climate change has also reached Antarctica and is visible on the EAP. This affects mainly directly measurable (atmospheric or climatic) properties like temperature and accumulation rate (South Pole: Clem et al., 2020, Kohlen Station: Medley et al., 2018). In turn, significant changes in climate proxies like stable water isotopes were not reported yet. In this section, I want to investigate whether the climatic changes over the last decades are already visible in snow on the EAP comparing decadal $\delta^{18}\text{O}$ values according to the local accumulation rate.

MATERIAL & METHODS

The original plan in this study provided an additional shallow firn core (up to 10 m) at each sampling site with a hand auger. Using depth information of volcanic horizons, i.e., the eruption of Pinatubo in June 1991 (Cole-Dai et al., 1997), the local accumulation rates could have been derived. However, as the hand auger was unfortunately unavailable at the traverse start, this plan had to be canceled.

For this alternative approach, five locations (Kohlen Station and locations 5, 12, 14, and 15) were chosen at which the accumulation rate is fairly known from literature or measurements within this study (publication III). At Kohlen station, I used an accumulation rate of $78.5 \text{ kg}^{-2}\text{a}^{-1}$ (according to Medley et al., 2018). At site 12, I used an accumulation rate of $30 \text{ kg}^{-2}\text{a}^{-1}$, a bit lower than derived by Arthern et al. (2006), as the remotely calculated accumulation rates tend to be overestimated on the interior EAP (Anschütz et al., 2011). The local accumulation rate was transposed into water equivalent. Subsequently, 10-year depth intervals were calculated for each location according to the water equivalent (of ten years) and the isotopic mean values ($\delta^{18}\text{O}$) in these intervals were derived. Here, the recent decade starts with 31.12.2017 and ranges until 01.01.2008. The values of the year 2017 for the samples of season 2016/17 were treated as not available (N/A). As the T4M samples were taken in season 2018/19, the first year covered in the snow profiles was omitted.

In this approach, the accumulation rate was used as the only measure. I did not consider the cyclicity of stable water isotopes or impurities to derive annual layers as the dating is afflicted by a large uncertainty (publications II & III).

Along the traverse, I used the available snow profiles presented in chapters 2.2.1 and 2.7.3. Profiles of all lengths were used (1 m, 2 m, 4 m), even if some 1 m profiles only cover one 10-year interval. The samples were cut and measured through CRDS, as mentioned in chapters 2.4 and 2.6. At Kohlen Station, T4M samples were used to be able to go back in time until year 1998. As more 1 m profiles are available, there are also more results regarding the most recent decade. The values of each profile were plotted individually for clarity (Fig. 13). At location 12, I additionally used data measured by means of continuous flow analysis from firn core B54 at the Desert Research Institute (unpublished; mentioned in publication II) (s. Tab. 2 in the appendix), including the time scale derived from volcanic layers.

RESULTS

In Fig. 13, the mean $\delta^{18}\text{O}$ of the 10-year intervals at the five selected locations are shown.

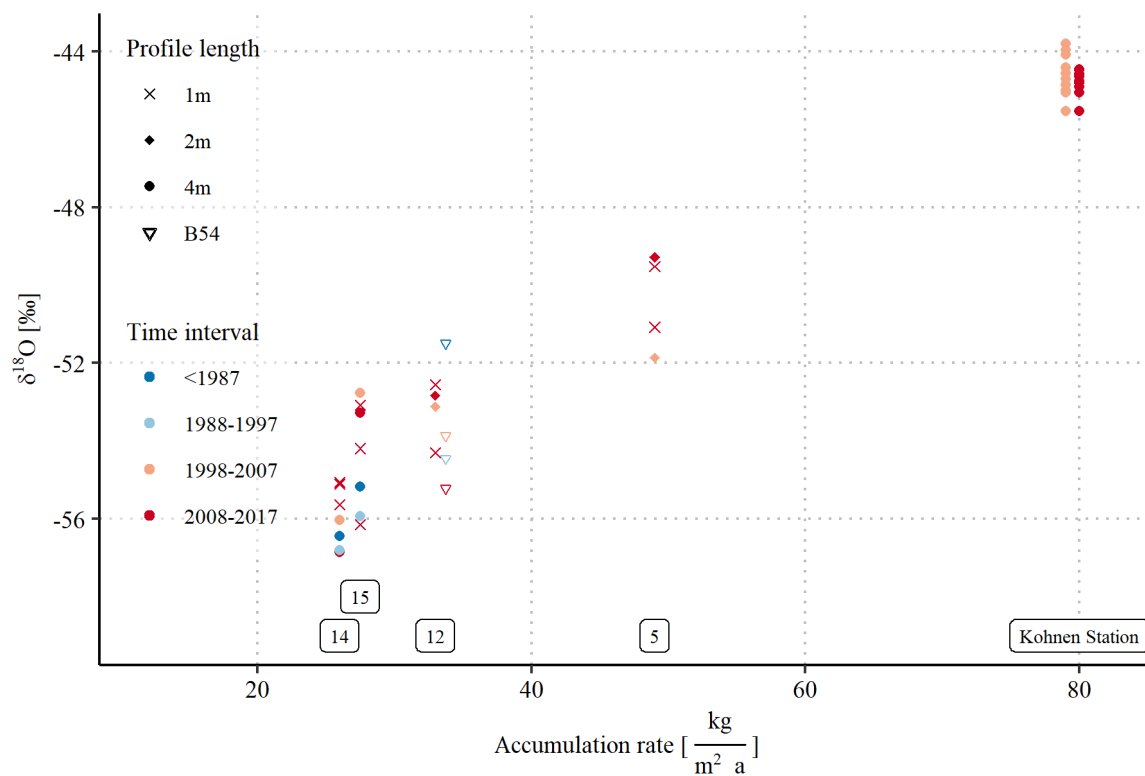


Fig. 13: $\delta^{18}\text{O}$ of the 10-year intervals separated by a color code and plotted against the accumulation rate. 1 m, 2 m, and 4 m profiles can be distinguished by different symbols. Samples at Kohnen Station and location 12 were plotted next to each other to avoid an overlay. Consider that 1 m and 4 m profiles have a lateral spacing of 10 m.

At Kohnen Station, there is no visible increase in $\delta^{18}\text{O}$ comparing the last two decades. While at location 5 the more recent decade shows higher $\delta^{18}\text{O}$ than the previous one (indicating warmer temperatures), at location 12, there is no unequivocal trend. Higher $\delta^{18}\text{O}$ values in the decade 2017-2008 than in 1998-2007 are visible in two of three profiles.

In the 4 m profiles at locations 14 and 15, a tendency towards higher $\delta^{18}\text{O}$ in the two more recent decades is visible, generally speaking comparing intervals before (including) 1997 and intervals after 1998. At location 14, three out of four samples of the most recent decade have the highest $\delta^{18}\text{O}$ values while the remaining one has the lowest $\delta^{18}\text{O}$.

In the scattering of the $\delta^{18}\text{O}$ of the recent decade (2017-2008), the local (spatial) variability of the 1 m means is also clearly visible. The decadal $\delta^{18}\text{O}$ values from B54 have a much larger scattering than the $\delta^{18}\text{O}$ from the snow profiles. The smoothing of the $\delta^{18}\text{O}$ in the CFA analysis, which is an accepted effect due to time efficiency, should not affect the mean values considerably (Fig. 14). However, the short-term variability in $\delta^{18}\text{O}$ (unless not the subject of this section) is much better represented in the snow profiles.

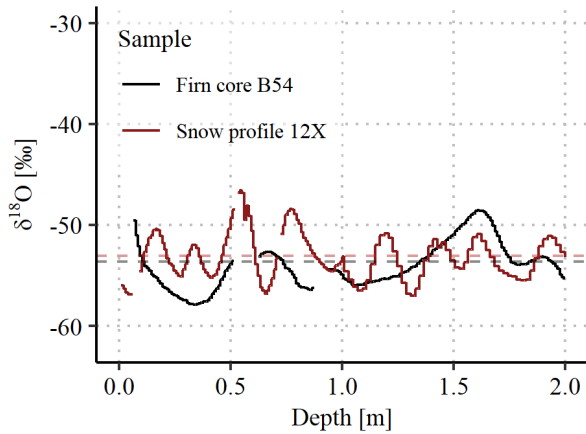


Fig. 14: $\delta^{18}\text{O}$ over depth in firn core B54 and snow profile 12X at location 12. Dashed lines show the respective mean $\delta^{18}\text{O}$ values from the surface to 2 m depth.

DISCUSSION

Although this approach is simplistic and does not consider temporal and spatial accumulation variability, it was still the most straightforward option using the available samples. One major uncertainty here is the accumulation rate or, being more precise, the annual layer thickness (vertical variability). As mentioned in publication III, temporal variability (including precipitation intermittency) (Casado et al., 2020, Laepple et al., 2011, Schlosser & Oerter, 2002, Servettaz et al., 2020) causes variations in the annual layer thickness each year. Of course, the accuracy of the decadal $\delta^{18}\text{O}$ values would increase with a) a more accurate dating and b) with a higher number of samples. Absolute time markers are needed (like initially planned) for a more accurate dating. For the decades earlier than 1998, only one value at locations 14 and 15 was available, which does not allow a very reliable conclusion.

Also inconsistency between temperature and stable water isotopes has been discussed recently (Ma et al., 2020, Münch et al., 2017) and can hamper a conclusion in this context. However, if the warming trend (1°C , Medley et al., 2018) is also present in snow on the EAP, one would expect an increase in the range of $0.6\text{‰}^\circ\text{C}^{-1}$ to $1.2\text{‰}^\circ\text{C}^{-1}$ over the two recent decades (Masson-Delmotte et al., 2008 or publication III). The warming trend at Kohlen Station is not visible in the data, at least in the mean isotopic values of the last two decades. Going back further in time might show different results here. On the remote EAP, the recent decadal $\delta^{18}\text{O}$ values are (for the most part) higher than the previous ones. Whether these observations are solid could be verified with a larger number of samples going further back in time than the year 1990. Still, these findings can indicate that global warming has also been recorded by climate proxies in snow of the EAP.

7 SUMMARY, CONCLUSION & OUTLOOK

This thesis was designed to a) further quantify the spatial variability of climate proxies in surface snow of East Antarctica, b) expand the knowledge of surface processes and snowpack formation for a more reliable interpretation of ice core records, which in consequence c) can improve our understanding for past and future, natural and anthropogenic changes of climate.

In the framework of this thesis, the large number of 83 snow profiles was collected along a traverse between Kohnen Station (0° 4'E, 75° 0'S) and former Plateau Station (40° 33'E, 79° 15'S) on the East Antarctic Plateau. At 22 sampling locations, four snow profiles (except for three sampling sites) were retrieved for a combination of physical and chemical analyses. Using four spatially independent samples at each location enabled us to derive locally and regionally more representative values than with single samples. We introduced a new sampling device for snow profiles for the laboratory work to cut the profiles into discrete samples.

7.1 SUMMARY & CONCLUSIONS OF THE SCIENTIFIC RESULTS

The surface snow density is an essential characteristic in field glaciology and not well constrained in the remote part of the East Antarctic Plateau. We were able to determine the surface snow density (0-1 m) at each sampling site with an error of the mean of less than 1.5%. The bulk density of the snow profiles along the traverse route (2200 km) was 355 kg m⁻³. The applied liner method has a much smaller sampling error than previously used sampling devices with different geometry and much smaller sampling volume (Conger & McClung, 2009). A comparison with existing datasets from the same region (Oerter, 2008) has shown that even the spatial variability on the local scale (tens of meters) is higher than a potential increase in density caused by warming temperatures. We therefore cannot conclude that a snow density increase over the past decade on the East Antarctic Plateau is linked to global warming, but can be explained with different sampling methods and the local density variability. Surprisingly, the snow surface density along the traverse route did not decrease dependent on temperature and accumulation rate but rather fluctuated around a mean value. We could show with our data that the spatial variability of snow density fluctuates stronger than assumed and the surface snow density is higher (around 10%) than modeled. Parameterized snow density for firn models in SMB calculations (e.g., Ligtenberg et al., 2011) therefore need further optimization to capture the conditions in the East Antarctic Plateau. Wrong snow density assumptions can lead to a miscalculation of ice sheet mass balances. In an example we showed an underestimation of mass in the firn column of the East Antarctic Plateau of 3%. Therefore, we see our results as an important baseline to tune snow density parameterizations to improve SMB calculations.

Crusts in polar snowpack have been observed, described and investigated in previous studies (e.g., Albert et al., 2004, Fegyveresi et al., 2018, Sommer et al., 2017). Using the gray value images and vertical density profiles derived from the μ CT scans, we created the first dataset of the spatial distribution of crusts including the orientation (obliquity) and intensity (thickness and density). This dataset did not only include many samples along the traverse, but also samples from Kohnen Station as well as northern Greenland. Contrary to our expectations to see more crusts due to a lower annual accumulation, we saw a decreasing number of crusts per meter in surface snow going from Kohnen Station towards former Plateau Station. This suggests, that the number of crusts and the accumulation rate are related. We found a linear relation on the spatial scale in our samples between the number of crusts and the logarithmic accumulation rate. Also a temporal relationship between accumulation rate and crust concentration in firn core B40 is observed unless a bit weaker than expected from the results on the spatial scale. Crusts are a

stratigraphic feature and they can – in combination with volumetric signals – be used as an additional dating approach (comp. Hoshina et al., 2016). As crusts have a completely different formation process than precipitation-related proxies like stable water isotopes and major ions, they add a different aspect in tracing back the snowpack history. Whether crusts can also serve as a new proxy still has to be evaluated, especially as the formation conditions of crusts remain not completely understood. However, we see the potential of crusts as a stratigraphic marker for surface exposition and accumulation additional to chemical measurements (stable water isotopes, major ions). Further studies might focus on the link between crusts and backscatter properties in remote sensing, the influence of crusts on firn ventilation and the microstructure of crusts to investigate their formation. Especially in regions with low accumulation rate, the effect of crusts as layer boundaries (remote sensing) and reduced firn ventilation (gas diffusivity in firn) might have been underestimated so far.

A case study of a joint stratigraphic and chemical analysis in one snow profile along the traverse revealed the possibility to reconstruct the deposition history of specific deposition events. Constant concentrations of major ions over one 35 cm snow layer suggested no precipitation-driven accumulation, but a continuous accumulation from one snow source (of potentially mixed drift snow). The combination with limited variations in snow density over depth and visible fine layering in the gray value image were interpreted as a drift event with constant deposition. Also the deuterium excess indicated the pile-up of a dune structure over time. Interestingly, the nitrate concentration increased with depth, which was also observed in layers of other profiles with similar density evolution. Whether this can be an identifier for an, e.g., drift event needs further investigation. Still, the combined analysis of stratigraphy and climate proxies has the potential to decipher the snowpack history.

Stable water isotopes measured in ice cores are an essential proxy to reconstruct past temperature changes on short (e.g., decadal) and long (e.g., glacial-interglacial) time scales (Masson-Delmotte et al., 2008). Understanding the processes during and shortly after the snow deposition also improves their interpretation as a paleotemperature proxy. A spatial overview of stable water isotopes between Kohnen Station and Plateau Station has shown the known correlation of $\delta^{18}\text{O}$ with temperature and elevation. While at Kohnen Station the temporal variability in $\delta^{18}\text{O}$ can be interpreted as seasonal signal, on the interior plateau the observed cycles are no longer consistent with the local accumulation rate. The cyclicity with roughly 20 cm length fits with previously published values for postdepositional diffusion (Laepplé et al., 2018), but in the uppermost meter diffusion alone is probably too weak to cause the observed patterns alone. The processes of sublimation, mechanical mixing and diffusion together overprint a seasonal signal where the accumulation rate is below $50 \text{ kg m}^{-2}\text{a}^{-1}$. This observation excludes an interpretation of seasonal cycles in $\delta^{18}\text{O}$ in East Antarctic snow profiles or firn and ice cores.

The comparison of our observations with the global circulation model ECHAM6-wiso (Cauquoin & Werner, in review, 2021) validates the model with a similar spatial trend along the traverse for $\delta^{18}\text{O}$, nevertheless with an offset of on average +5%. The trend in deuterium excess in turn is rather too weak, but strongly influenced by postdepositional sublimation, which is visible in the majority of the profiles. Contrasting mean $\delta^{18}\text{O}$ of the upper 5 cm and 1 m in the measured profiles, we find a similar spatial trend along the traverse. But when plotting them against geographical properties like elevation and temperature, we report an offset that does not fit with Antarctic-wide observations (Masson-Delmotte et al., 2008). We suggest to use samples up to 1 m depth to cover the interannual variability without seasonal bias and a reduced influence of surface processes.

At selected sites we compared the measured snow profiles to simulated profiles derived from ECHAM6-wiso data from surface to 2 m depth. In the first meter, the simulated profiles show distinct variations (i.e., seasonal deposition), which are not present in the observed profiles. In the second meter, the general trends of the profiles

are depicted well. We come to the conclusion that in the upper meter the processes of sublimation and mechanical mixing are dominant and can therefore explain the discrepancy between real and simulated profiles. Below 1 m the diffusion gets stronger and results in a better image of the real profile. How much of the “depositional events” create a measurable isotopic signal remains a major question, but we were able to assign some precipitation events from ECHAM6-wiso to the snow profiles. A further quantification of postdepositional processes and a reliable isotopic composition of fresh snow are necessary for improved paleotemperature reconstructions using $\delta^{18}\text{O}$ and d in ice core records.

Rising temperature and accumulation rate have been measured as consequences of global warming in East Antarctica (South Pole: Clem et al., 2020, Kohlen Station: Medley et al., 2018). A comparison of decadal $\delta^{18}\text{O}$ mean values at selected sites of the traverse suggests that global warming is also recorded in surface snow on the remote plateau of the East Antarctic ice sheet. As the sample number in this approach was very limited, a larger number of longer records with precise accumulation markers (e.g., volcanic horizons) is necessary to proof this observation. Generally, inconsistency of stable water isotopes with temperature due to postdepositional effects (e.g., Laepple et al., 2018, Ma et al., 2020) and the small-scale (tens of meters) spatial variability hamper the clarity of the results. However, the most recent decades tend to the highest $\delta^{18}\text{O}$ values, which can be interpreted as a temperature increase on the East Antarctic Plateau.

7.2 SUGGESTIONS FOR FURTHER STUDIES

Evaluating the sampling strategy, analysis, and results of this study, I want to summarize possible improvements and ideas for future studies:

Profiles 14X and 15X (from the surface to 4 m depth) were also analyzed through 3D- μCT . These data are available to learn about the firnification under cold and dry environmental conditions and can be processed in terms of layering and anisotropy.

Time constraints and limited measuring capacities lead to the fact that some samples were not cut and analyzed chemically (IC and CRDS; Tab. 2) during this project. Also, the samples of the OIR trench are only measured by means of the μCT and not further processed. All these samples are available for future projects, but for chemical analyses, a storage effect (alteration of proxies within the samples with time) should be taken into account, as the samples are stored now for over four years. At sites with analyzed samples, the storage effect might be quantified. For future studies, I suggest cutting of snow profiles soon after sampling, even if the measuring capacities do not allow a near-term measurement. Diffusion or volatilization is minimized when the snow profiles are cut and the distinct samples are stored in air-tight bags.

A revisit of OIR camp for another trench study (the trench position was marked with bamboo poles) could be a very interesting task to evaluate temporal changes of density, structural features, and stable water isotopes and major ions.

Tracing snow at the surface to study the redeposition mechanism should be another focus in the future. A feasible approach of a combined analysis of photography and snow samples was recently performed in Greenland (Zuhr et al., in review, 2021). This concept should be elaborated further and applied in Antarctica as well.

For the future use of the liner technique, I suggest markings at the outside of the carbon fiber tubes. The samples should then be measured by means of μCT in the same orientation as taken in the field. This way, snowpack

features (e.g., crusts, dunes, depth hoar, and more) can be analyzed with the correct orientation towards each other and be traced spatially on the local scale (in the order of meters).

7.3 CLOSING REMARKS

Coming back to the title question of the thesis: Long-term projections state the ice masses of East Antarctica to be in balance (Gardner et al., 2018, IMBIE Team, 2018, Rignot et al., 2019), but there are evidences for the arrival of climate change on the East Antarctic Plateau regarding temperature and accumulation rate (Clem et al., 2020, Medley et al., 2018). While temporal changes in snow density are entirely masked by the spatial variability and the sampling error, stable water isotopes indicate some trend towards higher temperatures recorded in surface snow. However, the change of $\delta^{18}\text{O}$ over the last decades is within the range of natural variability. Still, all the presented data in this study can serve as a solid data basis for further analyses on the East Antarctic Plateau. Furthermore, they could improve the understanding of signal formation at the very surface of the snowpack, and lower the uncertainty of future SMB calculations of the East Antarctic ice sheet.

In a personal conversation, once the question came up, whether there is not enough data and evidence to assess future climate change. Furthermore, whether humankind should rather spend money on projects to limit and adapt to climatic change and promote sustainability in all fields of socioeconomic interactions – instead of budgeting scientific expeditions and long-term projects for climate observations. Although there are many data available all around the globe to determine the share of an anthropogenic impact on the Earth's climate, after all, there is still a need for more data, especially from remote places on Earth. These data are not only needed to verify the climate change but also to further understand processes in the past, present, and future as well as to monitor the state of the Earth. Especially for East Antarctica, it is still unclear how this region, whose ice masses hold a huge sea level equivalent, will respond to a global climate change. Changing climatic conditions are reported to increase the snowfall in East Antarctica, which can buffer the potential sea level rise (Medley & Thomas, 2019, Seroussi et al., 2020, Zwally et al., 2015). Reducing the uncertainty in sea level projections for East Antarctica can help the adaption of humankind to climate change.

Although there is verified evidence for a changing climate: to act accordingly and see results in a political, economical, and social context takes time and probably even more pressure. This pressure can be created with enough evidence of a climate change, which in turn starts with the collection of field data.

8 REFERENCES

- ADOLPH, A.C. AND ALBERT, M.R., 2014: Gas diffusivity and permeability through the firn column at Summit, Greenland: measurements and comparison to microstructural properties. *Cryosphere*, **8**(1): 319-328. <https://doi.org/10.5194/tc-8-319-2014>
- AGETA, Y., AZUMA, N., FUJII, Y., FUJINO, K., FUJITA, S., FURUKAWA, T., HONDOH, T., KAMEDA, T., KAMIYAMA, K., KATAGIRI, K., KAWADA, K., KAWAMURA, T., KOBAYASHI, S., MAE, S., MAENO, H., MIYAHARA, T., MOTOYAMA, H., NAKAYAMA, Y., NARUSE, R., NISHIO, F., SAITOH, K., SAITOH, T., SHIMBORI, K., SHIRAIWA, T., SHOJI, H., TAKAHASHI, A., TAKAHASHI, S., TANAKA, Y., YOKOYAMA, K., WATANABE, O. AND GRP, D.-F.D.C., 1998: Deep ice-core drilling at Dome Fuji and glaciological studies in east Dronning Maud Land, Antarctica. *Annals of Glaciology*, Vol 27, 1998, **27**: 333-337. <https://doi.org/10.3189/1998AoG27-1-333-337>
- ALBERT, M., SHUMAN, C., COURVILLE, Z., BAUER, R., FAHNESTOCK, M. AND SCAMBOS, T., 2004: Extreme firn metamorphism: impact of decades of vapor transport on near-surface firn at a low-accumulation glazed site on the East Antarctic plateau. *Ann Glaciol-Ser*, **39**: 73-78. <https://doi.org/10.3189/172756404781814041>
- ALEXANDER, L.V., ZHANG, X., PETERSON, T.C., CAESAR, J., GLEASON, B., TANK, A.M.G.K., HAYLOCK, M., COLLINS, D., TREWIN, B., RAHMIZADEH, F., TAGIPOUR, A., KUMAR, K.R., REVADEKAR, J., GRIFFITHS, G., VINCENT, L., STEPHENSON, D.B., BURN, J., AGUILAR, E., BRUNET, M., TAYLOR, M., NEW, M., ZHAI, P., RUSTICUCCI, M. AND VAZQUEZ-AGUIRRE, J.L., 2006: Global observed changes in daily climate extremes of temperature and precipitation. *Journal of Geophysical Research-Atmospheres*, **111**(D5). <https://doi.org/10.1029/2005jd006290>
- ALLEY, R.B., CLARK, P.U., HUYBRECHTS, P. AND JOUGHIN, I., 2005: Ice-sheet and sea-level changes. *Science*, **310**(5747): 456-460. <https://doi.org/10.1126/science.1114613>
- AMAP, 2021: Arctic Climate Change Update 2021: Key Trends and Impacts. Summary for Policy-makers.
- ANSCHÜTZ, H., SINISALO, A., ISAKSSON, E., MCCONNELL, J.R., HAMRAN, S.E., BISIAUX, M.M., PASTERIS, D., NEUMANN, T.A. AND WINTHER, J.G., 2011: Variation of accumulation rates over the last eight centuries on the East Antarctic Plateau derived from volcanic signals in ice cores. *Journal of Geophysical Research-Atmospheres*, **116**: 12. <https://doi.org/10.1029/2011jd015753>
- ARCONE, S.A., SPIKES, V.B., HAMILTON, G.S. AND MAYEWSKI, P.A., 2004: Stratigraphic continuity in 400 MHz short-pulse radar profiles of firn in West Antarctica. *Ann Glaciol-Ser*, **39**: 195-200. <https://doi.org/10.3189/172756404781813925>
- ARTHERN, R.J., WINEBRENNER, D.P. AND VAUGHAN, D.G., 2006: Antarctic snow accumulation mapped using polarization of 4.3-cm wavelength microwave emission. *Journal of Geophysical Research-Atmospheres*, **111**(D6). <https://doi.org/10.1029/2004jd005667>
- BAGHERI DASTGERDI, S., BEHRENS, M., BONNE, J.-L., HÖRHOOLD, M., LOHMANN, G., SCHLOSSER, E. AND WERNER, M., in review, 2020: Continuous monitoring of surface water vapour isotopic compositions at Neumayer Station III, East Antarctica. *The Cryosphere Discuss.*, [preprint]. <https://doi.org/10.5194/tc-2020-302>
- BALSLEV-CLAUSEN, D., DAHL, T.W., SAAD, N. AND ROSING, M.T., 2013: Precise and accurate $\delta^{13}\text{C}$ analysis of rock samples using Flash Combustion–Cavity Ring Down Laser Spectroscopy. *Journal of Analytical Atomic Spectrometry*, **28**(4): 516-523. <https://doi.org/10.1039/c2ja30240c>
- BARBANTE, C. AND EISEN, O.: High-resolution geophysical survey confirms the deep Beyond EPICA ice-core drilling site (Press Release for the final site selection of the Beyond EPICA project), 2019
- BERDEN, G., PEETERS, R. AND MEIJER, G., 2010: Cavity ring-down spectroscopy: Experimental schemes and applications. *International Reviews in Physical Chemistry*, **19**(4): 565-607. <https://doi.org/10.1080/014423500750040627>
- BIGLER, M., SVENSSON, A., KETTNER, E., VALLELONGA, P., NIELSEN, M.E. AND STEFFENSEN, J.P., 2011: Optimization of high-resolution continuous flow analysis for transient climate signals in ice cores. *Environ Sci Technol*, **45**(10): 4483-4489. <https://doi.org/10.1021/es200118j>
- BIRNBAUM, G., BRAUNER, R. AND RIES, H., 2006: Synoptic situations causing high precipitation rates on the Antarctic plateau: observations from Kohlen Station, Dronning Maud Land. *Antarctic Science*, **18**(2): 279-288. <https://doi.org/10.1017/s0954102006000320>
- BÖHM, R., SCHÖNER, W., AUER, I., HYNEK, B., KROISLEITNER, C. AND WEYSS, G., 2007: *Gletscher im Klimawandel. Vom Eis der Polargebiete zum Goldbergkees in den Hohen Tauern*. Wien, Zentralanstalt für Meteorologie und Geodynamik. ISBN: 987-3200010130
- BRANAGAN, D.F., 2014: Carsten Egeberg Borchgrevink (1864-1934): The man who claimed to be the first to set foot on Antarctica. *Earth Sci. Hist.*, **33**(1): 67-121. <https://doi.org/10.17704/eshi.33.1.a0768366584n23vv>
- BROMWICH, D.H., 1988: Snowfall in high southern latitudes. *Reviews of Geophysics*, **26**(1): 149-168. <https://doi.org/10.1029/RG026i001p00149>
- BROMWICH, D.H., GUO, Z.C., BAI, L.S. AND CHEN, Q.S., 2004: Modeled antarctic precipitation. Part I: Spatial and temporal variability. *Journal of Climate*, **17**(3): 427-447. [https://doi.org/10.1175/1520-0442\(2004\)017<0427:Mappis>2.0.Co;2](https://doi.org/10.1175/1520-0442(2004)017<0427:Mappis>2.0.Co;2)
- BROMWICH, D.H. AND NICOLAS, J.P., 2014: New Reconstruction of Antarctic Near-Surface Temperatures: Multidecadal Trends and Reliability of Global Reanalyses. *Journal of Climate*, **27**(21): 8070-8093. <https://doi.org/10.1175/jcli-d-13-00733.1>
- BURTON-JOHNSON, A., BLACK, M., FRETWELL, P.T. AND KALUZA-GILBERT, J., 2016: An automated methodology for differentiating rock from snow, clouds and sea in Antarctica from Landsat 8 imagery: a new rock outcrop map and area estimation for the entire Antarctic continent. *Cryosphere*, **10**(4): 1665-1677. <https://doi.org/10.5194/tc-10-1665-2016>
- CAI, S., HSU, P.-C. AND LIU, F., 2021: Changes in polar amplification in response to increasing warming in CMIP6. *Atmospheric and Oceanic Science Letters*, **14**(3): 100043. <https://doi.org/10.1016/j.aosl.2021.100043>
- CAIAZZO, L., BECAGLI, S., FROSINI, D., GIARDI, F., SEVERI, M., TRAVERSI, R. AND UDISTI, R., 2016: Spatial and temporal variability of snow chemical composition and accumulation rate at Talos Dome site (East Antarctica). *Sci Total Environ*, **550**: 418-430. <https://doi.org/10.1016/j.scitotenv.2016.01.087>
- CASADO, M., LANDAIS, A., MASSON-DELMOTTE, V., GENTHON, C., KERSTEL, E., KASSI, S., ARNAUD, L., PICARD, G., PRIE, F., CATTANI, O., STEEN-LARSEN, H.C., VIGNON, E. AND CERMAK, P., 2016: Continuous measurements of isotopic composition

- of water vapour on the East Antarctic Plateau. *Atmos. Chem. Phys.*, **16**(13): 8521-8538. <https://doi.org/10.5194/acp-16-8521-2016>
- CASADO, M., MÜNCH, T. AND LAEPPEL, T., 2020: Climatic information archived in ice cores: impact of intermittency and diffusion on the recorded isotopic signal in Antarctica. *Climate of the Past*, **16**(4): 1581-1598. <https://doi.org/10.5194/cp-16-1581-2020>
- CAUQUOIN, A. AND WERNER, M., in review, 2021: High-resolution isotope modeling with ECHAM6-wiso nudged to ERA5 reanalyses: evaluation and perspectives for a better understanding of the water cycle. *Journal of Advances in Modelling Earth Systems*.
- CAVITTE, M.G.P., PARRENIN, F., RITZ, C., YOUNG, D.A., VAN LIEFFERINGE, B., BLANKENSHIP, D.D., FREZZOTTI, M. AND ROBERTS, J.L., 2018: Accumulation patterns around Dome C, East Antarctica, in the last 73 kyr. *The Cryosphere*, **12**(4): 1401-1414. <https://doi.org/10.5194/tc-12-1401-2018>
- CLARK, P.U., DYKE, A.S., SHAKUN, J.D., CARLSON, A.E., CLARK, J., WOHLFARTH, B., MITROVICA, J.X., HOSTETLER, S.W. AND MCCABE, A.M., 2009: The Last Glacial Maximum. *Science*, **325**(5941): 710-714. <https://doi.org/10.1126/science.1172873>
- CLARK, P.U., SHAKUN, J.D., MARCOTT, S.A., MIX, A.C., EBY, M., KULP, S., LEVERMANN, A., MILNE, G.A., PFISTER, P.L., SANTER, B.D., SCHRAG, D.P., SOLOMON, S., STOCKER, T.F., STRAUSS, B.H., WEAVER, A.J., WINKELMANN, R., ARCHER, D., BARD, E., GOLDNER, A., LAMBECK, K., PIERREHUMBERT, R.T. AND PLATTNER, G.-K., 2016: Consequences of twenty-first-century policy for multi-millennial climate and sea-level change. *Nature Climate Change*, **6**(4): 360-369. <https://doi.org/10.1038/nclimate2923>
- CLEM, K.R., FOGT, R.L., TURNER, J., LINTNER, B.R., MARSHALL, G.J., MILLER, J.R. AND RENWICK, J.A., 2020: Record warming at the South Pole during the past three decades. *Nature Climate Change*, **10**(8): 762-770. <https://doi.org/10.1038/s41558-020-0815-z>
- COLBECK, S.C., 1989: Air Movement in Snow Due to Windpumping. *Journal of Glaciology*, **35**(120): 209-213. <https://doi.org/10.3189/S002214300004524>
- COLBECK, S.C., 1991: The Layered Character of Snow Covers. *Reviews of Geophysics*, **29**(1): 81-96. <https://doi.org/10.1029/90rg02351>
- COLE-DAI, J., MOSLEY-THOMPSON, E. AND THOMPSON, L.G., 1997: Quantifying the Pinatubo volcanic signal in south polar snow. *Geophysical Research Letters*, **24**(21): 2679-2682. <https://doi.org/10.1029/97gl02734>
- COLGAN, W., MACHGUTH, H., MACFERRIN, M., COLGAN, J.D., VAN AS, D. AND MACGREGOR, J.A., 2016: The abandoned ice sheet base at Camp Century, Greenland, in a warming climate. *Geophysical Research Letters*, **43**(15): 8091-8096. <https://doi.org/10.1002/2016gl069688>
- CONGER, S.M. AND MCCLUNG, D.M., 2009: Comparison of density cutters for snow profile observations. *Journal of Glaciology*, **55**(189): 163-169. <https://doi.org/10.3189/002214309788609038>
- CRAIG, H., 1961: Isotopic Variations in Meteoric Waters. *Science*, **133**(3465): 1702-1703. <https://doi.org/10.1126/science.133.3465.1702>
- CRUTZEN, P.J., 2002: Geology of mankind. *Nature*, **415**(6867): 23. <https://doi.org/10.1038/415023a>
- DALLMAYR, R., FREITAG, J., HORHOLD, M., LAEPPEL, T., LEMBURG, J., DELLA-LUNGA, D. AND WILHELMS, F., 2021: A dual-tube sampling technique for snowpack studies. *Journal of Glaciology*, **67**(261): 84-90. <https://doi.org/10.1017/jog.2020.85>
- DALRYMPLE, G.B., 2001: The age of the Earth in the twentieth century: a problem (mostly) solved. *Geological Society, London, Special Publications*, **190**(1): 205-221. <https://doi.org/10.1144/gsl.sp.2001.190.01.14>
- DALRYMPLE, P.C. AND STROSCHEN, L.A., 1977: Micrometeorological System: Installation, Performance, and Problems. In Dalrymple, P.C., A.J. Riordan, A. Riordan, A.J. Riordan, G. Weller, H.H. Lettau, H. Lettau, L.A. Stroschein, L.S. Kundla, L.A. Stroschein, M. Kuhn, P. Schwerdtfeger, R.C. Lile and U. Radok (ed.), *Meteorological Studies at Plateau Station, Antarctica*, American Geophysical Union. (Antarctic Research Series 25). <https://doi.org/10.1002/9781118664872.ch1>
- DANSGAARD, W., 1964: Stable isotopes in precipitation. *Tellus*, **16**(4): 436-468. <https://doi.org/10.1111/j.2153-3490.1964.tb00181.x>
- DECONTO, R.M. AND POLLARD, D., 2003: Rapid Cenozoic glaciation of Antarctica induced by declining atmospheric CO₂. *Nature*, **421**(6920): 245-249. <https://doi.org/10.1038/nature01290>
- DECONTO, R.M. AND POLLARD, D., 2016: Contribution of Antarctica to past and future sea-level rise. *Nature*, **531**(7596): 591-597. <https://doi.org/10.1038/nature17145>
- DIBB, J.E. AND WHITLOW, S.I., 1996: Recent climate anomalies and their impact on snow chemistry at South Pole, 1987-1994. *Geophysical Research Letters*, **23**(10): 1115-1118. <https://doi.org/10.1029/96gl01039>
- DIERKING, W., LINOW, S. AND RACK, W., 2012: Toward a robust retrieval of snow accumulation over the Antarctic ice sheet using satellite radar. *Journal of Geophysical Research-Atmospheres*, **117**. <https://doi.org/10.1029/2011jd017227>
- DOME F. DEEP CORING GROUP, 1998: Deep ice-core drilling at Dome Fuji and glaciological studies in east Dronning Maud Land, Antarctica. *Annals of Glaciology*, **27**: 333-337. <https://doi.org/10.3189/1998AoG27-1-333-337>
- DONEY, S.C., FABRY, V.J., FEELY, R.A. AND KLEYPAS, J.A., 2009: Ocean Acidification: The Other CO₂ Problem. *Annu. Rev. Mar. Sci.*, **1**: 169-192. <https://doi.org/10.1146/annurev.marine.010908.163834>
- EICHLER, J., WEIKUSAT, C., WEGNER, A., TWARLOH, B., BEHRENS, M., FISCHER, H., HÖRHOLD, M., JANSEN, D., KIPFSTUHL, S., RUTH, U., WILHELMS, F. AND WEIKUSAT, I., 2019: Impurity Analysis and Microstructure Along the Climatic Transition From MIS 6 Into 5e in the EDML Ice Core Using Cryo-Raman Microscopy. *Front. Earth Sci.*, **7**. <https://doi.org/10.3389/feart.2019.00020>
- EISEN, O., FREZZOTTI, M., GENTHON, C., ISAKSSON, E., MAGAND, O., VAN DEN BROEKE, M.R., DIXON, D.A., EKAYKIN, A., HOLMLUND, P., KAMEDA, T., KARLÖF, L., KASPARI, S., LIPENKOV, V.Y., OERTER, H., TAKAHASHI, S. AND VAUGHAN, D.G., 2008: Ground-based measurements of spatial and temporal variability of snow accumulation in East Antarctica. *Reviews of Geophysics*, **46**(2). <https://doi.org/10.1029/2006rg000218>
- EKAYKIN, A.A., HONDOH, T., LIPENKOV, V.Y. AND MIYAMOTO, A., 2009: Post-depositional changes in snow isotope content: Preliminary results of laboratory experiments. *Clim. Past Discuss.*, **5**(2239-2009). <https://doi.org/10.5194/cpd-5-2239-2009>

- EKAYKIN, A.A., LIPENKOV, V.Y., BARKOV, N.I., PETIT, J.R. AND MASSON-DELMOTTE, V., 2002: Spatial and temporal variability in isotope composition of recent snow in the vicinity of Vostok station, Antarctica: implications for ice-core record interpretation. *Annals of Glaciology*, Vol 35, 35: 181-186. <https://doi.org/10.3189/172756402781816726>
- ELDERFIELD, H., FERRETTI, P., GREAVES, M., CROWHURST, S., MCCAVE, I.N., HOPELL, D. AND PIOTROWSKI, A.M., 2012: Evolution of ocean temperature and ice volume through the mid-Pleistocene climate transition. *Science*, 337(6095): 704-709. <https://doi.org/10.1126/science.1221294>
- EPICA COMMUNITY MEMBERS, 2004: Eight glacial cycles from an Antarctic ice core. *Nature*, 429(6992): 623-628. <https://doi.org/10.1038/nature02599>
- EPICA COMMUNITY MEMBERS, 2006: One-to-one coupling of glacial climate variability in Greenland and Antarctica. *Nature*, 444(7116): 195-198. <https://doi.org/10.1038/nature05301>
- FARIA, S.H., WEIKUSAT, I. AND AZUMA, N., 2014: The microstructure of polar ice. Part I: Highlights from ice core research. *Journal of Structural Geology*, 61: 2-20. <https://doi.org/10.1016/j.jsg.2013.09.010>
- FEJYVERESI, J.M., ALLEY, R.B., MUTO, A., ORSI, A.J. AND SPENCER, M.K., 2018: Surface formation, preservation, and history of low-porosity crusts at the WAIS Divide site, West Antarctica. *Cryosphere*, 12(1): 325-341. <https://doi.org/10.5194/tc-12-325-2018>
- FELDMANN, J. AND LEVERMANN, A., 2015: Collapse of the West Antarctic Ice Sheet after local destabilization of the Amundsen Basin. *Proc Natl Acad Sci U S A*, 112(46): 14191-14196. <https://doi.org/10.1073/pnas.1512482112>
- FISCHER, H., FUNDEL, F., RUTH, U., TWARLOH, B., WEGNER, A., UDISTI, R., BECAGLI, S., CASTELLANO, E., MORGANTI, A., SEVERI, M., WOLFF, E., LITTOT, G., RÖTHLISBERGER, R., MULVANEY, R., HUTTERLI, M.A., KAUFMANN, P., FEDERER, U., LAMBERT, F., BIGLER, M., HANSSON, M., JONSELL, U., DE ANGELIS, M., BOUTRON, C., SIGGAARD-ANDERSEN, M.-L., STEFFENSEN, J.P., BARBANTE, C., GASPARI, V., GABRIELLI, P. AND WAGENBACH, D., 2007: Reconstruction of millennial changes in dust emission, transport and regional sea ice coverage using the deep EPICA ice cores from the Atlantic and Indian Ocean sector of Antarctica. *Earth and Planetary Science Letters*, 260(1-2): 340-354. <https://doi.org/10.1016/j.epsl.2007.06.014>
- FISCHER, H., SEVERINGHAUS, J., BROOK, E., WOLFF, E., ALBERT, M., ALEMANY, O., ARTHERN, R., BENTLEY, C., BLANKENSHIP, D., CHAPPELLAZ, J., CREYTS, T., DAHL-JENSEN, D., DINN, M., FREZZOTTI, M., FUJITA, S., GALLEE, H., HINDMARSH, R., HUDSPETH, D., JUGIE, G., KAWAMURA, K., LIPENKOV, V., MILLER, H., MULVANEY, R., PARRENIN, F., PATTYN, F., RITZ, C., SCHWANDER, J., STEINHAGE, D., VAN OMMEN, T. AND WILHELMS, F., 2013: Where to find 1.5 million yr old ice for the IPICS "Oldest-Ice" ice core. *Climate of the Past*, 9(6): 2489-2505. <https://doi.org/10.5194/cp-9-2489-2013>
- FISCHER, H., WAHLEN, M., SMITH, J., MASTROIANNI, D. AND DECK, B., 1999: Ice core records of atmospheric CO₂ around the last three glacial terminations. *Science*, 283(5408): 1712-1714. <https://doi.org/10.1126/science.283.5408.1712>
- FISHER, D.A., REEH, N. AND CLAUSEN, H.B., 1985: Stratigraphic noise in time series derived from ice cores. *Annals of Glaciology*, 7: 76-83. <https://doi.org/10.3189/S0260305500005942>
- FLACH, J.D., PARTINGTON, K.C., RUIZ, C., JEANSOU, E. AND DRINKWATER, M.R., 2005: Inversion of the surface properties of ice sheets from satellite microwave data. *IEEE Trans. Geosci. Remote Sensing*, 43(4): 743-752. <https://doi.org/10.1109/tgrs.2005.844287>
- FREITAG, J. AND KIPFSTUHL, S., *pers. commun.*: Low deuterium excess can indicate a dune structure.
- FREITAG, J., KIPFSTUHL, S. AND LAEPPEL, T., 2013: Core-scale radioscopic imaging: a new method reveals density–calcium link in Antarctic firn. *Journal of Glaciology*, 59(218): 1009-1014. <https://doi.org/10.3189/2013JoG13J028>
- FRETWELL, P., PRITCHARD, H.D., VAUGHAN, D.G., BAMBER, J.L., BARRAND, N.E., BELL, R., BIANCHI, C., BINGHAM, R.G., BLANKENSHIP, D.D., CASASSA, G., CATANIA, G., CALLENS, D., CONWAY, H., COOK, A.J., CORR, H.F.J., DAMASKE, D., DAMM, V., FERRACCIOLI, F., FORSBERG, R., FUJITA, S., GIM, Y., GOGINENI, P., GRIGGS, J.A., HINDMARSH, R.C.A., HOLMLUND, P., HOLT, J.W., JACOBEL, R.W., JENKINS, A., JOKAT, W., JORDAN, T., KING, E.C., KOHLER, J., KRABILL, W., RIGER-KUSK, M., LANGLEY, K.A., LEITCHENKOV, G., LEUSCHEN, C., LUYENDYK, B.P., MATSUOKA, K., MOUGINOT, J., NITSCHKE, F.O., NOGI, Y., NOST, O.A., POPOV, S.V., RIGNOT, E., RIPPIN, D.M., RIVERA, A., ROBERTS, J., ROSS, N., SIEGERT, M.J., SMITH, A.M., STEINHAGE, D., STUDINGER, M., SUN, B., TINTO, B.K., WELCH, B.C., WILSON, D., YOUNG, D.A., XIANGBIN, C. AND ZIRIZZOTTI, A., 2013: Bedmap2: improved ice bed, surface and thickness datasets for Antarctica. *Cryosphere*, 7(1): 375-393. <https://doi.org/10.5194/tc-7-375-2013>
- FREZZOTTI, M., POURCHET, M., FLORA, O., GANDOLFI, S., GAY, M., URBINI, S., VINCENT, C., BECAGLI, S., GRAGNANI, R., PROPOSITO, M., SEVERI, M., TRAVERSI, R., UDISTI, R. AND FILY, M., 2005: Spatial and temporal variability of snow accumulation in East Antarctica from traverse data. *Journal of Glaciology*, 51(172): 113-124. <https://doi.org/10.3189/172756505781829502>
- FRIEDMAN, I., 1953: Deuterium content of natural waters and other substances. *Geochimica et Cosmochimica Acta*, 4(1-2): 89-103. [https://doi.org/10.1016/0016-7037\(53\)90066-0](https://doi.org/10.1016/0016-7037(53)90066-0)
- FRIELER, K., CLARK, P.U., HE, F., BUZZERT, C., REESE, R., LIGTENBERG, S.R.M., VAN DEN BROEKE, M.R., WINKELMANN, R. AND LEVERMANN, A., 2015: Consistent evidence of increasing Antarctic accumulation with warming. *Nature Climate Change*, 5(4): 348-352. <https://doi.org/10.1038/nclimate2574>
- FURUKAWA, T., KAMIYAMA, K. AND MAENO, H., 1996: Snow surface features along the traverse route from the coast to Dome Fuji Station, Queen Maud Land, Antarctica. *Proceedings of the NIPR Symposium on Polar Meteorology and Glaciology*, 10: 13-24.
- FURUKAWA, T., WATANABE, O., SEKO, K. AND FUJII, Y., 1992: Distribution of surface conditions of ice sheet in Enderby Land and east Queen Maud Land, East Antarctica. *Proc. NIPR Symp. Polar Meteorol. Glacil*, 5: 140-144.
- GARDNER, A.S., MOHOLDT, G., SCAMBOS, T., FAHNSTOCK, M., LIGTENBERG, S., VAN DEN BROEKE, M. AND NILSSON, J., 2018: Increased West Antarctic and unchanged East Antarctic ice discharge over the last 7 years. *Cryosphere*, 12(2): 521-547. <https://doi.org/10.5194/tc-12-521-2018>
- GENTHON, C., KRINNER, G. AND CASTEBRUNET, H., 2017: Antarctic precipitation and climate-change predictions: horizontal resolution and margin vs plateau issues. *Annals of Glaciology*, 50(50): 55-60. <https://doi.org/10.3189/172756409787769681>

- GISTEMP TEAM, 2020: GISS Surface Temperature Analysis (GISTEMP), version 4. <https://data.giss.nasa.gov/gistemp/>, last access: 10.12.2020
- GÖKTAS, F., FISCHER, H., OERTER, H., WELLER, R., SOMMER, S. AND MILLER, H., 2002: A glacio-chemical characterization of the new EPICA deep-drilling site on Amundsenisen, Dronning Maud Land, Antarctica. *Annals of Glaciology*, Vol 35, **35**: 347-354. <https://doi.org/10.3189/172756402781816474>
- GREGORY, S.A., ALBERT, M.R. AND BAKER, I., 2014: Impact of physical properties and accumulation rate on pore close-off in layered firn. *Cryosphere*, **8**(1): 91-105. <https://doi.org/10.5194/tc-8-91-2014>
- GUPTA, P., NOONE, D., GALEWSKY, J., SWEENEY, C. AND VAUGHN, B.H., 2009: Demonstration of high-precision continuous measurements of water vapor isotopologues in laboratory and remote field deployments using wavelength-scanned cavity ring-down spectroscopy (WS-CRDS) technology. *Rapid Commun Mass Spectrom*, **23**(16): 2534-2542. <https://doi.org/10.1002/rcm.4100>
- HANSEN, B.L. AND LANGWAY, C.C., 1966: Deep core drilling in ice and core analysis at Camp Century, Greenland, 1961-1966. *Antarctic Journal of the United States*, **1**(5): 207-208.
- HELD, I.M. AND SODEN, B.J., 2006: Robust responses of the hydrological cycle to global warming. *Journal of Climate*, **19**(21): 5686-5699. <https://doi.org/10.1175/jcli3990.1>
- HÖNISCH, B., HEMMING, N.G., ARCHER, D., SIDDALL, M. AND MCMANUS, J.F., 2009: Atmospheric carbon dioxide concentration across the mid-Pleistocene transition. *Science*, **324**(5934): 1551-1554. <https://doi.org/10.1126/science.1171477>
- HOSHINA, Y., FUJITA, K., IIZUKA, Y. AND MOTOYAMA, H., 2016: Inconsistent relationships between major ions and water stable isotopes in Antarctic snow under different accumulation environments. *Polar Science*, **10**(1): 1-10. <https://doi.org/10.1016/j.polar.2015.12.003>
- HOSHINA, Y., FUJITA, K., NAKAZAWA, F., IIZUKA, Y., MIYAKE, T., HIRABAYASHI, M., KURAMOTO, T., FUJITA, S. AND MOTOYAMA, H., 2014: Effect of accumulation rate on water stable isotopes of near-surface snow in inland Antarctica. *Journal of Geophysical Research-Atmospheres*, **119**(1): 274-283. <https://doi.org/10.1002/2013jd020771>
- HUGONNET, R., MCNABB, R., BERTHIER, E., MENOUNOS, B., NUTH, C., GIROD, L., FARINOTTI, D., HUSS, M., DUSSAILLANT, I., BRUN, F. AND KAAB, A., 2021: Accelerated global glacier mass loss in the early twenty-first century. *Nature*, **592**(7856): 726-731. <https://doi.org/10.1038/s41586-021-03436-z>
- IMBIE TEAM, 2018: Mass balance of the Antarctic Ice Sheet from 1992 to 2017. *Nature*, **558**(7709): 219-222. <https://doi.org/10.1038/s41586-018-0179-y>
- INDERMÜHLE, A., STOCKER, T.F., JOOS, F., FISCHER, H., SMITH, H.J., WAHLEN, M., DECK, B., MASTROIANNI, D., TSCHUMI, J., BLUNIER, T., MEYER, R. AND STAUFFER, B., 1999: Holocene carbon-cycle dynamics based on CO₂ trapped in ice at Taylor Dome, Antarctica. *Nature*, **398**(6723): 121-126. <https://doi.org/10.1038/18158>
- INTERNATIONAL GEOGRAPHICAL CONGRESS, 1896: *Report of the Sixth International Geographical Congress: Held in London, 1895*. London, J. Murray.
- IPCC, 1998: Principles governing IPCC work. <https://www.ipcc.ch/site/assets/uploads/2018/09/ipcc-principles.pdf>, last access: 08.12.2020
- IPCC, 2014: Climate Change 2014: Synthesis Report. *Contribution of Working Groups I, II and III to the Fifth Assessment Report of the Intergovernmental Panel on Climate Change [Core Writing Team, R.K. Pachauri and L.A. Meyer (eds.)]*. IPCC, Geneva, Switzerland: 151. <https://doi.org/10.1017/CB09781107415324>
- IPCC, 2019: IPCC Special Report on the Ocean and Cryosphere in a Changing Climate. In Pörtner, H.-O., D.C. Roberts, V. Masson-Delmotte, P. Zhai, M. Tignor, E. Poloczanska, K. Mintenbeck, A. Alegria, M. Nicolai, A. Okem, J. Petzold, B. Rama and N.M. Weyer (ed.).
- JOHNSEN, S., CLAUSEN, H.B., CUFFEY, K.M., HOFFMANN, G., SCHWANDER, J. AND CREYTS, T., 2000: Diffusion of stable isotopes in polar firn and ice: the isotope effect in firn diffusion. (ed.), *Physics of ice core records*, Sapporo, Hokkaido University, 121-140. <https://doi.org/10.7916/D8KW5D4X>
- JONES, T.R., WHITE, J.W.C., STEIG, E.J., VAUGHN, B.H., MORRIS, V., GKNIS, V., MARKLE, B.R. AND SCHOENEMANN, S.W., 2017: Improved methodologies for continuous-flow analysis of stable water isotopes in ice cores. *Atmospheric Measurement Techniques*, **10**(2): 617-632. <https://doi.org/10.5194/amt-10-617-2017>
- JOUGHIN, I., SMITH, B.E. AND MEDLEY, B., 2014: Marine ice sheet collapse potentially under way for the Thwaites Glacier Basin, West Antarctica. *Science*, **344**(6185): 735-738. <https://doi.org/10.1126/science.1249055>
- JOUZEL, J., 2013: A brief history of ice core science over the last 50 yr. *Climate of the Past*, **9**(6): 2525-2547. <https://doi.org/10.5194/cp-9-2525-2013>
- KARLÖF, L., ISAKSSON, E., WINTHER, J.G., GUNDESTRUP, N., MEIJER, H.A.J., MULVANEY, R., POURCHET, M., HOFSTEDE, C., LAPPEGARD, G., PETERSSON, R., VAN DEN BROEKE, M. AND VAN DE WAL, R.S.W., 2005: Accumulation variability over a small area in east Dronning Maud Land, Antarctica, as determined from shallow firn cores and snow pits: some implications for ice-core records. *Journal of Glaciology*, **51**(174): 343-352. <https://doi.org/10.3189/172756505781829232>
- KARLÖF, L., WINEBRENNER, D.P. AND PERCIVAL, D.B., 2006: How representative is a time series derived from a firn core? A study at a low-accumulation site on the Antarctic plateau. *Journal of Geophysical Research*, **111**(F4). <https://doi.org/10.1029/2006jf000552>
- KARLSSON, N.B., BINDER, T., EAGLES, G., HELM, V., PATTYN, F., VAN LIEFFERINGE, B. AND EISEN, O., 2018: Glaciological characteristics in the Dome Fuji region and new assessment for "Oldest Ice". *Cryosphere*, **12**(7): 2413-2424. <https://doi.org/10.5194/tc-12-2413-2018>
- KAUFMANN, P.R., FEDERER, U., HUTTERLI, M.A., BIGLER, M., SCHUPBACH, S., RUTH, U., SCHMITT, J. AND STOCKER, T.F., 2008: An improved continuous flow analysis system for high-resolution field measurements on ice cores. *Environ Sci Technol*, **42**(21): 8044-8050. <https://doi.org/10.1021/es800772z>
- KENNETT, J.P., 1977: Cenozoic evolution of Antarctic glaciation, the circum-Antarctic Ocean, and their impact on global paleoceanography. *Journal of Geophysical Research*, **82**(27): 3843-3860. <https://doi.org/10.1029/JC082i027p03843>
- KING, J.C., ANDERSON, P.S., VAUGHAN, D.G., MANN, G.W., MOBBS, S.D. AND VOSPER, S.B., 2004: Wind-borne redistribution of snow across an Antarctic ice rise. *Journal of Geophysical Research-Atmospheres*, **109**(D11). <https://doi.org/10.1029/2003jd004361>

- KING, J.C. AND TURNER, J., 1997: *Antarctic Meteorology and Climatology*. Cambridge, Cambridge University Press.
- KOERNER, R.M., 1971: A Stratigraphic Method of Determining the Snow Accumulation Rate at Plateau Station, Antarctica, and Application to South Pole-Queen Maud Land Traverse 2, 1965-1966. 225-238. <https://doi.org/10.1029/AR016p0225>
- KRATOCHWIL, N.A., DUEKER, S.R., MURI, D., SENN, C., YOON, H., YU, B.Y., LEE, G.H., DONG, F. AND OTTENEDER, M.B., 2018: Nanotracing and cavity-ring down spectroscopy: A new ultrasensitive approach in large molecule drug disposition studies. *PLoS One*, **13**(10): e0205435. <https://doi.org/10.1371/journal.pone.0205435>
- LACIS, A.A., SCHMIDT, G.A., RIND, D. AND RUEDY, R.A., 2010: Atmospheric CO₂: principal control knob governing Earth's temperature. *Science*, **330**(6002): 356-359. <https://doi.org/10.1126/science.1190653>
- LAEPPLE, T., HÖRHOOLD, M., MÜNCH, T., FREITAG, J., WEGNER, A. AND KIPFSTUHL, S., 2016: Layering of surface snow and firn at Kohlen Station, Antarctica: Noise or seasonal signal? *Journal of Geophysical Research-Earth Surface*, **121**(10): 1849-1860. <https://doi.org/10.1002/2016jf003919>
- LAEPPLE, T., MÜNCH, T., CASADO, M., HOERHOLD, M., LANDAIS, A. AND KIPFSTUHL, S., 2018: On the similarity and apparent cycles of isotopic variations in East Antarctic snow pits. *Cryosphere*, **12**(1): 169-187. <https://doi.org/10.5194/tc-12-169-2018>
- LAEPPLE, T., WERNER, M. AND LOHMANN, G., 2011: Synchronicity of Antarctic temperatures and local solar insolation on orbital timescales. *Nature*, **471**(7336): 91-94. <https://doi.org/10.1038/nature09825>
- LEGRAND, M. AND MAYEWSKI, P., 1997: Glaciochemistry of polar ice cores: A review. *Reviews of Geophysics*, **35**(3): 219-243. <https://doi.org/10.1029/96rg03527>
- LENAERTS, J.T.M. AND VAN DEN BROEKE, M.R., 2012: Modeling drifting snow in Antarctica with a regional climate model: 2. Results. *Journal of Geophysical Research: Atmospheres*, **117**(D5). <https://doi.org/10.1029/2010jd015419>
- LENAERTS, J.T.M., VAN MEIJAARD, E., VAN DEN BROEKE, M.R., LIGTENBERG, S.R.M., HORWATH, M. AND ISAKSSON, E., 2013: Recent snowfall anomalies in Dronning Maud Land, East Antarctica, in a historical and future climate perspective. *Geophysical Research Letters*, **40**(11): 2684-2688. <https://doi.org/10.1002/grl.50559>
- LENSSEN, N.J.L., SCHMIDT, G.A., HANSEN, J.E., MENNE, M.J., PERSIN, A., RUEDY, R. AND ZYSS, D., 2019: Improvements in the GISTEMP Uncertainty Model. *Journal of Geophysical Research: Atmospheres*, **124**(12): 6307-6326. <https://doi.org/10.1029/2018jd029522>
- LENTON, T.M., HELD, H., KRIEGLER, E., HALL, J.W., LUCHT, W., RAHMSTORF, S. AND SCHELLNHUBER, H.J., 2008: Tipping elements in the Earth's climate system. *Proceedings of the National Academy of Sciences*, **105**(6): 1786-1793. <https://doi.org/10.1073/pnas.0705414105>
- LENTON, T.M., ROCKSTROM, J., GAFFNEY, O., RAHMSTORF, S., RICHARDSON, K., STEFFEN, W. AND SCHELLNHUBER, H.J., 2019: Climate tipping points - too risky to bet against. *Nature*, **575**(7784): 592-595. <https://doi.org/10.1038/d41586-019-03595-0>
- LI, X., RIGNOT, E., MORLIGHEM, M., MOUGINOT, J. AND SCHEUCHL, B., 2015: Grounding line retreat of Totten Glacier, East Antarctica, 1996 to 2013. *Geophysical Research Letters*, **42**(19): 8049-8056. <https://doi.org/10.1002/2015gl065701>
- LIGTENBERG, S.R.M., HELSEN, M.M. AND VAN DEN BROEKE, M.R., 2011: An improved semi-empirical model for the densification of Antarctic firn. *Cryosphere*, **5**(4): 809-819. <https://doi.org/10.5194/tc-5-809-2011>
- LIMA, 2008: Antarctica in context. LIMA (British Antarctic Survey). <https://lima.usgs.gov/download.php>, last access: 12.03.2020
- LINDSAY, R.W. AND ZHANG, J., 2005: The thinning of Arctic sea ice, 1988-2003: Have we passed a tipping point? *Journal of Climate*, **18**(22): 4879-4894. <https://doi.org/10.1175/jcli3587.1>
- LISIECKI, L.E. AND RAYMO, M.E., 2005: A Pliocene-Pleistocene stack of 57 globally distributed benthic $\delta^{18}O$ records. *Paleoceanography*, **20**(1). <https://doi.org/10.1029/2004pa001071>
- MA, T.M., LI, L., SHI, G.T. AND LI, Y.S., 2020: Acquisition of Post-Depositional Effects on Stable Isotopes ($\delta^{18}O$ and δ^2D) of Snow and Firn at Dome A, East Antarctica. *Water*, **12**(6): 14. <https://doi.org/10.3390/w12061707>
- MANHES, G., ALLÈGRE, C.J., DUPRÉ, B. AND HAMELIN, B., 1980: Lead isotope study of basic-ultrabasic layered complexes: Speculations about the age of the earth and primitive mantle characteristics. *Earth and Planetary Science Letters*, **47**(3): 370-382. [https://doi.org/10.1016/0012-821x\(80\)90024-2](https://doi.org/10.1016/0012-821x(80)90024-2)
- MARZEION, B., JAROSCH, A.H. AND HOFER, M., 2012: Past and future sea-level change from the surface mass balance of glaciers. *The Cryosphere*, **6**(6): 1295-1322. <https://doi.org/10.5194/tc-6-1295-2012>
- MASELLI, O.J., FRITZSCHE, D., LAYMAN, L., MCCONNELL, J.R. AND MEYER, H., 2013: Comparison of water isotope-ratio determinations using two cavity ring-down instruments and classical mass spectrometry in continuous ice-core analysis. *Isotopes Environ Health Stud*, **49**(3): 387-398. <https://doi.org/10.1080/10256016.2013.781598>
- MASSON-DELMOTTE, V., HOU, S., EKAYKIN, A., JOUZEL, J., ARISTARAIN, A., BERNARDO, R.T., BROMWICH, D., CATTANI, O., DELMOTTE, M., FALOURD, S., FREZZOTTI, M., GALLEE, H., GENONI, L., ISAKSSON, E., LANDAIS, A., HELSEN, M.M., HOFFMANN, G., LOPEZ, J., MORGAN, V., MOTOYAMA, H., NOONE, D., OERTER, H., PETIT, J.R., ROYER, A., UEMURA, R., SCHMIDT, G.A., SCHLOSSER, E., SIMOES, J.C., STEIG, E.J., STENNI, B., STIEVENARD, M., VAN DEN BROEKE, M.R., DE WAL, R.S.W.V., DE BERG, W.J.V., VIMEUX, F. AND WHITE, J.W.C., 2008: A review of Antarctic surface snow isotopic composition: Observations, atmospheric circulation, and isotopic modeling. *Journal of Climate*, **21**(13): 3359-3387. <https://doi.org/10.1175/2007jcli2139.1>
- MCMILLAN, M., SHEPHERD, A., SUNDAL, A., BRIGGS, K., MUIR, A., RIDOUT, A., HOGG, A. AND WINGHAM, D., 2014: Increased ice losses from Antarctica detected by CryoSat-2. *Geophysical Research Letters*, **41**(11): 3899-3905. <https://doi.org/10.1002/2014gl060111>
- MEDLEY, B., MCCONNELL, J.R., NEUMANN, T.A., REIJMER, C.H., CHELLMAN, N., SIGL, M. AND KIPFSTUHL, S., 2018: Temperature and Snowfall in Western Queen Maud Land Increasing Faster Than Climate Model Projections. *Geophysical Research Letters*, **45**(3): 1472-1480. <https://doi.org/10.1002/2017gl075992>
- MEDLEY, B. AND THOMAS, E.R., 2019: Increased snowfall over the Antarctic Ice Sheet mitigated twentieth-century sea-level rise. *Nature Climate Change*, **9**(1): 34-39. <https://doi.org/10.1038/s41558-018-0356-x>
- MEEHL, G.A. AND TEBALDI, C., 2004: More intense, more frequent, and longer lasting heat waves in the 21st century. *Science*, **305**(5686): 994-997. <https://doi.org/10.1126/science.1098704>

- MEIER, M.F., DYURGEROV, M.B., RICK, U.K., O'NEEL, S., PFEFFER, W.T., ANDERSON, R.S., ANDERSON, S.P. AND GLAZOVSKY, A.F., 2007: Glaciers dominate eustatic sea-level rise in the 21st century. *Science*, **317**(5841): 1064-1067. <https://doi.org/10.1126/science.1143906>
- MEINSHAUSEN, M., NICHOLLS, Z.R.J., LEWIS, J., GIDDEN, M.J., VOGEL, E., FREUND, M., BEYERLE, U., GESSNER, C., NAUELS, A., BAUER, N., CANADELL, J.G., DANIEL, J.S., JOHN, A., KRUMMEL, P.B., LUDERER, G., MEINSHAUSEN, N., MONTZKA, S.A., RAYNER, P.J., REIMANN, S., SMITH, S.J., VAN DEN BERG, M., VELDEERS, G.J.M., VOLLMER, M.K. AND WANG, R.H.J., 2020: The shared socio-economic pathway (SSP) greenhouse gas concentrations and their extensions to 2500. *Geosci. Model Dev.*, **13**(8): 3571-3605. <https://doi.org/10.5194/gmd-13-3571-2020>
- MILES, B.W.J., STOKES, C.R. AND JAMIESON, S.S.R., 2016: Pan-ice-sheet glacier terminus change in East Antarctica reveals sensitivity of Wilkes Land to sea-ice changes. *Science Advances*, **2**(5): e1501350. <https://doi.org/10.1126/sciadv.1501350>
- MITCHELL, L.E., BUIZERT, C., BROOK, E.J., BRETON, D.J., FEGYVERESI, J., BAGGENSTOS, D., ORSI, A., SEVERINGHAUS, J., ALLEY, R.B., ALBERT, M., RHODES, R.H., MCCONNELL, J.R., SIGL, M., MASELLI, O., GREGORY, S. AND AHN, J., 2015: Observing and modeling the influence of layering on bubble trapping in polar firn. *Journal of Geophysical Research: Atmospheres*, **120**(6): 2558-2574. <https://doi.org/10.1002/2014jd022766>
- MONAGHAN, A.J., BROMWICH, D.H., CHAPMAN, W. AND COMISO, J.C., 2008: Recent variability and trends of Antarctic near-surface temperature. *Journal of Geophysical Research*, **113**(D4). <https://doi.org/10.1029/2007jd009094>
- MONAGHAN, A.J., BROMWICH, D.H., FOGT, R.L., WANG, S.H., MAYEWSKI, P.A., DIXON, D.A., EKAYKIN, A., FREZZOTTI, M., GOODWIN, I., ISAKSSON, E., KASPARI, S.D., MORGAN, V.I., OERTER, H., VAN OMMEN, T.D., VAN DER VEEN, C.J. AND WEN, J.H., 2006: Insignificant change in Antarctic snowfall since the International Geophysical Year. *Science*, **313**(5788): 827-831. <https://doi.org/10.1126/science.1128243>
- MOSER, D.E., HORHOLD, M., KIPFSTUHL, S. AND FREITAG, J., 2020: Microstructure of Snow and Its Link to Trace Elements and Isotopic Composition at Kohnen Station, Dronning Maud Land, Antarctica. *Front. Earth Sci.*, **8**. <https://doi.org/10.3389/feart.2020.00023>
- MOSS, R.H., EDMONDS, J.A., HIBBARD, K.A., MANNING, M.R., ROSE, S.K., VAN VUUREN, D.P., CARTER, T.R., EMORI, S., KAINUMA, M., KRAM, T., MEEHL, G.A., MITCHELL, J.F., NAKICENOVIC, N., RIAHI, K., SMITH, S.J., STOUFFER, R.J., THOMSON, A.M., WEYANT, J.P. AND WILBANKS, T.J., 2010: The next generation of scenarios for climate change research and assessment. *Nature*, **463**(7282): 747-756. <https://doi.org/10.1038/nature08823>
- MÜNCH, T., KIPFSTUHL, S., FREITAG, J., MEYER, H. AND LAEPPLÉ, T., 2016: Regional climate signal vs. local noise: a two-dimensional view of water isotopes in Antarctic firn at Kohnen Station, Dronning Maud Land. *Climate of the Past*, **12**(7): 1565-1581. <https://doi.org/10.5194/cp-12-1565-2016>
- MÜNCH, T., KIPFSTUHL, S., FREITAG, J., MEYER, H. AND LAEPPLÉ, T., 2017: Constraints on post-depositional isotope modifications in East Antarctic firn from analysing temporal changes of isotope profiles. *The Cryosphere*, **11**(5): 2175-2188. <https://doi.org/10.5194/tc-11-2175-2017>
- MUTO, A., SCAMBOS, T.A., STEFFEN, K., SLATER, A.G. AND CLOW, G.D., 2011: Recent surface temperature trends in the interior of East Antarctica from borehole firn temperature measurements and geophysical inverse methods. *Geophysical Research Letters*, **38**(15). <https://doi.org/10.1029/2011gl048086>
- NASA, 2021: Global Land-Ocean Temperature Index. In (GISS), N.s.G.I.f.S.S., ed.
- OERTER, H., 2008: High resolution density and $\delta 18O$ of snow pits DML76S05_11 to DML90S05_25. In Oerter, H., H. Fischer and P. Sperlich, eds., *Pangaea*. <https://doi.org/10.1594/PANGAEA.708082>
- OERTER, H., DRÜCKER, C., KIPFSTUHL, S. AND WILHELMS, F., 2009: Kohnen station - the drilling camp for the EPICA deep ice core in Dronning Maud Land. *Polarforschung*, **78**(1): 1-23.
- OERTER, H., GRAF, W., WILHELMS, F., MINIKIN, A. AND MILLER, H., 1999: Accumulation studies on Amundsenisen, Dronning Maud Land, Antarctica, by means of tritium, dielectric profiling and stable-isotope measurements: first results from the 1995-96 and 1996-97 field seasons. *Ann Glaciol*, **29**: 1-9. <https://doi.org/10.3189/172756499781820914>
- OPPENHEIMER, M., GLAVOVIC, B., HINKEL, J., VAN DE WAL, R., MAGNAN, A.K., ABD-ELGAWAD, A., CAI, R., CIFUENTES-JARA, M., DECONTO, R.M. AND GHOSH, T., 2019: Sea level rise and implications for low lying islands, coasts and communities. In Pörtner, H.-O., D.C. Roberts, V. Masson-Delmotte, P. Zhai, M. Tignor, E. Poloczanska, K. Mintenbeck, A. Alegria, M. Nicolai, A. Okem, J. Petzold, B. Rama and N.M. Weyer (ed.), *IPCC Special Report on the Ocean and Cryosphere in a Changing Climate*.
- PANG, H., HOU, S., LANDAIS, A., MASSON-DELMOTTE, V., JOUZEL, J., STEEN-LARSEN, H.C., RISI, C., ZHANG, W., WU, S., LI, Y., AN, C., WANG, Y., PRIE, F., MINSTER, B., FALOURD, S., STENNI, B., SCARCHILLI, C., FUJITA, K. AND GRIGIONI, P., 2019: Influence of Summer Sublimation on δD , $\delta 18O$, and $\delta 17O$ in Precipitation, East Antarctica, and Implications for Climate Reconstruction From Ice Cores. *Journal of Geophysical Research: Atmospheres*. <https://doi.org/10.1029/2018jd030218>
- PARISH, T.R. AND BROMWICH, D.H., 1987: The Surface Windfield over the Antarctic Ice Sheets. *Nature*, **328**(6125): 51-54. <https://doi.org/10.1038/328051a0>
- PARMESAN, C. AND YOHE, G., 2003: A globally coherent fingerprint of climate change impacts across natural systems. *Nature*, **421**(6918): 37-42. <https://doi.org/10.1038/nature01286>
- PARRENIN, F., CAVITTE, M.G.P., BLANKENSHIP, D.D., CHAPPELLAZ, J., FISCHER, H., GAGLIARDINI, O., MASSON-DELMOTTE, V., PASSALACQUA, O., RITZ, C., ROBERTS, J., SIEGERT, M.J. AND YOUNG, D.A., 2017: Is there 1.5-million-year-old ice near Dome C, Antarctica? *Cryosphere*, **11**(6): 2427-2437. <https://doi.org/10.5194/tc-11-2427-2017>
- PATTYN, F., RITZ, C., HANNA, E., ASAY-DAVIS, X., DECONTO, R., DURAND, G., FAVIER, L., FETTWEIS, X., GOELZER, H., GOLLEDGE, N.R., KUIPERS MUNNEKE, P., LENAERTS, J.T.M., NOWICKI, S., PAYNE, A.J., ROBINSON, A., SEROUSSI, H., TRUSEL, L.D. AND VAN DEN BROEKE, M., 2018: The Greenland and Antarctic ice sheets under 1.5 °C global warming. *Nature Climate Change*, **8**(12): 1053-1061. <https://doi.org/10.1038/s41558-018-0305-8>
- PAYNE, A.J., VIELI, A., SHEPHERD, A.P., WINGHAM, D.J. AND RIGNOT, E., 2004: Recent dramatic thinning of largest West Antarctic ice stream triggered by oceans. *Geophysical Research Letters*, **31**(23). <https://doi.org/10.1029/2004gl021284>
- PETIT, J.R., JOUZEL, J., RAYNAUD, D., BARKOV, N.I., BARNOLA, J.M., BASILE, I., BENDER, M., CHAPPELLAZ, J., DAVIS, M., DELAYGUE, G., DELMOTTE, M., KOTLYAKOV, V.M., LEGRAND, M., LIPENKOV, V.Y., LORIUS, C., PEPIN, L., RITZ, C.,

- SALTZMAN, E. AND STIEVENARD, M., 1999: Climate and atmospheric history of the past 420,000 years from the Vostok ice core, Antarctica. *Nature*, **399**(6735): 429-436. <https://doi.org/10.1038/20859>
- PFEFFER, W.T. AND MRUGALA, R., 2002: Temperature gradient and initial snow density as controlling factors in the formation and structure of hard depth hoar. *Journal of Glaciology*, **48**(163): 485-494. <https://doi.org/10.3189/172756502781831098>
- PHILIPPE, M., TISON, J.-L., FJØSNE, K., HUBBARD, B., KLÆR, H.A., LENAERTS, J.T.M., DREWS, R., SHELDON, S.G., DE BOND, K., CLAEYS, P. AND PATTYN, F., 2016: Ice core evidence for a 20th century increase in surface mass balance in coastal Dronning Maud Land, East Antarctica. *The Cryosphere*, **10**(5): 2501-2516. <https://doi.org/10.5194/tc-10-2501-2016>
- PICCIOTTO, E., CROZAZ, G. AND DE BREUCK, W., 1971: Accumulation on the South Pole-Queen Maud Land Traverse, 1964-1968. In Cray, A.P. (ed.), *Antarctic Snow and Ice Studies II*, Washington D.C., American Geophysical Union, 257-315. (Antarctic Research Series 16). <https://doi.org/10.1029/AR016p0257>
- PIDWIRNY, M., 2006: Glacial Processes. <http://www.physicalgeography.net/fundamentals/10ae.html>, last access: 02.11.2021
- R CORE TEAM, 2021: A language and environment for statistical computing. Vienna, Austria, R Foundation for Statistical Computing.
- RADOK, U. AND LILE, R.C., 1977: A Year of Snow Accumulation at Plateau Station. In Dalrymple, P.C., A.J. Riordan, A. Riordan, A.J. Riordan, G. Weller, H.H. Lettau, H. Lettau, L.A. Stroschein, L.S. Kundla, L.A. Stroschein, M. Kuhn, P. Schwerdtfeger, R.C. Lile and U. Radok (ed.), *Meteorological Studies at Plateau Station, Antarctica*, American Geophysical Union. (Antarctic Research Series 25). <https://doi.org/10.1002/9781118664872.ch2>
- REIJMER, C.H. AND VAN DEN BROEKE, M.R., 2003: Temporal and spatial variability of the surface mass balance in Dronning Maud Land, Antarctica, as derived from automatic weather stations. *Journal of Glaciology*, **49**(167): 512-520. <https://doi.org/10.3189/172756503781830494>
- RIGNOT, E., MOUGINOT, J., SCHEUCHL, B., VAN DEN BROEKE, M., VAN WESSEM, M.J. AND MORLIGHEM, M., 2019: Four decades of Antarctic Ice Sheet mass balance from 1979-2017. *Proc. Natl. Acad. Sci. U. S. A.*, **116**(4): 1095-1103. <https://doi.org/10.1073/pnas.1812883116>
- RUNDLE, A.S., 1971: Snow Accumulation and Firm Stratigraphy on the East Antarctic Plateau. In Cray, A.P. (ed.), *Antarctic Snow and Ice Studies II*, Washington D.C., American Geophysical Union, 239-255. (Antarctic Research Series 16). <https://doi.org/10.1029/AR016p0239>
- RUTH, U., BARBANTE, C., BIGLER, M., DELMONTE, B., FISCHER, H., GABRIELLI, P., GASPARI, V., KAUFMANN, P., LAMBERT, F., MAGGI, V., MARINO, F., PETIT, J.R., UDISTI, R., WAGENBACH, D., WEGNER, A. AND WOLFF, E.W., 2008: Proxies and measurement techniques for mineral dust in Antarctic ice cores. *Environ Sci Technol*, **42**(15): 5675-5681. <https://doi.org/10.1021/es703078z>
- SANZ RODRIGO, J., BUCHLIN, J.-M., VAN BEECK, J., LENAERTS, J.T.M. AND VAN DEN BROEKE, M.R., 2012: Evaluation of the antarctic surface wind climate from ERA reanalyses and RACMO2/ANT simulations based on automatic weather stations. *Climate Dynamics*, **40**(1-2): 353-376. <https://doi.org/10.1007/s00382-012-1396-y>
- SCAMBOS, T.A., BELL, R.E., ALLEY, R.B., ANANDAKRISHNAN, S., BROMWICH, D.H., BRUNT, K., CHRISTIANSON, K., CREYTS, T., DAS, S.B., DECONTO, R., DUTRIEUX, P., FRICKER, H.A., HOLLAND, D., MACGREGOR, J., MEDLEY, B., NICOLAS, J.P., POLLARD, D., SIEGFRIED, M.R., SMITH, A.M., STEIG, E.J., TRUSEL, L.D., VAUGHAN, D.G. AND YAGER, P.L., 2017: How much, how fast?: A science review and outlook for research on the instability of Antarctica's Thwaites Glacier in the 21st century. *Global and Planetary Change*, **153**: 16-34. <https://doi.org/10.1016/j.gloplacha.2017.04.008>
- SCAMBOS, T.A., CAMPBELL, G.G., POPE, A., HARAN, T., MUTO, A., LAZZARA, M., REIJMER, C.H. AND BROEKE, M.R., 2018: Ultralow Surface Temperatures in East Antarctica From Satellite Thermal Infrared Mapping: The Coldest Places on Earth. *Geophysical Research Letters*, **45**(12): 6124-6133. <https://doi.org/10.1029/2018gl078133>
- SCAMBOS, T.A., FREZZOTTI, M., HARAN, T., BOHLANDER, J., LENAERTS, J.T.M., VAN DEN BROEKE, M.R., JEZEK, K., LONG, D., URBINI, S., FARNES, K., NEUMANN, T., ALBERT, M. AND WINTHER, J.G., 2012: Extent of low-accumulation 'wind glaze' areas on the East Antarctic plateau: implications for continental ice mass balance. *Journal of Glaciology*, **58**(210): 633-647. <https://doi.org/10.3189/2012JoGI1J232>
- SCHALLER, C.F., 2017: Towards understanding the signal formation in polar snow, firn and ice using X-ray computed tomography. PhD Thesis Universität Bremen.
- SCHALLER, C.F., FREITAG, J. AND EISEN, O., 2017: Critical porosity of gas enclosure in polar firn independent of climate. *Climate of the Past*, **13**(11): 1685-1693. <https://doi.org/10.5194/cp-13-1685-2017>
- SCHALLER, C.F., FREITAG, J., KIPFSTUHL, S., LAEPPLE, T., STEEN-LARSEN, H.C. AND EISEN, O., 2016: A representative density profile of the North Greenland snowpack. *Cryosphere*, **10**(5): 1991-2002. <https://doi.org/10.5194/tc-10-1991-2016>
- SCHELLNHUBER, H.J., RAHMSTORF, S. AND WINKELMANN, R., 2016: Why the right climate target was agreed in Paris. *Nature Climate Change*, **6**(7): 649-653. <https://doi.org/10.1038/nclimate3013>
- SCHLOSSER, E., MANNING, K.W., POWERS, J.G., DUDA, M.G., BIRNBAUM, G. AND FUJITA, K., 2010: Characteristics of high-precipitation events in Dronning Maud Land, Antarctica. *Journal of Geophysical Research*, **115**(D14). <https://doi.org/10.1029/2009jd013410>
- SCHLOSSER, E. AND OERTER, H., 2002: Seasonal variations of accumulation and the isotope record in ice cores: a study with surface snow samples and firn cores from Neumayer station, Antarctica. *Annals of Glaciology*, Vol 35, **35**: 97-101. <https://doi.org/10.3189/172756402781817374>
- SCHRÖDER, L., HORWATH, M., DIETRICH, R., HELM, V., VAN DEN BROEKE, M.R. AND LIGTENBERG, S.R.M., 2019: Four decades of Antarctic surface elevation changes from multi-mission satellite altimetry. *Cryosphere*, **13**(2): 427-449. <https://doi.org/10.5194/tc-13-427-2019>
- SCHWANDER, J., 1996: Gas Diffusion in Firn. In Wolff, E.W. and R.C. Bales (ed.), *Chemical Exchange Between the Atmosphere and Polar Snow*, Berlin, Heidelberg, Springer Berlin Heidelberg, 527-540. (NATO ASI Series). https://doi.org/10.1007/978-3-642-61171-1_22
- SCHWANDER, J. AND STAUFFER, B., 1984: Age difference between polar ice and the air trapped in its bubbles. *Nature*, **311**(5981): 45-47. <https://doi.org/10.1038/311045a0>
- SCHYTT, V., 1958: Snow and ice studies in Antarctica. In: Norwegian-British-Swedish antarctic expedition, 1949-52. Scientific results; Vol. 4.

- SCREEN, J.A. AND SIMMONDS, I., 2010: The central role of diminishing sea ice in recent Arctic temperature amplification. *Nature*, **464**(7293): 1334-1337. <https://doi.org/10.1038/nature09051>
- SEIDLER, C., 2017: Verlassene Antarktisstation - Besuch in der Festung der Einsamkeit. Spiegel. <https://www.spiegel.de/wissenschaft/mensch/antarktis-forscher-besuchen-eine-seit-50-jahren-verlassene-station-a-1140427.html>, last access: 23.12.2020
- SEROUSSI, H., NOWICKI, S., PAYNE, A.J., GOELZER, H., LIPSCOMB, W.H., ABE-OUCHI, A., AGOSTA, C., ALBRECHT, T., ASAY-DAVIS, X., BARTHEL, A., CALOV, R., CULLATHER, R., DUMAS, C., GALTON-FENZI, B.K., GLADSTONE, R., GOLLEDGE, N.R., GREGORY, J.M., GREVE, R., HATTERMANN, T., HOFFMAN, M.J., HUMBERT, A., HUYBRECHTS, P., JOURDAIN, N.C., KLEINER, T., LAROUR, E., LEGUY, G.R., LOWRY, D.P., LITTLE, C.M., MORLIGHEM, M., PATTYN, F., PELLE, T., PRICE, S.F., QUIQUET, A., REESE, R., SCHLEGEL, N.-J., SHEPHERD, A., SIMON, E., SMITH, R.S., STRANEO, F., SUN, S., TRUSEL, L.D., VAN BREEDAM, J., VAN DE WAL, R.S.W., WINKELMANN, R., ZHAO, C., ZHANG, T. AND ZWINGER, T., 2020: ISMIP6 Antarctica: a multi-model ensemble of the Antarctic ice sheet evolution over the 21st century. *The Cryosphere*, **14**(9): 3033-3070. <https://doi.org/10.5194/tc-14-3033-2020>
- SERREZE, M.C. AND BARRY, R.G., 2011: Processes and impacts of Arctic amplification: A research synthesis. *Global and Planetary Change*, **77**(1-2): 85-96. <https://doi.org/10.1016/j.gloplacha.2011.03.004>
- SERVETTAZ, A.P.M., ORSI, A.J., CURRAN, M.A.J., MOY, A.D., LANDAIS, A., AGOSTA, C., WINTON, V.H.L., TOUZEAU, A., MCCONNELL, J.R., WERNER, M. AND BARONI, M., 2020: Snowfall and Water Stable Isotope Variability in East Antarctica Controlled by Warm Synoptic Events. *Journal of Geophysical Research-Atmospheres*, **125**(17): 14. <https://doi.org/10.1029/2020jd032863>
- SHAW, G.E., 1988: Antarctic Aerosols - a Review. *Reviews of Geophysics*, **26**(1): 89-112. <https://doi.org/10.1029/RG026i001p00089>
- SHEN, Q., WANG, H., SHUM, C.K., JIANG, L., HSU, H.T. AND DONG, J., 2018: Recent high-resolution Antarctic ice velocity maps reveal increased mass loss in Wilkes Land, East Antarctica. *Sci Rep*, **8**(1). <https://doi.org/10.1038/s41598-018-22765-0>
- SHEPHERD, A., WINGHAM, D. AND RIGNOT, E., 2004: Warm ocean is eroding West Antarctic Ice Sheet. *Geophysical Research Letters*, **31**(23). <https://doi.org/10.1029/2004gl021106>
- SHIRAIISHI, K., 2013: Dome Fuji Station in East Antarctica and the Japanese Antarctic Research Expedition. *Proceedings of the International Astronomical Union*, **8**(S288): 161-168. <https://doi.org/10.1017/s1743921312016821>
- SIEGERT, M.J., POPOV, S. AND STUDINGER, M., 2011: Vostok subglacial lake: A review of geophysical data regarding its discovery and topographic setting. In Siegert, M.J., C. Kennicutt and B. Bindschadler (ed.), *Subglacial Antarctic Aquatic Environments*, Washington DC, AGU Geophysical Monograph, 45-60. <https://doi.org/10.1029/2010gm000934>
- SOMMER, C.G., LEHNING, M. AND FIERZ, C., 2017: Wind tunnel experiments: saltation is necessary for wind-packing. *Journal of Glaciology*, **63**(242): 950-958. <https://doi.org/10.1017/jog.2017.53>
- SOMMER, C.G., LEHNING, M. AND FIERZ, C., 2018: Wind Tunnel Experiments: Influence of Erosion and Deposition on Wind-Packing of New Snow. *Front. Earth Sci.*, **6**. <https://doi.org/10.3389/feart.2018.00004>
- SORENSEN, L.S., SIMONSEN, S.B., LANGLEY, K., GRAY, L., HELM, V., NILSSON, J., STENSENG, L., SKOURUP, H., FORSBERG, R. AND DAVIDSON, M.W.J., 2018: Validation of CryoSat-2 SARIn Data over Austfonna Ice Cap Using Airborne Laser Scanner Measurements. *Remote Sens.*, **10**(9): 12. <https://doi.org/10.3390/rs10091354>
- SOWERS, T., BENDER, M., RAYNAUD, D. AND KOROTKEVICH, Y.S., 1992: $\delta^{15}\text{N}$ of N_2 in air trapped in polar ice: A tracer of gas transport in the firn and a possible constraint on ice age-gas age differences. *Journal of Geophysical Research: Atmospheres*, **97**(D14): 15683-15697.
- SPEKTRUM, 2005: Welcher Kontinent liegt durchschnittlich am höchsten? Spektrum. <https://www.spektrum.de/quiz/welcher-kontinent-liegt-durchschnittlich-am-hoechsten/783554>, last access: 19.03.2020
- STEEN-LARSEN, H.C., MASSON-DELMOTTE, V., HIRABAYASHI, M., WINKLER, R., SATOW, K., PRIÉ, F., BAYOU, N., BRUN, E., CUFFEY, K.M., DAHL-JENSEN, D., DUMONT, M., GUILLEVIC, M., KIPFSTUHL, S., LANDAIS, A., POPP, T., RISI, C., STEFFEN, K., STENNI, B. AND SVEINBJÖRNSDÓTTIR, A.E., 2014: What controls the isotopic composition of Greenland surface snow? *Climate of the Past*, **10**(1): 377-392. <https://doi.org/10.5194/cp-10-377-2014>
- STEFFEN, W., CRUTZEN, P.J. AND MCNEILL, J.R., 2007: The Anthropocene: Are humans now overwhelming the great forces of nature. *Ambio*, **36**(8): 614-621. [https://doi.org/10.1579/0044-7447\(2007\)36\[614:taahno\]2.0.co;2](https://doi.org/10.1579/0044-7447(2007)36[614:taahno]2.0.co;2)
- STENNI, B., CURRAN, M.A.J., ABRAM, N.J., ORSI, A., GOURSAUD, S., MASSON-DELMOTTE, V., NEUKOM, R., GOOSSE, H., DIVINE, D., VAN OMMEN, T., STEIG, E.J., DIXON, D.A., THOMAS, E.R., BERTLER, N.A.N., ISAKSSON, E., EKAYKIN, A., WERNER, M. AND FREZZOTTI, M., 2017: Antarctic climate variability on regional and continental scales over the last 2000 years. *Climate of the Past*, **13**(11): 1609-1634. <https://doi.org/10.5194/cp-13-1609-2017>
- STENNI, B., SCARCHILLI, C., MASSON-DELMOTTE, V., SCHLOSSER, E., CIARDINI, V., DREOSSI, G., GRIGIONI, P., BONAZZA, M., CAGNATI, A., KARLICEK, D., RISI, C., UDISTI, R. AND VALT, M., 2016: Three-year monitoring of stable isotopes of precipitation at Concordia Station, East Antarctica. *The Cryosphere*, **10**(5): 2415-2428. <https://doi.org/10.5194/tc-10-2415-2016>
- STROEVE, J.C., SERREZE, M.C., HOLLAND, M.M., KAY, J.E., MALANIK, J. AND BARRETT, A.P., 2011: The Arctic's rapidly shrinking sea ice cover: a research synthesis. *Climatic Change*, **110**(3-4): 1005-1027. <https://doi.org/10.1007/s10584-011-0101-1>
- SUTTER, J., FISCHER, H., GROSFELD, K., KARLSSON, N.B., KLEINER, T., VAN LIEFFERINGE, B. AND EISEN, O., 2019: Modelling the Antarctic Ice Sheet across the mid-Pleistocene transition – implications for Oldest Ice. *The Cryosphere*, **13**(7): 2023-2041. <https://doi.org/10.5194/tc-13-2023-2019>
- THOMAS, E.R., VAN WESSEM, J.M., ROBERTS, J., ISAKSSON, E., SCHLOSSER, E., FUDGE, T.J., VALLELONGA, P., MEDLEY, B., LENAERTS, J., BERTLER, N., VAN DEN BROEKE, M.R., DIXON, D.A., FREZZOTTI, M., STENNI, B., CURRAN, M. AND EKAYKIN, A.A., 2017: Regional Antarctic snow accumulation over the past 1000 years. *Climate of the Past*, **13**(11): 1491-1513. <https://doi.org/10.5194/cp-13-1491-2017>
- TOUZEAU, A., LANDAIS, A., STENNI, B., UEMURA, R., FUKUI, K., FUJITA, S., GUILBAUD, S., EKAYKIN, A., CASADO, M., BARKAN, E., LUZ, B., MAGAND, O., TESTE, G., LE MEUR, E., BARONI, M., SAVARINO, J., BOURGEOIS, I. AND RISI, C., 2016: Acquisition

- of isotopic composition for surface snow in East Antarctica and the links to climatic parameters. *Cryosphere*, **10**(2): 837-852. <https://doi.org/10.5194/tc-10-837-2016>
- TURNER, J., ANDERSON, P., LACHLAN-COPE, T., COLWELL, S., PHILLIPS, T., KIRCHGAESSNER, A., MARSHALL, G.J., KING, J.C., BRACEGIRDLE, T., VAUGHAN, D.G., LAGUN, V. AND ORR, A., 2009: Record low surface air temperature at Vostok station, Antarctica. *Journal of Geophysical Research*, **114**(D24). <https://doi.org/10.1029/2009jd012104>
- TURNER, J., COLWELL, S.R., MARSHALL, G.J., LACHLAN-COPE, T.A., CARLETON, A.M., JONES, P.D., LAGUN, V., REID, P.A. AND IAGOVKINA, S., 2005: Antarctic climate change during the last 50 years. *Int. J. Climatol.*, **25**(3): 279-294. <https://doi.org/10.1002/joc.1130>
- UNFCCC, 2015: Adoption of the Paris Agreement. UNFCCC. <http://unfccc.int/resource/docs/2015/cop21/eng/109r01.pdf>, last access: 09.12.2020
- URBINI, S., FREZZOTTI, M., GANDOLFI, S., VINCENT, C., SCARCHILLI, C., VITTUARI, L. AND FILY, M., 2008: Historical behaviour of Dome C and Talos Dome (East Antarctica) as investigated by snow accumulation and ice velocity measurements. *Global and Planetary Change*, **60**(3-4): 576-588. <https://doi.org/10.1016/j.gloplacha.2007.08.002>
- VAN GELDERN, R. AND BARTH, J.A.C., 2012: Optimization of instrument setup and post-run corrections for oxygen and hydrogen stable isotope measurements of water by isotope ratio infrared spectroscopy (IRIS). *Limnology and Oceanography: Methods*, **10**(12): 1024-1036. <https://doi.org/10.4319/lom.2012.10.1024>
- VAN LIEFFERINGE, B., PATTYN, F., CAVITTE, M.G.P., KARLSSON, N.B., YOUNG, D.A., SUTTER, J. AND EISEN, O., 2018: Promising Oldest Ice sites in East Antarctica based on thermodynamical modelling. *Cryosphere*, **12**(8): 2773-2787. <https://doi.org/10.5194/tc-12-2773-2018>
- VAN LIPZIG, N.P.M., TURNER, J., COLWELL, S.R. AND VAN DEN BROEKE, M.R., 2004: The near-surface wind field over the Antarctic continent. *Int. J. Climatol.*, **24**(15): 1973-1982. <https://doi.org/10.1002/joc.1090>
- VON SCHUCKMANN, K., CHENG, L., PALMER, M.D., HANSEN, J., TASSONE, C., AICH, V., ADUSUMILLI, S., BELTRAMI, H., BOYER, T., CUESTA-VALERO, F.J., DESBRUYÈRES, D., DOMINGUES, C., GARCÍA-GARCÍA, A., GENTINE, P., GILSON, J., GORFER, M., HAIMBERGER, L., ISHII, M., JOHNSON, G.C., KILLICK, R., KING, B.A., KIRCHENGAST, G., KOŁODZIEJCZYK, N., LYMAN, J., MARZEION, B., MAYER, M., MONIER, M., MONSELESAN, D.P., PURKEY, S., ROEMMICH, D., SCHWEIGER, A., SENEVIRATNE, S.I., SHEPHERD, A., SLATER, D.A., STEINER, A.K., STRANEO, F., TIMMERMANS, M.-L. AND WIFFELS, S.E., 2020: Heat stored in the Earth system: where does the energy go? *Earth System Science Data*, **12**(3): 2013-2041. <https://doi.org/10.5194/essd-12-2013-2020>
- WATANABE, O., KAMIYAMA, K., MOTOYAMA, H., FUJII, Y., IGARASHI, M., FURUKAWA, T., GOTO-AZUMA, K., SAITO, T., KANAMORI, S., KANAMORI, N., YOSHIDA, N. AND UEMURA, R., 2003: General tendencies of stable isotopes and major chemical constituents of the Dome Fuji deep ice core. *Memoirs of National Institute of Polar Research*, **57**: 1-24.
- WELLER, R., TRAUFFETER, F., FISCHER, H., OERTER, H., PIEL, C. AND MILLER, H., 2004: Postdepositional losses of methane sulfonate, nitrate, and chloride at the European Project for Ice Coring in Antarctica deep-drilling site in Dronning Maud Land, Antarctica. *Journal of Geophysical Research-Atmospheres*, **109**(D7). <https://doi.org/10.1029/2003jd004189>
- WINEBRENNER, D.P., ARTHERN, R.J. AND SHUMAN, C.A., 2001: Mapping Greenland accumulation rates using observations of thermal emission at 4.5-cm wavelength. *Journal of Geophysical Research-Atmospheres*, **106**(D24): 33919-33934. <https://doi.org/10.1029/2001jd900235>
- WINTER, A., STEINHAGE, D., CREYTS, T.T., KLEINER, T. AND EISEN, O., 2019: Age stratigraphy in the East Antarctic Ice Sheet inferred from radio-echo sounding horizons. *Earth System Science Data*, **11**(3): 1069-1081. <https://doi.org/10.5194/essd-11-1069-2019>
- WOLFF, E.W., FISCHER, H., FUNDEL, F., RUTH, U., TWARLOH, B., LITTOT, G.C., MULVANEY, R., ROTHLISBERGER, R., DE ANGELIS, M., BOUTRON, C.F., HANSSON, M., JONSELL, U., HUTTERLI, M.A., LAMBERT, F., KAUFMANN, P., STAUFFER, B., STOCKER, T.F., STEFFENSEN, J.P., BIGLER, M., SIGGAARD-ANDERSEN, M.L., UDISTI, R., BECAGLI, S., CASTELLANO, E., SEVERI, M., WAGENBACH, D., BARBANTE, C., GABRIELLI, P. AND GASPARI, V., 2006: Southern Ocean sea-ice extent, productivity and iron flux over the past eight glacial cycles. *Nature*, **440**(7083): 491-496. <https://doi.org/10.1038/nature04614>
- WOLFF, E.W., JONES, A.E., MARTIN, T.J. AND GRENFELL, T.C., 2002: Modelling photochemical NO_x production and nitrate loss in the upper snowpack of Antarctica. *Geophysical Research Letters*, **29**(20): 5-1-5-4. <https://doi.org/10.1029/2002gl015823>
- WORLD OCEAN REVIEW 6, 2019: *Arktis und Antarktis - extrem, klimarelevant, gefährdet*. Hamburg, maribus gGmbH. 978-3-86648-634-8
- YOUNG, D.A., ROBERTS, J.L., RITZ, C., FREZZOTTI, M., QUARTINI, E., CAVITTE, M.G.P., TOZER, C.R., STEINHAGE, D., URBINI, S., CORR, H.F.J., VAN OMMEN, T. AND BLANKENSHIP, D.D., 2017: High-resolution boundary conditions of an old ice target near Dome C, Antarctica. *The Cryosphere*, **11**(4): 1897-1911. <https://doi.org/10.5194/tc-11-1897-2017>
- YOUNG, G.M., 2013: Evolution of Earth's climatic system: Evidence from ice ages, isotopes, and impacts. *GSA Today*, **23**(10): 4-10. <https://doi.org/10.1130/gsatg183a.1>
- ZALICKI, P. AND ZARE, R.N., 1995: Cavity ring-down spectroscopy for quantitative absorption measurements. *The Journal of Chemical Physics*, **102**(7): 2708-2717. <https://doi.org/10.1063/1.468647>
- ZUHR, A.M., MÜNCH, T., STEEN-LARSEN, H.C., HÖRHOLD, M. AND LAEPPLE, T., in review, 2021: Local scale depositional processes of surface snow on the Greenland ice sheet. *The Cryosphere Discuss.*, [preprint]. <https://doi.org/10.5194/tc-2021-36>
- ZWALLY, H.J., LI, J., ROBBINS, J.W., SABA, J.L., YI, D.H. AND BRENNER, A.C., 2015: Mass gains of the Antarctic ice sheet exceed losses. *Journal of Glaciology*, **61**(230): 1019-1036. <https://doi.org/10.3189/2015JoG15J071>

9 ACKNOWLEDGMENTS

Although my time at AWI already started in 2014 as a student assistant in the Glaciology group, which led subsequently to writing my master thesis, the following lines focus on the time of my PhD project in chronological order, starting in spring 2016:

Although he might not be aware of it, **Christoph Schaller** got the ball for this project rolling with encouraging me to apply for a stipend at the German Environmental Foundation. Thank you for three years as a colleague, friend, and competitor in several Wikipedia challenges.

From the very beginning, meaning the conception of the application for the PhD project, continuing with the data analyses as well as many scientific discussions and hints, **Johannes Freitag** supported me throughout the whole time – thank you so much. I hope you enjoyed our scientific discussions as much as the political ones and the gymnastic sessions in the μ CT lab.

Also from the very beginning you supported me as well as this project, **Maria Hörhold**. Thank you not only for your scientific support, but also for just taking care and warm words at the right time.

Thank you, **Olaf Eisen**, for your support through the years – even if some requests were on short notice, you backed this project from the very beginning, starting with the application at DBU, continuing with lots of feedback to my manuscripts and ending with the assessment of this thesis.

I am deeply grateful for the opportunity to join not only a scientifically interesting, but also adventurous expedition to one of the most remote places on this planet. Two and a half months in Antarctica were a once-in-a-lifetime experience to me. Thanks to our expedition leader **Andreas Frenzel**, who introduced me very empathically into the life and the routines in the field. Furthermore, sharing six and a half weeks in isolation with the CoFi traverse team (Fig. 15) makes it definitely worth mentioning each one of the team: Thank you

Geron, not only for making the best food, but also keeping the motivation up with your life wisdom,

Martin, for your – luckily never necessary – medical support,

Peter, for your Swabian coolness,

Urs, for anecdotes from Switzerland (although I did not understand each single word)

Torsten, for leading us safe over the vast infinity and loneliness of the East Antarctic Plateau

Sverrir, for your constant work ethic during cold drilling days,

Alexandra, to stand us eight men in the wild and supporting my work in the field,

and, of course, **Sepp Kipfstuhl**, simply for sharing your infinite experience (including how to dig a snow pit, Fig. 16), which sometimes was even too much to digest at once.



Fig. 15: CoFi traverse crew, from left to right: Sepp, Alexandra, Alexander (me), Sverrir, Torsten, Geron, Urs, Peter, Martin.

During my time at AWI, I also shared the μ CT lab with **Tetsuro Taranczewski**. Thank you, for controversial coffee talks together with Johannes and Christoph – and sometimes also with **Melissa Mengert**. I am really thankful for your reliability at the analytical work in the cold labs, the accompanied conversations as well as the recipe for the best red wine chocolate cake.

When finally all the μ CT measurements were done, I needed (wo)manpower to cut the samples in the cold lab. Thanks to everybody, who stood at my side cutting snow profiles in the cold (listed in order of abundance): **Melissa Mengert, Pia Götz, Georgia Micha, Jana Kalmbach, Lisa Bouvet, Charlotte Fischer, Sonja Wahl, Lena Sophie Franz, Jennfier Gromes, Kyra Streng, Maria Eden, Linus Petterson, Tetsuro Taranczewski**. For some (not further evaluated) reason, the percentage of women is extraordinary high here.

Without the tireless efforts of the impurity and stable water isotope labs the enormous dataset for this thesis would not exist. Thank you **Thaddäus Bluszcz, Birthe Twarloh, Melanie Behrens & York Schlomann** for your work ‘behind the scenes’.

Thank you **Remi Dallmayr, Emma Smith, Svenja Schiwek, Nicole Syring, Nicolas Stoll & Steven Franke** for lunch & coffee chats, AWI rooftop parties, good music and making my life at AWI a good one. I want to thank **Alexander Rösner** for sharing small but very useful hints once in a while. Finishing the thesis during the upcoming COVID-19 pandemic was not the easiest, so the virtual workspace with **Rebecca Schlegel** was a good way to keep the focus in endless home office. To make the text frame of this thesis comprehensible, I want to thank **Birk Stern** for proofreading – I hope we find a date for a dinner in return soon.

I want to thank the whole **Glaciology group** for their hospitality, especially the **ice core group** providing a nice work atmosphere at AWI and **Hubertus Fischer & Frank Wilhelms** to act as the assessors of this thesis.

Last but not least, I want to thank the **DBU** for financial support, **my parents** for always standing at my side and **Franziska Martens** for keeping me on track.



Fig. 16: View out of a snow pit – the first one I dug – on a sunny day at Kohnen Station.

10 APPENDIX

10.1 SAMPLING PROTOCOLS

Tab. 2: Sample overview (methods applied as at 10.04.2020)

Location number in this study	Official location name listed in PANGAEA (ANT-Land_2016_)	Available snow profiles	Latitude [°S]	Longitude [°E]	Altitude [m asl]	Sampling date	Density measured	Discrete samples	IC measured	CRDS measured	Optical levelling	Additional samples
1	CoFi_4	A, B, C, X (2m)	75.106	2.891	2989	14.12.2016	<input checked="" type="checkbox"/>	<input checked="" type="checkbox"/>	<input checked="" type="checkbox"/>	<input checked="" type="checkbox"/>		
2	CoFi_8	A, B, C, X (2m)	75.178	6.117	3146	15.12.2016	<input checked="" type="checkbox"/>	<input checked="" type="checkbox"/>	<input checked="" type="checkbox"/>	<input checked="" type="checkbox"/>		
3	CoFi_12	A, B, C, X (2m)	75.206	9.582	3301	16.12.2016	<input checked="" type="checkbox"/>	<input checked="" type="checkbox"/>	<input checked="" type="checkbox"/>	<input checked="" type="checkbox"/>		
4	CoFi_16	A, B, C, X (2m)	75.185	12.661	3400	17.12.2016	<input checked="" type="checkbox"/>	<input checked="" type="checkbox"/>	<input checked="" type="checkbox"/>	<input checked="" type="checkbox"/>		
5	CoFi_19	A, B, C, X (2m)	75.133	15.399	3470	18.12.2016	<input checked="" type="checkbox"/>	<input checked="" type="checkbox"/>	<input checked="" type="checkbox"/>	A,B,X	4 profiles	B51 (2012/13)
6	CoFi_21	A, B, C, X (2m)	75.475	16.321	3484	19.12.2016	<input checked="" type="checkbox"/>	<input checked="" type="checkbox"/>	<input checked="" type="checkbox"/>	<input checked="" type="checkbox"/>		
7	CoFi_22	A, B, C, X (2m)	76.186	18.328	3463	20.12.2016	<input checked="" type="checkbox"/>	<input checked="" type="checkbox"/>	<input checked="" type="checkbox"/>	<input checked="" type="checkbox"/>		
8	CoFi_23	A, B, C, X (2m)	76.898	20.661	3456	21.12.2016	<input checked="" type="checkbox"/>	<input checked="" type="checkbox"/>	<input checked="" type="checkbox"/>	<input checked="" type="checkbox"/>		
9	CoFi_24	A, B, C, X (2m)	77.571	23.186	3458	22.12.2016	<input checked="" type="checkbox"/>	<input checked="" type="checkbox"/>	<input checked="" type="checkbox"/>	<input checked="" type="checkbox"/>		
10	CoFi_25	A, B, C, X (2m)	78.287	26.296	3455	23.12.2016	<input checked="" type="checkbox"/>	<input checked="" type="checkbox"/>	<input checked="" type="checkbox"/>	<input checked="" type="checkbox"/>		
11	CoFi_26	A, X (2m)	78.888	29.375	3461	24.12.2016	<input checked="" type="checkbox"/>	<input checked="" type="checkbox"/>	<input checked="" type="checkbox"/>	<input checked="" type="checkbox"/>		
12	CoFi_27	A, B, C, X (2m)	79.001	29.999	3473	26.12.2016	<input checked="" type="checkbox"/>	<input checked="" type="checkbox"/>	<input checked="" type="checkbox"/>	A,B,X	4 profiles	B54; OIR trench
13	CoFi_56	A, B	79.181	35.692	3576	06.01.2017	<input checked="" type="checkbox"/>					
14	CoFi_60	A, B, C, X (4m)	79.242	40.555	3665	09-11.01.2017	<input checked="" type="checkbox"/>	<input checked="" type="checkbox"/>	<input checked="" type="checkbox"/>	<input checked="" type="checkbox"/>	Transects	B55
15	CoFi_64	A, B, C, X (4m)	79.332	34.965	3544	16-18.01.2017	<input checked="" type="checkbox"/>	<input checked="" type="checkbox"/>		<input checked="" type="checkbox"/>	Transects	B56
16	CoFi_69	A, B, C, X (2m)	78.839	27.284	3416	23.01.2017	<input checked="" type="checkbox"/>					
17	CoFi_71	A, B, C, X (2m)	78.501	22.640	3325	24.01.2017	<input checked="" type="checkbox"/>	<input checked="" type="checkbox"/>	<input checked="" type="checkbox"/>	A		
18	CoFi_73	A, B, C, X (2m)	78.02	17.621	3259	25.01.2017	<input checked="" type="checkbox"/>	<input checked="" type="checkbox"/>	A,B,X(1)	X(2)		
19	CoFi_75	A, B, X (2m)	77.317	12.029	3153	26.01.2017	<input checked="" type="checkbox"/>	A,X(2)	X(2)	A		
20	CoFi_77	A, B, C, X (2m)	76.539	7.198	3067	27.01.2017	<input checked="" type="checkbox"/>					
21	CoFi_79	A, B, C, X (2m)	75.674	2.903	2959	28.01.2017	<input checked="" type="checkbox"/>					
22	CoFi_44	A, B, C, X (2m)	76.793	31.900	3737	26.12.2016	<input checked="" type="checkbox"/>	C		C		B53 (2012/13)

Tab. 3: Sampling protocol of the OIR trench. The wall orientation is $\sim 127^\circ$ (true north).

Position	Distance from the first position	Relative surface height	KF number	Depth	Comments
1	0	0	361	0-1 m	5 cm offset into the wall
			391	1-2 m	
			421	2-3 m	
2	125	15.1	362	0-1 m	
			392	1-2 m	
			422	2-3 m	
3	237	16.9	363	0-1 m	
			393	1-2 m	
			423	2-3 m	
4	309	25.8	364	0-1 m	
			394	1-2 m	
			424	2-3 m	
5	462	28.8	365	0-1 m	
			395	1-2 m	
			425	2-3 m	
6	556	15.8	366	0-1 m	
			396	1-2 m	
			426	2-3 m	
7	672	8.3	367	0-1 m	10 cm offset to the left
			397	1-2 m	
			577	2-3 m	
8	800	6.4	368	0-1 m	
			398	1-2 m	
			578	2-3 m	
9	970	8	369	0-1 m	
			399	1-2 m	
			579	2-3 m	
10	1088	6.2	370	0-1 m	
			400	1-2 m	
			580	2-3 m	
11	1209	5.1	371	0-1 m	
			401	1-2 m	
			581	2-3 m	
12	1343	13.6	372	0-1 m	
			402	1-2 m	
			582	2-3 m	
13	1440	7.2	373	0-1 m	10 cm offset to the left
			403	1-2 m	
			583	2-3 m	
14	1575	10.1	374	0-1 m	
			404	1-2 m	
			584	2-3 m	
15	1750	18.3	375	0-1 m	
			405	1-2 m	
			585	2-3 m	
16	1832	20.9	376	0-1 m	
			406	1-2 m	
			586	2-3 m	
17	1934	15.9	377	0-1 m	
			407	1-2 m	
			587	2-3 m	
18	2056	21.4	378	0-1 m	
			408	1-2 m	
			588	2-3 m	

19	2145	13.9	379 409 589	0-1 m 1-2 m 2-3 m	
20	2282	10.3	380 410 590	0-1 m 1-2 m 2-3 m	
21	2449	9.6	381 411 591	0-1 m 1-2 m 2-3 m	Upper 4 cm lost
22	2545	12.9	382 412 592	0-1 m 1-2 m 2-3 m	
23	2700	13.3	383 413 593	0-1 m 1-2 m 2-3 m	20 cm offset to the left 20 cm offset to the left 20 cm offset to the left
24	2815	6.7	384 414 594	0-1 m 1-2 m 2-3 m	
25	3051	20.2	385 415 595	0-1 m 1-2 m 2-3 m	
26	3177	22.5	386 416 596	0-1 m 1-2 m 2-3 m	
27	3310	23.9	387 417 597	0-1 m 1-2 m 2-3 m	
28	3412	33.9	388 418 598	0-1 m 1-2 m 2-3 m	
29	3453	35.3	389 419 599	0-1 m 1-2 m 2-3 m	
30	3522	38.5	390 420 600	0-1 m 1-2 m 2-3 m	

10.2 DATASETS

10.2.1 SNOW DENSITY

10.2.1.1 SURFACE SNOW DENSITY ALONG THE COFI TRAVERSE

Surface snow density along an overland traverse between Kohlen Station and former Plateau Station
(East Antarctica)

Weinhart, A. H., Freitag, J., Hörhold, M., Kipfstuhl, S. and Eisen, O.

Pangaea, published on 14 April 2021

Doi: 10.1594/PANGAEA.928079

10.2.2 SPATIAL DISTRIBUTION OF CRUSTS IN GREENLAND AND ANTARCTICA

10.2.2.1 CRUSTS IN SNOW FROM GREENLAND AND ANTARCTICA

Compilation of high-density crusts in snow from various locations in Dronning Maud Land (East
Antarctica) and northern Greenland

Weinhart, A. H. and Freitag, J.

Pangaea, published on 18 October 2021

Doi: 10.1594/PANGAEA.935872

10.2.2.2 CRUSTS IN TWO ANTARCTIC FIRN CORES

High-density crust record from firn cores B40 and B54, East Antarctica

Weinhart, A. H., Kipfstuhl, S. and Freitag, J.

Pangaea, published on 23 July 2021

Doi: 10.1594/PANGAEA.933926

10.2.3 STABLE WATER ISOTOPES & MAJOR IONS

Stable water isotopes and major ions in snow along a traverse route between Kohlen Station and former Plateau Station, East Antarctica

Weinhart, A. H., Kipfstuhl, S., Mengert, M., Götz, P., Micha, G., Freitag, J. and Hörhold, M.

Pangaea, published on 04 May 2021

Doi: 10.1594/PANGAEA.929966

10.3 CONFERENCE POSTER CONTRIBUTIONS

10.3.1 EGU 2019

Challenges and limitations in interpreting climate proxies in snow of low accumulation areas – insights from a traverse on the East Antarctic Plateau

Weinhart, A. H., Freitag, J., Hörhold, M. and Kipfstuhl, S.

Geophysical Research Abstracts Vol. 21, EGU General Assembly 2019. EGU2019-17769, 2019.

Ice cores can give us precious information about past climate conditions. Proxies obtained from ice cores, such as stable water isotopes, are used to reconstruct paleoclimate records. Depending on the accumulation rate, even seasonal cycles can be resolved in some regions of Greenland and coastal Antarctica. But in areas with low accumulation it becomes difficult to resolve these proxies even on annual to decadal time scales.

For the Coldest Firn project at AWI two traverses have been carried out in season 2012/13 and 2016/17 on the East Antarctic Plateau, covering the barely sampled region between Kohnen Station and Dome Fuji / Plateau Station. Five firn cores of 200 meters length each have been drilled to investigate the firn metamorphosis at low-temperature and low accumulation.

Additionally in 2016/17, 115 snow profiles have been taken along the traverse using the snow liner technique. From the snow surface up to two meters depth samples in a high spatial coverage are available to investigate several climate proxies. The snow profiles have been analyzed for density and microstructure with the non-destructive Ice-CT at AWI. Cut into discrete samples in two centimeter resolution, they are further analyzed for stable water isotopes as well as several trace species using CRDS and IC measurements.

Accumulation rates for the area are estimated from comparing dated and extrapolated DEP (Dielectric Profiling) data of the drilled firn cores and existing satellite derived data. In some regions of the investigated area, values can easily fall below $25 \text{ kg m}^{-2} \text{ a}^{-1}$. Still, our isotope and impurity record does not show consecutive annual or seasonal layering. With structural features derived from the μ CT analysis we are able to partly resolve the snowpack history. While wind crusts form with long exposition time at the snow surface and without any precipitation, finely stratified or cross bedded layers are indicators for coherent precipitation events in a certain time interval. Our findings clearly imply unequally distributed precipitation over the year and re-deposition of snow, which strongly affects the stable water isotope and impurity record in the snowpack. Interpretation of seasonal or annual cycles is barely possible and challenges the reconstruction of paleo-climate records from proxies in low accumulation areas.

10.3.2 EGU 2020 #1 (CO-AUTHORSHIP)

The genesis of a climate archive: snow pack studies at four polar sites

Freitag, J., Hörhold, M., **Weinhart, A. H.**, Kipfstuhl, S. and Laepple, T.

Doi: 10.5194/egusphere-egu2020-19249

Understanding the deposition history and signal formation in ice cores from polar ice sheets is fundamental for the interpretation of paleoclimate reconstruction based on climate proxies. Polar surface snow responds to environmental changes on a seasonal time scale by snow metamorphism, displayed in the snow microstructure and archived in the snowpack. However, the seasonality of snow metamorphism and its link to the deposited signal in isotopes and impurity load is poorly known. Here, we apply core-scale microfocus X-ray computer tomography to continuously measure snow microstructure of four snow cores from Greenlandic (Renland ice cap-drill site (2 m), EGRIP drill site (5 m)) and Antarctic sites (EDML-drill site (3 m), CoFi 7/Plateau Station (4 m)) covering a wide range of annual temperatures from -18°C down to -56°C. In our multi-parameter approach we compare the derived microstructural properties on the mm- to cm-scale to discretely measured trace components and stable water isotopes, commonly used as climate proxies. We will show how ice and pore intercepts, the geometrical anisotropy, specific surface area, crusts anomalies and small-scale density distributions are represented under different climate conditions. Their profiles will be discussed in the context of snow metamorphism and deposition history using trace components and isotopes as additional constraints on timing.

10.3.3 EGU 2020 #2 (CO-AUTHORSHIP)

Spatial variability of surface snow isotopic composition on the East Antarctic Plateau and implications for climate reconstructions

Hörhold, M., **Weinhart, A. H.**, Kipfstuhl, S., Freitag, J., Micha, G., Werner, M. and Lohmann, G.

Doi: 10.5194/egusphere-egu2020-13653

The reconstruction of past temperatures based on ice core records relies on the quantitative but empirical relationship of stable water isotopes and annual mean temperature. However, its relation varies through space and time. On the East Antarctic Plateau, temperature reconstructions from ice cores are poorly constrained or even fail on decadal and smaller time scales. The observed discrepancy between annual mean temperature and isotopic composition partly relies on surface processes altering the signal after deposition but also, to a great deal, on spatially coherent processes prior to or during deposition. However, spatial coverage over larger areas on the East Antarctic Plateau is challenging. We here present in-situ measurements of the isotopic composition of surface snow with unprecedented statistical quality and coverage. 1 m surface snow profiles were collected during an overland traverse between Kohnen Station and Plateau Station, covering a 1200 km long transect. We explore regional differences of the temperature-isotope relationship and discuss possible mechanisms affecting the isotopic composition in areas with accumulation rates lower than 60 kg m⁻² a⁻¹.

10.4 MISCELLANEOUS

10.4.1 CURIOSITIES FROM THE ICE LAB

While spending – by rule of thumb – 292 hours in the ice lab cutting the snow profiles into discrete samples, we also stumbled upon two curiosities.

The first one is most likely a piece of paper from a notepad, about 1 cm in diameter (Fig. 17). How this piece of paper got there is pure speculation. The sample was from a snow profile taken in season 2013/14 (at location 5, chapter 2.7.2.1), one year after the drilling of B51 took place. A hypothesis is that this piece of paper was blown away by wind during the drilling operation or fieldwork around the drill site. Also the depth of 11-12 cm below the surface, in which the piece of paper was found, fits with the annual accumulation rate at location 5 (Karlöf et al., 2005) and supports the hypothesis.



Fig. 17: Finding in a snow profile at location 5 from season 13/14 in sample number 12.

For the other find, so far there is no plausible explanation. The round, droplet-like, amber structure (Fig. 18) was found in a snow profile at Plateau Station at a depth of 22-23 cm. It might be a frozen drop of a liquid but will probably remain a mystery.



Fig. 18: Finding in a snow profile at Plateau Station in sample number 23.

10.4.2 A VISIT TO ABANDONED PLATEAU STATION (ACTIVE 1966-1969)

Plateau Station was a research base operated by the United States from 1966 to 1969 and buried in snow since then. One of the lowest 10 m firn temperatures of -58.4°C has been recorded here and the accumulation rate ($\leq 32 \text{ kg m}^{-2} \text{ a}^{-1}$) is among the lowest of the whole Antarctic continent (e.g., Koerner, 1971, Radok & Lile, 1977). It was used for mainly atmospheric, meteorological, and geomagnetic studies (Dalrymple & Stroschein, 1977). After drilling of firn core B55, the five of us took the chance for a sneak peek into the abandoned station. The top of the former, roughly 4 m high observational tower is level with the snow surface now and marked with bamboo poles. After opening the skylight, we stepped down into the (roughly) -55°C cold darkness equipped with flashlights and photo cameras. The station appeared to be left head over heels because food stocks, medical equipment, furniture, and tools were still there – just the electric generator was removed. Our visit was described and printed in a Spiegel article (Seidler, 2017). Impressions through my eyes are shown below in Fig. 19.



Fig. 19: From top left to bottom right: The entrance to the station via the former skylight, engine room without generator, telephone, living room, kitchen with spice rack, a sleeping cabin, fire extinguisher, medicine cabinet, and workshop.